Improving In Vitro Bioassays: Addressing Chemical Transformation and Baseline Toxicity

Dissertation

der Mathematisch-Naturwissenschaftlichen Fakultät
der Eberhard Karls Universität Tübingen
zur Erlangung des Grades eines
Doktors der Naturwissenschaften
(Dr. rer. nat.)

vorgelegt von
M. Sc. Julia Huchthausen
aus Uelzen

Tübingen
2024

Gedruckt mit Genehmigung der Mathematisch-Naturwissenschaftlichen Fakultät der Eberhard Karls Universität Tübingen.

Tag der mündlichen Qualifikation:	08.03.2024
Dekan:	Prof. Dr. Thilo Stehle
1. Berichterstatter/-in:	Prof. Dr. Beate I. Escher
2. Berichterstatter/-in:	Prof. Dr. Stefan Stolte

Contents

Preface

This doctoral thesis was performed at the Helmholtz Centre for Environmental Research, Leipzig, in the Department of Cell Toxicology between 2020 and 2024. It is part of a project that has received funding from the European Union's Horizon 2020 research and innovation programme under Grant Agreement No. 965406. The thesis was written in cumulative form and is based on the following research articles:

Publication I: Huchthausen, J., Henneberger, L., Mälzer, S., Nicol, B., Sparham, C., Escher, B. I. (2022) High-Throughput Assessment of the Abiotic Stability of Test Chemicals in *In Vitro* Bioassays. *Chemical Research in Toxicology* 35 (5), 867-879. DOI: 10.1021/acs.chemrestox.2c00030.

Publication II: Huchthausen, J., Escher, B. I., Grasse, N., König, M., Beil, S., Henneberger, L. (2023) Reactivity of Acrylamides Causes Cytotoxicity and Activates Oxidative Stress Response. *Chemical Research in Toxicology* 36 (8), 1374-1385. DOI: 10.1021/acs.chemrestox.3c00115.

Publication III: Huchthausen, J., Braasch, J., Escher,B. I., König, M., Henneberger, L. (2024) Effects of Chemicals in Reporter Gene Bioassays with Different Metabolic Activity Compared to Baseline Toxicity. *Chemical Research in Toxicology.* DOI: 10.1021/acs.chemrestox.4c00017.

Parts of the thesis are taken from the original publications without further indication. The original publications are included at the end of the thesis.

The Figures of the thesis were created using BioRender (www.BioRender.com) and GraphPad Prism (version 10.1.0).

Summary

The widespread use of chemicals in today's world has led to significant concerns about their impact on human health and the environment. The traditional use of animal testing to establish safe levels for chemicals is impractical due to cost and time constraints, animal ethics and concerns about the relevance of animal data to humans. In response, there is a growing call for a paradigm shift towards new approach methodologies (NAMs) that are animal-free and include *in silico* and *in vitro* methods. *In vitro* bioassays using reporter gene cell lines are a key component of the 3R (Replacement, Refinement, Reduction) strategy, as they offer a promising, cost-effective and automatable alternative with high-throughput capabilities. To generate reliable *in vitro* data, the planning, execution and evaluation of the bioassays must be carried out with the utmost care. Chemicals are subject to various loss processes in the bioassay, which can lead to a deviation between the dosed concentration and the actual bioavailable concentration. These processes include reversible distribution and binding to media components and plastic, but also irreversible loss processes due to volatilization or abiotic or biotic degradation processes. If the latter loss processes remain unnoticed, this can lead to an incorrect interpretation of the bioassay results and an underestimation of the chemical hazard. The primary objective of this thesis was to improve the use of high-throughput cell-based bioassays used for single chemical screening. The study aimed to identify potential challenges and limitations, especially considering the influence of chemical transformation processes on bioassay results. Baseline toxicity, the minimal toxicity of a chemical, is caused by accumulation in the cell membrane and can be used to classify chemical toxicity. Chemicals with higher measured toxicity than baseline toxicity may have a specific mode of toxicity and lower experimental toxicity may indicate experimental artifacts and loss processes. A novel baseline toxicity model was developed based on a critical membrane burden derived from freely dissolved effect concentrations of charged and hydrophilic chemicals to consider distribution processes to media components and to make the model applicable to a wide range of chemicals. The measured cytotoxicity of 94 chemicals in three bioassays with different cell lines (AREc32, ARE-*bla*, and GR-*bla*) were compared with baseline toxicity by calculating the toxic ratio (TR). Between 44 and 50 chemicals could be identified as baseline toxicants and 22 to 28 chemicals showed a specific toxicity mechanism ($TR \geq 10$). However, seven chemicals showed $TR < 0.1$, which could be an indication of possible artifacts or loss processes. To identify abiotic transformation processes of chemicals in *in vitro* bioassays, a high-throughput workflow was developed based on 22 potentially unstable chemicals. Chemical stability was assessed in

different bioassay media, buffer solutions (pH 4, 7.4 and 9) and solutions of bovine serum albumin and glutathione to examine the influence of hydrolysis and covalent reactions with proteins. Photodegradation and abiotic oxidative degradation were also investigated, but were found to be less relevant for *in vitro* bioassay conditions. To assess the degradation kinetics of the chemicals, a high-throughput solid-phase microextraction (SPME) workflow using a BioSPME 96-Pin Device was established for extracting chemicals from the exposure solutions. The results indicated that the main contributors to the depletion of test chemicals in the bioassay media were reactions with hydroxide ions and covalent interactions with proteins. *In silico* models predicting the half-life of the hydrolytic degradation of chemicals in the environment and qualitative models based on structural features predicting reactivity towards proteins were compared with the experimental results. Since these models were not tailored to the bioassay conditions, there were deviations from the experimental results but the models provided a useful initial estimate of stability. The reactivity of the chemicals with glutathione could not reflect the stability in the bioassay medium but gave indications of the possible reactive toxicity of the chemicals. This relationship was further investigated using ten (meth)acrylamides by comparing their measured cytotoxicity and activation of oxidative stress response with their reactivity towards glutathione. Notably, there was a linear relationship between the reactivity of the tested acrylamides and the toxicity and activation of the oxidative stress response, while methacrylamides did not react with glutathione and acted as baseline toxicants. The differences in reactivity were explained by the lower electrophilicity of methacrylamides caused by their different chemical structure. The metabolic activity was found to be different in all three cell lines (AREc32, ARE-*bla*, and GR-*bla*) and ARE-*bla* showed the highest metabolic activity. Cytochrome P450 enzymes could be induced by xenobiotic chemicals in ARE-*bla* and AREc32. The effect concentrations of 94 chemicals measured in the three cell lines were compared and none of the cell lines showed significantly higher or lower toxicity, which implies that the differences in metabolic activity had no influence on the bioassay results. In summary, this work contributes significantly to refining the interpretation of bioassay data by providing a new baseline toxicity model and developing an experimental approach to assess chemical stability. The knowledge gained from this work on the high-throughput testing of chemicals improved the understanding of potential confounding factors in bioassay results and laid the foundation for improved risk assessment methods using *in vitro* bioassays.

Zusammenfassung

Die weitverbreitete Verwendung von Chemikalien in der heutigen Welt hat erhebliche Bedenken hinsichtlich ihrer Auswirkungen auf die menschliche Gesundheit und die Umwelt verursacht. Die herkömmliche Verwendung von Tierversuchen zur Festlegung sicherer Grenzwerte für Chemikalien ist aufgrund von Kosten- und Zeitbeschränkungen, ethischen Bedenken im Umgang mit Tieren und Zweifel hinsichtlich der Relevanz von Tierversuchsdaten für den Menschen unpraktisch geworden. Die Reaktion darauf ist ein zunehmendes Verlangen nach einem Paradigmenwechsel hin zu sogenannten „New Approach Methodologies“ (NAMs), die frei von Tierversuchen sind und *in-silico* sowie *in-vitro* Methoden einschließen. *In-vitro* Biotests mit Reportergen Zelllinien sind ein wesentlicher Bestandteil der 3R-Strategie (Replacement, Refinement, Reduction), da sie eine vielversprechende, kostengünstige und automatisierbare Alternative mit der Möglichkeit auf Hochdurchsatz bieten. Um zuverlässige *in-vitro* Daten zu generieren, müssen die Planung, Durchführung und Auswertung der Biotestverfahren mit größter Sorgfalt erfolgen. Chemikalien unterliegen verschiedenen Verlustprozessen im Biotest, die zu Abweichungen zwischen der dosierten Konzentration und der tatsächlich bioverfügbaren Konzentration führen können. Diese Prozesse umfassen reversible Verteilung und Bindung an Bestandteilen des Mediums und Plastik, aber auch irreversible Verlustprozesse aufgrund von Verflüchtigung oder abiotischen oder biotischen Abbauvorgängen. Wenn die zuletzt genannten Verlustprozesse unbeachtet bleiben, kann dies zu einer falschen Interpretation der Biotest-Ergebnisse und einer Unterschätzung des chemischen Risikos führen. Das Hauptziel dieser Arbeit war es, die Anwendung von Hochdurchsatz-Biotests zur Testung von Einzelstoffen zu verbessern. Die Studie hatte zum Ziel, potenzielle Herausforderungen und Einschränkungen zu identifizieren, insbesondere unter Berücksichtigung der Einflüsse von chemischen Transformationsprozessen auf die Biotest-Ergebnisse. Die Grundlinientoxizität (Basistoxizität), die minimale Toxizität einer Chemikalie, wird durch die Anreicherung in der Zellmembran verursacht und kann zur Klassifizierung der chemischen Toxizität verwendet werden. Chemikalien mit höherer gemessener Toxizität als die Basistoxizität können einen spezifischen Toxizitätsmechanismus aufweisen, während eine geringere experimentelle Toxizität auf experimentelle Artefakte und Verlustprozesse hinweisen kann. Ein neuartiges Modell für die Basistoxizität wurde entwickelt, basierend auf einer kritischen Membrankonzentration, die aus frei-gelösten Effektkonzentrationen geladener und hydrophiler Chemikalien abgeleitet wurde, um Verteilungsprozesse zu Medienkomponenten zu berücksichtigen und das Modell für eine Vielzahl von Chemikalien anwendbar zu machen. Die gemessene Zytotoxizität von 94 Chemikalien aus drei Biotests mit verschiedenen Zelllinien

(AREc32, ARE-*bla* und GR-*bla*) wurde mit der Basistoxizität verglichen, indem das toxische Verhältnis (TR) berechnet wurde. Zwischen 44 und 50 Chemikalien konnten als basistoxisch eingestuft werden, und 22 bis 28 Chemikalien zeigten einen spezifischen Toxizitätsmechanismus (TR ≥ 10). Allerdings zeigten sieben Chemikalien TR < 0,1, was auf mögliche Artefakte oder Verlustprozesse hindeuten könnte. Um abiotische Transformationsprozesse von Chemikalien in *in-vitro* Biotests zu identifizieren, wurde ein Hochdurchsatz-Arbeitsablauf basierend auf 22 potenziell instabilen Chemikalien entwickelt. Die chemische Stabilität wurde in verschiedenen Biotest-Medien, Pufferlösungen (pH 4, 7,4 und 9) sowie Lösungen von bovinem Serumalbumin und Glutathion gemessen, um den Einfluss von Hydrolyse und kovalenten Reaktionen mit Proteinen zu untersuchen. Der Photoabbau und die abiotische oxidative Degradation wurden ebenfalls untersucht, erwiesen sich jedoch als weniger relevant für *in-vitro* Biotest-Bedingungen. Um die Abbaukinetik der Chemikalien zu ermitteln, wurde ein Hochdurchsatz-Festphasenmikroextraktion (SPME) Arbeitsablauf unter Verwendung eines BioSPME 96-Pin-Device etabliert, um die Chemikalien aus den Expositionslösungen zu extrahieren. Die Ergebnisse deuteten darauf hin, dass Reaktionen mit Hydroxidionen sowie kovalente Reaktionen mit Proteinen die Hauptursache für die Abnahme der Testchemikalienkonzentration im Biotest-Medium waren. *In-silico* Modelle, die die Halbwertszeit des hydrolytischen Abbaus von Chemikalien in der Umwelt vorhersagen, und qualitative Modelle basierend auf strukturellen Merkmalen, die die Reaktivität gegenüber Proteinen vorhersagen, wurden mit den experimentellen Ergebnissen verglichen. Da diese Modelle nicht auf die Biotest-Bedingungen zugeschnitten waren, gab es Abweichungen von den experimentellen Ergebnissen, aber die Modelle lieferten eine nützliche erste Schätzung der Stabilität. Die Reaktivität der Chemikalien mit Glutathion konnte die Stabilität im Biotest-Medium nicht widerspiegeln, gab jedoch Hinweise auf die mögliche reaktive Toxizität der Chemikalien. Diese Beziehung wurde weiter untersucht, indem die gemessene Zytotoxizität und Aktivierung der oxidativen Stressantwort von zehn (Meth)acrylamiden mit ihrer Reaktivität gegenüber Glutathion verglichen wurden. Bemerkenswerterweise gab es einen linearen Zusammenhang der Reaktivität der getesteten Acrylamide mit der Toxizität und Aktivierung der oxidativen Stressantwort, während Methacrylamide nicht mit Glutathion reagierten und basistoxisch wirkten. Die Unterschiede in der Reaktivität wurden durch die geringere Elektrophilie der Methacrylamide aufgrund ihrer unterschiedlichen Struktur erklärt. Die metabolische Aktivität war in allen drei Zelllinien (AREc32, ARE-*bla* und GR-*bla*) unterschiedlich, wobei ARE-*bla* die höchste metabolische Aktivität zeigte. Cytochrom P450-Enzyme konnten durch xenobiotische Chemikalien in ARE-*bla* und AREc32 induziert werden.

Die Effektkonzentrationen von 94 Chemikalien, die in den drei Zelllinien gemessen wurden, wurden verglichen, und keine der Zelllinien zeigte signifikant höhere oder niedrigere Toxizität, was darauf hindeutet, dass die Unterschiede in der Stoffwechselaktivität keinen Einfluss auf die Biotest-Ergebnisse hatten. Zusammenfassend trägt diese Arbeit erheblich dazu bei, die Interpretation von Biotest-Daten zu verfeinern, indem sie ein neues Modell für die Basistoxizität eingeführt hat und einen experimentellen Ansatz zur Bewertung der chemischen Stabilität entwickelt hat. Die aus dieser Arbeit gewonnenen Erkenntnisse zur Hochdurchsatzprüfung von Chemikalien verbessern das Verständnis potenzieller Störfaktoren in Biotest-Ergebnissen und legen den Grundstein für verbesserte Methoden der Risikobewertung mit *in vitro* Biotests.

Acknowledgements

“Are you sure that it is worth it? Doing a PhD will be hard and full of sacrifice.” Quotes like this are the first things that you hear when you tell people you are going to do a PhD. Sure, it is true that a PhD is a long journey that can be exhausting from time to time, but now, after three years, I can tell those people that for me, this journey never felt like a rocky road. It was more like a boat ride on a mostly gentle river that took me steadily forward. Even a river can be full of currents and rocks from time to time, but I was always lucky to be surrounded by people who helped me overcome these obstacles. This trip has flown by and I still cannot quite believe that I am writing these words right now. I have grown a lot during my journey. I became stronger, more confident and gained a lot of knowledge. I feel blessed and grateful that I was able to gain so many new experiences, meet interesting and lovely people and travel to new countries. First and foremost, I would like to express my sincere gratitude to Beate Escher for being a role model for young (female) scientists, a great mentor and supervisor. Your energy, curiosity and passion for science are infectious and inspiring and I am glad that I was able to benefit from your advice, guidance, and encouragement throughout my PhD. I would also like to thank Luise Henneberger from the bottom of my heart. You and Beate ultimately convinced me to do my PhD and always believed in me, even though I sometimes lacked self-confidence. Thank you, Luise, for always being there for me during this time, always having an open ear for my questions and always having a solution ready for every problem. I also want to express my gratitude to Stefan Stolte for always being supportive and interested in my research and giving valuable feedback from a different perspective. Next, I want to thank the whole Celltox team, especially Maria König, Sophia Mälzer, Jenny Braasch, Vanessa Srebny, Niklas Wojtysiak and Rita Schlichting. We spend an average of 11 years of our lives at work, so I am very lucky to be part of such a great team and be surrounded by so many great people every day. Thank you for your support in the lab, your expertise and all the conversations, coffee breaks and team events. Many thanks also to the team of PrecisionTox, especially Stefan Scholz, for coordinating the project and all your feedback on my research. Thanks a lot, to all my friends, especially Hanna, Thyra and Sophia, who have always believed in me and supported me throughout my life. I can laugh and cry with you and you always have an open ear. I would also like to thank my parents for making my studies possible and for supporting me along the way, even though they still do not know exactly what I am doing. Last but not least, I would like to thank the person who is by my side every day, who goes through thick and thin with me and gives me strength for everything I do. William, I love you from the bottom of my heart.

1. Introduction

1.1 Chemical risk assessment

Chemicals play a crucial role in our modern society, offering numerous advantages across various industrial domains, including healthcare, commodities, and agriculture. They are utilized in the production of drugs, plastics, pesticides, and a variety of other applications. Consequently, the chemical industry is growing worldwide and the number of registered chemicals is increasing. Since June 2008, the European Chemicals Agency (ECHA) has done 104,078 registrations, comprising 22,502 chemicals, under the Registration, Evaluation, Authorization and Restriction of Chemicals (REACH) and around 1700 registrations are added each year (ECHA 2023b; Muir et al. 2023). In addition to all the positive aspects, there is also a growing concern about the effects of this increasing number of chemicals on people and our planet (Arp et al. 2023). The World Health Organization (WHO) estimated that more than 2 million deaths were linked to chemical exposures worldwide in 2019 (WHO 2021). A number of steps have already been taken in recent years to restrict the use of harmful chemicals. For example, the ban on bisphenol A in thermal paper, which came into force in 2017 (EC 2016), or the proposed ban on the class of per- and polyfluoroalkyl substances (PFAS) in the European Union, which was presented at the beginning of 2023 (ECHA 2023a) and has been discussed by representatives of politics, science and industry to date. The European Commission has taken steps to address the imperative for public safety by publishing its “Chemicals Strategy” within the framework of the European Green Deal (EC 2020). This strategy outlines a series of initiatives aimed at fostering a toxic-free environment and safeguarding both people and the ecosystem from potentially harmful chemicals (Magurany et al. 2023). Risk assessment of chemicals is therefore an important task for the governments of countries worldwide and decisions on banning or restricting chemicals must be made according to the latest scientific knowledge to protect people and our planet. As depicted in Figure 1, risk is defined as the likelihood of a chemical to cause an adverse effect, which is determined by the toxic potential of the chemical (hazard) and the amount of the chemical to which organisms are exposed (exposure). The first step in chemical risk assessment is the identification of hazardous chemicals. This involves considering chemical properties, like persistence, bioaccumulation and toxicity (PBT) (EP&EC 2006) or possible modes of toxicity, such as carcinogenicity, mutagenicity or reproductive toxicity (CMR). Toxicity assessment evaluates the adverse effects of chemicals on living organisms by studying the dose-response relationship and by identifying the specific target organs and modes of toxic action (Adeleye et al. 2015). Exposure assessment determines the levels of exposure to a chemical through various routes, such as inhalation,

ingestion, and dermal contact. This step considers factors like frequency, duration, and concentration of exposure (Rice et al. 2008).

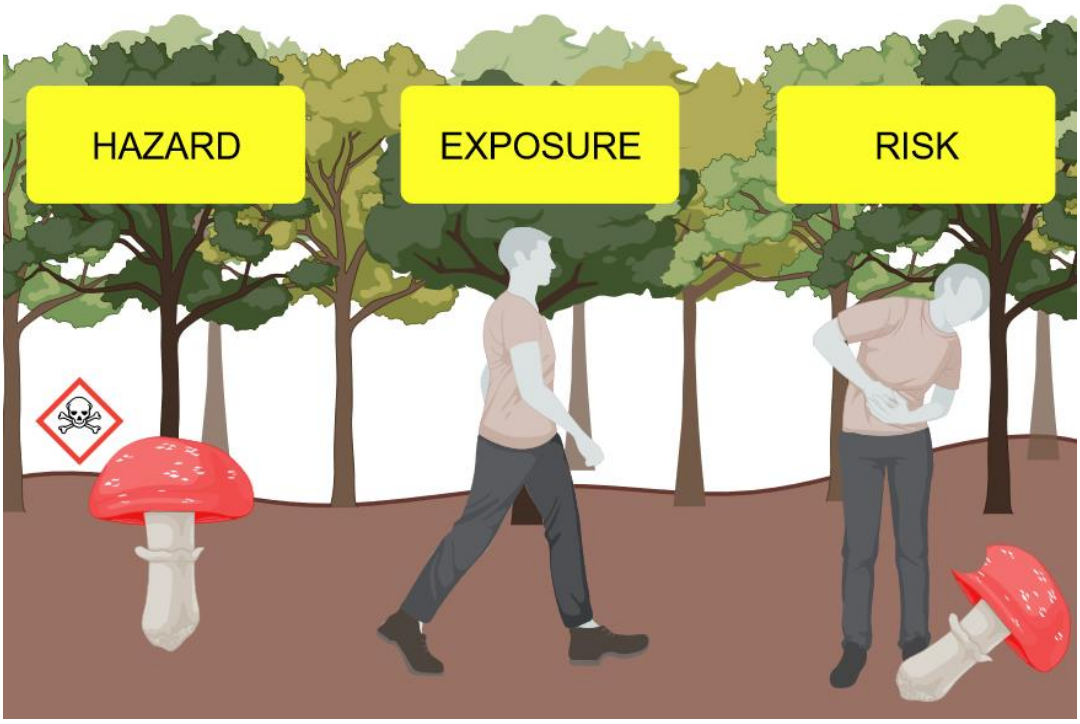

Figure 1: Graphical depiction of the meaning of the terms hazard, exposure and risk in the context of risk assessment.

The conventional approach of using animal studies to define safe levels of chemicals for humans has been standard for many years. However, a comprehensive risk assessment of chemicals using animal-based studies is not feasible, as animal testing for the risk assessment of a single chemical is extremely costly and can take several years to complete (Van Norman 2019). In addition, the relevance of toxicity data from laboratory animals for humans is questionable, as biological variability and interspecies extrapolation are possible sources of error (Leist and Hartung 2013). Therefore, in recent years, there have been calls for a paradigm shift to improve the relevance, efficiency and ethical acceptance of chemical risk assessment (Schmeisser et al. 2023; van der Zalm et al. 2022). These so-called new approach methodologies (NAMs) are characterized by the principle of the 3Rs, meaning the "Replacement, Refinement and Reduction" of animals in research (Burden et al. 2015) and the use of advanced technologies such as high-throughput screening methods, omics technologies (genomics, proteomics and metabolomics), and computational modeling to generate large-scale data sets for comprehensive risk assessment (Thomas et al. 2013).

1.2 *In vitro* bioassays for single chemical screening

The publication of the Toxicity Testing in the 21st Century (Tox21) strategy by the U.S. National Research Council in 2007 has been one of the most groundbreaking achievements in *in vitro* toxicology of the recent past (NRC 2007). As part of Tox21, which is a collaboration between various research institutions and government agencies in the United States, around 10,000 chemicals were tested in a high-throughput screening (HTS) format and the resulting data was made publicly available. Over 50 bioassays were used in this project to identify molecular initial events (MIE) or key events (KE) associated with nuclear receptors and cellular stress response pathways and to develop adverse outcome pathways (AOP) of these chemicals in humans (Ankley et al. 2010).

In vitro bioassays are a promising alternative to animal testing and therefore an important part of the 3R principle. They are cost-effective, can be automated and can be carried out in high-throughput format using multi-well plates and robotic platforms (Hartung 2011). Many different multi-well plate systems have already been established using different model organisms *in vivo*, such as nematodes (*Caenorhabditis elegans)*, fruit flies (*Drosophila melanogaster*) or zebrafish embryos (*Danio rerio*), as well as *in vitro* systems using primary cells or cell lines from humans or different animal species. The use of human cell lines for human risk assessment of chemicals eliminates the need for interspecies extrapolation, making data from *in vitro* bioassays even more meaningful than *in vivo* data from distant species in some cases (Leist and Hartung 2013). Many *in vitro* cell-based bioassays utilize immortalized reporter gene cell lines, which can identify specific toxicity mechanisms on the cellular level. The cell lines are usually genetically modified and contain genes for molecular receptors or other cellular targets coupled with a reporter gene. The expression of the reporter protein visualizes the activation of the molecular target by a test substance (Wang et al. 2020). Reporter enzymes are, for example, β-lactamase or luciferase, which are able to generate fluorescence or luminescence using appropriate substrates. This signal can then be quantified and the measured fluorescence or luminescence is proportional to the activation of the molecular target (Wang et al. 2006; Zlokarnik 2000). In addition to unspecific cytotoxicity, these assays measure specific biological endpoints or responses, which can include (hormone) receptor activation or inhibition, xenobiotic metabolism, adaptive stress response or reactive toxicity (Escher et al. 2021). By testing the effects of chemicals in multiple *in vitro* bioassays with different endpoints, modes of toxic action (MOA) of the chemicals can be identified.

After damage caused by stressors, adaptive stress response pathways are triggered to reestablish cellular homeostasis. Many diseases, like diabetes, cancer, and neurodegenerative conditions, involve oxidative stress, which can be induced by a variety of xenobiotic chemicals (Barnham et al. 2004; Gorrini et al. 2013). Electrophilic chemicals and chemicals generating reactive oxygen species (ROS) can activate the oxidative stress response. Various mammalian reporter gene assays assess this response, such as the AREc32 cell line (Wang et al. 2006) or CellSensor™ ARE-*bla* Hep G2 cell line (Bogen 2017). Figure 2A shows the oxidative stress response via the Kelch-like ECH-associated protein 1 (Keap-1) and nuclear factor erythroid 2-related factor 2 (NRF-2) pathway. Nrf-2 activity is regulated by the repressor protein Keap-1 in the cytoplasm and is constantly degraded through the ubiquitin–proteasome pathway. In the presence of oxidative stress, Nrf-2 undergoes dissociation from Keap-1 and moves to the nucleus, where it forms heterodimers with small musculoaponeurotic fibrosarcoma (Maf) proteins. Binding of this complex to the antioxidant response elements (ARE) of the DNA initiates the transcription of protective genes as a defense mechanism against oxidative stress (Deshmukh et al. 2017; Taguchi et al. 2011). In reporter gene cell lines, multiple copies of the ARE are located upstream of a reporter gene such as β-lactamase or luciferase, which is expressed after exposure to chemicals that activate the oxidative stress response, such as the reference compound *tert*-butylhydroquinone (tBHQ) and can be quantified via fluorescence or luminescence detection (Wang et al. 2006; Zhao et al. 2016).

A growing amount of endocrine-disrupting chemicals (EDCs) in the environment has been a focus of science for several years. Nuclear hormone receptors like the glucocorticoid receptor (GR), estrogen receptor (ER) or androgen receptor (AR) are primary targets of EDCs (Gore et al. 2015). In the past decade, bioassays have played a crucial role in identifying nuclear receptor agonists or antagonists. As depicted in Figure 2B, reporter gene cell lines for GR activation (e.g. GeneBLAzer™ GR-UAS-*bla* HEK 293T cell line) express the ligand-binding domain of human GR, which is present in the cytoplasm. When chemicals bind to the receptor binding domain, the resulting receptor-ligand complex dimerizes and is translocated into the nucleus. There it interacts with the glucocorticoid response elements (GRE) of the DNA, which are located upstream of the target genes and, in the case of the GR-*bla* cell line, upstream of a β-lactamase reporter gene. The expression of the target genes and of β-lactamase is induced and can be quantified (Oakley and Cidlowski 2013). Corticosteroid receptors, such as GR, are widely distributed in organisms and play a role in various diseases. They mediate the actions of steroid hormones (glucocorticoids) involved in numerous physiological processes. Disturbances in glucocorticoid action have can lead to adverse effects in humans, for example,

congenital malformation, affective disorders, immune, cardiovascular and allergic diseases or cancer (Odermatt and Gumy 2008; Zhang et al. 2019). Dexamethasone is a glucocorticoid pharmaceutical and known GR agonist and it was used as a reference chemical for the GR-*bla* bioassay.

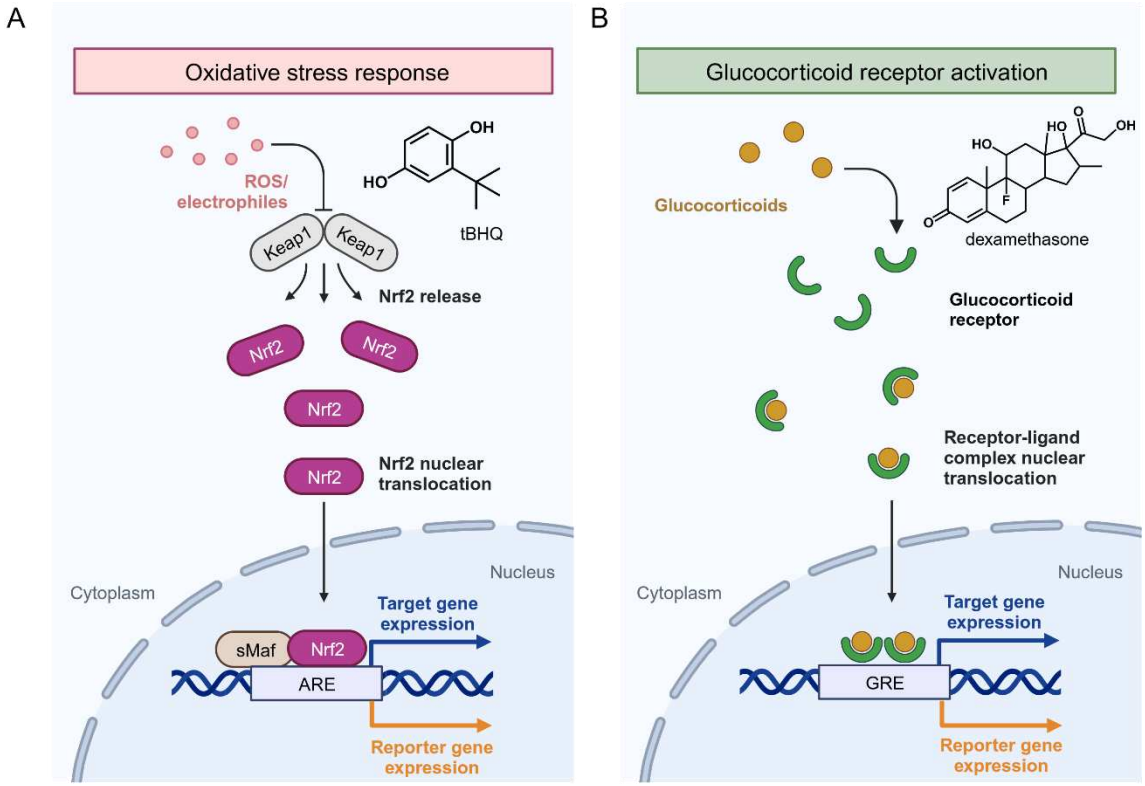

Figure 2: Cellular pathways of oxidative stress response activation (A) and glucocorticoid receptor activation (B) in reporter gene cell lines. ROS = reactive oxygen species, tBHQ = *tert*-butylhydroquinone, Keap1 = Kelch-like ECH-associated protein 1, Nrf2 = Nuclear factor erythroid 2-related factor 2, sMaf = Small musculoaponeurotic fibrosarcoma proteins, ARE = antioxidant response element, GRE = glucocorticoid response element. Adapted from "Keap1–Nrf2 Pathway", by BioRender.com (2023). Retrieved from https://app.biorender.com/biorender-templates.

1.3 Baseline Toxicity

In 1992, Verhaar et al. developed a classification scheme for the toxicity of chemicals (Verhaar et al. 1992). The four chemical classes were inert chemicals, less inert chemicals, reactive chemicals and specifically acting chemicals. Later, the difference between the first two groups was explained by the use of the octanol-water partitioning constant (K_{ow}) as a descriptor of hydrophobicity. By using more appropriate descriptors, such as the liposome-water partitioning constant ($K_{lip/w}$), both classes could be summarized as baseline toxicants (Vaes et al. 1998). Baseline toxicity, often referred to as narcosis, means the loss of membrane integrity and function leading to cell death, as shown in Figure 3 (van Wezel and Opperhuizen 1995). The underlying mechanisms of baseline toxicity are still not fully explained and there are various theories according to which either the structure of the lipids or the proteins of the membrane is disturbed or the interaction of the two (van Wezel and Opperhuizen 1995). Baseline toxicity is a non-specific toxicity mechanism and caused by chemical accumulation in the membrane, which means that it is not the nature but only the concentration of the chemical in the cell membrane that is responsible for the toxicity, which means that hydrophobic chemicals have a higher baseline toxicity than hydrophilic chemicals because they accumulate in the membrane to a greater extent (Könemann 1981). The relationship between toxicity and hydrophobicity is used by so-called quantitative structure-activity relationship (QSAR) models to predict the baseline toxicity of a chemical. Comparing observed toxicity with the predicted baseline toxicity can indicate a specific or reactive MOA. Empirical baseline toxicity QSARs for various aquatic species (Escher et al. 2017; Klüver et al. 2016) and reporter gene cells (Escher et al. 2019; Lee et al. 2021) have been published, which use only $K_{lip/w}$ as an input parameter. Since experimental data for $K_{lip/w}$ are rare, linear solvation energy relationships (LSER) (Ulrich et al. 2017) or linear free energy relationships (LFER) (Endo et al. 2011) are often used for the prediction of $K_{lip/w}$. QSAR models can also be applied to ionizable chemicals if the $D_{lip/w}$ is used as an input parameter instead of the $K_{lip/w}$, as it includes the speciation of the chemical at a certain pH (usually 7.4) (Escher et al. 2017; Escher and Schwarzenbach 2002).

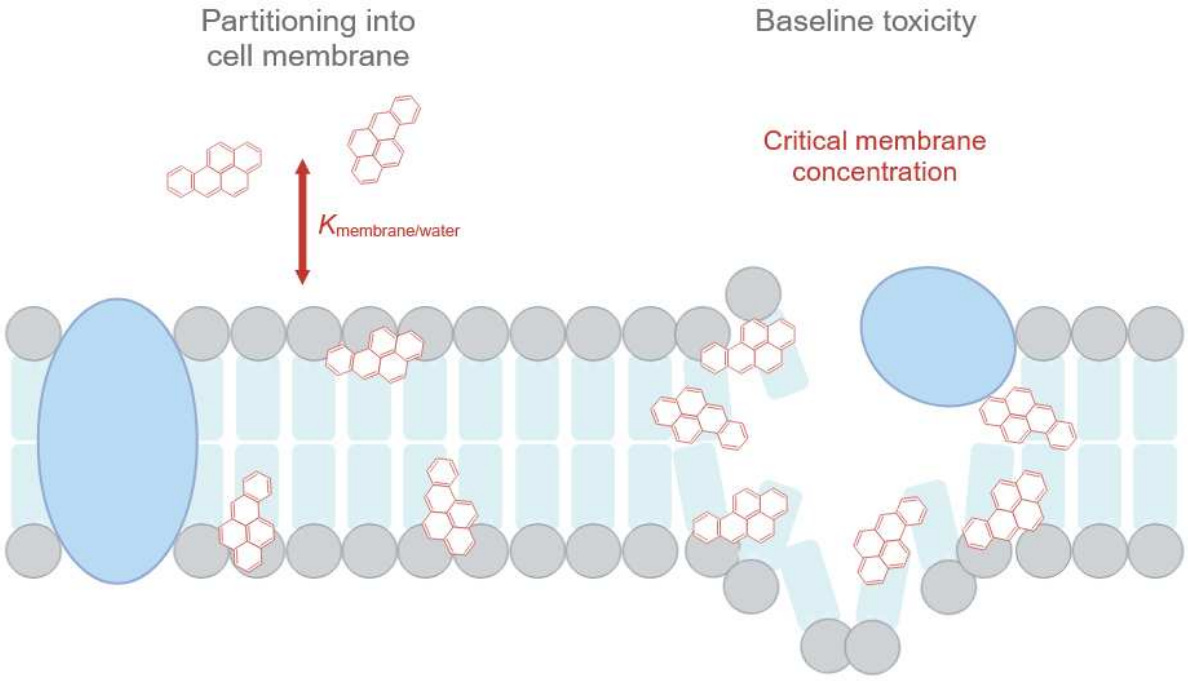

Figure 3: Mechanism of baseline toxicity caused by xenobiotic chemicals. $K_{membrane/water}$ is the partitioning constant of the chemical between the cell membrane and the water.

1.4 Chemical exposure in *in vitro* bioassays

A chemical undergoes the toxicokinetic and toxicodynamic phases between exposure to a chemical and the occurrence of a biological effect (Figure 4). The toxicokinetic phase, determines the concentration of a chemical that reaches the cellular target site. The toxicodynamic phase involves all cellular toxicity pathways that lead from a molecular interaction to an observable effect (Wang and Tan 2019).

In vitro reporter gene bioassays can be used to identify the toxicodynamic processes of a chemical, as they delve into the mechanisms and effects of the chemical at the cellular and molecular levels (Andersen and Krewski 2009). They can identify MIEs like receptor binding, modulation of protein or lipid structures or DNA, and thus indicate cellular toxicity pathways. MOAs and AOPs of chemicals can be unraveled using *in vitro* bioassay effect data by linking cellular toxicity mechanisms to organ-level responses or whole organism effects (Escher and Hermens 2002). Toxicokinetic processes define the behavior of a chemical in the body and comprise absorption, distribution, metabolism, and excretion (ADME). Toxicokinetics are dependent on the physicochemical properties of the chemical and the metabolic capacity of the cells and determine how much of a substance reaches the target site and its potential for accumulation (Dixit et al. 2003).

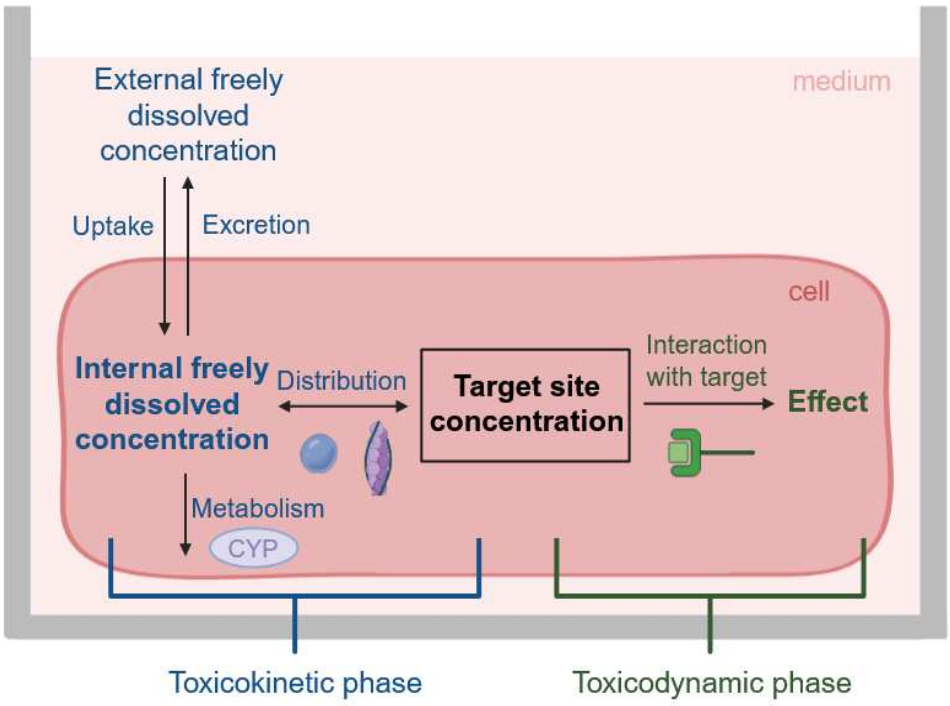

Figure 4: Toxicokinetic and toxicodynamic processes in *in vitro* bioassays. The Figure was adapted from Escher B, Neale P, Leusch F. 2021. Bioanalytical Tools in Water Quality Assessment. IWA Publishing.

In vitro tests offer advantages over *in vivo* tests for the determination of toxicodynamic processes, but one downside is that they can only partially represent toxicokinetic processes and *in vivo* tests are still necessary to investigate the toxicokinetic behavior and ADME processes of chemicals. Toxicokinetics are essential to translating external chemical exposure concentrations (e.g. from inhalation) into concentrations at the target site (e.g. in the cells of the respiratory epithelium). Quantitative *in vitro* to *in vivo* extrapolation (QIVIVE) compares *in vitro* effect concentrations from cell-based tests with measured or modeled plasma concentrations to assess the chemical risk for exposed people (Wilk-Zasadna et al. 2015; Yoon et al. 2015).

The exposure concentration of the chemical in the *in vitro* bioassay should be taken into account to provide reliable input parameters for QIVIVE. The chemical is subject to various toxicokinetic processes in the *in vitro* system that determine its concentration at the target site. This information is lost if nominal *in vitro* effect concentrations are used, because these are based on the initial chemical concentration added to the test system and can therefore cause an inaccurate assessment of the chemical risk. Various reversible distribution processes, as well as irreversible transformation processes of the chemical, can result in incorrect *in vitro* data, reducing the reliability and trust in *in vitro* bioassays. To circumvent these problems, a careful assessment of chemical exposure in *in vitro* bioassays is necessary (Heringa et al. 2003; Yoon et al. 2012).

1.4.1 Chemical partitioning and loss processes *in vitro* bioassays

Within the *in vitro* bioassay well, test chemicals can be distributed between different compartments. The largest compartment is the bioassay medium, but the cells, the air above the medium and the well plate can also play a role (Figure 5).

The composition of the bioassay medium depends on the assay and cell type and should provide optimal cell nutrition. The major component of the medium is water, which is supplemented with nutrients, salts, hormones and growth factors (Davis 2002). An important component of most cell culture media is fetal bovine serum (FBS), which is a multicomponent mixture of important growth factors, hormones, vitamins, trace elements and other proteins that are necessary for good cell growth and proliferation (Brunner et al. 2010). Since a main component of FBS is bovine serum albumin (BSA), cell culture media that are supplemented with different percentages (usually between 2% (v/v) and 20% (v/v)) of FBS have different protein contents. Some chemicals, such as hydrophobic chemicals or acids, show a high affinity for serum albumin and have low freely dissolved concentrations (C_{free}) compared to nominal

concentrations (C_{nom}) in FBS-rich media. Therefore, the actual bioavailable concentration is reduced by chemical partitioning to components of the bioassay medium (Henneberger et al. 2019a; Henneberger et al. 2020). On the one hand, the binding of the test chemicals to the medium proteins causes a discrepancy between *in vitro* and *in vivo* conditions and makes it difficult to compare the effects of bioassays with different media. On the other hand, the sorption, especially of hydrophobic chemicals, to the components of the medium can also be utilized. Fischer et al. (2019) established the term "serum-mediated passive dosing" (SMPD), using the high protein content of FBS in the bioassay medium as a reservoir for chemicals, similar to conventional passive samplers (e.g. PDMS). Since binding to FBS is an equilibrium process, SMPD can stabilize the concentration of chemicals in the bioassay and increase chemical solubility in the bioassay medium. The binding behavior of albumin and xenobiotic chemicals has been intensely investigated in recent years and three main high-affinity binding sites have been identified (Peters 1995; Zsila 2013) that can interact with organic acids and hydrophobic chemicals. However, these binding sites can also be saturated, which leads to a lower binding affinity at high chemical concentrations. Especially organic acids often show a concentration-dependent, non-linear binding to albumin (Henneberger et al. 2019a). BSA-water distribution ratios ($D_{BSA/w}$) can be determined using ultracentrifugation, ultrafiltration, equilibrium dialysis and solid-phase microextraction (SPME) (Buscher et al. 2014). Although equilibrium dialysis is the conventional and most widely used method, the relevance of SPME for the measurement of distribution ratios and freely dissolved concentrations of chemicals has increased in recent years (Peltenburg et al. 2015). If experimental $D_{BSA/w}$ are not available, they can also be predicted using LSER (Ulrich et al. 2017) or QSAR models (Endo and Goss 2011; Qin et al. 2024). In addition to albumin and other proteins, FBS also contains lipids in the form of different lipoproteins. However, these only make up a very small percentage of the medium and are therefore less relevant for the distribution of chemicals. However, hydrophobic chemicals can also bind to lipids in the medium, reducing C_{free}. This can be described by the liposome-water distribution ratio ($D_{lip/w}$), which can either be determined experimentally (Escher et al. 2002) or modeled (Endo et al. 2011; Ulrich et al. 2017).

Microtiter plates are commonly made of polystyrene (PS), which is an important sorption phase for neutral, hydrophobic chemicals that can bind to plastic via adsorption as well as absorption (Fischer et al. 2018b; Kramer 2010). Even if distribution to PS is relatively slow, this can be important, especially for bioassays using media with low FBS content in high-tier well plates. Chemical distribution into the well plate can be up to 99% of the total chemical amount within 96 h for chemicals with logarithmic octanol-water partitioning constants (log

K_{ow}) > 5 (Fischer et al. 2018b). Higher levels of FBS in the medium can prevent this distribution process since the FBS represents an additional sorption phase and thus stabilizes the exposure concentration in the bioassay (Fischer et al. 2018b; Fischer et al. 2019).

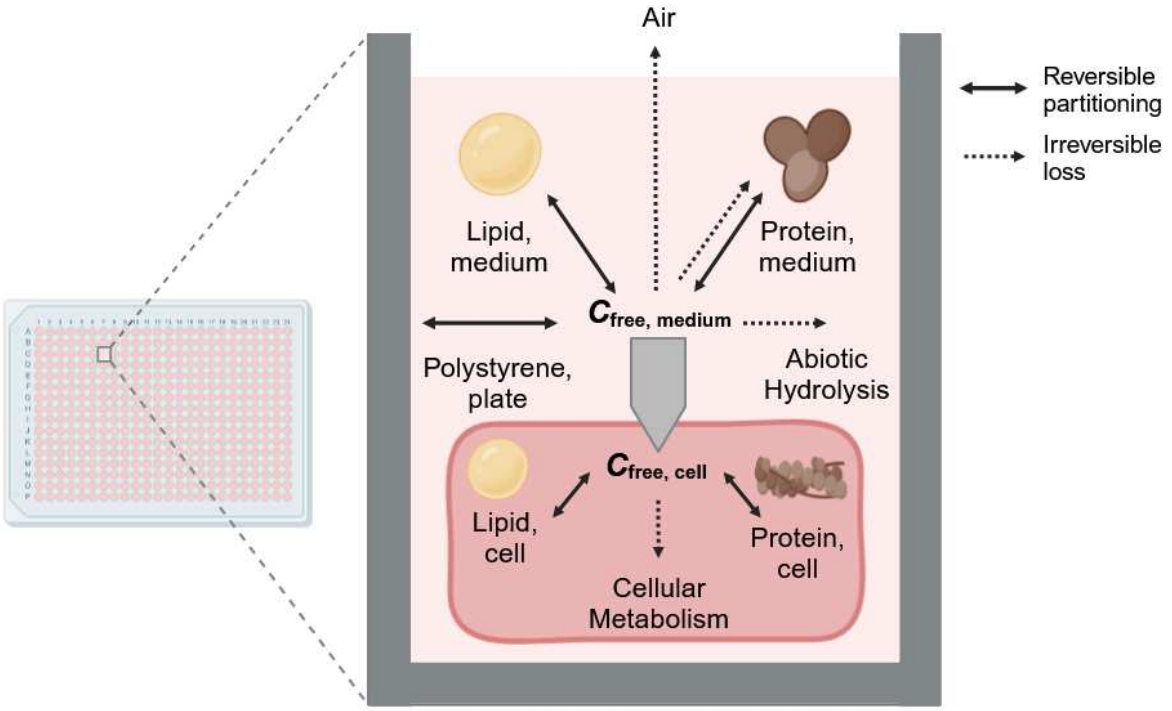

Figure 5: Distribution and loss processes of test chemicals in *in vitro* bioassays. C_{free} is the freely dissolved concentration in the bioassay medium or the cell.

While chemical partitioning to medium components or well plate plastic is a reversible process, there are also irreversible loss processes that can deplete the chemical from the bioassay medium. Volatile chemicals can evaporate from the bioassay medium into the headspace of the well and since the well plate cannot be sealed airtight for the necessary gas exchange, the chemicals can evaporate from the plate and thus disappear from the bioassay system (Riedl and Altenburger 2007). High-throughput bioassays in multi-well plate format are therefore not applicable for volatile chemicals and special exposure-controlled systems need to be applied (Kramer et al. 2010). Dosing of semi-volatile chemicals can lead to cross-contamination of neighboring wells, affecting bioassay responses. The protein content of the medium can influence the volatility of the test chemicals since only the free fraction of the chemical can evaporate from the medium. Therefore, Escher et al. proposed a volatility cut-off for *in vitro* bioassays based on the medium-air partitioning constant ($K_{medium/air}$) of the chemical,

saying that chemicals with $K_{medium/air} \leq 10{,}000$ L/L cannot be tested in standard HTS bioassays because of possible loss to the air (Escher et al. 2019).

The target site of the chemical in the bioassay is the cell, which is why the concentration in the cell (C_{cell}) is the most accurate concentration metric for the description of toxicity (Groothuis et al. 2015). Due to the small volume of cells compared to the other compartments of the bioassay, it is difficult to determine C_{cell} experimentally and only possible using very large cell quantities in cell culture flasks or via fluorescence microscopy with fluorescent test chemicals (Fischer et al. 2018a). It can be assumed that chemicals usually enter the cell via passive diffusion, although active transport may play a role for some chemicals. In the cell, chemicals undergo the same partitioning processes as in the bioassay medium, since cells also contain water, proteins and lipids as partitioning phases. However, the types of proteins and lipids in the cell can differ from those in the medium, which can lead to differences in distribution. Unlike the bioassay medium, cellular proteins are not mainly albumin, so especially for chemicals with specific binding to albumin (e.g. organic acids), $D_{BSA/w}$ should not be used to describe the distribution to cellular proteins. Instead, partitioning constants or distribution ratios to structural proteins should be used, as these better represent the non-specific binding to cellular proteins (Henneberger et al. 2016; Henneberger et al. 2020). QSAR models for the prediction of structural protein-water partitioning constants ($K_{SP/w}$) for neutral or cationic chemicals (Endo et al. 2012) as well as structural protein-water distribution ratios for anionic PFAS ($D_{SP/w}$) (Qin et al. 2024) have been developed.

Chemical partitioning into cell membranes can be described using $D_{lip/w}$, as liposomes are phospholipid bilayer vesicles that are very similar to the cell membrane structure. Cells also contain storage lipids, which are less polar and mostly consist of triglycerides and sterol esters (Walther and Farese 2012). For the prediction of the distribution to storage lipids, $D_{lip/w}$ is less suitable, especially for ionizable chemicals. Partitioning constants to other lipids or oils like triolein, octanol or olive oil can be used instead to better predict this distribution (Geisler et al. 2012; Quinn et al. 2014).

Simple mass-balance models (MBMs) have been developed to estimate the external freely dissolved concentration (C_{free}), the cellular concentration (C_{cell}) or the concentration in the cell membrane ($C_{membrane}$) from C_{nom} and partitioning constants of the chemicals between water and the lipid or protein phase of the medium ($K_{lip/w}$ or $K_{prot/w}$) or the cells ($K_{cell/w}$) (Armitage et al. 2021; Armitage et al. 2014; Fischer et al. 2017). By using distribution ratios ($D_{lip/w}$, $D_{prot/w}$, $D_{cell/w}$) instead of partitioning constants, which include chemical speciation, the

models can also be applied to ionizable chemicals. While C_{free} predicted with MBMs showed good agreement with measured C_{free} for neutral chemicals and bases, most of the models did not show good agreement with experimentally determined C_{free} for organic acids, as they do not consider the non-linear binding to proteins (Henneberger et al. 2020; Huchthausen et al. 2020). C_{free} must therefore either be determined experimentally or more complex models must be developed for this group of chemicals (Qin et al. 2023). A calculation of the chemical distribution using mass-balance models only works if the chemical concentration remains stable over time. Abiotic transformation processes like hydrolysis, oxidation or covalent reactions with proteins are an irreversible source of chemical loss in the bioassay medium and metabolic degradation reactions can take place in the cells. These processes must therefore be excluded in advance to allow reliable prediction of C_{free}.

1.4.2 Experimental exposure assessment

Quantitative *in vitro*-to-*in vivo* extrapolation (QIVIVE) is a method utilized to translate effect concentrations from *in vitro* bioassays into human exposure concentrations that can cause the same effects in the human target organ or tissue (Yoon et al. 2012). The nominal concentration (C_{nom}), i.e., the dosed concentration, is mostly used as an input parameter for QIVIVE models as it is easily available. A thorough investigation of these processes is necessary to gain a better understanding of the chemical exposure in the bioassay and to provide reliable data for QIVIVE since *in vitro* bioassays are subject to different partitioning and loss processes of chemicals (Gülden and Seibert 2003). The freely dissolved concentration (C_{free}), the total cellular concentration (C_{cell}) or the concentration in the cell membrane ($C_{membrane}$) were considered to be better dose metrics, as they better reflect the effective concentration at the target side of the chemical (Groothuis et al. 2015). C_{free} has been proven to be a suitable metric for assessing exposure in *in vitro* bioassays, as it can be determined experimentally, whereas the experimental determination of C_{cell} or $C_{membrane}$ is very laborious.

Henneberger et al. (2019a) developed a solid-phase microextraction (SPME) method for the measurement of distribution ratios of chemicals to biological materials, like proteins and lipids, and applied the method successfully to measure C_{free} of chemicals in *in vitro* bioassays (Henneberger et al. 2019b; Huchthausen et al. 2020). SPME has been developed by Arthur and Pawliszyn as a simple sample extraction technique using polyimide-coated single SPME fibers (Arthur and Pawliszyn 1990). Sample extraction is based on the equilibrium partitioning of chemicals between the sample and the coating material (Pawliszyn 2012). Through the development of versatile, biocompatible coating materials like C18 or polydimethylsiloxane

(PDMS) (Musteata et al. 2007), SPME has become a universal tool for the determination of distribution ratios of chemicals to biological materials or the measurement of C_{free}. SPME can be applied for *in vitro* bioassays as it can remove biological materials that would disturb the instrumental analysis, requires only small sample volumes down to 30 µL and has relatively short equilibration times (Huchthausen et al. 2023; Peltenburg et al. 2015; Vaes et al. 1996). The commercial release of a BioSPME 96-Pin Device (Roy et al. 2021) allowed an increase in sample throughput and automation of the SPME procedure in this thesis.

1.4.3 Abiotic transformation

All chemicals have a lifetime and are able to change their chemical structure as a result of external influences, meaning that so-called parent chemicals are converted into transformation products with altered chemical properties. Chemical transformation can therefore also be relevant in the context of *in vitro* bioassays, as the concentration of a test substance can decrease over time and the concentration of transformation products can increase (Figure 6). Chemical transformation processes can occur abiotically or biotically and are subject to the principles of reaction kinetics and thermodynamics.

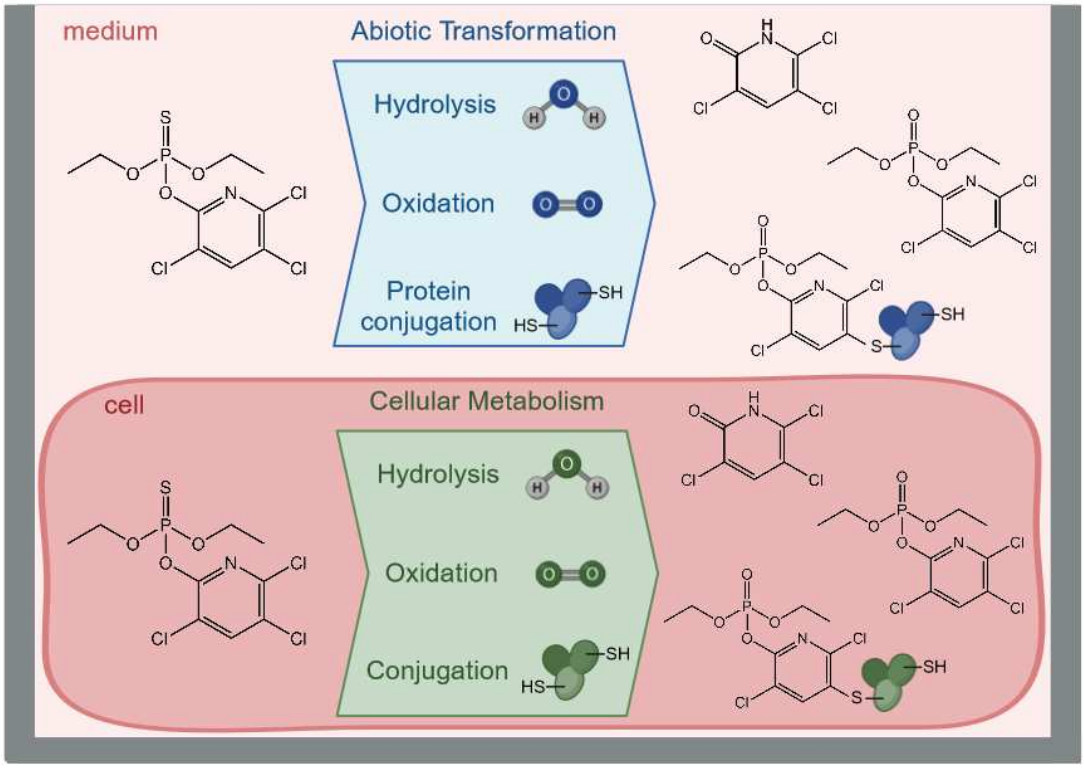

Figure 6: Abiotic transformation processes and cellular metabolism in *in vitro* bioassays.

While persistent chemicals can remain in the environment for multiple decades, half-lives of unstable chemicals in the range of a few hours to minutes are not uncommon (Mansouri

et al. 2017; Queen 1967). In order to evaluate the relevance of transformation processes for the conditions and time scales of *in vitro* bioassays, it is important to determine which reaction processes play a role, which transformation products are formed and what the kinetics of the transformation reactions are in order to determine the degradation rate of the test substance. The reaction rate is the speed at which reactants are degraded and products are formed. These reactions are defined by rate laws, which describe the relationship between the rate of a chemical reaction and the concentrations of its reactants. In first-order reactions, the rate is directly proportional to the concentration of a single reactant A, with k being the first-order rate constant (Eq. 1) (Schwarzenbach et al. 2002).

$$\frac{d[\mathrm{A}]}{d\mathrm{t}} = -k \times [\mathrm{A}] \quad (1)$$

If the concentration of two reactants A and B determines the reaction rate, it is a second-order reaction, with k' being the second-order rate constant (Eq. 2) (Schwarzenbach et al. 2002).

$$\frac{d[\mathrm{A}]}{d\mathrm{t}} = -k' \times [\mathrm{A}] \times [\mathrm{B}] \quad (2)$$

In reactions of two chemicals where one reactant (e.g. reactant B) is present in excess, the rate law can be simplified by setting $k = k'[\mathrm{B}]_0$ since the concentration of B stays apparently constant over time. The rate law that appears first-order with respect to the limiting reactant is therefore called pseudo-first-order kinetics and k is called the pseudo-first-order rate constant (Schwarzenbach et al. 2002).

The main component of bioassay media is water, which is why hydrolysis is an important transformation process for *in vitro* bioassays. Hydrolytic reactions are usually substitution reactions that replace an atom or functional group of a molecule with water. Hydrolysis usually occurs via nucleophilic substitution (S_N1 or S_N2) or via addition-elimination mechanisms, depending on the type of the leaving group (Bouyacoub et al. 1996; Hegarty and Frost 1973). Since water is present in excess in the bioassay medium, hydrolysis reactions are usually pseudo-first-order reactions. These can be catalyzed by both acids (protons, H^+) and bases (hydroxide ions, OH^-). Since water always consists of the three components that are in equilibrium ($H_2O \rightleftarrows H^+ + OH^-$), the overall hydrolysis kinetics can be described with three individual reactions.

$$k = k_{H^+} \times [H^+] + k_{H_2O} + k_{OH^-} \times [OH^-] \quad (3)$$

In hydrolysis reactions, water or hydroxide ions (base-catalyzed hydrolysis) act as nucleophiles. As defined by Lewis, a nucleophile (Lewis base) is a substance that can donate an electron pair, while an electrophile (Lewis acid) can accept an electron pair (Lewis 1923). Pearson extended this classification by introducing the concept of hard and soft acids and bases (HSAB principle). The hardness of an electrophile or nucleophile can therefore be related to its polarizability. Hard electrophiles and nucleophiles are relatively small and difficult to polarize, while soft electrophiles and nucleophiles are relatively large and easy to polarize (Pearson 1990). According to the HSAB principle, molecules with the same polarizability, i.e., hard electrophiles with hard nucleophiles and soft electrophiles with soft nucleophiles, react preferentially with each other (Lopachin et al. 2012).

With the addition of serum proteins to the bioassay medium, additional reaction partners for test chemicals in addition to water and hydroxide ions are added. While water and hydroxide ions are rather hard nucleophiles, soft electrophiles react primarily with easily polarizable thiol groups of cysteines. For this reason, especially soft electrophiles such as type-2 alkenes, form covalent bonds with medium proteins (LoPachin and Gavin 2012).

Autoxidation is the spontaneous reaction of a chemical with molecular oxygen in the absence of light (Richardson 1932). Photooxidation is triggered by ultraviolet (UV) or visible light, which accelerates the oxidation reactions (Altshuller et al. 1962). In both processes, reactive oxygen species are formed, which can lead to chemical transformations. Autoxidation takes place very slowly for most chemicals without catalysts. Photooxidation is particularly relevant for the transformation of chemicals in the environment but likely to play a minor role in *in vitro* systems without exposure to light.

1.4.4 Metabolism

Similar to the bioassay medium, abiotic transformation processes like hydrolysis or covalent reactions with proteins can also occur after the chemical has entered the cell. However, enzymatically catalyzed metabolic transformation processes are of greater importance inside the cell (Caldwell et al. 1995) (Figure 6). The so-called biotransformation of xenobiotic chemicals is a highly regulated process that involves several different enzymes and serves the detoxification and elimination of foreign substances from the cell or the body (Caldwell et al. 1995). Liver cells are the primary location of biotransformation in the body, but other organs such as the kidneys and intestine also play a role. Xenobiotic metabolism is regulated by multiple complex signaling pathways, which mostly use nuclear receptors such as the aryl

hydrocarbon receptor (AhR) and the pregnane X receptor (PXR) as sensors for xenobiotic stress and regulate the expression of important metabolizing enzymes (Zanger and Schwab 2013).

The process of biotransformation consists of three phases (phase I, II and III). Phase I involves oxidative reactions mostly catalyzed by cytochrome P450 monooxygenases (CYP), increasing the chemical polarity and reactivity. Phase II is a detoxification phase involving conjugation reactions of hydrophilic chemicals or phase I products with polar molecules to increase the polarity for excretion (Williams 1959). Phase III involves the excretion of polar conjugates from phase II by active transport (Kim 2002).

Phase I metabolism is especially relevant for hydrophobic chemicals, which are difficult to remove from the cell or body. CYP enzymes represent a superfamily of highly conserved, heme-containing proteins that occur in almost all species and play a central role in phase I biotransformation. The group of CYP450 enzymes comprises numerous isoforms, enabling them to catalyze the oxidation of a variety of structurally diverse substrates (Esteves et al. 2021). The active site of CYP450 enzymes contains a heme-iron center, which enables the activation of molecular oxygen. Nicotinamide adenine dinucleotide phosphate (NADPH) or nicotinamide adenine dinucleotide (NADH) usually serve as reduction equivalents for this redox reaction (Denisov et al. 2005). Other phase I enzymes are flavin-containing monooxygenases (FMO), dehydrogenases, amide oxidases and epoxide hydrolases. All of these enzymes catalyze reactions such as dealkylation, epoxidation, hydroxylation and oxidation, which increase the hydrophilicity, polarity and reactivity of the substrates, making them suitable substrates for phase II enzymes (Croom 2012). Due to their high reactivity, phase I transformation products often have a higher toxicity than the parent substances, which can lead to undesirable adverse effects on cellular metabolism (Coecke et al. 2006).

Phase II metabolism is characterized by the conjugation of hydrophilic, reactive xenobiotics or transformation products from phase I with polar molecules such as glutathione, sulfate, glucuronic acid or N-acetylcysteine. In this phase, hydrophilic chemicals and reactive intermediates are detoxified and prepared to be eliminated from the cell. Phase II enzymes are transferases such as glutathione S-transferases, glucuronosyltransferases or sulfotransferases (Croom 2012; LeBlanc 2008).

Metabolic transformation is highly relevant for *in vitro* bioassays as it can lead to chemical loss and detoxification on the one hand and to the bioactivation of the test chemical and the generation of toxic transformation products on the other.

1.5 Aims of this thesis

The aim of this thesis was to improve bioassay screening of single chemicals with regard to exposure, chemical transformation and baseline toxicity to increase the quality and reliability of *in vitro* effect data used for human risk assessment.

For the evaluation of *in vitro* effect concentrations, baseline toxicity is often used to distinguish specifically acting chemicals from baseline toxicants, but existing baseline toxicity QSARs were not validated for their applicability for very hydrophilic chemicals ($\log D_{lip/w} < 0$) or anionic chemicals (Lee et al. 2021). One aim of *Publication III* was to define the critical membrane burden for cell-based *in vitro* bioassays on the basis of neutral, hydrophilic chemicals and measured freely dissolved concentrations of ionizable chemicals and to develop a nominal baseline toxicity QSAR using a mass balance model (Fischer et al. 2017). This QSAR enables the prediction of baseline toxicity for neutral as well as charged and hydrophilic as well as hydrophobic chemicals. The use of freely dissolved effect concentrations allowed a direct derivation of the critical membrane burden with only $D_{lip/w}$ as an input parameter and chemical partitioning processes were taken into account. The predicted baseline toxicity was compared with measured cytotoxicity from high-throughput screening of 94 chemicals in three bioassays. Specifically acting chemicals were identified by comparison with baseline toxicity. In addition, special attention was paid to chemicals showing lower effects than baseline toxicity, as this artifact may indicate loss of the chemical due to problems or errors in experimental performance, such as precipitation of the test chemicals, or degradation of the chemical in the bioassay.

In the next part of the thesis, potential transformation processes in the bioassay were investigated that could have led to such underestimation of toxicity. The aim of *Publication I* was to develop a framework for the experimental determination of abiotic transformation processes, including hydrolysis, oxidation, photodegradation and irreversible reactions with proteins in the assay medium. A selection of 22 presumably unstable chemicals was used to develop an experimental workflow for abiotic stability testing to identify chemical transformation processes and determine degradation rates. The method used in this workflow was solid-phase microextraction (SPME) with a Supel^{TM} BioSPME 96-Pin Device and chemical concentrations were quantified using liquid chromatography and mass spectrometry (LC-MS). The obtained experimental data were compared with predictions from *in silico* models developed for environmental degradation processes to examine the applicability of these models under bioassay conditions.

The developed workflow was applied to a set of reactive acrylamides and non-reactive methacrylamides in *Publication II* to measure their reactivity toward the two biological nucleophiles glutathione and 2-deoxyguanosine, representing reactivity against proteins and DNA in the cell. Soft electrophiles like acrylamides react preferably with soft nucleophiles like thiol groups of glutathione (Lopachin et al. 2012), which should be confirmed with this work. In order to achieve a higher throughput and minimize experimental variations, the workflow was partially automated as part of *Publication II.* Measured degradation rates of different acrylamides were compared with bioassay effects (cytotoxicity and oxidative stress response activation) in three cell lines to examine the relationship between abiotic reactivity and the toxicity of chemicals. Quantum chemical calculations were used to scrutinize this relationship.

The last part of the thesis aimed to investigate the relevance of cellular metabolism in *in vitro* bioassays. In *Publication III*, the metabolic activity of three different cell lines was characterized with and without the use of chemical inducers. Measured *in vitro* effect concentrations (cytotoxicity and oxidative stress response activation) from cell lines with different metabolic activities were compared to investigate the impact of cytochrome P450 enzyme (CYP) activity on bioassay results.

The overarching goal of this thesis was to demonstrate the relevance of baseline toxicity, chemical exposure and transformation for *in vitro* bioassays and how this knowledge can be utilized to improve bioassay planning, execution and data evaluation. Special attention was paid to the abiotic and metabolic stability of test chemicals in *in vitro* systems to increase the understanding of abiotic and biotic transformation processes, to provide methods to determine the stability of chemicals in the assay system and to evaluate the influence of chemical transformation on bioassay results.

2. High-throughput screening of single chemicals

2.1 Cell-based reporter gene bioassays

High-throughput bioassays have emerged as powerful tools in the field of chemical risk assessment in recent years, revolutionizing the way we evaluate the potential hazards and risks associated with exposure to various chemicals (Judson et al. 2010). The rise of technological advancements in our society is resulting in a growing release of chemicals into the environment, presenting potential risks to both humans and animals. For this reason, there is a growing need for efficient experimental and predictive methods to assess the safety of these compounds (Basketter et al., 2012; NRC, 2007). Cell-based high-throughput reporter gene bioassays enable the testing of a large number of chemicals in a short time, which has become an important component of toxicity screening, mode of action elucidation and hazard identification (Adeleye et al. 2015). The use of cell-based bioassays is not only more time- and cost-effective but also reduces the ethical concerns associated with animal testing (Tice et al. 2013). This change is in line with the 3Rs principle for animal testing, which emphasizes the need to minimize the use of animals in research (Burden et al. 2015). *In vitro* bioassays also provide valuable information on a variety of endpoints, such as the activation of cellular stress response pathways or endocrine disruption, which may indicate adverse effects in humans (NRC 2007). *In vitro* bioassays thus represent a promising alternative to the traditional risk assessment of chemicals, which relied on time-consuming and resource-intensive animal testing.

The use of multi-well plates (96 to 1536-well) and robotic liquid handling platforms allows for high sample throughput, automation and standardization of *in vitro* bioassay workflows. The bioassay workflow applied in *Publication II* and *Publication III* is shown in Figure 7. Bioassays were performed over three consecutive days, with cell seeding on day one, chemical dosing on day two and detection of cytotoxicity and reporter gene activation on day three. Detailed protocols for the *in vitro* bioassays used can be found in *Publication II* and *Publication III* and in the literature (Escher et al. 2012; König et al. 2017; Neale et al. 2017). Briefly, cell suspensions in the corresponding bioassay media were prepared and cells were dispensed into 384-well plates using a MultiFlow dispenser. The number of cells was adapted so that at the end of the bioassay (after 48 h), a confluence of approximately 80% was achieved in the unexposed wells. Cells were incubated at 37 °C and 5% CO_2 for 24 h to allow the cells to settle and attach to the plates. Chemical solutions in bioassay medium were prepared by directly dissolving the pure chemicals in medium or by pipetting an aliquot of a solvent stock solution (e.g., methanol or DMSO) into an aliquot of medium. Chemical solutions were diluted

serially with bioassay medium using a Hamilton Microlab Star robotic system and transferred to the cell plates. Cell confluency was determined utilizing an IncuCyte S3 Live-Cell Analysis System directly after and 24 hours after chemical dosing as a measure of cytotoxicity. After the confluency measurement, reporter gene activation was quantified using a multimode plate reader (Tecan), measuring either luminescence or fluorescence depending on the reporter enzyme used (Escher et al. 2012; König et al. 2017; Neale et al. 2017).

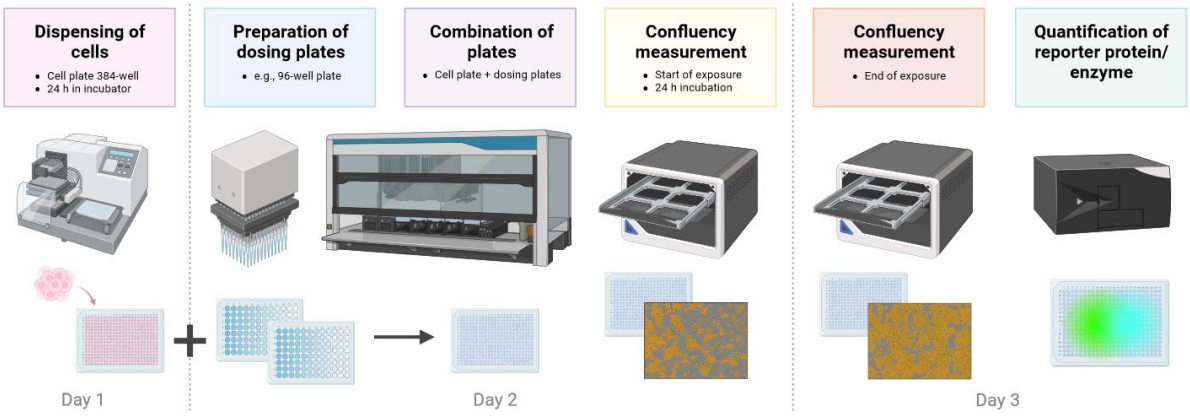

Figure 7: Workflow for high-throughput reporter gene bioassays. The Figure was created by Luise Henneberger.

The assays used in *Publication II* and *Publication III* were AREc32, ARE-*bla* and GR-*bla*. AREc32 and ARE-*bla* carry multiple copies of the antioxidant response element (ARE) and detect the oxidative stress response of chemicals via activation of the Nuclear Factor Erythroid 2 related Factor 2/Kelch-like ECH-associated protein 1 (Nrf-2/Keap-1) pathway (Figure 2A) (Shukla et al. 2012; Wang et al. 2006). GR-*bla* detects glucocorticoid receptor (GR) activation (Figure 2B) (Wilkinson et al. 2008).

Measured effects were plotted against tested concentrations to derive concentration-response curves (CRC) for the test chemicals. Full CRCs are normally log-concentration-response plots with a sigmoidal form, but on a linear concentration scale, CRCs have been shown to be linear up to 30% effect (Escher et al. 2018). The IC_{10} is the concentration at which cell viability is reduced by 10% and was calculated from the slope of the regression of the linear range of the concentration-response curve (Eq. 4).

$$IC_{10} = \frac{10\%}{\text{slope}} \qquad (4)$$

Cytotoxicity can cause artifacts in reporter gene bioassays, e.g., it can mask reporter gene activation. In addition, the so-called “cytotoxicity burst,” which means an unspecific

activation of various metabolic pathways shortly before cell death, can lead to an apparent activation of reporter gene activity (Judson et al. 2016). For this reason, only concentrations that are below cytotoxicity were considered for the evaluation of reporter gene activation. The IC_{10} served as a threshold for cytotoxicity and only concentrations below the IC_{10} were considered for the CRCs of reporter gene activation.

Analogous to the calculation of cytotoxicity, the activation of GR was also calculated from the slope of the linear part of the CRC. Dexamethasone was the reference chemical in the GR-*bla* assay and was also dosed on all bioassay plates to determine the maximum effect. The responses of the test chemicals were calculated relative to the maximum effect of the reference compound. The concentration where 10% of the maximum effect was reached (EC_{10}) was reported as a measure of GR activation and calculated with Eq. 5.

$$EC_{10} = \frac{10\%}{\text{slope}} \tag{5}$$

No maximum effect could be determined for AREc32 and ARE-*bla*, as there is no maximum for the oxidative stress response activation. Therefore, the induction ratio (IR) was used as a measure of reporter gene activation instead of the percentage of maximum effect. As a measure of the amount of luciferase, the relative light units (RLU) were measured and the IR was calculated by dividing the RLU of the sample by the RLU of the control (Eq. 6). The CRCs for oxidative stress response are mostly linear up to an IR of 5, so only values below an IR of 5 and below IC_{10} were used for the CRCs.

$$IR = \frac{\text{RLU (sample)}}{\frac{\sum_{i=1}^{n} \text{RLU (control)}}{n}} \tag{6}$$

CRCs for the oxidative stress response were obtained by plotting IR against the concentration. The concentration that led to an IR of 1.5 ($EC_{IR1.5}$) was used as a threshold for activity as it is three times the standard deviation of the effect of the unexposed cells (Eq. 7) (Escher et al. 2012).

$$EC_{IR1.5} = \frac{0.5}{\text{slope}} \tag{7}$$

The specificity ratio (SR) is the ratio between cytotoxicity (IC_{10}) and reporter gene activation (EC_{10} or $EC_{IR1.5}$) and can be calculated using either measured cytotoxicity ($SR_{cytotoxicity}$) or baseline toxicity ($SR_{baseline}$) (Eq. 8). A SR $\geq$ 10 means that the measured effect is specific and a SR < 10 represents unspecific effects that are connected to cytotoxicity (Escher et al. 2020).

$$\text{specificity ratio } \left(SR_{cytotoxicity} \text{ or } SR_{baseline}\right) = \frac{IC_{10,experimental} \text{ or } IC_{10,baseline}}{EC_{IR1.5} \text{ or } EC_{10}} \quad (8)$$

2.1.1 Challenges of single chemical screening

High-throughput *in vitro* reporter gene bioassays have many advantages over animal testing. They are more cost-effective, ethically acceptable, can be automated and have a higher sample throughput. They therefore allow the generation of a large amount of toxicity data, which, in combination with suitable *in silico* models, represents a promising possibility for human risk assessment of chemicals (next generation risk assessment, NGRA) (Dent et al. 2021; Moxon et al. 2020). Despite all of these benefits, there are also obstacles that complicate the routine use of *in vitro* bioassays in the risk assessment of chemicals. If left unaddressed, these can lead to misjudgments and, thus, a loss of confidence in bioassay data.

(1) Partitioning of chemicals to components of the bioassay medium or the plastic material of the well plates can lead to a lower bioavailable concentration but can also stabilize the chemical concentration (Fischer et al. 2018b; Henneberger et al. 2019b; Huchthausen et al. 2020).

(2) Volatile chemicals are not suitable for high-throughput testing as they can dissipate from the bioassay medium and semi-volatile chemicals can spread over the bioassay plate and contaminate neighboring wells (Escher et al. 2019).

(3) Hydrophobic chemicals with low water solubility can precipitate in the bioassay medium, leading to false dosing concentrations (Fischer et al. 2019).

(4) Unstable or reactive chemicals are prone to transformation processes like hydrolysis or covalent reactions with proteins in the bioassay medium (*Publication I*) or chemicals can be taken up and metabolized by the cells (Fischer et al. 2018a; Fischer et al. 2020).

Unnoticed, all these effects can have a negative impact on the quality of the bioassay data and, in the worst case, lead to a misinterpretation of the toxicity of the chemical. In recent years, however, experimental strategies and models have been developed to uncover some of these processes and decipher their impact on the *in vitro* effect data. In the following chapters, irreversible chemical loss processes such as abiotic or biotic transformation will be discussed in detail and experimental methods for determining these processes and their significance for *in vitro* bioassays will be explained. A new model for assessing baseline toxicity, combined with insights into chemical transformation, will help to enhance the accuracy of *in vitro* screening of single chemicals. This will lead to more reliable data for assessing the risk of chemicals.

2.2 Baseline toxicity

Baseline toxicity results from the accumulation of chemicals into cellular membranes, a phenomenon associated with the lethal body burden principle (Mccarty 1986), where the membrane serves as the target site of the chemical. Similarly, a critical membrane burden can be derived that is independent of the chemical's physicochemical properties. The critical membrane burden for 10% cytotoxicity ($IC_{10,membrane}$) for reporter gene cell lines was found to be 69 mmol/L_{Lip} (Escher et al. 2019). However, this value was derived for neutral chemicals from nominal effect concentrations ($IC_{10,nom}$) using a mass balance model. In *Publication III,* a new $IC_{10,membrane}$ was derived from freely dissolved effect concentrations ($IC_{10,free}$), which consider the partitioning of the chemicals to components of the bioassay medium and cells and are therefore directly linked to the $IC_{10,membrane}$ (Eq. 9).

$$IC_{10,membrane} = IC_{10,free} \times D_{lip/w} \quad (9)$$

For hydrophilic chemicals ($K_{lip/w} < 1$), $IC_{10,nom}$ equals $IC_{10,free}$ (Henneberger et al. 2019b), as these chemicals do not show binding to medium components. For more hydrophobic chemicals, a mass-balance model can predict nominal baseline toxicity ($IC_{10,nom,\ baseline}$) from $IC_{10,membrane}$ by dividing the bioassay medium into different partitioning phases (lipid, protein, water) (Eq. 10) (Fischer et al. 2017).

$$IC_{10,nom,baseline} = \frac{IC_{10,membrane}}{D_{lip/w}} \times (1 + D_{BSA/w} \times VF_{protein,medium} + D_{lip/w} \times VF_{lipid,medium}) \quad (10)$$

Partitioning to cells can be neglected as they make up only a small fraction of the total protein and lipid volume of the bioassay (Qin et al. 2024). To calculate the $IC_{10,nom,\ baseline}$, the volumes of lipid and protein in the bioassay medium and the distribution coefficients between the water and these phases were obtained from the literature or predicted with QSAR models (Endo et al. 2011; Gobas et al. 1988; Qin et al. 2024; Ulrich et al. 2017).

Chemicals can be classified based on their MOA. The toxic ratio (TR) is the ratio of the $IC_{10,nom,baseline}$ and the experimental cytotoxicity and serves as an indicator of the specificity of a compound's toxicity (Eq. 11) (Verhaar et al. 1992). A TR between 0.1 and 10 suggests baseline toxicity, while a TR equal to or above 10 indicates a reactive or specific mode of toxic action (Maeder et al. 2004; Verhaar et al. 1992). TR below 0.1 can indicate experimental artifacts or loss of the chemicals since baseline toxicity is the minimal toxicity a chemical can have.

$$\text{toxic ratio (TR)} = \frac{IC_{10,baseline}}{IC_{10,experimental}} \quad (11)$$

Baseline toxicity provides important information for *in vitro* bioassays, as it allows better planning of bioassay dosing and a classification of the measured effects (Escher et al. 2019).

2.2.1 Baseline toxicity QSAR

IC_{10} values of 14 hydrophilic chemicals with log $K_{lip/w}$ between -1.04 and 0.81, measured for AREc32, ARE-*bla* and GR-*bla* in *Publication III* and $IC_{10,free}$ values of 14 ionizable chemicals and caffeine measured for AREc32 (Huchthausen et al. 2020) were used to derive an $IC_{10,membrane}$ of 26 mmol/L_{lip} ± 3.3 mmol/L_{lip} by linear regression of log 1/$IC_{10,free}$ against log $D_{lip/w}$ and a slope fixed to 1 (Figure 8A+B). The newly defined $IC_{10,membrane}$ was a factor 2.65 lower than the previously published $IC_{10,membrane}$ for reporter gene bioassays that was based on nominal concentrations only (Escher et al. 2019). Chemical partitioning to medium proteins and lipids must be considered to derive $IC_{10,nom,baseline}$ from the newly defined $IC_{10,membrane}$. The distribution ratio to bovine serum albumin ($D_{BSA/w}$) can be used as a proxy for the partitioning to medium proteins and the distribution ratio to liposomes ($D_{lip/w}$) as a proxy for the partitioning to medium lipids. $D_{BSA/w}$ can be calculated directly from the $D_{lip/w}$, but the linear relationship for neutral and cationic chemicals is different than that for anionic chemicals, resulting in different QSAR equations for the different substance classes.

By insertion of the newly defined $IC_{10,membrane}$ and the QSAR for the calculation of $D_{BSA/w}$ for neutral chemicals (Endo and Goss 2011) or anions (Qin et al. 2024) in Eq. 10, a QSAR for $IC_{10,nom,baseline}$ can be derived.

$$IC_{10,nom,baseline}\ (\text{neutral}) = \frac{26\ \text{mmol/L}_{lip}}{D_{lip/w}} \times (1 + 10^{0.70 \times \log D_{lip/w} + 0.34} \times VF_{protein,medium} + D_{lip/w} \times VF_{lipid,medium}) \quad (11)$$

$$IC_{10,nom,baseline}\ (\text{anionic}) = \frac{26\ \text{mmol/L}_{lip}}{D_{lip/w}} \times (1 + 10^{0.75 \times \log D_{lip/w} + 1.01} \times VF_{protein,medium} + D_{lip/w} \times VF_{lipid,medium}) \quad (12)$$

AREc32 and ARE-*bla* bioassay media were supplemented with 10% FBS or dialyzed FBS, so for both bioassays, a generic QSAR with measured protein and lipid contents of 3.00×10^{-3} L/L protein and 7.00×10^{-5} L/L lipid was applied. GR-*bla* bioassay medium was supplemented with 2% charcoal-stripped FBS with a protein content of 9.40×10^{-4} L/L and a lipid content of 1.47×10^{-5} L/L (Qin et al. 2024).

All resulting QSAR models for $IC_{10,nom,baseline}$ for neutral and anionic chemicals in AREc32 and ARE-*bla* or GR-*bla* bioassays are shown in Figure 8C.

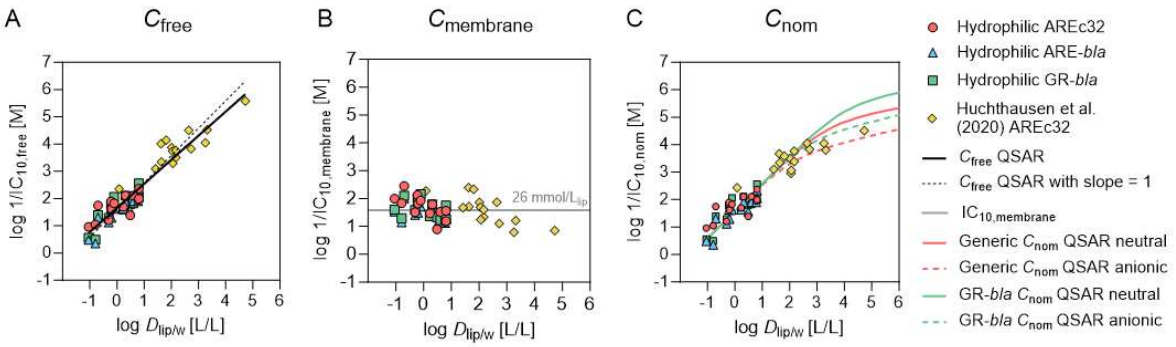

Figure 8: Experimental derivation of nominal baseline toxicity QSARs for neutral and anionic chemicals for AREc32, ARE-*bla* and GR-*bla* cell lines. A: Logarithmic reciprocal $IC_{10,free}$ (log 1/$IC_{10,free}$) of test chemicals plotted against logarithmic liposome-water distribution ratios ($D_{lip/w}$). The black solid line is the linear regression of the data points and the dotted black line is the linear regression with a slope fixed to 1, which was used to derive the critical membrane concentration for baseline toxicity ($IC_{10,membrane}$). B: Logarithmic reciprocal $IC_{10,membrane}$ (log 1/$IC_{10,membrane}$) of test chemicals plotted against $D_{lip/w}$. The solid grey line indicates the constant CMB of 26 mmol/L_{lip} derived from the linear regression from A. C: Logarithmic reciprocal $IC_{10,nom}$ (log 1/IC_{10}) of test chemicals plotted against $D_{lip/w}$ derived with the mass-balance models for neutral and anionic chemicals. The red solid line indicates the generic QSAR for AREc32 and ARE-*bla* for neutral chemicals and the red dotted line indicates the generic anionic QSAR. The green solid line indicates the generic QSAR for GR-*bla* for neutral chemicals and the green dotted line indicates the anionic QSAR for GR-*bla.* The Figure was taken from *Publication III.*

2.2.2 Effects of single chemicals compared to baseline toxicity

The selection of chemicals in *Publication III* was based on various aspects. Chemicals with different biological activity, target site and endpoints, as well as baseline toxicants, were selected to cover different modes of action. In addition, the chemicals should have an environmental relevance or relevance to humans. The chemicals should cover diverse physicochemical properties, although hydrophobic and volatile chemicals were excluded due to their inapplicability in some biological test systems. A complete list and more detailed information on the 94 chemicals selected can be found in *Publication III.* All chemicals were screened for their toxicity in the AREc32, ARE-*bla* and GR-*bla* bioassays in *Publication III*. The $IC_{10,baseline}$ were calculated for all chemicals with experimental or predicted $D_{lip/w}$ and

compared with the experimental IC_{10} of the chemicals from the AREc32, ARE-*bla* and GR-*bla* assays (Figure 9). The newly derived baseline QSAR was found to be superior to previously published models as it was able to predict $IC_{10,baseline}$ also for hydrophilic chemicals with $D_{lip/w} < 0$ and anionic chemicals. The toxic ratio of the chemicals was used to identify chemicals with specific toxicity (TR ≥ 10) and baseline toxicants (10 > TR ≥ 0.1). The number of specifically acting chemicals was between 22 (ARE-*bla*) and 28 (GR-*bla*), which accounts for 23% to 30% of all tested chemicals and azacytidine, a cytostatic pharmaceutical, had the highest TR in all assays. The majority of chemicals (between 44 and 50 chemicals) were classified as baseline toxicants in all assays.

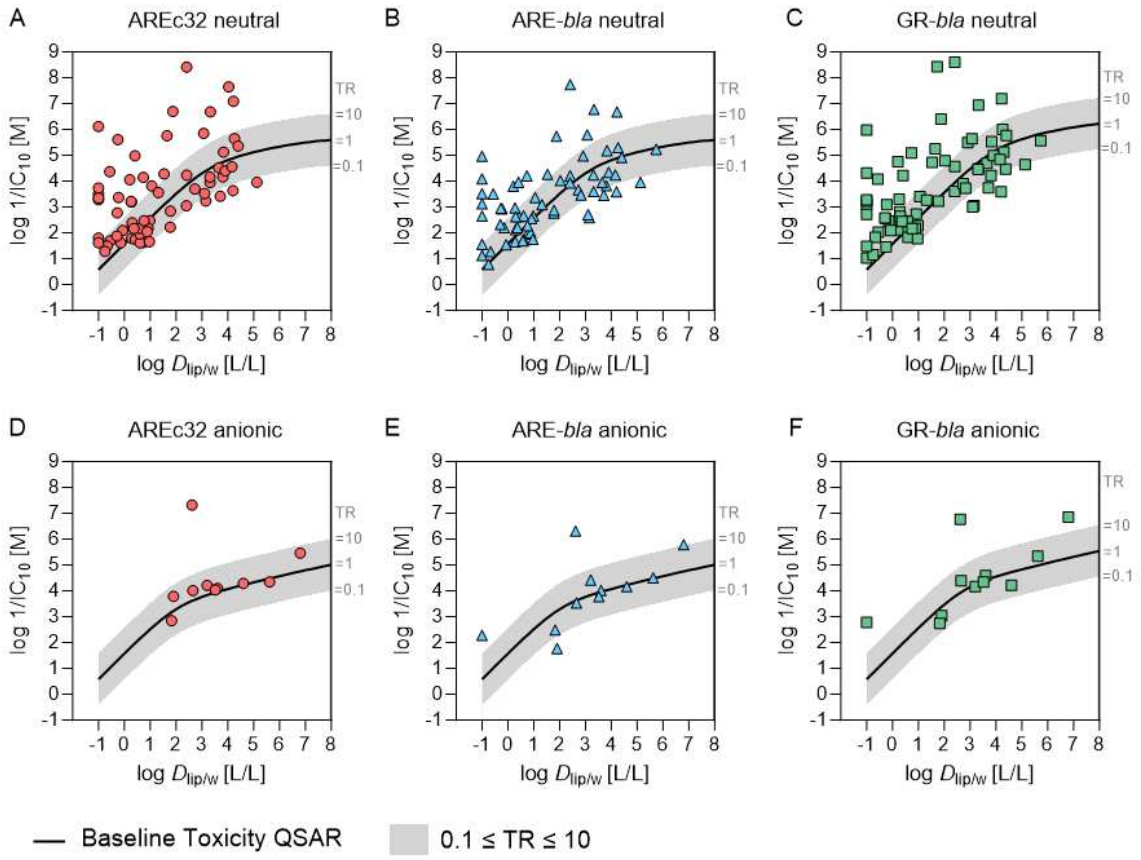

Figure 9: Cytotoxicity of test chemicals compared to baseline toxicity. Logarithmic reciprocal IC_{10} were plotted against logarithmic liposome-water distribution ratios (log $D_{lip/w}$) of the test chemicals. The black line indicates $IC_{10,baseline}$, the grey area indicates a toxic ratio (TR) between 0.1 and 10. A and D show data from the AREc32 assay for neutral (A) and anionic chemicals (D). B and E show data from the ARE-*bla* assay for neutral (B) and anionic chemicals (E). C and F show data from the GR-*bla* assay for neutral (C) and anionic chemicals (F). The Figure was adapted from *Publication III.*

Seven chemicals had TR below 0.1 in the three bioassays, which is an artifact that can indicate chemical loss or experimental errors, as discussed in more detail in *Publication III*. Baseline toxicity is the minimal toxicity of a chemical and measured toxicity cannot be lower. Possible causes of the loss of chemicals in *in vitro* bioassays are precipitation, volatilization, abiotic degradation or metabolization and the latter two will be discussed in more detail in the following chapters. Hence, TRs below 0.1 may indicate experimental problems or chemical instability and effect data for such chemicals should be carefully analyzed and possible loss processes excluded.

3. Chemical transformation in *in vitro* bioassays

3.1 Abiotic transformation processes

In order to use the data from *in vitro* bioassays for human risk assessment of chemicals, stable chemical exposure is necessary, since models for quantitative *in-vitro*-to *in vivo* extrapolation mostly use nominal chemical concentrations rather than measured concentrations. It is known that various loss processes that occur during the bioassay can lead to a decrease in chemical concentration. These processes include volatilization, sorption to the plastic of the well plate, and partitioning to components of the medium or the cells. Left unnoticed, the deviation of the actual bioavailable concentration from the nominal concentration may result in an underestimated toxicity and thus weaken the confidence in *in vitro* data for the risk assessment of chemicals. These loss processes are well known and both experimental methods and models exist to calculate the losses (Escher et al. 2019; Fischer et al. 2018b; Fischer et al. 2017; Henneberger et al. 2019b).

Abiotic transformation reactions of chemicals with components of the bioassay medium have remained unnoticed for a long time, although these transformation processes can reduce the concentration of chemicals in the medium, which can lead to an underestimation of *in vitro* effects. In addition to this problem, active transformation products can be formed that might have higher toxicity than the parent chemicals. If these processes are not detected, this can lead to serious errors in the interpretation of *in vitro* bioassay results. However, the stability measurement of chemicals in *in vitro* tests is time-consuming and labor-intensive and therefore not compatible with high-throughput screening methods. This is why chemical stability is not routinely measured and predictive models mostly only predict degradation under environmental conditions and not for the specific conditions of *in vitro* bioassays.

In the next chapters, a framework for the stability assessment of chemicals in *in vitro* bioassays, including an experimental workflow for determining abiotic stability as well as the influence of hydrolysis reactions and covalent reactions with proteins, will be explained in more detail.

3.1.1 Experimental workflow

In *Publication I,* a high-throughput framework for the determination and quantification of abiotic degradation processes under *in vitro* bioassay conditions has been developed and is shown in Figure 10. For the development of this framework, 22 potentially unstable chemicals were selected from the literature. As a first step, degradation kinetics in bioassay medium were

measured. Chemicals with degradation half-lives ($t_{1/2}$) in bioassay medium ≥ 100 h, which is two times the maximum duration of a standard *in vitro* bioassay, were classified as stable and bioassays for these chemicals could be run without chemical quantification. For chemicals with $t_{1/2}$ < 100 h, abiotic degradation during the bioassay could not be excluded, so the chemical concentration in the assay medium before and after the bioassay should be measured to ensure a stable exposure. The workflow was further used to unravel the mechanisms of abiotic transformation in the bioassay medium. The two most important abiotic transformation processes were hydrolysis and reactions with proteins, as the bioassay medium consists mainly of water and protein supplements (FBS).

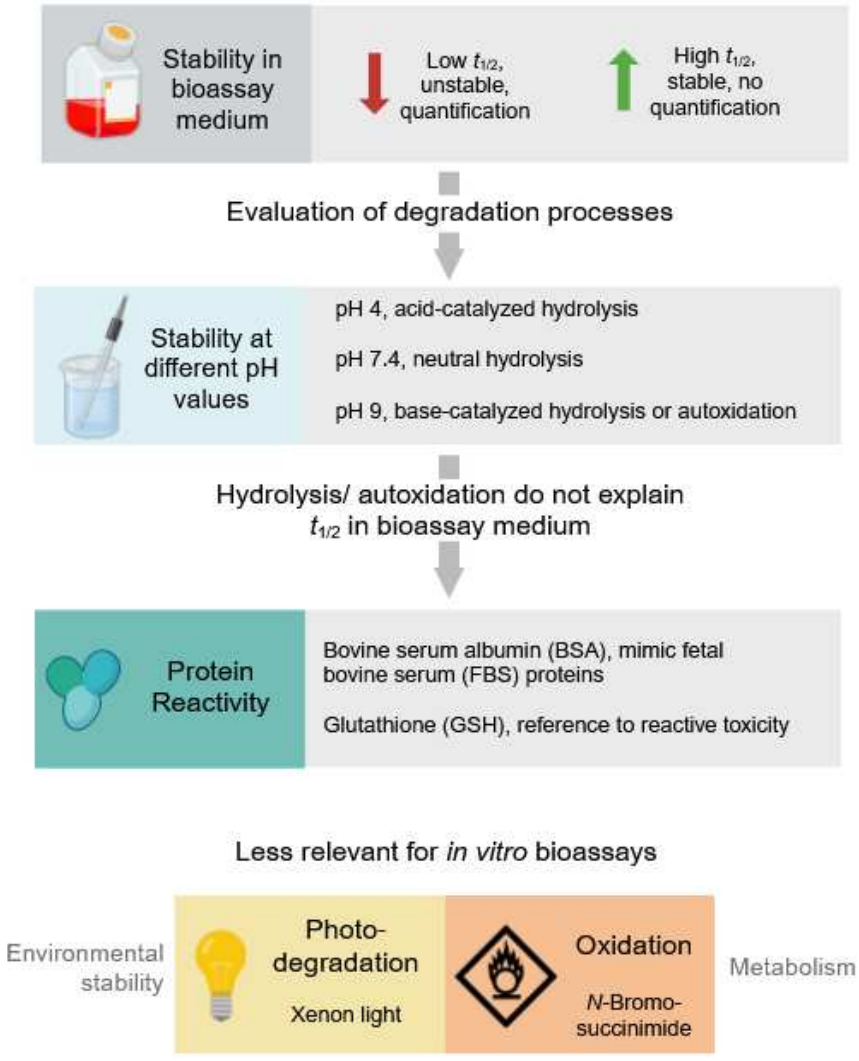

Figure 10: Framework for high-throughput abiotic stability assessment of chemicals. $t_{1/2}$ is the degradation half-life. The Figure was adapted from *Publication I*.

Hydrolysis reactions at neutral pH were a ubiquitous source of chemical loss in the bioassay medium. In order to gain insight into the hydrolysis mechanism, the degradation kinetics of the chemicals were also measured at acidic (pH 4) and basic (pH 9) pH values. Autoxidation, i.e., the reaction with atmospheric oxygen, can also take place in the bioassay medium, as oxygen is omnipresent. Autoxidation is also pH-dependent and occurs primarily at a basic pH (Jiang et al. 2015). Therefore, it cannot be differentiated from base-catalyzed hydrolysis using this workflow.

If degradation in bioassay medium was faster than in PBS, reactions with the proteins in the medium probably played a role. The reactivity toward proteins was investigated using bovine serum albumin (BSA) as a surrogate for fetal bovine serum (FBS), a component of many bioassay media. In addition, the reactivity toward reduced glutathione (GSH, y-Glu-Cys-Gly) was tested, which simulated the reaction potential of chemicals with a free thiol group and thus represents an indication of possible reactive toxicity of the chemicals (Chapter 3.1.5).

In *Publication I*, photodegradation under xenon-light and abiotic oxidation with *N*-bromosucchinimide were also investigated. These processes were found to be less relevant for *in vitro* bioassays as they do not reflect the experimental conditions, as the assay medium does not contain strong oxidizing agents and plates were incubated in the dark. However, the results of this study can provide an indication of possible degradation of the chemicals in the environment (photodegradation) as well as biotic degradation (oxidation) of the chemicals.

Figure 11 shows the depiction of a workflow for the experimental determination of degradation half-lives, which was developed in *Publication I* and automated in *Publication II*. The workflow was applied to measure degradation half-lives at different pH values to determine the degradation kinetics and mechanism of autoxidation or hydrolysis. pH-buffered solutions at pH 4 and pH 9 were prepared to measure either acid-catalyzed hydrolysis or reactions with hydroxide ions as nucleophile ("base-catalyzed hydrolysis"). Degradation half-lives in phosphate-buffered saline (PBS, pH 7.4) were measured to determine neutral hydrolysis and reactions with water. Reactivity with proteins was measured in the presence of bovine serum albumin (BSA) or GSH and different concentrations of GSH were used to determine second-order degradation kinetics.

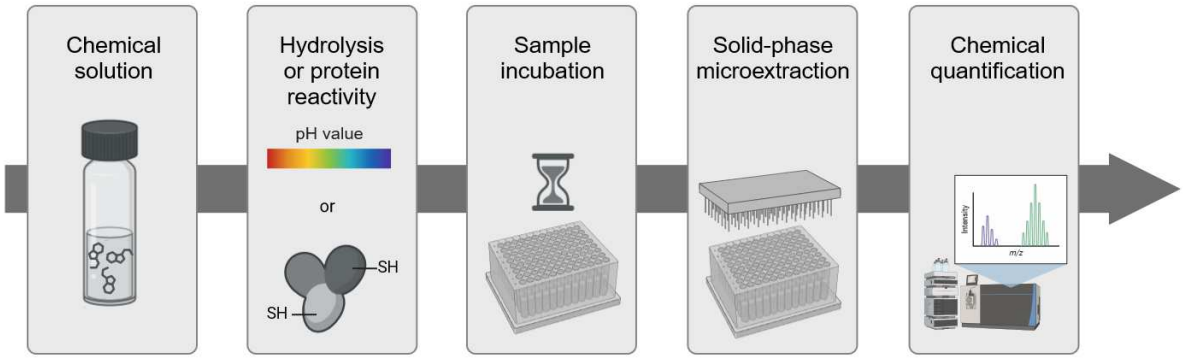

Figure 11: Experimental workflow for determination of abiotic stability and degradation kinetics of test chemicals.

Chemical solutions in the different buffers or BSA or GSH solutions were prepared and incubated for different periods of time between 30 min and 48 h. The incubation times were selected based on the time frame of the *in vitro* bioassays in *Publication II* and *Publication III,* which was 24 hours of incubation after chemical dosing. Chemicals were extracted from the incubation solutions using the SPME method described in *Publication I* and *Publication II* using the Supel™ BioSPME 96-Pin Device (Sigma-Aldrich). The Supel™ BioSPME 96-Pin Device allows simultaneous extraction of samples from 96-well plates, significantly increasing sample throughput compared to single SPME fibers. The SPME method consisted of four steps (conditioning, washing, extraction and desorption), as shown in Figure 12. Firstly, SPME pins were conditioned in isopropanol for 20 minutes and washed with deionized water for 10 seconds. Afterwards, the pin device was transferred to the sample plates and chemicals were extracted. Extraction times were 15 min at 37 °C and 1000 rpm in *Publication I* and *Publication II*. Chemicals were desorbed from the pin coating in a desorption plate filled with solvent-water mixtures whose composition depended on the chemical hydrophobicity. All steps of the SPME procedure were performed manually in *Publication I* and automated on a Hamilton Microlab Star robotic system in *Publication II* to increase sample throughput and reduce experimental variability. After the SPME extraction, the chemical concentration in the desorption solvent was quantified.

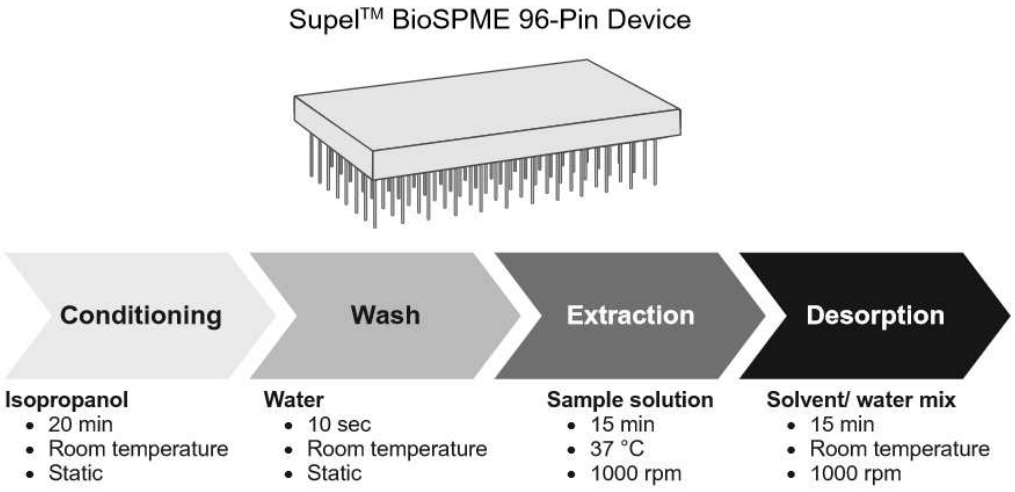

Figure 12: Solid-phase microextraction (SPME) workflow for the Supel™ BioSPME 96-Pin Device. Parts of the Figure were created by Luise Henneberger.

The strategy for the calculation of degradation half-lives is shown in Figure 13. Since reaction partners (hydroxide ions or glutathione) were used in excess, their concentration was assumed to be constant and pseudo-first-order kinetics were assumed. This means that only the concentration of the test chemical determined the reaction rate. The plot of the natural logarithm of the measured chemical concentrations against time showed a linear curve with a slope of *-k*, which is the pseudo-first-order degradation rate constant.

$$\ln(C)_t = -k \times t + C_0 \quad (13)$$

The degradation half-live ($t_{1/2}$) was calculated from *k* using Eq. 14.

$$t_{1/2} = \frac{\ln(2)}{k} \quad (14)$$

Reactions in the test system could be broken down into reactions with water and reactions with the present nucleophile (hydroxide ions (OH^-) or GSH). Since the concentration of water was constant, *k* only depended on the concentration of the nucleophile.

$$k = k_{H_2O} + k_{OH^-} \times [OH^-] \text{ or } k = k_{H_2O} + k_{GSH} \times [GSH] \quad (15)$$

A plot of *k* against the nucleophile concentration gave a linear curve with a slope of k_{OH^-} or k_{GSH} and an intercept of k_{H2O}.

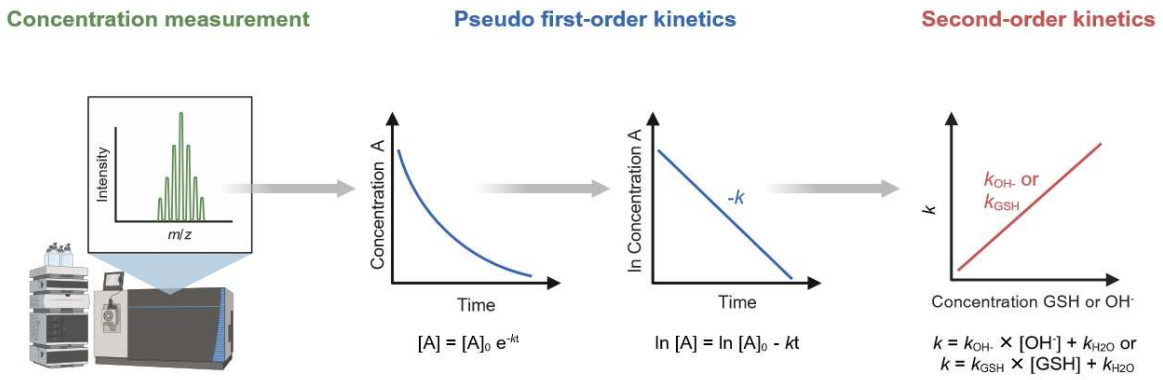

Figure 13: Experimental determination of reaction rates of pseudo-first-order and second-order reactions. k = pseudo-first-order degradation rate constant, k_{OH^-} = second-order degradation rate constant of the reaction of the chemical with hydroxide ion, k_{GSH} = second-order degradation rate constant of the reaction of the chemical with glutathione.

3.1.2 Stability in bioassay medium

As a first part of the framework developed in *Publication I* (Figure 10), chemical stability in three bioassay media was determined. Figure 14 shows the degradation half-lives ($t_{1/2}$) of the chemicals from *Publication I* in three bioassay media, phosphate-buffered saline (PBS) and pH 4, pH 7.4 and pH 9 aqueous buffers. Half of the chemicals were found to be unstable in bioassay medium and/or PBS. The majority of these chemicals (phosmet, bendiocarb, quercetin, malathion, andrographolide, L-sulforaphane, acetylsalicylic acid and carbofuran) showed $t_{1/2}$ < 24 h in at least one bioassay medium. Phosmet had the lowest $t_{1/2}$ in all bioassay media and PBS with 0.95 h in AREc32 medium being the lowest degradation half-life measured in *Publication I*. Some of the chemicals (phosmet, bendiocarb, quercetin, acetylsalicylic acid) had similar $t_{1/2}$ in all three media as well as PBS, which indicates degradation independent of the protein content of the solution. Hence, hydrolysis or autoxidation might be responsible for this degradation. Other chemicals such as malathion, andrographolide, L-sulforaphane, carbofuran and amoxicillin showed different $t_{1/2}$ in the three media and PBS, indicating reactivity towards proteins in the bioassay medium as a possible loss process of these chemicals.

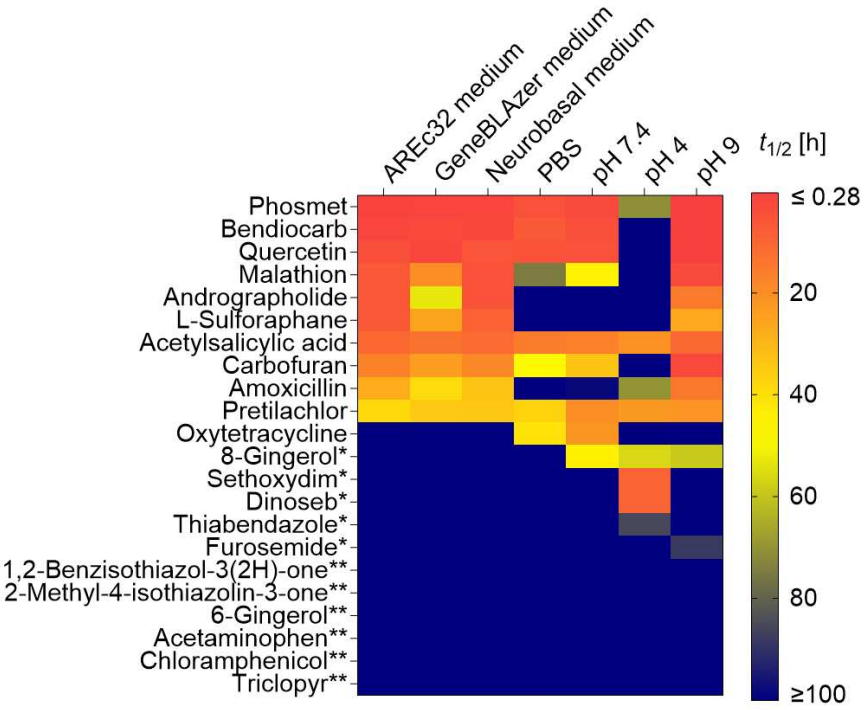

Figure 14: Stability of test chemicals in three bioassay media, PBS, and three pH buffers. The different colors indicate the degradation half-life ($t_{1/2}$) of the chemical in the respective medium or buffer. Chemicals that were stable in all media and PBS are marked with an asterisk, and chemicals that were stable in all media and buffers are marked with two asterisks. The Figure was taken from *Publication I*.

3.1.3 Hydrolysis

In a hydrolytic reaction a chemical is cleaved through the addition of water. The reaction mechanism of hydrolysis reactions is mostly a nucleophilic substitution, with water acting as the nucleophile (neutral and acid-catalyzed hydrolysis). In base-catalyzed hydrolysis reactions, the hydroxide ion acts as a nucleophile (Parekh et al. 2011). Hydrolysis reactions of chemicals are common in industry, the environment and biological systems since many chemical groups are prone to hydrolysis (e.g., esters, carboxylic acids, lactones, amides) (Fenner et al. 2013). For many environmental contaminants, hydrolysis reactions in the environment are desirable, as increasing contamination of the environment with persistent chemicals poses a major risk for humans and wildlife (Hale et al. 2020). In *in vitro* bioassays, however, hydrolysis reactions can lead to an unstable exposure of the test chemical, which can lead to an unnoticed misinterpretation of the bioassay results. Media for cell-based bioassays normally include buffers to stabilize pH during the assay at the physiological level. However, in reality, the pH of the media is often higher (approximately 7.7) to compensate for the acidic metabolites of the cells (Michl et al. 2019). Variations in the pH value of the medium can influence the stability

of the test chemicals and thus reduce the comparability between different assays and with the *in vivo* situation.

Ten chemicals investigated in *Publication I* showed degradation in all bioassay media (Figure 14). This degradation could either be caused by hydrolysis reactions or by covalent reactions with proteins in the medium. Eight of the chemicals also showed degradation in two different buffers at pH 7.4, indicating hydrolytic degradation of the chemicals at physiological pH. Autoxidation, meaning the oxidation by oxygen in the air (Crounse et al. 2013), could also be a potential degradation mechanism for these chemicals. However, the two processes can only be distinguished experimentally by identifying specific transformation products. For the differentiation of acid- or base-catalyzed hydrolysis, the degradation kinetics of the test chemicals were measured at different pH values. Most of the chemicals had a lower degradation half-life at pH 9 compared to pH 7.4 (Figure 14), which suggests that base-catalyzed hydrolysis was the predominant reaction. The second-order reaction rate constant of the reaction with hydroxide ions could be determined from the pseudo-first-order degradation rate constants plotted against the pH (hydroxide ion concentration). Figure 15 shows the pseudo-first-order and second-order kinetics and suspected chemical reaction of carbofuran. The reaction of carbofuran was supposed to be base-catalyzed carbamate hydrolysis (Seiber 1978) and the second-order reaction rate constant was found to be 3.42×10^4 $M^{-1}h^{-1}$. The reaction rate of the reaction with water could be derived from the intercept of the fit in Figure 15B and was close to zero. Apparently, neutral hydrolysis played no role in the degradation of carbofuran and acid-catalyzed reactions at pH 4 were observed only for sethoxydim and dinoseb (Figure 14).

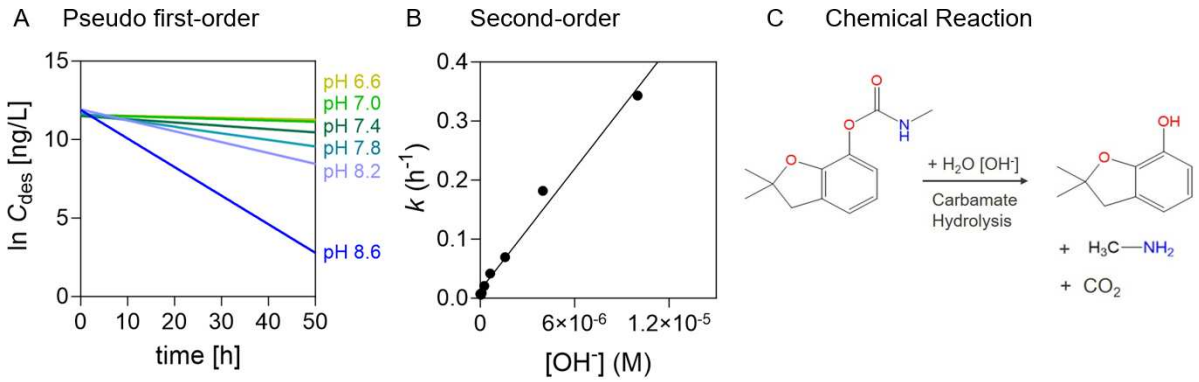

Figure 15: pH-dependent degradation of carbofuran with pseudo-first-order degradation at different pH values (A), resulting second-order degradation of reaction with hydroxide ions (OH^-) (B) and proposed chemical reaction mechanism (Seiber 1978) (C). The Figure was adapted from *Publication I*.

3.1.4 Reactivity towards proteins

Reversible binding of mostly hydrophobic or acidic chemicals to proteins is a known process in biological systems that limits the bioavailability of chemicals (Groothuis et al. 2015; Gülden and Seibert 1997). These processes have been extensively studied in the past in the context of *in vitro* bioassays and experimental methods as well as predictive models have been developed to determine the freely dissolved fraction of chemicals (Fischer et al. 2017; Henneberger et al. 2019b; Huchthausen et al. 2020). The ability of chemicals to form covalent, irreversible bonds with proteins or peptides has long been neglected in this context. These processes are common in toxicology, as they often lead to a dysfunction of proteins inside the cell and thus to a toxic outcome, which will be discussed in detail in the next chapter. With regard to exposure assessment, however, such irreversible reactions can lead to a reduction in chemical concentration, which in turn can falsify bioassay results. Five of the test chemicals from *Publication I* showed faster degradation in bioassay medium than in buffer solution at pH 7.4 (Figure 14). Apparently, for these chemicals, reactions with proteins play a role. The degradation half-lives of the chemicals in BSA and GSH solutions were determined to confirm the hypothesis. Five chemicals showed significantly faster degradation in either BSA or GSH solutions compared to buffer solution at pH 7.4. The reaction of 1,2-benzisothiazol-3(2H)-one, 2-methyl-4-isothiazolinone and L-sulforaphane with GSH took place immediately, so no degradation rate could be calculated. With BSA as well as in the medium, however, 1,2-benzisothiazol-3(2H)-one and 2-methyl-4-isothiazolinone showed no degradation. This means that the reactivity of the chemicals with GSH does not allow a direct conclusion about the stability of the chemicals in bioassay medium but can provide information about their reactive toxicity (Chapter 3.1.5). For andrographolide and pretilachlor, the second-order degradation rate constants of the reaction with GSH could be determined and were 438 $M^{-1}h^{-1}$ and 38 $M^{-1}h^{-1}$, respectively. Andrographolide, bendiocarb, L-sulforaphane, malathion, and oxytetracycline showed faster degradation in the BSA solution compared to buffer at pH 7.4, indicating covalent reactions with proteins as a loss process. However, for bendiocarb, malathion and oxytetracycline, hydrolysis was also observed, which makes it difficult to say whether there is an additional reaction with proteins or whether the results were caused by experimental variations of the hydrolytic degradation.

3.1.5 Reactive toxicity

In *Publication I*, reactions of the test chemicals with the proteins of the bioassay medium and with glutathione were observed. If these reactions occur in the bioassay medium, this leads to a reduction in the chemical concentration, which can lead to a misinterpretation of the toxicity of the chemicals. However, it has been shown in numerous studies that reactivity towards proteins or glutathione in cells can be the molecular initiating event of many adverse effects and associated diseases (Divkovic et al. 2005; Lopachin and Decaprio 2005). Therefore, the relationship between protein reactivity and the cytotoxicity of chemicals was investigated in *Publication II*. A subset of ten acrylamides and methacrylamides was selected for this purpose, as acrylamides are electrophilic and reactive chemicals whose toxicity exceeds baseline toxicity (Blaschke et al. 2012; Freidig et al. 1999a). Their high toxicity is usually caused by irreversible interactions with biological nucleophiles containing thiol, amino or hydroxyl groups (Harder et al. 2003a). In Michael addition reactions with biological nucleophiles (Michael donors), acrylamides act as a Michael acceptors (Ramirez-Montes et al. 2022). They belong to the so-called soft (polarizable) electrophiles, which react preferentially with soft nucleophiles such as thiols (Pearson 1990). Since glutathione (GSH) is abundant in cells and has a free thiol group, it serves as a cellular target for reactive electrophiles, protects cells from oxidative stress and supports cellular homeostasis. (Ketterer 1982; Reed 1990). Pseudo-first-order degradation rate constants of ten differently substituted (meth)acrylamides were measured at different concentrations of GSH and second-order degradation rate constants of the reaction with GSH were derived. Figure 16 shows the results for acrylamide.

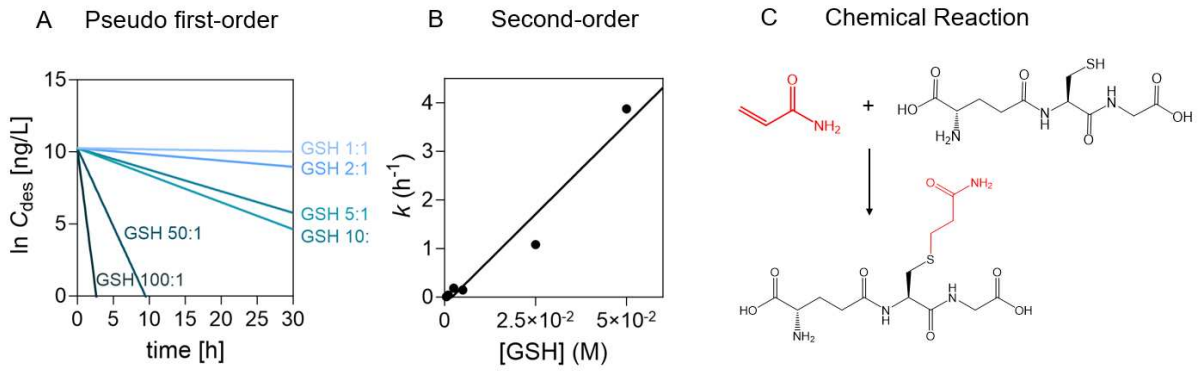

Figure 16: Pseudo-first-order degradation of acrylamide at different glutathione (GSH) concentrations (A), resulting second-order degradation of the reaction with GSH (B) and proposed chemical reaction. The Figure was adapted from *Publication II*.

None of the tested methacrylamides showed reactivity with GSH, which could be explained using quantum chemical calculations by the electron-donating effect of the methyl group, which lowered the electrophilicity of these chemicals (Freidig et al. 1999b; McCarthy et al. 1994). The methacrylamides also showed the lowest cytotoxicity of the ten test chemicals in the AREc32, ARE-*bla* and GR-*bla* assays and could all be classified as baseline toxicants. The tested acrylamides had TR between 0.2 (*N*-benzylacylamide) and 2227.7 (*N,N'*-methylenebisacrylamide), indicating either baseline toxicity or a highly specific toxicity mechanism. For all acrylamides, *in vitro* bioassay effects from the three assays were compared with second-order degradation rate constants with GSH (k_{GSH}) (Figure 17).

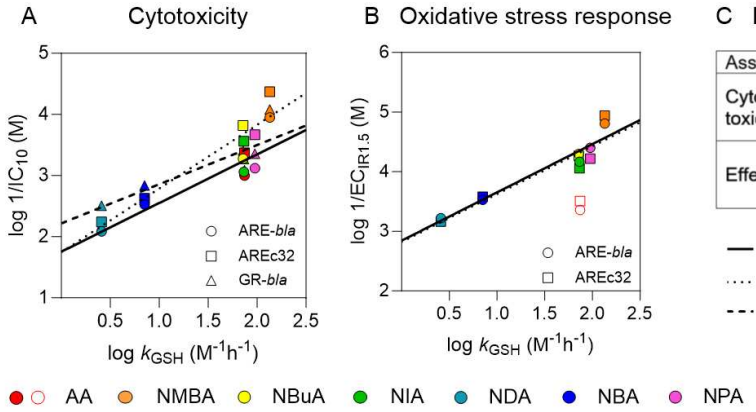

C Linear Regression

Assay		ARE-*bla*	AREc32	GR-*bla*
Cyto-toxicity	Slope	0.797	1.042	0.640
	Intercept	1.757	1.749	2.220
	R^2	0.806	0.896	0.729
Effect	Slope	0.810	0.802	
	Intercept	2.845	2.823	
	R^2	0.943	0.853	

Linear regression of ARE-*bla*
Linear regression of AREc32
Linear regression of GR-*bla*

Figure 17: Linear regression of cytotoxicity (log $1/IC_{10}$) (A) and activation of the oxidative stress response ($EC_{IR1.5}$) (B) plotted against reactivity with GSH (k_{GSH}). (C) Regression parameters of linear regression. AA was excluded from the fit of the oxidative stress response. The Figure was taken from *Publication II.*

There was a linear relationship between measured effect concentrations and k_{GSH} for all acrylamides and for cytotoxicity as well as activation of the oxidative stress response. *N,N*-diethylacrylamide (NDA) and *N*-benzylacrylamide (NBA) showed the lowest *in vitro* effects and also the lowest reactivity. This observation was consistent with the results of quantum chemical calculations. These calculations suggested that the presence of two ethyl groups on the nitrogen atom of NDA hinders the formation of the intermediate state in the reaction with GSH (Bent et al. 2015). Additionally, the merging of the orbitals of the phenyl ring of NBA with those of C_α and C_β reduces the electrophilicity. Since GSH reactivity correlated with both measured effects, it could be concluded that the effects are connected and do not happen independently. The predominant mode of toxic action was supposed to be the formation of reactive oxygen species (ROS), which trigger the oxidative stress response of the cells and ultimately cause cell death. In addition, a direct reaction of the chemicals with GSH disturbs

the intracellular redox homeostasis, making the cells more vulnerable to ROS (Zhao et al. 2022a; Zhao et al. 2022b).

The study has shown that the reactivity of chemicals to proteins or GSH does not only represent the loss of the chemical during the *in vitro* bioassay. Rather, these reactions could also be directly linked to the toxicity of the chemical. Additionally, none of the (meth)acrylamides showed reactivity towards 2-deoxyguanosine (2DG) which served as a proxy for DNA reactivity. This result was expected due to the softness of the electrophiles and could be confirmed experimentally. Mutagenic or carcinogenic effects of these chemicals are therefore unlikely without further chemical activation. In conclusion, it can be said that measuring the chemical reactivity not only helps to assess the exposure of the chemical in the bioassay but can also be used directly to interpret the toxicity and make statements about the mode of action.

3.1.6 Models for abiotic transformation

The need to assess the abiotic stability of chemicals has been known for a long time and is omnipresent, especially in environmental sciences, as the fate of xenobiotic chemicals has been investigated in numerous studies (Chu et al. 2009; Kumar et al. 2023). Also, in the pharmaceutical and agrochemical industries, stability studies are integrated into the drug or pesticide development process as they provide important information about shelf-life and degradation products and pathways (Bajaj and Singh 2018; Foti et al. 2013; Zhang and Yang 2021). However, the need for abiotic stability testing has not yet fully arrived in *in vitro* toxicology. Experimental assessment of the abiotic stability of test chemicals is labor- and cost-intensive and not compatible with high-throughput *in vitro* bioassays in 384- or 1536-well plates. Nevertheless, it is necessary to generate reliable data and avoid false-negative or false-positive bioassay results. Therefore, there is a great interest in simplifying the stability assessment by using *in silico* models for the prediction of abiotic stability. Hydrolysis was identified as one of the main degradation pathways in *in vitro* bioassay medium, so modeling the potential hydrolytic degradation of test chemicals would increase the reliability of bioassay results. Many models and programs for hydrolytic stability assessment are based on data from drug development or the environmental fate of chemicals. There are numerous databases collecting chemical stability data for pharmaceuticals like Pharma D3 (Alsante et al. 2014) or DELPHI (Pole et al. 2007) or data for the environmental fate of chemicals (EPA 1998). There are also many open-source programs for the prediction of chemical stability, like HYDROWIN (EPI Suite, US Environmental Protection Agency) (EPA 2012) or Chemical Transformation

Simulator (CTS, US Environmental Protection Agency) (EPA 2019). HYDROWIN predicts acid- or base-catalyzed hydrolysis rate constants and half-lives for six chemical classes (Howard and Meylan 1992) and CTS predicts biological and environmental degradation pathways and products as well as half-lives (Tebes-Stevens et al. 2017; Yuan et al. 2020).

Data and models for protein reactivity are mainly based on toxicological profiling of chemicals for their skin sensitization, respiratory sensitization or aquatic toxicity potential, as all of these endpoints involve covalent reactions of chemicals with proteins (Aptula et al. 2009; Enoch et al. 2009; Schultz et al. 2007). Analysis of these endpoints has been used to generate a number of structural alerts that identify functional groups associated with covalent binding to proteins (Enoch et al. 2011). These alerts are implemented in a number of software programs, such as Derek Nexus (Lhasa Limited, https://www.lhasalimited.org/solutions/skin-sensitisation-assessment/), TOPKAT (Enslein 1988) or the modules of the OECD QSAR toolbox (Dimitrov et al. 2016) among many others.

In *Publication I*, the experimental stability data for hydrolysis at pH 7.4 and reactivity toward bovine serum BSA and GSH were compared with predictions of six different models (CTS and HYDROWIN for hydrolysis and four models from the QSAR toolbox for protein reactivity), as shown in Figure 18.

For hydrolysis at pH 7.4, HYDROWIN identified four of the eight chemicals that were unstable in the experiment and CTS identified five chemicals. Both models also predicted additional chemicals to be hydrolyzed. Both 8-gingerol and oxytetracycline, which showed hydrolysis in the experiments, were not predicted by any of the models. Eight chemicals showed reactivity with BSA or GSH in the experiment and four models were used to predict protein reactivity. None of the models was able to predict all of the chemicals that showed reactivity in the experiment and some models also generated warnings for chemicals that were stable in the experiment. The protein binding OASIS model was able to correctly classify the most reactive chemicals of all models (six of the eight chemicals), but gave warnings for seven additional chemicals. The protein binding CYS model could only identify three of the reactive chemicals but also only gave a wrong alert for one chemical.

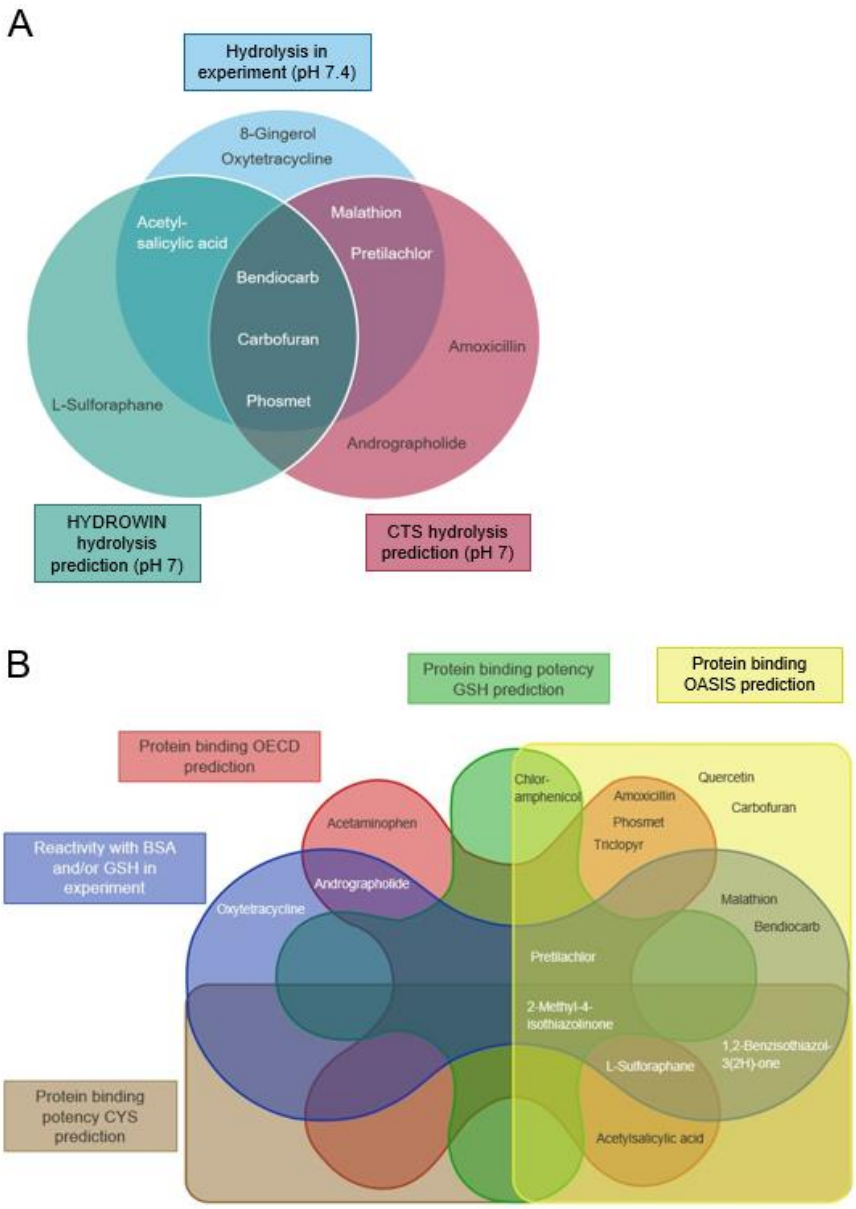

Figure 18: Comparison of experimental stability at pH 7.4 (A) or with glutathione (GSH) or bovine serum albumin (BSA) (B) with stability predictions from different *in silico* models.

All in all, it can be concluded that models for the abiotic stability of chemicals that are not designed for the specific conditions of *in vitro* bioassays do not allow a quantitative assessment of chemical stability in the bioassay. However, these models can be used to increase awareness of degradation processes and to scrutinize bioassay data for suspect chemicals. Also, structural alerts for reactivity with proteins can be used not only to assess stability in the bioassay medium but also to provide an indication of the reactive toxicity of the chemicals.

3.2 Metabolic activity of reporter gene cell lines

Cellular metabolism, or biotransformation of xenobiotic chemicals, means the transformation of a chemical into structurally different metabolites inside the cell (Coecke et al. 2006). In the body, biotransformation is a crucial process that takes place primarily in the liver and influences the physicochemical properties of chemicals, their distribution and their toxicity. Xenobiotic metabolism can be separated in two phases. In phase I, mainly oxidation reactions take place, which are catalyzed by cytochrome P450 (CYP) enzymes. The aim of these reactions is to increase the polarity of xenobiotic substances and thus facilitate their excretion (Croom 2012). In phase II, the metabolites formed in phase I undergo conjugation with polar molecules like glutathione or glucuronic acid to further increase the polarity of the metabolites (Iyanagi 2007). In phase I of xenobiotic metabolism reactive intermediates can be formed (bioactivation). These metabolites can have a higher toxicity than the parent substances and can be involved in various adverse effects, such as carcinogenesis or neurotoxicity, by reacting with proteins or DNA (Maggio et al. 2021; Souza et al. 2016).

It has been shown in many studies that reporter gene cell lines have limited metabolic activity and therefore cannot represent the *in vivo* situation (Coecke et al. 2006; Qu et al. 2021). Still, there is evidence in the literature that cytochrome P450 (CYP) enzyme activity can be induced by some xenobiotic chemicals, resulting in a higher metabolic capacity of the cells (Choi et al. 2015; Fischer et al. 2020). To ensure accurate *in vitro* data, it is necessary to determine the metabolic activity of reporter gene cell lines with and without xenobiotic activation and examine how it affects the bioassay results. The biotransformation of chemicals can have two consequences, as shown in Figure 19. Firstly, degradation of the chemical can decrease the chemical concentration, leading to lower toxicity (detoxification). Secondly, cellular CYP enzymes can produce one or more reactive metabolites, which may have a higher toxicity than the parent substance. In this case, it must be ensured that the metabolization of the test substance also takes place in the bioassay, as otherwise the toxicity of the substance may be misjudged.

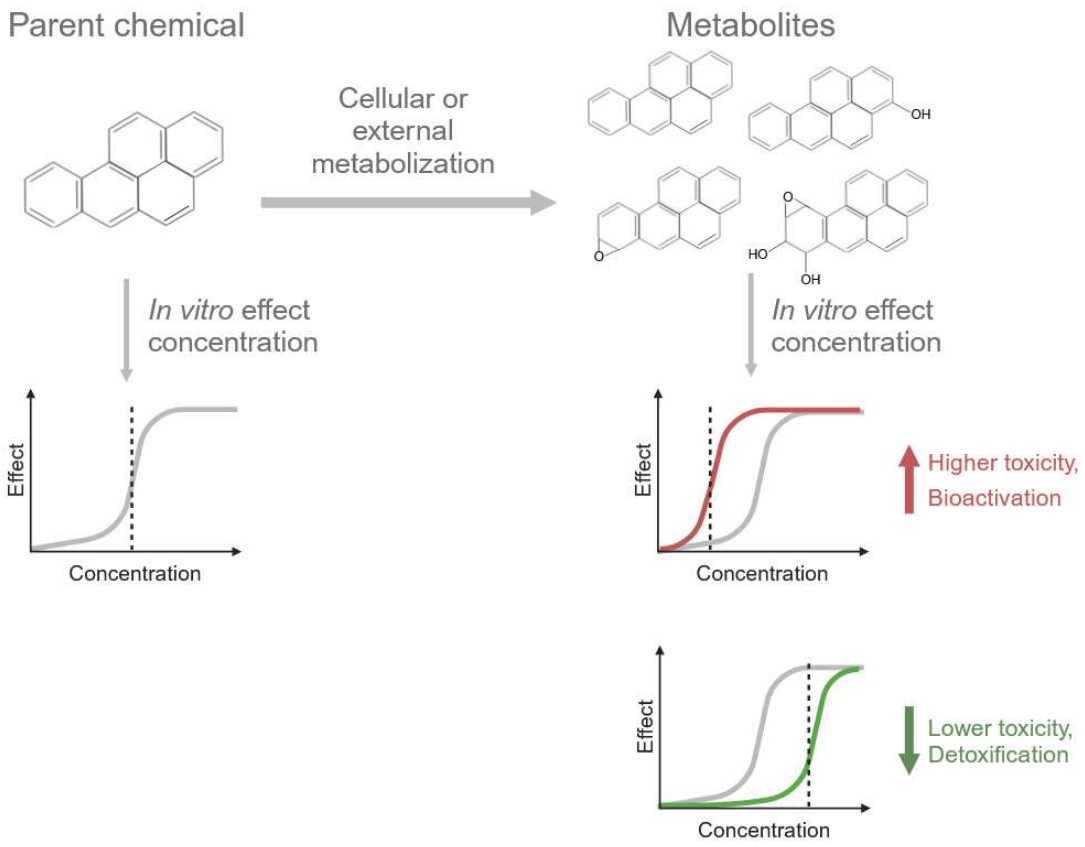

Figure 19: Possible impact of metabolic transformation of test chemicals on *in vitro* bioassay results.

3.2.1 Metabolic characterization of reporter gene cell lines

In *Publication III*, the metabolic activity of the three reporter gene cell lines AREc32, ARE-*bla* and GR-*bla* was measured with and without previous incubation of the cells with the CYP inducers omeprazole (Novotna et al. 2014) and benzo[a]pyrene (Pushparajah et al. 2017). All reporter gene cells are based on different cell lines, so different metabolic activity was expected. AREc32 is based on the MCF-7 human breast cancer cell line. ARE-*bla* is based on the HepG2 human liver cancer cell line and GR-*bla* is based on the HEK293T human embryonic kidney cell line. Figure 20 shows the results of the metabolic characterization. CYP activity was measured using the 7-ethoxyresorufin O-deethylation (EROD) assay, the 7-ethoxy-4-trifluoromethylcoumarin O-deethylation (EFCOD) assay and the 7-benzyloxy-4-trifluoromethylcoumarin O-deethylation (BFCOD) assay. All three cell lines had low or non-detectable basal CYP activities in all three assays. ARE-*bla* had the highest basal CYP activity of the three cell lines, as expected from its liver cell background. CYP activity was not or only very slightly induced by omeprazole and benzo[a]pyrene (BaP) in GR-*bla* cells. A slightly higher induction was achieved for AREc32, with BaP being the stronger inducer. The strongest

induction was achieved for ARE-*bla*, with the highest CYP activity measured after incubation with BaP in the EROD assay (151.00 pmol of resorufin formed per minute per $mg_{protein}$ ($pmol_{resorufin}$ min^{-1} $mg_{protein}^{-1}$)). As a comparison, the CYP activities of rat liver S9 were also quantified. The EROD activity of the S9 was 695.17 $pmol_{resorufin}$ min^{-1} $mg_{protein}^{-1}$ which is 4.6 times higher than the EROD activity of ARE-*bla*.

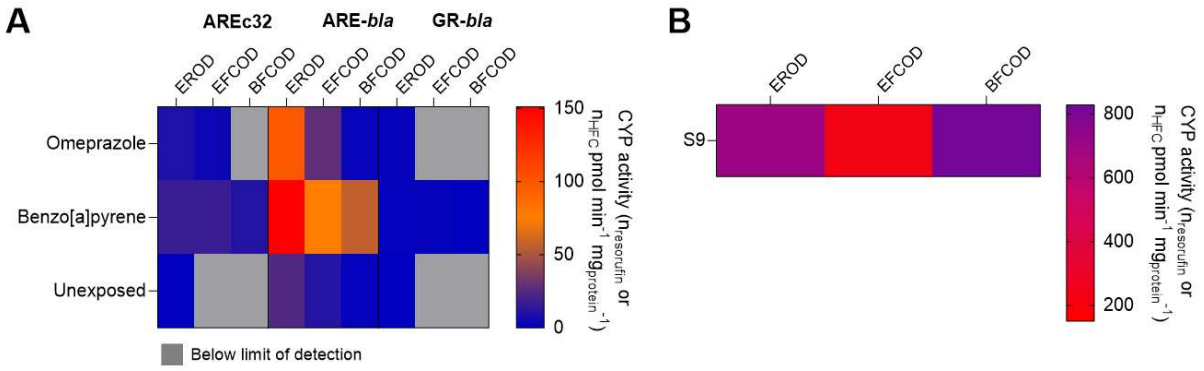

Figure 20: Results of EROD, EFCOD and BFCOD assays for AREc32 (MCF-7), ARE-*bla* (HepG2) and GR-*bla* (HEK293T) cells without chemical exposure and after exposure to omeprazole or benzo[a]pyrene (A) and for rat liver S9 as a positive control (B). CYP activity was measured as amount of resorufin ($n_{resorufin}$, EROD) or amount of 7-hydroxy-4-trifluoromethylcoumarin (n_{HFC}, EFCOD and BFCOD) formed per minute and per $mg_{protein}$. The Figure was taken from *Publication III*.

The results shown in *Publication III* prove that the CYP activity of reporter gene cell lines can be activated by xenobiotic chemicals, as previously reported in the literature (Fischer et al. 2020). Especially HepG2 cells showed a strong inducibility of CYP activity. These results suggest that test chemicals in the *in vitro* bioassay may increase the CYP activity of the cells, potentially causing a metabolic transformation of the chemicals in the assay. However, the quantification of CYP activity does not allow a conclusion about the impact on the bioassay results. Chemical metabolization can lead to bioactivation as well as detoxification, and in the latter case, the cellular concentration of the chemical must be significantly reduced to have an effect. It must therefore be clarified how this will affect the bioassay results of the respective cell lines and chemicals. Data from metabolically active cells (HepG2) in particular should be critically reviewed and examined for possible metabolization of the test substances.

3.2.2 Comparison of *in vitro* effects from cell lines with different metabolic activity

In *Publication III*, 94 chemicals were systematically screened for their cytotoxicity in three different cell lines of different origin and with different CYP activities (AREc32: MCF-7, ARE-*bla*: HepG2 and GR-*bla*: HEK293T). The ARE-*bla* cell line, derived from a HepG2 cell line, showed the highest basal CYP activity and inducibility of all three cell lines. It also had the highest number of chemicals for which no IC_{10} value could be determined (16 chemicals). For example, dexamethasone showed low IC_{10} in GR-*bla* but was not cytotoxic in AREc32 or ARE-*bla*, which can be explained by a specific toxicity mechanism of dexamethasone, which is also the reference compound for the GR-*bla* cell line (Li et al. 2012b). Chlorpyrifos-oxon was also only cytotoxic in the GR-*bla* assay, which might be explained by the higher protein content of the AREc32 and ARE-*bla* bioassay media and a suspected loss through reaction with medium proteins (Schopfer and Lockridge 2019).

A comparison of all measured IC_{10} values of all assays showed slightly lower cytotoxicity (higher IC_{10}) for most chemicals in ARE-*bla*. However, an analysis of variance (ANOVA) of the three datasets showed no significant difference with a P-value of 0.3647. Compared to the IC_{10} values of GR-*bla* (Figure 21A), which showed no CYP activity, the measured effect concentrations of AREc32 and ARE-*bla* showed a good agreement within a factor of 10 in most cases. There are larger deviations for some chemicals, but these mostly also occur for AREc32, which showed only a slight inducibility and no basal CYP activity.

The basal CYP activity of ARE-*bla* was between 9.5 and 870.8 times lower than the measured CYP activity of rat liver S9. Apparently, this is not sufficient to metabolize the test substances in the *in vitro* bioassay or the metabolites and parent chemicals have similar cytotoxic effects. There was a noticeable trend that, for many chemicals, the measured IC_{10} values in ARE-*bla* were slightly higher than those of the other two cell lines. This difference was found to be not significant and less than a factor of 10 for the majority of chemicals, and therefore below the measurement uncertainty of the biological system. However, in order to exclude a metabolic transformation of the chemicals with certainty, it is necessary to measure the concentration before and after incubation with the cells and/or to identify metabolites formed. Furthermore, none of the chemicals were found to have significantly higher cytotoxicity in ARE-*bla*, which contradicts the formation of reactive metabolites through metabolic activation. For example, cyclophosphamide is known to be metabolized *in vivo* to the bioactive products phosphoramide mustard and acrolein (Steinbrecht et al. 2020), which

would cause significant higher cytotoxicity in *in vitro* cell-based bioassays than the parent chemical. In *Publication III* however, cyclophosphamide had the same effects in all cell lines.

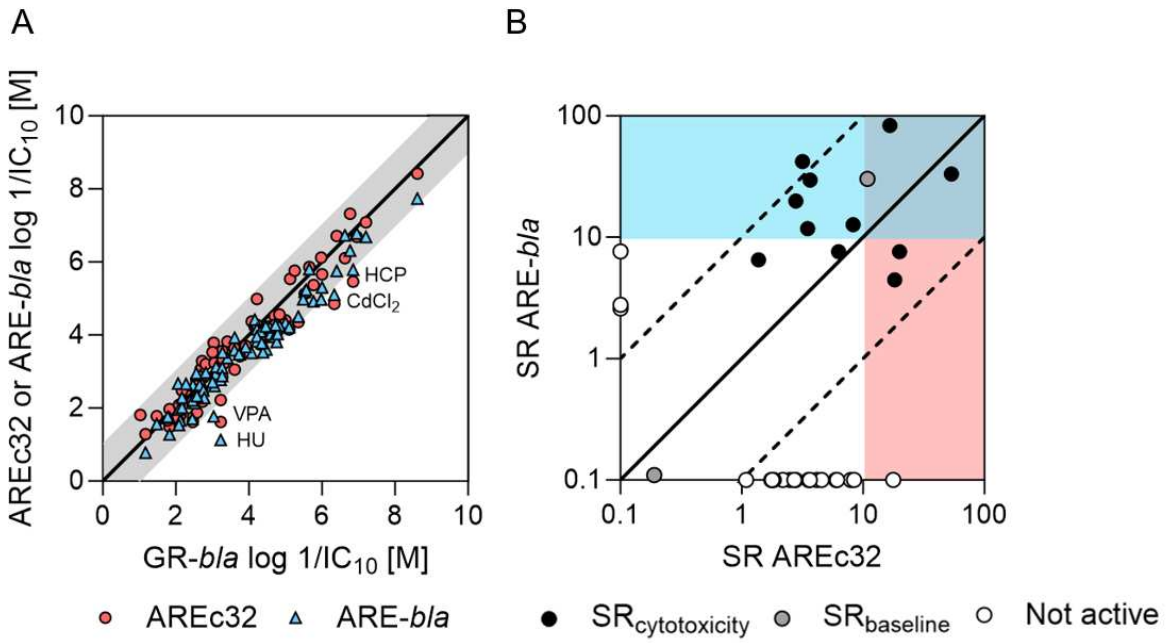

Figure 21: A: log $1/IC_{10}$ measured in AREc32 or ARE-*bla* plotted against $1/IC_{10}$ measured in GR-*bla*. Red circles indicate results for AREc32, blue triangles indicate results for ARE-*bla.* The black line indicates a perfect agreement between the results of the cell lines. The grey area indicates a deviation by a factor of ten. HCP = Hexachlorophene, $CdCl_2$ = Cadmium chloride, VPA = Valproic acid, HU = hydroxyurea. B: Specificity ratios (SR) of oxidative stress response activation in ARE-*bla* plotted against SR in AREc32. $SR_{cytotoxicity}$ is shown when cytotoxicity could be determined in both assays (black circles). For chemicals without measured cytotoxicity in at least one assay, $SR_{baseline}$ was used (grey circles). Chemicals that showed oxidative stress response activation only in one assay are indicated with white circles. The Figures were taken from *Publication III.*

Figure 21B shows a comparison of the specificity ratio (SR) of the oxidative stress response activation from AREc32 and ARE-*bla.* 31 chemicals activated the oxidative stress response in AREc32, but only 17 chemicals in ARE-*bla.* For the chemicals that were active in both assays, the SR of both assays had a good agreement, but 17 chemicals that were moderately specific ($1 < SR < 10$) in AREc32 did not activate the oxidative stress response at concentrations below cytotoxicity in ARE-*bla* and cadmium chloride that had an SR of 17.8 in AREc32 was not active in ARE-*bla*. Apparently, ARE-*bla* has a lower sensitivity for oxidative stress response activation as moderately specific chemicals are not identified. Furthermore, the $EC_{IR1.5}$

of the reference chemical *tert*-butylhydroquinone was 1.75 times higher for ARE-*bla* than for AREc32 and showed a higher variability between replicates, emphasizing the lower sensitivity of the ARE-*bla* assay.

The confirmation that the different basal CYP activity and inducibility of CYP activity of the different reporter gene cell lines have no significant influence on the results of the bioassays is encouraging for the use of *in vitro* bioassays for chemical risk assessment. A loss of the test chemicals due to metabolic degradation would have falsified the results of the bioassay and reduced the reliability of the *in vitro* data, since a stable exposure of the chemicals in the bioassay is essential. The results obtained confirm those of previous studies, which found that reporter gene cell lines have negligible metabolic activity (Qu et al. 2021; Wilkening et al. 2003). Nevertheless, in some cases, it is necessary to metabolize chemicals before or during the bioassay in order to assess the toxic effects of the metabolites. This is relevant for a number of endpoints, especially genotoxicity (Shah et al. 2016), neurotoxicity (Flaskos 2012) and skin sensitization (Nilsson et al. 2005). Since reporter gene cells apparently cannot metabolize these compounds sufficiently, additional metabolizing systems must be used. If this investigation is neglected, it can also lead to a misjudgment of the toxicity of a chemical and its metabolites generated *in vivo*.

4. Implications:

4.1 Key findings

This doctoral thesis focused on the difficulties of single chemical screening in high-throughput bioassays, considering baseline toxicity and both abiotic and biotic transformation processes. Chemical transformation processes can lead to a deviation between the bioavailable concentration in the test system and the dosed nominal concentration and can cause incorrect effect concentrations and, thus, an incorrect assessment of the toxicity of a test chemical. Apart from this, transformation products can also have more toxic effects than their parent chemicals, even if metabolism mostly leads to detoxification and an overall decrease in toxicity.

For this reason, the importance of careful experimental planning of bioassay dosing and examination of the physicochemical properties of the test chemical, as well as an exposure assessment in the bioassay using experimental methods or models, was emphasized. A baseline toxicity QSAR was developed in *Publication III* based on freely dissolved effect concentrations of hydrophilic and ionizable chemicals that can be applied to a wider range of test chemicals than previous QSARs. The predicted baseline toxicity can serve as guidance for choosing appropriate dosing concentrations, can identify specific toxicity mechanisms and can also be used as a quality control for bioassay data. In a high-throughput screening of 94 chemicals in three bioassays, approximately 7% of the chemicals showed significantly lower toxicity than the predicted baseline toxicity. This observation may indicate experimental artifacts and suggest a loss of the chemical in the assay. Thus, possible abiotic transformation processes should be verified for these chemicals using *in silico* models or experimentally.

An experimental workflow for abiotic stability assessment of chemicals was established in *Publication I* using a high-throughput solid-phase microextraction (SPME) method. This workflow can be applied to identify chemical transformation processes in *in vitro* bioassays and to elucidate their impact on bioassay results. By using this workflow, degradation half-lives of test chemicals in different bioassay media could be determined. Abiotic hydrolysis and covalent reactions with proteins could be identified as the main abiotic degradation pathways in *in vitro* bioassays, while photodegradation and oxidation played only minor roles. In *Publication II*, the workflow was automated on a Hamilton robotic platform and used to determine the reactivity of acrylamides towards glutathione. The linear correlation between glutathione reactivity and cytotoxicity, as well as oxidative stress response activation, allowed conclusions about the mode of action of these substances. This correlation showed that abiotic transformation processes can not only lead to a loss of the chemical over time and thus reduce the *in vitro*

effect, but that abiotic reactions such as covalent reactions with proteins can also be directly linked to the toxic effect of the chemical.

Cytochrome P450 activities were found to be low in AREc32, ARE-*bla* and GR-*bla* cell lines, which are based on MCF-7, HepG2 and HEK293T cells, but could be induced by chemicals like omeprazole or benzo[a]pyrene (*Publication III*). There was no significant difference between the effect concentration measured for the different cell lines for 94 single chemicals, so the low cellular xenobiotic metabolism activities of the three cell lines were found to have no impact on chemical toxicity. If the toxicity of chemical metabolites should be investigated, external metabolization systems must be used to achieve biotransformation of the chemicals.

Although there is no simple general strategy for dealing with chemical transformation in *in vitro* biotests, the tools developed in this thesis can help to diagnose if transformation, whether abiotic or biotic, has affected the bioassay results. The consequences and necessary measures always depend on the chemical, the type of transformation and the bioassay. It is important to keep in mind the possibility of chemical transformation in the *in vitro* system and to understand its relevance and significance for bioassay results. Careful planning of the biotests and a critical review of the results can help uncover possible loss processes and thus avoid inaccurate effect concentrations. The methods and guidelines provided in this thesis can give some guidance.

4.2 Exposure assessment for single chemical screening

Back in 1538, Paracelsus wrote a sentence that became one of the fundamental principles of toxicology and remains valid centuries later: “All things are poison, and nothing is without poison; the dosage alone makes it so a thing is not a poison” (Paracelsus 1538). This quote underlines the importance of considering the dose in *in vitro* toxicology. Toxicity is determined by the concentration of a chemical at the cellular target site and the potential to trigger the molecular initiating event (MIE) (Proenca et al. 2021). The nominal concentration (C_{nom}) is the most widely used concentration metric for *in vitro* bioassays because it is easily accessible. C_{nom} can differ greatly from the biologically effective concentration in the *in vitro* system due to various loss processes such as binding to proteins of the medium or the plastic material of the plates, volatilization or abiotic degradation processes. The experimental measurement of the freely dissolved concentration (C_{free}) in the *in vitro* bioassay can be a promising alternative, as it can reveal these loss processes (Groothuis et al. 2015). Measured C_{free} can be a valuable input for QIVIVE models as they allow a better comparability of the *in vitro* and *in vivo* situations and give a better representation of the concentration at the target site (Heringa et al. 2004; Kisitu et al. 2020). Studies measuring C_{free} in *in vitro* bioassays showed a linear relationship between C_{free} and C_{nom} for the majority of chemicals, whereby C_{free} was similar to C_{nom} for neutral, hydrophilic chemicals and bases, as these did not show strong binding to medium components (Henneberger et al. 2019b; Huchthausen et al. 2020). For neutral, hydrophobic chemicals, strong binding to the proteins and lipids of the bioassay medium was observed, so C_{free} was much lower than C_{nom} for these chemicals (Henneberger et al. 2020; Henneberger et al. 2019b). For organic acids, a concentration-dependent binding to proteins was observed, showing a high affinity at low concentrations and a low affinity at high concentrations (Henneberger et al. 2019a; Henneberger et al. 2019b; Huchthausen et al. 2020). The measurement of C_{free} at different time points also allowed an assessment of the stability of the chemical concentration over the time of the assay (Henneberger et al. 2019b; Huchthausen et al. 2020). However, experimental measurement of C_{free} is very labor-intensive and incompatible with high-throughput screening and the need for rapid data generation for a large number of chemicals. Mass-balance models can reliably predict C_{free} for various groups of chemicals, but are not applicable if irreversible loss processes occur. New approach methodologies in HTS format often rely on a combination of experimental and modeling approaches to account for chemical loss processes.

There is not a single relevant concentration metric for *in vitro* bioassays and the selection of the concentration metric should always consider the purpose and function of the *in*

vitro data. For many chemicals and testing scenarios, the nominal concentration can be enough to describe the *in vitro* effect. However, a careful consideration of the assay setup and physicochemical properties of the chemicals prior to the bioassay is essential to identify all possible sources of chemical loss processes (Groothuis et al. 2015). If data from *in vitro* bioassays is used as an input parameter for QIVIVE for the assessment of safe exposure levels for humans, the most accurate *in vitro* models should be used to guarantee a good agreement between the *in vitro* and *in vivo* concentrations, either by measuring C_{free} or by validating mass-balance models for a realistic prediction. Without exposure estimation, *in vitro* bioassay data can still be useful for qualitative hazard identification or prioritization of chemicals, but careful planning, including (1) the examination of physicochemical properties, (2) solubility in bioassay medium, (3) possible volatilization or (4) abiotic or biotic degradation, and finally (5) critically scrutinizing the bioassay results, should always be included in *in vitro* toxicological testing (Yoon et al. 2012).

4.3 Influence of abiotic transformation processes on *in vitro* data

The previous chapter described the importance of exposure assessment for the reliable use of *in vitro* bioassay data and the use of mass-balance models to estimate exposure concentrations of chemicals. However, these models can only be applied if the test chemical concentration is stable over the course of the bioassay. Irreversible loss processes like volatilization, abiotic degradation processes or cellular metabolism will lead to changes in the chemical equilibrium and false model predictions. Volatile chemicals are out of the applicability domain of high-throughput bioassays and special setups are necessary to test the toxicity of these chemicals (Escher et al. 2019; Kramer et al. 2010).

Abiotic hydrolysis and covalent reactions with proteins were identified as the two major abiotic degradation processes in the *in vitro* bioassay medium. The degradation half-lives of test chemicals were found to be as low as 0.95 h, leading to a complete chemical transformation within the 24-hour incubation time of the bioassays used in this thesis. Only the comparison of measured total or freely dissolved concentrations at different time points in the course of the bioassay could detect these loss processes. Without experimental exposure measurement, degradation processes would remain unnoticed and could lead to an underestimation of the toxicity of chemicals.

As long as it is not ensured that degradation processes occur equally in humans, *in vitro* data for unstable chemicals should not be used for human risk assessment. However, measuring chemical stability is not easy to integrate into a routine high-throughput screening of chemicals, as both extraction methods and analytical methods have to be developed and the appropriate instruments must be available. Prediction models based on the stability of chemicals in the environment can be used for the prediction of the hydrolytic half-lives of chemicals. The "Virtual Cell Based Assay" developed by the European Union's Joint Research Centre is a dynamic model for the simulation of the kinetics and of test chemicals in cell-based *in vitro* assays and includes predicted degradation rates of the test chemicals to estimate chemical exposure concentrations (JRC et al. 2010; JRC et al. 2011). Nevertheless, such predictions should be handled with caution, as they may differ from the actual degradation under bioassay conditions because they are not tailored to the conditions of *in vitro* bioassays. Larger data sets with measured degradation rates under bioassay conditions are needed for quantitative prediction of chemical transformation in *in vitro* bioassays and to build more reliable and quantitative models. *In vitro* data of unstable chemicals can only be used for qualitative estimations of toxicity mechanisms *in vivo* as long as no toxic transformation products are

formed. A comprehensive identification and quantification of formed transformation products and a comparison of *in vitro* and *in vivo* degradation rates would be necessary to make quantitative statements about toxicity. Furthermore, the question arises whether unstable chemicals have toxicological relevance, since such chemicals are usually degraded quickly in the environment and also in the body and so human exposure to these chemicals should be low.

Models for reactivity to proteins are mostly qualitative and based on structural alerts. Reactivity towards proteins in the bioassay medium represents an additional chemical loss source that could cause apparently lower *in vitro* effects. Moreover, these processes can indicate a mode of toxic action within the cell that is involved in different adverse outcomes such as neurotoxicity (Lopachin and Decaprio 2005), skin sensitization (Aptula et al. 2005) or hepatotoxicity (Yang et al. 2017). The measurement of chemical reaction rates with glutathione can usually be directly linked to toxicity *in vitro* and corresponding QSAR models have already been published for many *in vitro* systems (Harder et al. 2003b; Hermens 1990; Niederer et al. 2004). Overall, models for hydrolysis and protein reactivity can give an indication of possible transformation and *in vitro* data for affected chemicals should be carefully examined and experimental concentration measurements should be carried out if required.

Photooxidation was found to be negligible for *in vitro* systems with plate incubation in the dark, but can be more relevant for assays that require incubation under light (e.g. algae test) (Glauch and Escher 2020). Autooxidation could not be distinguished from hydrolysis without the identification of transformation products and is only relevant for chemicals with certain structural features (Hagvall et al. 2011).

4.4 Influence of biotic transformation processes on *in vitro* data

Classic biotic transformation by microorganisms is not possible in *in vitro* systems due to the sterile conditions, under which the assay is run. Biotic transformation by the cell lines, i.e., metabolism, can be considered as a loss process or part of the toxic response, where the formed metabolites are either of lower toxicity (detoxification) or higher toxicity (toxification, activation). Metabolism can only be considered as part of the toxic response if the cultured cells have similar metabolic capacity as cells *in vivo* (Coecke et al. 2006).

Reporter gene cell lines used in high-throughput chemical screening showed limited metabolic activity due to low CYP enzyme expression (Qu et al. 2021). However, the CYP enzyme activity of certain cell lines could be increased by xenobiotic chemicals such as benzo[a]pyrene (Fischer et al. 2020). The screening of 94 chemicals in three bioassays in *Publication III* showed that different metabolic activities had no significant effect on the bioassay results for the selected chemicals and assays. On the one hand, this means that the unintentional loss of chemicals through metabolism and the associated detoxification of test chemicals can be excluded for the majority of chemicals, which strengthens the significance of the obtained *in vitro* data. On the other hand, the lack of metabolic capacity of reporter gene cell lines represents an apparent discrepancy between the *in vitro* systems and the conditions that actually prevail *in vivo*. The *in vivo* formation of reactive (intermediate) metabolites leading to increased toxicity is particularly well known in drug development (Thompson et al. 2016) and also plays an important role in chemical risk assessment (Coecke et al. 2006).

Direct testing of known metabolites is often not possible because identification and quantification are expensive and time-consuming and metabolites are often not commercially available or unstable (Coecke et al. 2006). A better and therefore more widely used approach for the risk assessment of metabolites is to increase the metabolic competence of *in vitro* systems. This can be done with different approaches by adding either endogenous or exogenous metabolization systems. Endogenous metabolization is based on the use of metabolically competent cells and cell lines, such as primary or cryopreserved hepatocytes or various hepatoma cell lines (e.g. HepaRG), which express all relevant metabolic liver enzymes (Antherieu et al. 2012; Li et al. 2012a). The disadvantages of such cell-based systems include the biological variability and short lifetime of primary hepatocytes, as well as the lengthy and costly establishment of culture methods for such complex cell systems, which cannot be combined with high-throughput screening of chemicals (Combes et al. 2002). Exogenous metabolization systems normally use subcellular fractions, which are commercially available

and much simpler to use and are therefore routinely utilized for the identification of adverse effects of metabolites in the micronucleus or Ames test (OECD 2016; OECD 2020). The most common systems are S9 fractions or microsomes obtained from chemically induced rat livers, which contain the most important metabolizing enzymes (e.g., CYPs, glucuronosyltransferase, esterase). In most cases, cofactors such as nicotinamide adenine dinucleotide phosphate (NADPH) must be added for metabolic transformation (Ooka et al. 2020). The problem with these exogenous systems is the biological variability of the subcellular fractions and their animal origin, which is ethically questionable and does not fully represent human metabolizing enzymes. In addition, both S9 and microsomes show cytotoxic effects when dosed directly to the cells (Cox et al. 2016). Labor-intensive washing or extraction steps are necessary to avoid these artifacts, which are time-consuming and also carry the risk of losing unstable metabolites. Recently, immobilized S9 fractions were developed using alginate microspheres, which showed better compatibility with *in vitro* bioassays (Deisenroth et al. 2020). A promising alternative to the conventional methods using biological enzyme fractions are so-called biomimetic catalysts. These metalloporphyrins mimic the active side of CYP enzymes and catalyze a number of oxidation reactions of xenobiotic chemicals that are also catalyzed by biological CYP enzymes (Lohmann and Karst 2008). They have therefore been successfully used for the bioactivation of test substances for Ames tests (Inami et al. 2009). One disadvantage of biomimetic catalysts is their low regioselectivity compared to natural CYP enzymes (Chauhan et al. 2001). Apart from experimental methods for chemical metabolization, *in silico* models for the metabolization of chemicals, such as BioTransformer (Djoumbou-Feunang et al. 2019) or Metatox (Rudik et al. 2017) can be combined with *in vitro* bioassay data to predict possible effects in humans.

4.5 Using baseline toxicity to improve single chemical screening

The concept of baseline toxicity was introduced over 30 years ago (Verhaar et al. 1992) and can be used to evaluate the specificity of a toxic effect of a chemical. Instead of simply comparing measured effect concentrations of chemicals, they can be normalized to their minimal toxicity by calculating the toxic ratio (TR). Baseline toxicity occurs when chemicals accumulate in the cell membrane, leading to cellular dysfunction. This is why hydrophobic chemicals typically cause toxic effects at lower concentrations (Escher and Hermens 2002). These effects do not necessarily indicate a specific toxicity mechanism but rather indicate a stronger accumulation in the membrane. By using the TR as another indicator for toxicity, we can separate the hydrophobicity-driven component of toxicity, which essentially determines the internal concentration in cells (toxicokinetics) from the mode-of-action component of the effect (toxicodynamics).

To predict baseline toxicity for a broad range of chemicals with different physicochemical properties, a new baseline toxicity QSAR based on a newly derived critical membrane burden of 26 mmol/L_{lip} for 10% cytotoxicity ($IC_{10,membrane}$) was developed in *Publication III*. This critical membrane burden is more robust than the previously published $IC_{10,membrane}$ for *in vitro* bioassays (Escher et al. 2019), as it was determined on the basis of effect concentrations of hydrophilic chemicals or measured freely dissolved effect concentrations ($IC_{10,free}$) of ionizable chemicals. Hydrophilic chemicals do not bind to the proteins and lipids of the bioassay medium. Therefore, their nominal effect concentration is similar to $IC_{10,free}$. Thus, the critical membrane concentration can be derived directly from the measured effect concentrations of hydrophilic chemicals without having to consider the loss processes of the chemical due to partitioning to medium components. By including both hydrophilic and charged chemicals in the derivation of the QSAR model, it can be used to predict the baseline toxicity of neutral and charged chemicals, as well as hydrophilic chemicals, down to a $D_{lip/w}$ of -1.

Approximately half of the tested chemicals in *Publication III* could be identified as baseline toxicants without a specific toxicity mechanism and approximately a quarter to a third of the chemicals showed TR ≥ 10, indicating specific toxicity mechanisms. Chemicals showing TR < 0.1 were of special interest, as this artifact may suggest experimental artifacts or loss processes of the chemicals during the bioassay.

4.6 Recommendations for future work

In the past years, *in vitro* toxicology has made good progress with regard to exposure assessment of chemicals. The need to consider bioavailable chemical concentrations in bioassays is nowadays well recognized, especially if *in vitro* data is used for human risk assessment (Proenca et al. 2021). However, the need for high-throughput screening and the generation of big data sets, as well as a lack of instrumentation and expertise, are obstacles to the implementation of systematic concentration assessment of test chemicals. For this reason, it is important to further increase the awareness of the relevance of experimental concentration measurements and the application of models for exposure prediction. The ultimate goal is the development of a universal exposure assessment strategy for a wide range of chemicals and bioassays.

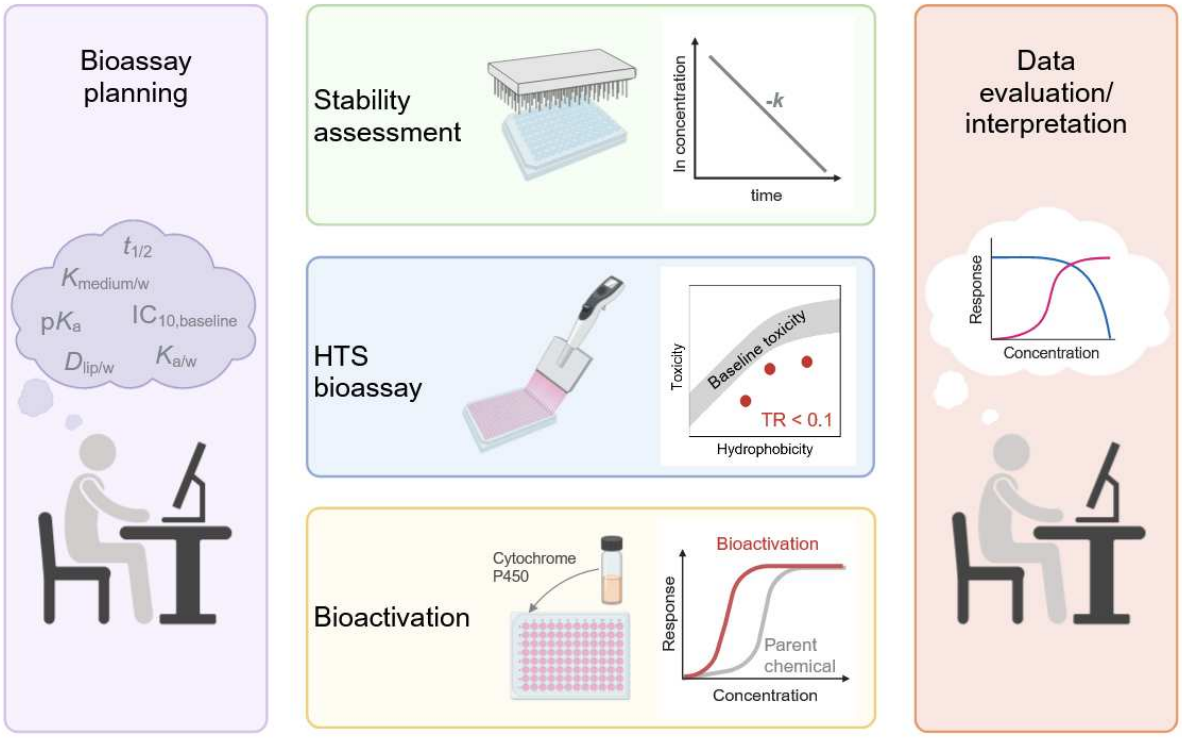

Figure 22: Proposed framework for exposure and stability assessment of chemicals in *in vitro* bioassays used for chemical risk assessment. $t_{1/2}$ = degradation half-life, $K_{medium/w}$ = medium-water partitioning constant, $IC_{10,baseline}$ = baseline toxicity for 10% inhibition of cell viability, $D_{lip/w}$ = liposome-water distribution ratio, $K_{a/w}$ = air-water partitioning constant, $-k$ = pseudo-first-order degradation rate constant, TR = toxic ratio, CYP = cytochrome P450 enzyme

Figure 22 shows a framework for the investigation of exposure and stability of chemicals in the *in vitro* bioassay, which summarizes the most important findings of this work. The framework provides information on the necessary steps in bioassay dosing, performance

and interpretation to identify chemicals for which experimental exposure measurements are necessary, e.g. unstable chemicals, and gives guidance how abiotic and biotic transformation can be further investigated.

4.6.1 Bioassay dosing planning

Prior to the bioassay, physicochemical properties of the chemicals should be compiled and carefully reviewed. QSARs can be used to model physicochemical properties used as input parameters, but experimentally measured physicochemical properties should be used if available to increase the accuracy of the exposure predictions. Exposure predictions should also be used to plan dosing of chemicals based on their maximum solubility in bioassay medium (Fischer et al. 2019). Chemicals with $K_{medium/air}$ below the volatility cut-off for *in vitro* bioassays ($K_{medium/air} \leq 10{,}000$ L/L) are out of the applicability domain of standard HTS bioassays (Escher et al. 2019). Precautions should also be taken when dosing semi-volatile chemicals, such as sealing the test plate with air-permeable films and filling rows only with medium between rows with chemicals to prevent contamination of neighboring wells (Escher et al. 2019). In addition, chemically defined media without animal components, such as FBS (Rafnsdottir et al. 2023; van der Valk et al. 2010), should be used when possible to minimize the variation in protein and lipid content and thus provide reproducible exposure conditions. Furthermore, baseline toxicity models should be used to predict the minimal toxicity as an anchor for dosing concentrations (normally three times $IC_{10,baseline}$) if this is below medium solubility. For this purpose, the already published baseline toxicity models for cell-based assays (*Publication III* and (Escher et al. 2019; Lee et al. 2021; Qin et al. 2024)) should be reviewed and validated in order to be able to make a clear prediction for each substance class. *In silico* models for the prediction of hydrolytic stability, possible reactivity toward proteins or biotransformation should be used to obtain first indications of possible instability.

4.6.2 Execution of HTS bioassays and interpretation of the results

In vitro bioassays in high-throughput format should be performed according to best scientific practice with a high degree of standardization and automation. Bioassays normally apply a large number of quality controls, such as a sufficient number of replicates, negative and positive controls or long-term records of reference chemicals to ensure high data quality. Directly using nominal effect concentrations from *in vitro* bioassays can be sufficient to estimate the risk of chemicals, but for certain groups of chemicals, exposure in the bioassay must be considered and C_{free} can be a better dose metric than the nominal concentration. For a large number of chemical classes, exposure can already be predicted using existing mass-

balance models. For example, loss processes due to partitioning to media components, plastic or the air are considered by these models (Escher et al. 2019; Fischer et al. 2018b; Fischer et al. 2017). However, irreversible loss processes due to abiotic or biotic degradation cannot be modeled quantitatively. Predictions from mass balance models are only reliable if the chemical concentration remains stable over time. Based on the $IC_{10,baseline}$, the toxic ratio (TR) can be calculated to assess the specificity of chemical toxicity compared to baseline toxicity. In addition, a TR < 0.1 should be considered an indicator of experimental artifacts and the data of the respective chemicals should be critically reviewed or experiments repeated to exclude experimental errors. If experimental errors can be excluded, chemical transformation processes should be considered as a cause for bioassay artifacts.

4.6.3 Stability assessment

The chemical stability should be determined experimentally for suspect chemicals with predicted transformation and/or TR < 0.1. By focusing on the susceptible chemicals, the number of experiments can be greatly reduced. However, it should be kept in mind that TR < 0.1 only indicate artifacts or degradation for baseline toxicants, whereas for specifically acting chemicals these processes could only lead to a lower TR or a wrong classification as baseline toxicants. Direct exposure measurements in the *in vitro* bioassay would allow the best estimation of chemical stability. However, such detailed investigations are often not possible in a high-throughput environment without analytical capacities. Nevertheless, at least the concentration at the beginning of the bioassay should be compared with the concentration at the end of the bioassay in order to exclude transformation processes. Alternatively, the framework for stability testing provided in *Publication I* can be used to unravel the transformation processes involved (hydrolysis and reactivity toward proteins) and measure degradation half-lives. Measuring the reaction rate constant of chemicals with GSH may give an indication of reactive toxicity in the bioassay. Some chemicals can form toxic transformation products, which usually occurs through metabolic transformation, but is also possible abiotically, for example, the formation of disinfection by-products in water treatment (Mian et al. 2018). Most *in vitro* reporter gene cell lines show only low metabolic activity and cannot reproduce the bioactivation of test chemicals. For this reason, test chemicals must be transformed using external metabolism systems to assess the toxicity of the metabolites. However, there is a lack of standardized methods for this metabolization and existing methods often cause bioassay artifacts and are based on animal materials (Coecke et al. 2006). The novel approach of using biomimetic catalysts for the bioactivation of chemicals represents a promising alternative to conventional methods and should therefore be investigated in the future for its compatibility with *in vitro*

bioassays and the comparability of the metabolites formed with the *in vivo* situation. Chemicals can be screened with and without bioactivation and thus the effects of possible metabolites can be determined. The implementation of such a system would significantly increase the relevance of *in vitro* data for human risk assessment, as the lack of metabolic capacity has been a major disadvantage of *in vitro* bioassays to date.

5. References

Adeleye Y, Andersen M, Clewell R, Davies M, Dent M, Edwards S, Fowler P, Malcomber S, Nicol B, Scott A, Scott S, Sun B, Westmoreland C, White A, Zhang Q, Carmichael PL (2015) Implementing Toxicity Testing in the 21st Century (TT21C): Making safety decisions using toxicity pathways, and progress in a prototype risk assessment. Toxicology 332:102-11

Alsante KM, Huynh-Ba K, Baertschi SW, Reed RA, Landis MS, Kleinman MH, Foti C, Rao VM, Meers P, Abend A, Reynolds DW, Joshi BK (2014) Recent trends in product development and regulatory issues on impurities in active pharmaceutical ingredient (API) and drug products. Part 1: Predicting degradation related impurities and impurity considerations for pharmaceutical dosage forms. AAPS PharmSciTech 15(1):198-212

Altshuller AP, Cohen IR, Sleva SF, Kopczynski SL (1962) Air pollution: photooxidation of aromatic hydrocarbons. Science 138(3538):442-3

Andersen ME, Krewski D (2009) Toxicity testing in the 21st century: bringing the vision to life. Toxicol Sci 107(2):324-30

Ankley GT, Bennett RS, Erickson RJ, Hoff DJ, Hornung MW, Johnson RD, Mount DR, Nichols JW, Russom CL, Schmieder PK, Serrrano JA, Tietge JE, Villeneuve DL (2010) Adverse outcome pathways: a conceptual framework to support ecotoxicology research and risk assessment. Environ Toxicol Chem 29(3):730-41

Antherieu S, Chesne C, Li R, Guguen-Guillouzo C, Guillouzo A (2012) Optimization of the HepaRG cell model for drug metabolism and toxicity studies. Toxicol In Vitro 26(8):1278-85

Aptula AO, Enoch SJ, Roberts DW (2009) Chemical mechanisms for skin sensitization by aromatic compounds with hydroxy and amino groups. Chem Res Toxicol 22(9):1541-7

Aptula AO, Patlewicz G, Roberts DW (2005) Skin sensitization: reaction mechanistic applicability domains for structure-activity relationships. Chem Res Toxicol 18(9):1420-6

Armitage JM, Sangion A, Parmar R, Looky AB, Arnot JA (2021) Update and Evaluation of a High-Throughput In Vitro Mass Balance Distribution Model: IV-MBM EQP v2.0. Toxics 9(11):315

Armitage JM, Wania F, Arnot JA (2014) Application of mass balance models and the chemical activity concept to facilitate the use of in vitro toxicity data for risk assessment. Environ Sci Technol 48(16):9770-9

Arp HPH, Aurich D, Schymanski EL, Sims K, Hale SE (2023) Avoiding the Next Silent Spring: Our Chemical Past, Present, and Future. Environ Sci Technol 57(16):6355-6359

Arthur CL, Pawliszyn J (1990) Solid-Phase Microextraction with Thermal-Desorption Using Fused-Silica Optical Fibers. Anal Chem 62(19):2145-2148

Bajaj S, Singh S (2018) Methods for Stability Testing of Pharmaceuticals, vol 1. Humana Press, New York, NY

Barnham KJ, Masters CL, Bush AI (2004) Neurodegenerative diseases and oxidative stress. Nat Rev Drug Discov 3(3):205-214

Bent GA, Maragh P, Dasgupta T, Fairman RA, Grierson L (2015) Kinetic and density functional theory (DFT) studies of in vitro reactions of acrylamide with the thiols: captopril, L-cysteine, and glutathione. Toxicol Res-Uk 4(1):121-131

Blaschke U, Eismann K, Böhme A, Paschke A, Schüürmann G (2012) Structural alerts for the excess toxicity of acrylates, methacrylates, and propiolates derived from their short-term and long-term bacterial toxicity. Chem Res Toxicol 25(1):170-80

Bogen KT (2017) Low-Dose Dose-Response for In Vitro Nrf2-ARE Activation in Human HepG2 Cells. Dose Response 15(2):1559325817699696

Bouyacoub A, Jean Y, Volatron F (1996) Hydrolysis of unsubstituted and alkyl-substituted aziridinium cations: selectivity and reaction mechanism (SN1 vs. SN2). J Mol Struct: THEOCHEM 371:51-57

Brunner D, Frank J, Appl H, Schöffl H, Pfaller W, Gstraunthaler G (2010) The serum-free media interactive online database. ALTEX 27(1):53-62

Burden N, Chapman K, Sewell F, Robinson V (2015) Pioneering better science through the 3Rs: an introduction to the national centre for the replacement, refinement, and reduction of animals in research (NC3Rs). J Am Assoc Lab Anim Sci 54(2):198-208

Buscher B, Laakso S, Mascher H, Pusecker K, Doig M, Dillen L, Wagner-Redeker W, Pfeifer T, Delrat P, Timmerman P (2014) Bioanalysis for plasma protein binding studies in drug discovery and drug development: views and recommendations of the European Bioanalysis Forum. Bioanalysis 6(5):673-682

Caldwell J, Gardner I, Swales N (1995) An introduction to drug disposition: the basic principles of absorption, distribution, metabolism, and excretion. Toxicol Pathol 23(2):102-14

Chauhan SM, Kandadai SA, Sahoo B (2001) Regioselective biomimetic oxidation of etodolac with iodosylbenzene catalyzed by halogenated and perhalogenated metalloporphyrins in dichloromethane. Chem Pharm Bull (Tokyo) 49(10):1375-6

Choi JM, Oh SJ, Lee SY, Im JH, Oh JM, Ryu CS, Kwak HC, Lee JY, Kang KW, Kim SK (2015) HepG2 cells as an in vitro model for evaluation of cytochrome P450 induction by xenobiotics. Arch Pharm Res 38(5):691-704

Chu V, Einolf HJ, Evers R, Kumar G, Moore D, Ripp S, Silva J, Sinha V, Sinz M, Skerjanec A (2009) In vitro and in vivo induction of cytochrome p450: a survey of the current practices and recommendations: a pharmaceutical research and manufacturers of america perspective. Drug Metab Dispos 37(7):1339-54

Coecke S, Ahr H, Blaauboer BJ, Bremer S, Casati S, Castell J, Combes R, Corvi R, Crespi CL, Cunningham ML, Elaut G, Eletti B, Freidig A, Gennari A, Ghersi-Egea JF, Guillouzo A, Hartung T, Hoet P, Ingelman-Sundberg M, Munn S, Janssens W, Ladstetter B, Leahy D, Long A, Meneguz A, Monshouwer M, Morath S, Nagelkerke F, Pelkonen O, Ponti J, Prieto P, Richert L, Sabbioni E, Schaack B, Steiling W, Testai E, Vericat JA, Worth A (2006) Metabolism: a bottleneck in in vitro toxicological test development. The report and recommendations of ECVAM workshop 54. Altern Lab Anim 34(1):49-84

Combes R, Balls M, Bansil L, Barratt M, Bell D, Botham P, Broadhead C, Clothier R, George E, Fentem J, Jackson M, Indans I, Loizu G, Navaratnam V, Pentreath V, Phillips B, Stemplewski H, Stewart J (2002) An assessment of progress in the use of alternatives in toxicity testing since the publication of the report of the second FRAME Toxicity Committee (1991). Altern Lab Anim 30(4):365-406

Cox JA, Fellows MD, Hashizume T, White PA (2016) The utility of metabolic activation mixtures containing human hepatic post-mitochondrial supernatant (S9) for in vitro genetic toxicity assessment. Mutagenesis 31(2):117-30

Croom E (2012) Metabolism of xenobiotics of human environments. Prog Mol Biol Transl Sci 112:31-88

Crounse JD, Nielsen LB, Jorgensen S, Kjaergaard HG, Wennberg PO (2013) Autoxidation of Organic Compounds in the Atmosphere. Journal of Physical Chemistry Letters 4(20):3513-3520

Davis JM (2002) Basic Cell Culture Second Edition: A Practical Approach, 2 edn. Oxford University Press, Oxford

Deisenroth C, DeGroot DE, Zurlinden T, Eicher A, McCord J, Lee MY, Carmichael P, Thomas RS (2020) The Alginate Immobilization of Metabolic Enzymes Platform Retrofits an Estrogen Receptor Transactivation Assay With Metabolic Competence. Toxicol Sci 178(2):281-301

Denisov IG, Makris TM, Sligar SG, Schlichting I (2005) Structure and chemistry of cytochrome P450. Chem Rev 105(6):2253-77

Dent MP, Vaillancourt E, Thomas RS, Carmichael PL, Ouedraogo G, Kojima H, Barroso J, Ansell J, Barton-Maclaren TS, Bennekou SH, Boekelheide K, Ezendam J, Field J, Fitzpatrick S, Hatao M, Kreiling R, Lorencini M, Mahony C, Montemayor B, Mazaro-Costa R, Oliveira J, Rogiers V, Smegal D, Taalman R, Tokura Y, Verma R, Willett C, Yang C (2021) Paving the way for application of next generation risk assessment to safety decision-making for cosmetic ingredients. Regul Toxicol Pharmacol 125:105026

Deshmukh P, Unni S, Krishnappa G, Padmanabhan B (2017) The Keap1-Nrf2 pathway: promising therapeutic target to counteract ROS-mediated damage in cancers and neurodegenerative diseases. Biophys Rev 9(1):41-56

Dimitrov SD, Diderich R, Sobanski T, Pavlov TS, Chankov GV, Chapkanov AS, Karakolev YH, Temelkov SG, Vasilev RA, Gerova KD, Kuseva CD, Todorova ND, Mehmed AM, Rasenberg M, Mekenyan OG (2016) QSAR Toolbox - workflow and major functionalities. SAR QSAR Environ Res 27(3):203-219

Divkovic M, Pease CK, Gerberick GF, Basketter DA (2005) Hapten-protein binding: from theory to practical application in the in vitro prediction of skin sensitization. Contact Dermatitis 53(4):189-200
Dixit R, Riviere J, Krishnan K, Andersen ME (2003) Toxicokinetics and physiologically based toxicokinetics in toxicology and risk assessment. J Toxicol Environ Health B Crit Rev 6(1):1-40
Djoumbou-Feunang Y, Fiamoncini J, Gil-de-la-Fuente A, Greiner R, Manach C, Wishart DS (2019) BioTransformer: a comprehensive computational tool for small molecule metabolism prediction and metabolite identification. J Cheminform 11(1):2
EC (2016) Commission Regulation (EU) 2016/2235 of 12 December 2016 amending Annex XVII to Regulation (EC) No 1907/2006 of the European Parliament and of the Council concerning the Registration, Evaluation, Authorisation and Restriction of Chemicals (REACH) as regards bisphenol A.
EC (2020) Communication from the Commission to the European Parliament, the Council, the European Economic and Social Committee and the Committee of the Regions. Chemicals Strategy for Sustainability Towards a Toxic-Free Environment., Brussels
ECHA (2023a) Annex XV Restriction Report: Proposal for a Restriction.
ECHA (2023b) REACH Registration Statistics. In. https://echa.europa.eu/documents/10162/2741157/registration_statistics_en.pdf/58c2d7bd-2173-4cb9-eb3b-a6bc14a6754b?t=1686750748164 Accessed 07.11.2023
Endo S, Bauerfeind J, Goss KU (2012) Partitioning of neutral organic compounds to structural proteins. Environ Sci Technol 46(22):12697-703
Endo S, Escher BI, Goss KU (2011) Capacities of Membrane Lipids to Accumulate Neutral Organic Chemicals. Environ Sci Technol 45(14):5912-5921
Endo S, Goss KU (2011) Serum albumin binding of structurally diverse neutral organic compounds: data and models. Chem Res Toxicol 24(12):2293-301
Enoch SJ, Ellison CM, Schultz TW, Cronin MT (2011) A review of the electrophilic reaction chemistry involved in covalent protein binding relevant to toxicity. Crit Rev Toxicol 41(9):783-802
Enoch SJ, Roberts DW, Cronin MT (2009) Electrophilic Reaction Chemistry of Low Molecular Weight Respiratory Sensitizers. Chem Res Toxicol 22(8):1447-1453
Enslein K (1988) An Overview of Structure-Activity Relationships as an Alternative To Testing in Animals for Carcinogenicity, Mutagenicity, Dermal and Eye Irritation, and Acute Oral Toxicity. Toxicol Ind Health 4(4):479-498
EP&EC (2006) Regulation (EC) No 1907/2006 of the European Parliament and of the Council of 18 December 2006 concerning the Registration, Evaluation, Authorisation and Restriction of Chemicals (REACH), establishing a European Chemicals Agency, amending Directive 1999/45/EC and repealing Council Regulation (EEC) No 793/93 and Commission Regulation (EC) No 1488/94 as well as Council Directive 76/769/EEC and Commission Directives 91/155/EEC, 93/67/EEC, 93/105/EC and 2000/21/EC (Text with EEA relevance)
EPA (1998) ENVIRONMENTAL FATE DATABASE (ENVIROFATE). In. https://cfpub.epa.gov/si/si_public_record_report.cfm?Lab=&dirEntryId=2896
EPA (2012) Estimation Programs Interface Suite™ for Microsoft® Windows, v 4.11. United States Environmental Protection Agency, Washington, DC, USA
EPA (2019) CTS: Chemical Transformation Simulator. In. https://qed.epa.gov/cts/gentrans/ 2021
Escher BI, Neale P, Leusch F (2021) Modes of action and toxicity pathways Bioanalytical Tools in Water Quality Assessment. IWA Publishing
Escher BI, Baumer A, Bittermann K, Henneberger L, König M, Kühnert C, Klüver N (2017) General baseline toxicity QSAR for nonpolar, polar and ionisable chemicals and their mixtures in the bioluminescence inhibition assay with Aliivibrio fischeri. Environ Sci Process Impacts 19(3):414-428
Escher BI, Berg M, Muhlemann J, Schwarz MA, Hermens JL, Vaes WH, Schwarzenbach RP (2002) Determination of liposome/water partition coefficients of organic acids and bases by solid-phase microextraction. Analyst 127(1):42-8
Escher BI, Dutt M, Maylin E, Tang JY, Toze S, Wolf CR, Lang M (2012) Water quality assessment using the AREc32 reporter gene assay indicative of the oxidative stress response pathway. J Environ Monit 14(11):2877-85

Escher BI, Glauch L, König M, Mayer P, Schlichting R (2019) Baseline Toxicity and Volatility Cutoff in Reporter Gene Assays Used for High-Throughput Screening. Chem Res Toxicol 32(8):1646-1655

Escher BI, Henneberger L, König M, Schlichting R, Fischer FC (2020) Cytotoxicity Burst? Differentiating Specific from Nonspecific Effects in Tox21 in Vitro Reporter Gene Assays. Environ Health Perspect 128(7):77007

Escher BI, Hermens JL (2002) Modes of action in ecotoxicology: their role in body burdens, species sensitivity, QSARs, and mixture effects. Environ Sci Technol 36(20):4201-17

Escher BI, Neale PA, Villeneuve DL (2018) The advantages of linear concentration-response curves for in vitro bioassays with environmental samples. Environ Toxicol Chem 37(9):2273-2280

Escher BI, Schwarzenbach RP (2002) Mechanistic studies on baseline toxicity and uncoupling of organic compounds as a basis for modeling effective membrane concentrations in aquatic organisms. Aquat Sci 64(1):20-35

Esteves F, Rueff J, Kranendonk M (2021) The Central Role of Cytochrome P450 in Xenobiotic Metabolism-A Brief Review on a Fascinating Enzyme Family. J Xenobiot 11(3):94-114

Fenner K, Canonica S, Wackett LP, Elsner M (2013) Evaluating pesticide degradation in the environment: blind spots and emerging opportunities. Science 341(6147):752-8

Fischer FC, Abele C, Droge STJ, Henneberger L, König M, Schlichting R, Scholz S, Escher BI (2018a) Cellular Uptake Kinetics of Neutral and Charged Chemicals in in Vitro Assays Measured by Fluorescence Microscopy. Chem Res Toxicol 31(8):646-657

Fischer FC, Abele C, Henneberger L, Klüver N, König M, Mühlenbrink M, Schlichting R, Escher BI (2020) Cellular Metabolism in High-Throughput In Vitro Reporter Gene Assays and Implications for the Quantitative In Vitro-In Vivo Extrapolation. Chem Res Toxicol 33(7):1770-1779

Fischer FC, Cirpka OA, Goss KU, Henneberger L, Escher BI (2018b) Application of Experimental Polystyrene Partition Constants and Diffusion Coefficients to Predict the Sorption of Neutral Organic Chemicals to Multiwell Plates in in Vivo and in Vitro Bioassays. Environ Sci Technol 52(22):13511-13522

Fischer FC, Henneberger L, König M, Bittermann K, Linden L, Goss KU, Escher BI (2017) Modeling Exposure in the Tox21 in Vitro Bioassays. Chem Res Toxicol 30(5):1197-1208

Fischer FC, Henneberger L, Schlichting R, Escher BI (2019) How To Improve the Dosing of Chemicals in High-Throughput in Vitro Mammalian Cell Assays. Chem Res Toxicol 32(8):1462-1468

Flaskos J (2012) The developmental neurotoxicity of organophosphorus insecticides: a direct role for the oxon metabolites. Toxicol Lett 209(1):86-93

Foti C, Alsante K, Cheng G, Zelesky T, Zell M (2013) Tools and workflow for structure elucidation of drug degradation products. TrAC Trends Anal Chem 49:89-99

Freidig AP, Verhaar HJM, Hermens JLM (1999a) Comparing the potency of chemicals with multiple modes of action in aquatic toxicology: Acute toxicity due to narcosis versus reactive toxicity of acrylic compounds. Environ Sci Technol 33(17):3038-3043

Freidig AP, Verhaar HJM, Hermens JLM (1999b) Quantitative structure-property relationships for the chemical reactivity of acrylates and methacrylates. Environ Toxicol Chem 18(6):1133-1139

Geisler A, Endo S, Goss KU (2012) Partitioning of Organic Chemicals to Storage Lipids: Elucidating the Dependence on Fatty Acid Composition and Temperature. Environ Sci Technol 46(17):9519-9524

Glauch L, Escher BI (2020) The Combined Algae Test for the Evaluation of Mixture Toxicity in Environmental Samples. Environ Toxicol Chem 39(12):2496-2508

Gobas FA, Lahittete JM, Garofalo G, Shiu WY, Mackay D (1988) A novel method for measuring membrane-water partition coefficients of hydrophobic organic chemicals: comparison with 1-octanol-water partitioning. J Pharm Sci 77(3):265-72

Gore AC, Chappell VA, Fenton SE, Flaws JA, Nadal A, Prins GS, Toppari J, Zoeller RT (2015) EDC-2: The Endocrine Society's Second Scientific Statement on Endocrine-Disrupting Chemicals. Endocr Rev 36(6):E1-E150

Gorrini C, Harris IS, Mak TW (2013) Modulation of oxidative stress as an anticancer strategy. Nat Rev Drug Discov 12(12):931-947

Groothuis FA, Heringa MB, Nicol B, Hermens JL, Blaauboer BJ, Kramer NI (2015) Dose metric considerations in in vitro assays to improve quantitative in vitro-in vivo dose extrapolations. Toxicology 332:30-40
Gülden M, Seibert H (1997) Influence of protein binding and lipophilicity on the distribution of chemical compounds in in vitro systems. Toxicol In Vitro 11(5):479-83
Gülden M, Seibert H (2003) In vitro-in vivo extrapolation: estimation of human serum concentrations of chemicals equivalent to cytotoxic concentrations in vitro. Toxicology 189(3):211-22
Hagvall L, Backtorp C, Norrby PO, Karlberg AT, Borje A (2011) Experimental and theoretical investigations of the autoxidation of geranial: a dioxolane hydroperoxide identified as a skin sensitizer. Chem Res Toxicol 24(9):1507-15
Hale SE, Arp HPH, Schliebner I, Neumann M (2020) Persistent, mobile and toxic (PMT) and very persistent and very mobile (vPvM) substances pose an equivalent level of concern to persistent, bioaccumulative and toxic (PBT) and very persistent and very bioaccumulative (vPvB) substances under REACH. Environ Sci Eur 32(1):155
Harder A, Escher BI, Landini P, Tobler NB, Schwarzenbach RP (2003a) Evaluation of bioanalytical assays for toxicity assessment and mode of toxic action classification of reactive chemicals. Environ Sci Technol 37(21):4962-70
Harder A, Escher BI, Schwarzenbach RP (2003b) Applicability and limitation of OSARs for the toxicity of electrophilic chemicals. Environ Sci Technol 37(21):4955-61
Hartung T (2011) From alternative methods to a new toxicology. Eur J Pharm Biopharm 77(3):338-49
Hegarty AF, Frost LN (1973) Elimination–addition mechanism for the hydrolysis of carbamates. Trapping of an isocyanate intermediate by an o-amino-group. J Chem Soc, Perkin Transactions 2(12):1719-1728
Henneberger L, Goss KU, Endo S (2016) Partitioning of Organic Ions to Muscle Protein: Experimental Data, Modeling, and Implications for in Vivo Distribution of Organic Ions. Environ Sci Technol 50(13):7029-36
Henneberger L, Mühlenbrink M, Fischer FC, Escher BI (2019a) C18-Coated Solid-Phase Microextraction Fibers for the Quantification of Partitioning of Organic Acids to Proteins, Lipids, and Cells. Chem Res Toxicol 32(1):168-178
Henneberger L, Mühlenbrink M, Heinrich DJ, Teixeira A, Nicol B, Escher BI (2020) Experimental Validation of Mass Balance Models for in Vitro Cell-Based Bioassays. Environ Sci Technol 54(2):1120-1127
Henneberger L, Mühlenbrink M, König M, Schlichting R, Fischer FC, Escher BI (2019b) Quantification of freely dissolved effect concentrations in in vitro cell-based bioassays. Arch Toxicol 93(8):2295-2305
Heringa MB, Schreurs RH, van der Saag PT, van der Burg B, Hermens JLM (2003) Measurement of free concentration as a more intrinsic dose parameter in an in vitro assay for estrogenic activity. Chem Res Toxicol 16(12):1662-1663
Heringa MB, Schreurs RH, Busser F, van der Saag PT, van der Burg B, Hermens JLM (2004) Toward more useful in vitro toxicity data with measured free concentrations. Environ Sci Technol 38(23):6263-70
Hermens JLM (1990) Electrophiles and acute toxicity to fish. Environ Health Perspect 87:219-25
Howard PH, Meylan WM (1992) Hydrolysis Rate Program. Taylor & Francis
Huchthausen J, König M, Escher BI, Henneberger L (2023) Experimental exposure assessment for in vitro cell-based bioassays in 96- and 384-well plates. Front Toxicol 5
Huchthausen J, Mühlenbrink M, König M, Escher BI, Henneberger L (2020) Experimental Exposure Assessment of Ionizable Organic Chemicals in In Vitro Cell-Based Bioassays. Chem Res Toxicol 33(7):1845-1854
Inami K, Okazawa M, Mochizuki M (2009) Mutagenicity of aromatic amines and amides with chemical models for cytochrome P450 in Ames assay. Toxicol In Vitro 23(6):986-91
Iyanagi T (2007) Molecular mechanism of phase I and phase II drug-metabolizing enzymes: implications for detoxification. Int Rev Cytol 260:35-112
Jiang C, Garg S, Waite TD (2015) Hydroquinone-Mediated Redox Cycling of Iron and Concomitant Oxidation of Hydroquinone in Oxic Waters under Acidic Conditions: Comparison with Iron-Natural Organic Matter Interactions. Environ Sci Technol 49(24):14076-84

JRC, Bouhifd M, Rodrigues R, Mennecozzi M, Zaldívar J (2010) A biology-based dynamic approach for the modelling of toxicity in cell-based assays. Part I, fate modelling. Publications Office
JRC, Macko P, Zaldívar J, Mennecozzi M, Rodrigues R, Bouhifd M, Baraibar J (2011) A biology-based dynamic approach for the modelling of toxicity in cell assays. part II, models for cell population growth and toxicity. Publications Office
Judson RS, Houck KA, Martin MT, Richard AM, Knudsen TB, Shah I, Little S, Wambaugh J, Woodrow Setzer R, Kothiya P, Phuong J, Filer D, Smith D, Reif DM, Rotroff D, Kleinstreuer N, Sipes N, Xia M, Huang R, Crofton K, Thomas RS (2016) Editor's Highlight: Analysis of the Effects of Cell Stress and Cytotoxicity on In Vitro Assay Activity Across a Diverse Chemical and Assay Space. Toxicol Sci 152(2):323-39
Judson RS, Houck KA, Kavlock RJ, Knudsen TB, Martin MT, Mortensen HM, Reif DM, Rotroff DM, Shah I, Richard AM, Dix DJ (2010) In vitro screening of environmental chemicals for targeted testing prioritization: the ToxCast project. Environ Health Perspect 118(4):485-92
Ketterer B (1982) The role of nonenzymatic reactions of glutathione in xenobiotic metabolism. Drug Metab Rev 13(1):161-87
Kim RB (2002) Transporters and xenobiotic disposition. Toxicology 181-182:291-7
Kisitu J, Hollert H, Fisher C, Leist M (2020) Chemical concentrations in cell culture compartments (C5) - free concentrations. ALTEX 37(4):693-708
Klüver N, Vogs C, Altenburger R, Escher BI, Scholz S (2016) Development of a general baseline toxicity QSAR model for the fish embryo acute toxicity test. Chemosphere 164:164-173
Könemann H (1981) Quantitative structure-activity relationships in fish toxicity studies Part 1: Relationship for 50 industrial pollutants. Toxicology 19(3):209-221
König M, Escher BI, Neale PA, Krauss M, Hilscherova K, Novak J, Teodorovic I, Schulze T, Seidensticker S, Kamal Hashmi MA, Ahlheim J, Brack W (2017) Impact of untreated wastewater on a major European river evaluated with a combination of in vitro bioassays and chemical analysis. Environ Pollut 220(Pt B):1220-1230
Kramer NI (2010) Measuring, Modeling, and Increasing the Free Concentration of Test Chemicals in Cell Assays. University of Utrecht
Kramer NI, Busser FJ, Oosterwijk MT, Schirmer K, Escher BI, Hermens JLM (2010) Development of a partition-controlled dosing system for cell assays. Chem Res Toxicol 23(11):1806-14
Kumar P, Arshad M, Gacem A, Soni S, Singh S, Kumar M, Yadav VK, Tariq M, Kumar R, Shah D, Wanale SG, Al Mesfer MKM, Bhutto JK, Yadav KK (2023) Insight into the environmental fate, hazard, detection, and sustainable degradation technologies of chlorpyrifos-an organophosphorus pesticide. Environ Sci Pollut Res Int 30(50):108347-108369
LeBlanc GA (2008) Chapter 12 - Phase II Conjugation of Toxicants. In: Smart RC, Hodgson E (eds) Molecular and Biochemical Toxicology. vol 4th ed John Wiley New York
Lee J, Braun G, Henneberger L, König M, Schlichting R, Scholz S, Escher BI (2021) Critical Membrane Concentration and Mass-Balance Model to Identify Baseline Cytotoxicity of Hydrophobic and Ionizable Organic Chemicals in Mammalian Cell Lines. Chem Res Toxicol 34(9):2100-2109
Leist M, Hartung T (2013) Inflammatory findings on species extrapolations: humans are definitely no 70-kg mice. Arch Toxicol 87(4):563-567
Lewis GN (1923) Valence and the Structure of Atoms and Molecules. Chemical Catalog Company, Incorporated
Li AP, Uzgare A, LaForge YS (2012a) Definition of metabolism-dependent xenobiotic toxicity with co-cultures of human hepatocytes and mouse 3T3 fibroblasts in the novel integrated discrete multiple organ co-culture (IdMOC) experimental system: results with model toxicants aflatoxin B1, cyclophosphamide and tamoxifen. Chem Biol Interact 199(1):1-8
Li H, Qian W, Weng X, Wu Z, Li H, Zhuang Q, Feng B, Bian Y (2012b) Glucocorticoid receptor and sequential P53 activation by dexamethasone mediates apoptosis and cell cycle arrest of osteoblastic MC3T3-E1 cells. PLoS One 7(6):e37030
Lohmann W, Karst U (2008) Biomimetic modeling of oxidative drug metabolism : Strategies, advantages and limitations. Anal Bioanal Chem 391(1):79-96
Lopachin RM, Decaprio AP (2005) Protein adduct formation as a molecular mechanism in neurotoxicity. Toxicol Sci 86(2):214-25
LoPachin RM, Gavin T (2012) Molecular mechanism of acrylamide neurotoxicity: lessons learned from organic chemistry. Environ Health Perspect 120(12):1650-7

Lopachin RM, Gavin T, Decaprio AP, Barber DS (2012) Application of the Hard and Soft, Acids and Bases (HSAB) theory to toxicant-target interactions. Chem Res Toxicol 25(2):239-51
Maeder V, Escher BI, Scheringer M, Hungerbuhler K (2004) Toxic ratio as an indicator of the intrinsic toxicity in the assessment of persistent, bioaccumulative, and toxic chemicals. Environ Sci Technol 38(13):3659-66
Maggio SA, Janney PK, Jenkins JJ (2021) Neurotoxicity of chlorpyrifos and chlorpyrifos-oxon to Daphnia magna. Chemosphere 276:130120
Magurany KA, Chang X, Clewell R, Coecke S, Haugabrooks E, Marty S (2023) A Pragmatic Framework for the Application of New Approach Methodologies in One Health Toxicological Risk Assessment. Toxicol Sci 192(2):155-77
Mansouri A, Cregut M, Abbes C, Durand MJ, Landoulsi A, Thouand G (2017) The Environmental Issues of DDT Pollution and Bioremediation: a Multidisciplinary Review. Appl Biochem Biotechnol 181(1):309-339
McCarthy TJ, Hayes EP, Schwartz CS, Witz G (1994) The reactivity of selected acrylate esters toward glutathione and deoxyribonucleosides in vitro: structure-activity relationships. Fundam Appl Toxicol 22(4):543-8
Mccarty LS (1986) The relationship between aquatic toxicity QSARs and bioconcentration for some organic chemicals. Environ Toxicol Chem 5(12):1071-1080
Mian HR, Hu G, Hewage K, Rodriguez MJ, Sadiq R (2018) Prioritization of unregulated disinfection by-products in drinking water distribution systems for human health risk mitigation: A critical review. Water Res 147:112-131
Michl J, Park KC, Swietach P (2019) Evidence-based guidelines for controlling pH in mammalian live-cell culture systems. Commun Biol 2:144
Moxon TE, Li H, Lee MY, Piechota P, Nicol B, Pickles J, Pendlington R, Sorrell I, Baltazar MT (2020) Application of physiologically based kinetic (PBK) modelling in the next generation risk assessment of dermally applied consumer products. Toxicol In Vitro 63:104746
Muir DCG, Getzinger GJ, McBride M, Ferguson PL (2023) How Many Chemicals in Commerce Have Been Analyzed in Environmental Media? A 50 Year Bibliometric Analysis. Environ Sci Technol 57(25):9119-9129
Musteata ML, Musteata FM, Pawliszyn J (2007) Biocompatible Solid-Phase Microextraction Coatings Based on Polyacrylonitrile and Solid-Phase Extraction Phases. Anal Chem 79(18):6903-6911
Neale PA, Altenburger R, Ait-Aissa S, Brion F, Busch W, de Aragao Umbuzeiro G, Denison MS, Du Pasquier D, Hilscherova K, Hollert H, Morales DA, Novak J, Schlichting R, Seiler TB, Serra H, Shao Y, Tindall AJ, Tollefsen KE, Williams TD, Escher BI (2017) Development of a bioanalytical test battery for water quality monitoring: Fingerprinting identified micropollutants and their contribution to effects in surface water. Water Res 123:734-750
Niederer C, Behra R, Harder A, Schwarzenbach RP, Escher BI (2004) Mechanistic approaches for evaluating the toxicity of reactive organochlorines and epoxides in green algae. Environ Toxicol Chem 23(3):697-704
Nilsson AM, Bergstrom MA, Luthman K, Nilsson JL, Karlberg AT (2005) A conjugated diene identified as a prohapten: contact allergenic activity and chemical reactivity of proposed epoxide metabolites. Chem Res Toxicol 18(2):308-16
Novotna A, Srovnalova A, Svecarova M, Korhonova M, Bartonkova I, Dvorak Z (2014) Differential effects of omeprazole and lansoprazole enantiomers on aryl hydrocarbon receptor in human hepatocytes and cell lines. PLoS One 9(6):e98711
NRC (2007) Toxicity Testing in the 21st Century: A Vision and a Strategy, Washington DC
Oakley RH, Cidlowski JA (2013) The biology of the glucocorticoid receptor: new signaling mechanisms in health and disease. J Allergy Clin Immunol 132(5):1033-44
Odermatt A, Gumy C (2008) Disruption of Glucocorticoid and Mineralocorticoid Receptor-Mediated Responses by Environmental Chemicals. CHIMIA 62(5):335
OECD (2016) Test No. 487: In Vitro Mammalian Cell Micronucleus Test
OECD (2020) Test No. 471: Bacterial Reverse Mutation Test
Ooka M, Lynch C, Xia M (2020) Application of In Vitro Metabolism Activation in High-Throughput Screening. Int J Mol Sci 21(21):8182
Paracelsus T (1538) Septem Defensiones, Darmstadt

Parekh VJ, Rathod VK, Pandit AB (2011) 2.10 - Substrate Hydrolysis: Methods, Mechanism, and Industrial Applications of Substrate Hydrolysis. In: Moo-Young M (ed) Comprehensive Biotechnology (Second Edition). Academic Press, Burlington, p 103-118
Pawliszyn J (2012) Handbook of Solid Phase Microextraction, 1. edn. Elsevier
Pearson RG (1990) Hard and Soft Acids and Bases - the Evolution of a Chemical Concept. Coordin Chem Rev 100:403-425
Peltenburg H, Bosman IJ, Hermens JL (2015) Sensitive determination of plasma protein binding of cationic drugs using mixed-mode solid-phase microextraction. J Pharm Biomed Anal 115:534-42
Peters T (1995) 3 - Ligand Binding by Albumin. In: Peters T (ed) All About Albumin. Academic Press, San Diego, p 76-132
Pole DL, Ando HY, Murphy ST (2007) Prediction of drug degradants using DELPHI: an expert system for focusing knowledge. Mol Pharm 4(4):539-49
Proenca S, Escher BI, Fischer FC, Fisher C, Gregoire S, Hewitt NJ, Nicol B, Paini A, Kramer NI (2021) Effective exposure of chemicals in in vitro cell systems: A review of chemical distribution models. Toxicol In Vitro 73:105133
Pushparajah DS, Plant KE, Plant NJ, Ioannides C (2017) Synergistic and antagonistic interactions of binary mixtures of polycyclic aromatic hydrocarbons in the upregulation of CYP1 activity and mRNA levels in precision-cut rat liver slices. Environ Toxicol 32(3):764-775
Qin W, Henneberger L, Glüge J, König M, Escher BI (2024) Baseline toxicity model to identify the specific and non-specific effects of per- and polyfluoroalkyl substances in cell-based bioassays Environ Sci Technol 58(13):5727–5738
Qin W, Henneberger L, Huchthausen J, König M, Escher BI (2023) Role of bioavailability and protein binding of four anionic perfluoroalkyl substances in cell-based bioassays for quantitative in vitro to in vivo extrapolations. Environ Int 173:107857
Qu W, Crizer DM, DeVito MJ, Waidyanatha S, Xia M, Houck K, Ferguson SS (2021) Exploration of xenobiotic metabolism within cell lines used for Tox21 chemical screening. Toxicol In Vitro 73:105109
Queen A (1967) Kinetics of the hydrolysis of acyl chlorides in pure water. Can J Chem 45(14):1619-1629
Quinn CL, van der Heijden SA, Wania F, Jonker MT (2014) Partitioning of polychlorinated biphenyls into human cells and adipose tissues: evaluation of octanol, triolein, and liposomes as surrogates. Environ Sci Technol 48(10):5920-8
Rafnsdottir OB, Kiuru A, Teback M, Friberg N, Revstedt P, Zhu J, Thomasson S, Czopek A, Malakpour-Permlid A, Weber T, Oredsson S (2023) A new animal product free defined medium for 2D and 3D culturing of normal and cancer cells to study cell proliferation and migration as well as dose response to chemical treatment. Toxicol Rep 10:509-520
Ramirez-Montes S, Zarate-Hernandez LA, Rodriguez JA, Santos EM, Cruz-Borbolla J (2022) A DFT Study of the Reaction of Acrylamide with L-Cysteine and L-Glutathione. Molecules 27(23):8220
Reed DJ (1990) Glutathione: toxicological implications. Annu Rev Pharmacol Toxicol 30(1):603-31
Rice G, MacDonell M, Hertzberg RC, Teuschler L, Picel K, Butler J, Chang YS, Hartmann H (2008) An approach for assessing human exposures to chemical mixtures in the environment. Toxicol Appl Pharmacol 233(1):126-36
Richardson GM (1932) The autoxidation of dialuric acid. Biochem J 26(6):1959-77
Riedl J, Altenburger R (2007) Physicochemical substance properties as indicators for unreliable exposure in microplate-based bioassays. Chemosphere 67(11):2210-20
Roy KS, Nazdrajic E, Shimelis OI, Ross MJ, Chen Y, Cramer H, Pawliszyn J (2021) Optimizing a High-Throughput Solid-Phase Microextraction System to Determine the Plasma Protein Binding of Drugs in Human Plasma. Anal Chem 93(32):11061-11065
Rudik AV, Bezhentsev VM, Dmitriev AV, Druzhilovskiy DS, Lagunin AA, Filimonov DA, Poroikov VV (2017) MetaTox: Web Application for Predicting Structure and Toxicity of Xenobiotics' Metabolites. J Chem Inf Model 57(4):638-642
Schmeisser S, Miccoli A, von Bergen M, Berggren E, Braeuning A, Busch W, Desaintes C, Gourmelon A, Grafström R, Harrill J, Hartung T, Herzler M, Kass GEN, Kleinstreuer N, Leist M, Luijten M, Marx-Stoelting P, Poetz O, van Ravenzwaay B, Roggeband R, Rogiers V, Roth A, Sanders

P, Thomas RS, Marie Vinggaard A, Vinken M, van de Water B, Luch A, Tralau T (2023) New approach methodologies in human regulatory toxicology - Not if, but how and when! Environ Int 178:108082
Schopfer LM, Lockridge O (2019) Mass Spectrometry Identifies Isopeptide Cross-Links Promoted by Diethylphosphorylated Lysine in Proteins Treated with Chlorpyrifos Oxon. Chem Res Toxicol 32(4):762-772
Schultz TW, Ralston KE, Roberts DW, Veith GD, Aptula AO (2007) Structure-activity relationships for abiotic thiol reactivity and aquatic toxicity of halo-substituted carbonyl compounds. SAR QSAR Environ Res 18(1-2):21-9
Schwarzenbach RP, Gschwend PM, Imboden DM (2002) Thermodynamics and Kinetics of Transformation Reactions. In: Schwarzenbach RP, Gschwend PM, Imboden DM (eds) Environmental Organic Chemistry. p 461-488
Seiber JN (1978) Loss of carbofuran from rice paddy water: chemical and physical factors. J Environ Sci Health B 13(2):131-48
Shah UK, Seager AL, Fowler P, Doak SH, Johnson GE, Scott SJ, Scott AD, Jenkins GJ (2016) A comparison of the genotoxicity of benzo[a]pyrene in four cell lines with differing metabolic capacity. Mutat Res Genet Toxicol Environ Mutagen 808:8-19
Shukla SJ, Huang R, Simmons SO, Tice RR, Witt KL, Vanleer D, Ramabhadran R, Austin CP, Xia M (2012) Profiling environmental chemicals for activity in the antioxidant response element signaling pathway using a high throughput screening approach. Environ Health Perspect 120(8):1150-6
Souza T, Jennen D, van Delft J, van Herwijnen M, Kyrtoupolos S, Kleinjans J (2016) New insights into BaP-induced toxicity: role of major metabolites in transcriptomics and contribution to hepatocarcinogenesis. Arch Toxicol 90(6):1449-58
Steinbrecht S, Kiebist J, Konig R, Thiessen M, Schmidtke KU, Kammerer S, Kupper JH, Scheibner K (2020) Synthesis of cyclophosphamide metabolites by a peroxygenase from Marasmius rotula for toxicological studies on human cancer cells. AMB Express 10(1):128
Taguchi K, Motohashi H, Yamamoto M (2011) Molecular mechanisms of the Keap1-Nrf2 pathway in stress response and cancer evolution. Genes Cells 16(2):123-40
Tebes-Stevens C, Patel JM, Jones WJ, Weber EJ (2017) Prediction of Hydrolysis Products of Organic Chemicals under Environmental pH Conditions. Environ Sci Technol 51(9):5008-5016
Thomas RS, Philbert MA, Auerbach SS, Wetmore BA, Devito MJ, Cote I, Rowlands JC, Whelan MP, Hays SM, Andersen ME, Meek ME, Reiter LW, Lambert JC, Clewell HJ, 3rd, Stephens ML, Zhao QJ, Wesselkamper SC, Flowers L, Carney EW, Pastoor TP, Petersen DD, Yauk CL, Nong A (2013) Incorporating new technologies into toxicity testing and risk assessment: moving from 21st century vision to a data-driven framework. Toxicol Sci 136(1):4-18
Thompson RA, Isin EM, Ogese MO, Mettetal JT, Williams DP (2016) Reactive Metabolites: Current and Emerging Risk and Hazard Assessments. Chem Res Toxicol 29(4):505-33
Tice RR, Austin CP, Kavlock RJ, Bucher JR (2013) Improving the human hazard characterization of chemicals: a Tox21 update. Environ Health Perspect 121(7):756-65
Ulrich N, Endo S, Brown TN, Watanabe N, Bronner G, Abraham MH, Goss KU (2017) UFZ-LSER database v 3.2.1 [Internet]. In. http://www.ufz.de/lserd
Vaes WHJ, Ramos EU, Verhaar HJM, Hermens JLM (1998) Acute toxicity of nonpolar versus polar narcosis: Is there a difference? Environ Toxicol Chem 17(7):1380-1384
Vaes WHJ, Ramos EU, Verhaar HJM, Seinen W, Hermens JLM (1996) Measurement of the Free Concentration Using Solid-Phase Microextraction: Binding to Protein. Anal Chem 68(24):4463-4467
van der Valk J, Brunner D, De Smet K, Fex Svenningsen A, Honegger P, Knudsen LE, Lindl T, Noraberg J, Price A, Scarino ML, Gstraunthaler G (2010) Optimization of chemically defined cell culture media--replacing fetal bovine serum in mammalian in vitro methods. Toxicol In Vitro 24(4):1053-63
van der Zalm AJ, Barroso J, Browne P, Casey W, Gordon J, Henry TR, Kleinstreuer NC, Lowit AB, Perron M, Clippinger AJ (2022) A framework for establishing scientific confidence in new approach methodologies. Arch Toxicol 96(11):2865-2879
Van Norman GA (2019) Limitations of Animal Studies for Predicting Toxicity in Clinical Trials: Is it Time to Rethink Our Current Approach? JACC Basic Transl Sci 4(7):845-854

van Wezel AP, Opperhuizen A (1995) Narcosis due to environmental pollutants in aquatic organisms: residue-based toxicity, mechanisms, and membrane burdens. Crit Rev Toxicol 25(3):255-79
Verhaar HJM, Vanleeuwen CJ, Hermens JLM (1992) Classifying Environmental-Pollutants .1. Structure-Activity-Relationships for Prediction of Aquatic Toxicity. Chemosphere 25(4):471-491
Walther TC, Farese RV, Jr. (2012) Lipid droplets and cellular lipid metabolism. Annu Rev Biochem 81:687-714
Wang L, Yu C, Wang J (2020) Development of reporter gene assays to determine the bioactivity of biopharmaceuticals. Biotechnol Adv 39:107466
Wang WX, Tan QG (2019) Applications of dynamic models in predicting the bioaccumulation, transport and toxicity of trace metals in aquatic organisms. Environ Pollut 252:1561-1573
Wang XJ, Hayes JD, Wolf CR (2006) Generation of a stable antioxidant response element-driven reporter gene cell line and its use to show redox-dependent activation of nrf2 by cancer chemotherapeutic agents. Cancer Res 66(22):10983-94
WHO (2021) The Public Health Impact of Chemicals: Knowns and Unknowns - Data Addendum for 2019. In. https://www.who.int/publications/i/item/WHO-HEP-ECH-EHD-21.01
Wilk-Zasadna I, Bernasconi C, Pelkonen O, Coecke S (2015) Biotransformation in vitro: An essential consideration in the quantitative in vitro-to-in vivo extrapolation (QIVIVE) of toxicity data. Toxicology 332:8-19
Wilkening S, Stahl F, Bader A (2003) Comparison of Primary Human Hepatocytes and Hepatoma Cell Line HepG2 with Regard to their Biotransformation Properties. Drug Metab Disposition 31(8):1035-1042
Wilkinson JM, Hayes S, Thompson D, Whitney P, Bi K (2008) Compound profiling using a panel of steroid hormone receptor cell-based assays. J Biomol Screen 13(8):755-65
Williams RT (1959) Detoxication Mechanisms: The Metabolism and Detoxication of Drugs, Toxic Substances, and Other Organic Compounds. Wiley
Yang X, Li W, Sun Y, Guo X, Huang W, Peng Y, Zheng J (2017) Comparative Study of Hepatotoxicity of Pyrrolizidine Alkaloids Retrorsine and Monocrotaline. Chem Res Toxicol 30(2):532-539
Yoon M, Blaauboer BJ, Clewell HJ (2015) Quantitative in vitro to in vivo extrapolation (QIVIVE): An essential element for in vitro-based risk assessment. Toxicology 332:1-3
Yoon M, Campbell JL, Andersen ME, Clewell HJ (2012) Quantitative in vitro to in vivo extrapolation of cell-based toxicity assay results. Crit Rev Toxicol 42(8):633-52
Yuan C, Tebes-Stevens C, Weber EJ (2020) Reaction Library to Predict Direct Photochemical Transformation Products of Environmental Organic Contaminants in Sunlit Aquatic Systems. Environ Sci Technol 54(12):7271-7279
Zanger UM, Schwab M (2013) Cytochrome P450 enzymes in drug metabolism: regulation of gene expression, enzyme activities, and impact of genetic variation. Pharmacol Ther 138(1):103-41
Zhang J, Yang Y, Liu W, Schlenk D, Liu J (2019) Glucocorticoid and mineralocorticoid receptors and corticosteroid homeostasis are potential targets for endocrine-disrupting chemicals. Environ Int 133:105133
Zhang JJ, Yang H (2021) Metabolism and detoxification of pesticides in plants. Sci Total Environ 790:148034
Zhao J, Shukla SJ, Xia M (2016) Cell-Based Assay for Identifying the Modulators of Antioxidant Response Element Signaling Pathway. Methods Mol Biol 1473:55-62
Zhao M, Deng L, Lu X, Fan L, Zhu Y, Zhao L (2022a) The involvement of oxidative stress, neuronal lesions, neurotransmission impairment, and neuroinflammation in acrylamide-induced neurotoxicity in C57/BL6 mice. Environ Sci Pollut Res Int 29(27):41151-41167
Zhao M, Zhang B, Deng L (2022b) The Mechanism of Acrylamide-Induced Neurotoxicity: Current Status and Future Perspectives. Front Nutr 9:859189
Zlokarnik G (2000) [15] Fusions to β-lactamase as a reporter for gene expression in live mammalian cells Methods Enzymol. vol 326. Academic Press, p 221-241
Zsila F (2013) Subdomain IB Is the Third Major Drug Binding Region of Human Serum Albumin: Toward the Three-Sites Model. Mol Pharm 10(5):1668-1682

6. Thesis publications

Publication I

Huchthausen, J., Henneberger, L., Mälzer, S., Nicol, B., Sparham, C., Escher, B. I. (2022) High-Throughput Assessment of the Abiotic Stability of Test Chemicals in *In Vitro* Bioassays. *Chemical Research in Toxicology* 35 (5), 867-879. DOI: 10.1021/acs.chemrestox.2c00030.

Publication II

Huchthausen, J., Escher, B. I., Grasse, N., König, M., Beil, S., Henneberger, L. (2023) Reactivity of Acrylamides Causes Cytotoxicity and Activates Oxidative Stress Response. *Chemical Research in Toxicology* 36 (8), 1374-1385. DOI: 10.1021/acs.chemrestox.3c00115.

Publication III

Huchthausen, J., Braasch, J., Escher,B. I., König, M., Henneberger, L. (2024) Effects of Chemicals in Reporter Gene Bioassays with Different Metabolic Activity Compared to Baseline Toxicity. *Chemical Research in Toxicology.* DOI: 10.1021/acs.chemrestox.4c00017.

EBERHARD KARLS
UNIVERSITÄT
TÜBINGEN

Mathematisch-Naturwissenschaftliche Fakultät

Erklärung nach § 5 Abs. 2 Nr. 8 der Promotionsordnung der Math.-Nat. Fakultät
-Anteil an gemeinschaftlichen Veröffentlichungen-
Nur bei kumulativer Dissertation erforderlich!

Declaration according to § 5 Abs. 2 No. 8 of the PhD regulations of the Faculty of Science
-Collaborative Publications-
For Cumulative Theses Only!

Last Name, First Name:

List of Publications

1. Huchthausen, J.; Henneberger, L.; Mälzer, S.; Nicol, B.; Sparham, C.; Escher, B. I. High-Throughput Assessment of the Abiotic Stability of Test Chemicals in In Vitro Bioassays. *Chem. Res. Toxicol.* **2022**, *35* (5), 867-879. DOI: 10.1021/acs.chemrestox.2c00030
2. Huchthausen, J.; Escher, B. I.; Grasse, N.; König, M.; Beil, S.; Henneberger, L. Reactivity of Acrylamides Causes Cytotoxicity and Activates Oxidative Stress Response. *Chem. Res. Toxicol.* **2023**, *36* (8), 1374-1385. DOI: 10.1021/acs.chemrestox.3c00115
3. Huchthausen, J.; Braasch, J.; Escher, B. I.; König, M.; Henneberger, L. Effects of Chemicals in Reporter Gene Bioassays with Different Metabolic Activity Compared to Baseline Toxicity. (submitted).

Nr.	Accepted publication yes/no	List of authors	Position of candidate in list of authors	Scientific ideas by the candidate (%)	Data generation by the candidate (%)	Analysis and Interpretation by the candidate (%)	Paper writing done by the candidate (%)
1	Yes	6	1	40	70	80	70
2	Yes	6	1	40	80	80	80
3	No	5	1	40	30	60	90

I confirm that the above-stated is correct

05.02.24 [redacted]

Date, Signature of the candidate

I/We certify that the above-stated is correct. [redacted]

05.02.24

Date, Signature of the doctoral committee or at least of one of the supervisors

Publication I

High-Throughput Assessment of the Abiotic Stability of Test Chemicals in *In Vitro* Bioassays

Julia Huchthausen[†], Luise Henneberger[†], Sophia Mälzer[†], Beate Nicol[¶], Chris Sparham[¶], Beate I. Escher[†‡*]

[†] Helmholtz Centre for Environmental Research – UFZ, Department of Cell Toxicology, Permoserstr. 15, 04318 Leipzig, Germany

[¶] Safety and Environmental Assurance Centre, Unilever, Colworth House, Sharnbrook, Bedford MK44 1LQ, UK

[‡] Eberhard Karls University Tübingen, Environmental Toxicology, Center for Applied Geoscience, Scharrenbergstr. 94-96, 72076 Tübingen, Germany

Corresponding author: beate.escher@ufz.de

Published in Chemical Research in Toxicology, DOI: 10.1021/acs.chemrestox.2c00030.

Chemical Research in Toxicology

pubs.acs.org/crt

Article

High-Throughput Assessment of the Abiotic Stability of Test Chemicals in *In Vitro* Bioassays

Julia Huchthausen, Luise Henneberger, Sophia Mälzer, Beate Nicol, Chris Sparham, and Beate I. Escher*

Cite This: *Chem. Res. Toxicol.* 2022, 35, 867−879

Read Online

ACCESS | Metrics & More | Article Recommendations | Supporting Information

ABSTRACT: Abiotic stability of chemicals is not routinely tested prior to performing *in vitro* bioassays, although abiotic degradation can reduce the concentration of test chemicals leading to the formation of active or inactive transformation products, which may lead to misinterpretation of bioassay results. A high-throughput workflow was developed to measure the abiotic stability of 22 test chemicals in protein-rich aqueous media under typical bioassay conditions at 37 °C for 48 h. These test chemicals were degradable in the environment according to a literature review. The chemicals were extracted from the exposure media at different time points using a novel 96-pin solid-phase microextraction. The conditions were varied to differentiate between various reaction mechanisms. For most hydrolyzable chemicals, pH-dependent degradation in phosphate-buffered saline indicated that acid-catalyzed hydrolysis was less important than reactions with hydroxide ions. Reactions with proteins were mainly responsible for the depletion of the test chemicals in the media, which was simulated by bovine serum albumin (BSA) and glutathione (GSH). 1,2-Benzisothiazol-3(2*H*)-one, 2-methyl-4-isothiazolinone, and L-sulforaphane reacted almost instantaneously with GSH but not with BSA, indicating that GSH is a good proxy for reactivity with electrophilic amino acids but may overestimate the actual reaction with three-dimensional proteins. Chemicals such as hydroquinones or polyunsaturated chemicals are prone to autoxidation, but this reaction is difficult to differentiate from hydrolysis and could not be simulated by the oxidant *N*-bromosuccinimide. Photodegradation played a minor role because cells are exposed in incubators in the dark and simulations with high light intensities did not yield realistic degradation. Stability predictions from various *in silico* prediction models for environmental conditions can give initial indications of the stability but were not always consistent with the experimental stability in bioassays. As the presented workflow can be performed in high throughput under realistic bioassay conditions, it can be used to provide an experimental database for developing bioassay-specific stability prediction models.

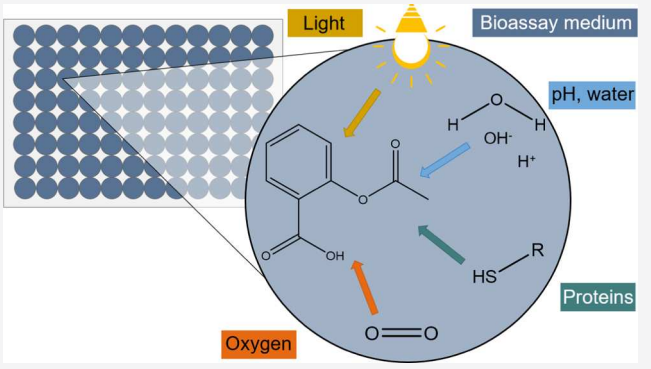

INTRODUCTION

The field of human risk assessment of chemicals has undergone a paradigm shift in recent years, moving away from animal testing to mechanistic *in vitro* toxicology.[1−4] New methods are being developed to enable reliable risk assessment without causing animal suffering. These so-called new approach methodologies (NAMs) also include the use of *in vitro* reporter gene bioassays, which can detect early cellular indicators for adverse outcomes in humans.[5] In various parts of the world, institutions such as the U.S. National Research Council (NRC) or the U.K. National Centre for the Replacement, Refinement, and Reduction of Animals in Research (NC3Rs) have worked to implement and optimize *in vitro* assays for toxicity assessment.[6,7] Compared to conventional animal experiments, *in vitro* bioassays are more cost-effective, can be automated, and, if fit-for-purpose, are ethically more acceptable.

Quantitative *in vitro* to *in vivo* extrapolation (QIVIVE) methods are used to extrapolate data from *in vitro* bioassays to the *in vivo* situation and to draw conclusions about the safety of chemicals in humans and the environment.[8] QIVIVE models rely on constant chemical exposure *in vitro* as they are typically based on the extrapolation of nominal effect concentrations *in vitro* to predicted maximum plasma concentrations *in vivo*.[9]

The dosed (nominal) concentration is the primary concentration metric used in *in vitro* toxicology.[10] Various loss processes, like volatilization, sorption to the plastic of the well plate, and interactions with components of the medium or the cells, can cause the actual bioavailable concentration to deviate from the nominal concentration.[11−14] Less attention has so far been paid to abiotic transformation of the test chemicals, although it has been shown that test chemicals can react with components of the bioassay medium.[15,16] Transformation

Received: January 27, 2022
Published: April 8, 2022

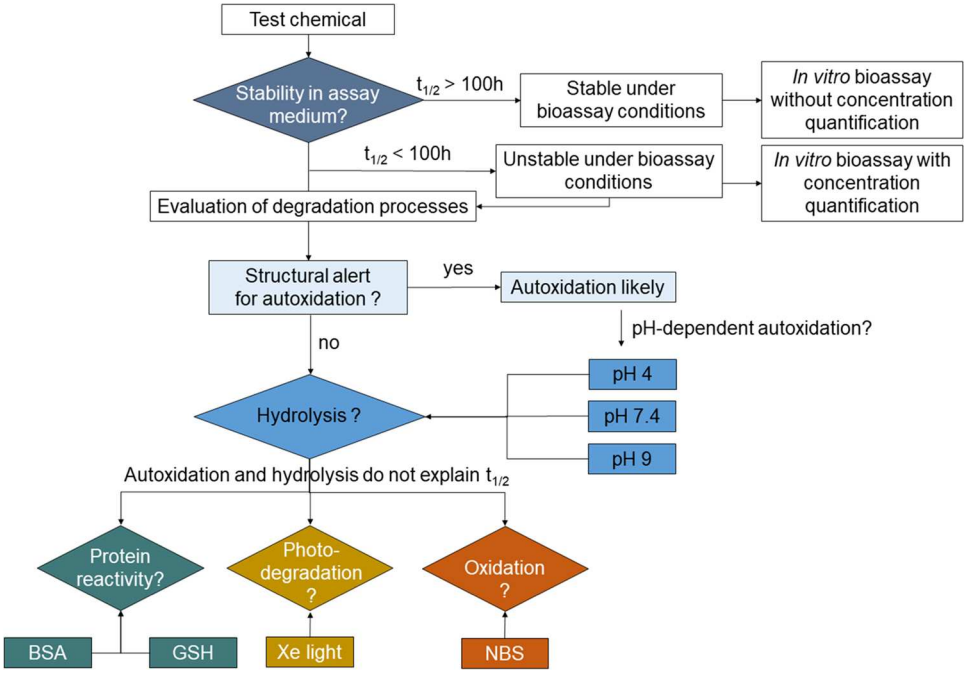

Figure 1. Framework for HT abiotic stability assessment of the test chemicals. Abbreviations: $t_{1/2}$, degradation half-life; BSA, bovine serum albumin; GSH, glutathione; NBS, *N*-bromosuccinimide.

processes may lead to a decrease in the concentration of the parent chemical over time, leading to an apparently lower effect. In addition, inactive or active transformation products can be formed, resulting in an underestimation or overestimation of the toxicity of the chemical.[16,17] If these processes remain unnoticed, this might lead to considerable errors in QIVIVE models.[18] The stability of chemicals in *in vitro* assays is not routinely monitored, and prediction models are not tailored to bioassay conditions but rather to environmental degradation.[19−22]

The aim of this study was to develop a high-throughput (HT) method to quantify degradation kinetics of chemicals in bioassay media in the absence of cells to assess whether the chemical is abiotically degraded in the time course of an *in vitro* bioassay. A second aim was to decipher the transformation processes involved, which might lead to conclusions about possible transformation products. Understanding abiotic processes under *in vitro* test conditions, both qualitatively and quantitatively, is important as these processes have an impact on how *in vitro* assay response data can be interpreted in a QIVIVE context. In addition, the abiotic stability of the test chemicals in the environment and mechanisms of transformation were predicted with various freely available *in silico* models[19−22] to evaluate if it is possible to waive the experimental stability assessment or have a screening step before running the experimental workflow.

EXPERIMENTAL FRAMEWORK FOR STABILITY TESTING

The framework for stability testing is depicted in Figure 1. As first step, the (pseudo) first-order degradation rate constants k and degradation half-lives ($t_{1/2}$) of all test chemicals in three different assay media were determined over the relevant time window for routine *in vitro* bioassays (48 h) used for risk assessment[23,24] and environmental monitoring.[5]

Chemicals with $t_{1/2} \geq 100$ h can be considered abiotically stable under bioassay conditions, and the *in vitro* bioassay can be performed without experimental quantification of exposure concentrations (Figure 1). For the method development and validation of the proposed workflow, however, all subsequent tests were performed for all chemicals. If $t_{1/2}$ was <100 h, the abiotic stability should be investigated in more detail and the relevant degradation processes identified (Figure 1). In this case, the experimental quantification of exposure concentrations in the bioassay is recommended.

Four representative degradation processes in the bioassay medium were evaluated: hydrolysis, reactivity toward proteins, photodegradation, and oxidation/autoxidation. Degradation in phosphate-buffered saline (PBS) at pH 7.4, the pH of cell-based *in vitro* assays, is the core experiment, as these degradation processes also occur in all other test systems. If the $t_{1/2}$ in PBS equal those in the bioassay medium, no further tests would be needed.

Autoxidation, *i.e.*, the oxidation by oxygen in the air,[25] often catalyzed by traces of iron, cannot be experimentally distinguished from hydrolysis using the present experimental setup but there are clear structural alerts for autoxidation such as hydroquinone moieties in polyphenols or benzohydroquinones.[16,26] Autoxidation can also be pH-dependent.[26,27] Hence, if such a structural alert was present in an investigated molecule, we assumed that autoxidation was the dominant mechanism over hydrolysis.

For those chemicals that were unstable in PBS, the mechanism of hydrolysis/autoxidation was assessed with pH-dependent experiments (Figure 1). Acid-catalyzed hydrolysis was assessed at pH 4, and the role of the hydroxide ion as a nucleophile was determined at pH 9. This setup was based on the "Fate, Transport and Transformation Test Guideline" of the Office of Prevention, Pesticides and Toxic Substances, United States Environmental Protection Agency (OPPTS).[2826]

Whenever the $t_{1/2}$ in PBS was higher than the $t_{1/2}$ in the bioassay medium, additional degradation processes must have played a role (Figure 1). Reactivity toward proteins was probed with bovine serum albumin (BSA) as a surrogate for fetal bovine serum (FBS), which contains mainly albumin. Since the potentially reactive amino acids might be buried due to the three-dimensional structure and folding of BSA, reduced glutathione (GSH, y-Glu-Cys-Gly), which is commonly used to simulate the reaction potential of chemicals with proteins, was also used to mimic a direct reaction with a free thiol group.

Photodegradation is highly relevant for chemicals in the environment, as they are constantly exposed to sunlight.[29,30] In cell-based *in*

https://doi.org/10.1021/acs.chemrestox.2c00030
Chem. Res. Toxicol. 2022, 35, 867−879

vitro bioassays, photodegradation plays a minor role, as the incubation of the plates takes place in the dark. Nevertheless, the chemicals might be exposed to various light sources during the preparation of the assay. For this reason, the photodegradation potential of the test substances was investigated using a xenon test chamber (Q-SUN Xe-1, Q-LAB). The test setup was based on the Organization for Economic Cooperation and Development (OECD) guideline: "Phototransformation of Chemicals in Water—Direct Photolysis".[31]

The mild oxidizing agent *N*-bromosuccinimide (NBS)[32] was used to examine the general susceptibility of the test substances to oxidation, which might be an indicator for autoxidation in the bioassay medium.

Using the proposed HT workflow for stability testing (Figure 1), unstable chemicals and their mechanisms of abiotic transformation can be identified under conditions that match those of a realistic *in vitro* bioassay, *i.e.*, in a well plate format under identical exposure conditions (with the exception of photodegradation and oxidation). The workflow is HT because a novel solid-phase microextraction (SPME) device (Supel BioSPME 96-Pin Device) was used to extract the chemicals from the exposure medium, which enables the extraction of chemicals from 96-well plates in one easy process.[33] This device allowed us to upscale the experiments to a 96-well plate format, which greatly increased the throughput of the experiment.

MATERIALS AND METHODS

Chemicals. A set of 22 test chemicals suspected to be prone to abiotic transformation were selected for this study (Table 1). The chemical structures can be found in Table S8. All test chemicals had a purity of ≥90%, were nonvolatile with water−air partitioning constants (K_{wa}) > 10 000 L/L, and were of moderate hydrophobicity with octanol−water partitioning constants log K_{ow} < 5 (Table S1). For all test chemicals, except for L-sulforaphane, aliquots were weighed and dissolved in methanol immediately before the experiment. The stocks were discarded after the end of the experiment. L-Sulforaphane was purchased from the provider as a solution in ethanol (10 g/L) and used directly for the experiments. The content of methanol or ethanol in the test system was kept below 0.6% for all tests.

Table 1. Test Chemicals of This Study with Suspected Transformation Processes

chemical	suspected transformation process	reference
1,2-benzisothiazol-3(2*H*)-one	reactivity toward proteins	ref 34
2-methyl-4-isothiazolinone	reactivity toward proteins	ref 34
6-gingerol	hydration−dehydration	ref 35
8-gingerol	hydration−dehydration	ref 35
acetaminophen	photodegradation	ref 36
acetylsalicylic acid	hydrolysis	ref 37
amoxicillin	hydrolysis, photodegradation	refs 38 and 39
andrographolide	hydrolysis, reactivity toward proteins	refs 40 and 41
bendiocarb	hydrolysis, photodegradation	refs 42 and 43
carbofuran	hydrolysis, photodegradation	refs 44 and 45
chloramphenicol	hydrolysis, photodegradation	refs 46 and 47
dinoseb	photodegradation	ref 48
furosemide	hydrolysis, photodegradation	refs 49 and 50
L-sulforaphane	hydrolysis, reactivity toward proteins	refs 51 and 52
malathion	hydrolysis	ref 53
oxytetracycline	hydrolysis, photodegradation	ref 54
phosmet	photodegradation	ref 55
pretilachlor	photodegradation, reactivity toward proteins	refs 56 and 57
quercetin	oxidation, photodegradation	refs 58 and 59
sethoxydim	photodegradation	ref 60
thiabendazole	photodegradation	ref 61
triclopyr	photodegradation, reactivity toward proteins	refs 62 and 57

Materials. The Supel BioSPME 96-Pin Devices (Sigma-Aldrich; 59683-U) had 96 polypropylene pins with a length of 24.7 mm. The tip of each pin was coated with C18 particles, which were attached to the pins with a polyacrylonitrile (PAN) binder. The coating length was 2.1 mm, and the average coating thickness was 12.5 μm, resulting in an approx. coating volume of 80 nL.[33] The experiments were performed in glass-coated deep-well plates (Product Nos. 60180-P306 and 60180-P336) from Thermo Scientific. Oxidation experiments were performed in polystyrene deep-well plates from Labsolute (Product No. 7696548) to prevent oxidation of the glass-coating material. During incubation, the plates were sealed with adhesive sealing film from Brand (Product No. 701367). The water for the experiments was obtained from a Milli-Q water purification system from Merck.

The components of the bioassay media were purchased from Thermo Fisher Scientific. More detailed information about the chemicals and solvents used can be found in Table S2.

Chemical Stability in Bioassay Media. The stability of the test chemicals was tested in three different bioassay media: the AREc32 medium (10% untreated FBS and 90% Dulbecco's modified Eagle's medium (DMEM) Glutamax) had a protein content of 8.93 mL/L and a lipid content of 0.14 mL/L,[63] the GeneBLAzer medium (2% charcoal-stripped FBS and 98% OptiMEM) had a protein content of 4.84 mL/L and a lipid content of 0.02 mL/L,[63] and the neurobasal medium (2% B-27 supplement, 2% GlutaMAX supplement) had a protein content of 2.58 mL/L and a negligible lipid content.[64] All media contained 100 U/mL penicillin and 100 μg/mL streptomycin.

Eight milliliters of each medium or buffer solution were spiked with the individual test chemicals. The final concentration was 5 mg/L for all test chemicals, except 1,2-benzisothiazol-3(2*H*)-one (20 mg/L), 2-methyl-4-isothiazolinone (20 mg/L), acetaminophen (20 mg/L), acetylsalicylic acid (20 mg/L), amoxicillin (10 mg/L), chloramphenicol (20 mg/L), L-sulforaphane (10 mg/L), and oxytetracycline (20 mg/L). Aliquots of 600 μL per well of each medium and buffer were transferred into six glass-coated deep-well plates with one column per chemical and two rows per medium (Figure S1). One plate was preheated to 37 °C for 15 min and extracted immediately with solid-phase microextraction (SPME). The other plates were incubated at 37 °C for 2, 4, 7, 24, or 48 h. After the respective incubation time, the plates were extracted with SPME. The plate for the 16 h incubation time was prepared separately by pipetting 600 μL of each medium into one well of a glass-coated deep-well plate following the pipetting scheme (Figure S1). The medium or buffer was spiked with the test chemicals directly in the plate leading to the same final concentrations as mentioned above. The plate was shaken at 1000 rpm (BioShake iQ, Quantifoil Instruments) for 5 min and then incubated at 37 °C for 16 h. The experiments were performed at least twice and three times for chemicals that showed degradation.

Chemical Stability at Different pH Values. The pH-driven degradation was tested in phosphate-buffered saline (PBS, 137 mM NaCl, 12 mM phosphate) and three different buffer solutions, pH 4 buffer (50 mM potassium phthalate, 0.4 mM NaOH), pH 7.4 buffer (50 mM KH_2PO_4, 39.5 mM NaOH), and pH 9 buffer (50 mM KCl, 50 mM H_3BO_3, 21.3 mM NaOH). The experiments were performed in the same way as the experiments with medium. In one additional experiment, the degradation kinetics were determined for two chemicals (carbofuran and quercetin) at additional pH values covering the pH range where degradation could be detected, which was pH 6.6−8.6 (carbofuran) or pH 5.4−7.8 (quercetin) using the buffers described in Table S3.

Reactivity toward Proteins. The pH of the BSA and GSH solutions in PBS was adjusted to 7.4 with 5 M NaOH and 5 M HCl. Since GSH is also unstable at pH 7.4 and might be oxidized rapidly by air,[65] an Ellman's test was performed to assess the stability of the GSH in the test solutions.[66] More information can be found in the Supporting Information (Text S2). Eight milliliters of the BSA or GSH solution in PBS were spiked with the individual test chemicals. 1,2-Benzisothiazol-3(2*H*)-one, 2-methyl-4-isothiazolinone, acetamino-

https://doi.org/10.1021/acs.chemrestox.2c00030
Chem. Res. Toxicol. 2022, 35, 867−879

phen, acetylsalicylic acid, chloramphenicol, and L-sulforaphane were spiked at a final concentration of 1.74×10^{-4} M. The concentration of BSA or GSH was 10 times higher (1.74×10^{-3} M). The other chemicals were spiked at a final concentration of 2.48×10^{-5} M with a BSA or GSH concentration of 2.48×10^{-4} M. As hydrolysis control, 8 mL of PBS was spiked with the corresponding concentration of the test chemicals. Aliquots of 600 μL per well were transferred into six glass-coated deep-well plates according to the pipetting scheme (Figure S1). The plates were incubated and extracted as described above. The plate for the 16 h incubation time was prepared separately as described above using the same chemical concentrations. The experiment was repeated up to three times for chemicals that showed degradation. In one additional experiment, the degradation kinetics were determined at additional GSH concentrations (1.24×10^{-3}, 2.48×10^{-3}, and 1.24×10^{-2} M) for two chemicals (pretilachlor and andrographolide).

Photodegradation. The photodegradation potential of the test chemicals was investigated using a xenon test chamber (Q-SUN Xe-1, Q-LAB) equipped with a Daylight-Q optical filter. Seven milliliters of PBS were spiked with the individual test chemicals at a final concentration of 5 mg/L for all test chemicals except 1,2-benzisothiazol-3(2*H*)-one (20 mg/L), 2-methyl-4-isothiazolinone (20 mg/L), acetaminophen (20 mg/L), acetylsalicylic acid (20 mg/L), amoxicillin (10 mg/L), chloramphenicol (20 mg/L), L-sulforaphane (10 mg/L), and oxytetracycline (20 mg/L). Aliquots of 600 μL per well were transferred to six glass-coated deep-well plates according to the pipetting scheme (Figure S1). One plate was preheated for 15 min at 37 °C and extracted immediately without further incubation. The other plates were placed in the xenon test chamber and covered with a quartz glass plate to reduce volatilization of water from the samples without reducing the light intensity. The air temperature of the chamber was set at 37 °C, but the actual temperature in the sample could not be measured. The plates were incubated in three independent experiments at an irradiance at 340 nm of 0.77 W/m^2 for 1.5, 2, 3, 4, 4.5, 6, or 7.5 h with full-spectrum sunlight and extracted with SPME.

Oxidation. *N*-Bromosuccinimide (NBS) was used as a mild oxidizing reagent. In a preliminary test, 4 mL of an NBS solution in PBS was spiked with the test chemicals. 1,2-Benzisothiazol-3(2*H*)-one, 2-methyl-4-isothiazolinone, acetaminophen, acetylsalicylic acid, chloramphenicol, and L-sulforaphane were spiked at a final concentration of 1.74×10^{-4} M. The concentration of NBS was 10 times higher (1.74×10^{-3} M). The other chemicals were spiked at a concentration of 2.48×10^{-5} M with an NBS concentration of 2.48×10^{-4} M. Four milliliters of PBS were spiked with the respective concentration of the test chemicals as hydrolysis control. Aliquots of 600 μL of each spiked solution were pipetted into three glass-coated deep-well plates according to the pipetting scheme (Figure S1). Ascorbic acid was added to each well of one plate at a concentration of 1.74×10^{-2} or 2.48×10^{-3} M to stop the reaction. The plate was shaken at 1000 rpm (BioShake iQ, Quantifoil Instruments) for 5 min, preheated to 37 °C for 15 min, and extracted with SPME. The other plates were incubated at 37 °C for 2 or 48 h, ascorbic acid was added, and the plates were extracted with SPME, as described below.

Since oxidation was fast for most chemicals, additional incubation times below 2 h were tested. The plates were prepared separately by pipetting 600 μL of PBS or NBS solution into one well of a glass-coated deep-well plate following the pipetting scheme (Figure S1). The solutions were spiked with the test chemicals directly in the plate leading to the same final concentrations as mentioned above. The plates were shaken at 1000 rpm (BioShake iQ, Quantifoil Instruments) for 5 min and then incubated for 10, 15, 20, 30, 40, 45, 50, 60, 70, or 90 min at 37 °C. After incubation, 1.74×10^{-2} or 2.48×10^{-3} M ascorbic acid was added to each well to stop the reaction. The plates were shaken at 1000 rpm (BioShake iQ, Quantifoil Instruments) for 5 min and extracted with SPME.

Solid-Phase Microextraction. The plates from all stability tests were extracted using SPME immediately after spiking and after the respective incubation times. The BioSPME 96-pin device was conditioned for 20 min in a glass-coated deep-well plate containing 800 μL of isopropanol per well and washed for 10 s in a glass-coated deep-well plate with 900 μL of Milli-Q water per well. It was transferred to the sample plate, attached to the plate with adhesive tape, and shaken at 37 °C and 1000 rpm (BioShake iQ, Quantifoil Instruments) for 15 min. The desorption plate was prepared with 600 μL of the respective desorption solvent (Table S1) per well. The pin device was transferred to the desorption plate, attached, and shaken at 1000 rpm without temperature control (BioShake iQ, Quantifoil Instruments) for 15 min. The transport time of the pin device between the plates was below 6 s to prevent the pin coating from drying out. After desorption, the desorption plates were stored at 4 °C until chemical analysis. Pin-water partitioning and the reproducibility of the SPME extraction are described in detail in Text S1, Figures S2 and S3, and Table S4.

Instrumental Analysis. The concentration of the chemicals in the desorption solvents and in the PBS samples was quantified with a liquid chromatography instrument (Agilent 1260 Infinity II) coupled to a triple quadrupole mass spectrometer (Agilent 6420 Triple Quad). A Kinetex 1.7 μm, C18, 100 Å, LC column (50 × 2.1 mm), a BioZen 1.6 μm, peptide PS-C18 LC column (50 × 2.1 mm), or a LunaOmega 1.6 μm, Polar C18, 100 Å, LC column (50 × 2.1 mm) were the columns used, depending on the test chemical. All LC and MS parameters can be found in the Supporting Information (Tables S5 and S6). PBS samples of 6-gingerol, 8-gingerol, dinoseb, phosmet, and pretilachlor were diluted 1:1 with acetonitrile before measurement. Calibration standards with a concentration range of 1−10 000 ng/mL were prepared in the respective desorption solvent or PBS and measured with the samples. Acetonitrile blanks were measured after approx. every 10th sample.

Data Evaluation. In a second-order reaction between two reactants A and B, the reaction rate depends on the concentration of the two reactants (eq 1), where $k_{\text{second-order}}$ is the reaction rate constant

$$\frac{\delta[\text{A}]}{\delta t} = -k_{\text{second}-\text{order}} \times [\text{A}] \times [\text{B}] \tag{1}$$

If one of the reactants is present in large excess (*e.g.*, [B] ≫ [A]), its concentration remains constant over time and [B] can be combined with $k_{\text{second-order}}$ to obtain a pseudo-first-order reaction rate constant $k_{\text{pseudo first-order}}$ (eq 2)

$$\frac{\delta[\text{A}]}{\delta t} = -k_{\text{pseudo first}-\text{order}} \times [\text{A}]$$
$$\text{with } k_{\text{pseudo first}-\text{order}} = k_{\text{second}-\text{order}} \times [\text{B}] \tag{2}$$

For all stability tests, the reaction partner [B] of the test substances was used in excess to assure that pseudo-first-order kinetics apply. The natural logarithm (ln) of the concentration in the desorption solvent after SPME (C_{des}) was plotted against the incubation time (t) to determine the degradation rate constant of the test chemicals.[67,68] It was not necessary to convert C_{des} to the concentration in the assay because all reactions were apparently first order. The experimental first-order rate constant k was derived from a linear regression of $\ln(C_{\text{des}})$ against t (eq 3)

$$\ln(C_{\text{des}})_t = -k \times t \tag{3}$$

The degradation half-life ($t_{1/2}$) of the (pseudo) first-order decay constant k was calculated with eq 4

$$t_{1/2} = \frac{\ln(2)}{k} \tag{4}$$

***In Silico* Prediction of Chemical Stability.** Three freely available *in silico* prediction programs were used to obtain an indication of the stability of the test chemicals (Table 2). HYDROWIN, a model of the EPI-Suite from the United States Environmental Protection Agency (EPA), predicts aqueous hydrolysis rate constants for acid- and base-catalyzed hydrolysis and degradation half-lives.[22] The web-based chemical transformation simulator (CTS),[77] developed by EPA, predicts different environmental and biological transformation pathways including abiotic hydrolysis[19] and photodegradation[20] and suggests possible degradation products.

The OECD quantitative structure−activity relationship (QSAR) toolbox provides QSAR-based prediction models for the prediction of

https://doi.org/10.1021/acs.chemrestox.2c00030
Chem. Res. Toxicol. 2022, 35, 867−879

adverse effects of chemicals.[21] Autoxidation of the test chemicals was predicted using two models in neutral and alkaline conditions, and five different models were applied to predict the reactivity of the test chemicals toward proteins. Although the QSAR Toolbox models are called "protein binding potency" models, in this case, protein binding refers to a chemical reaction, that is, the formation of irreversible covalent bonds between the test chemicals and a biological nucleophile. Possible reactions that can be predicted by the models are, for example, acylation, Michael addition, Schiff base formation, S_N2 reaction, or S_NAr reaction. Reversible bonds of chemicals to proteins formed by interactions such as van der Waals forces or hydrogen bonds are not considered.

RESULTS AND DISCUSSION

Chemical Stability in Bioassay Media. Eleven of 22 chemicals were stable in bioassay media and PBS (Figure 2)

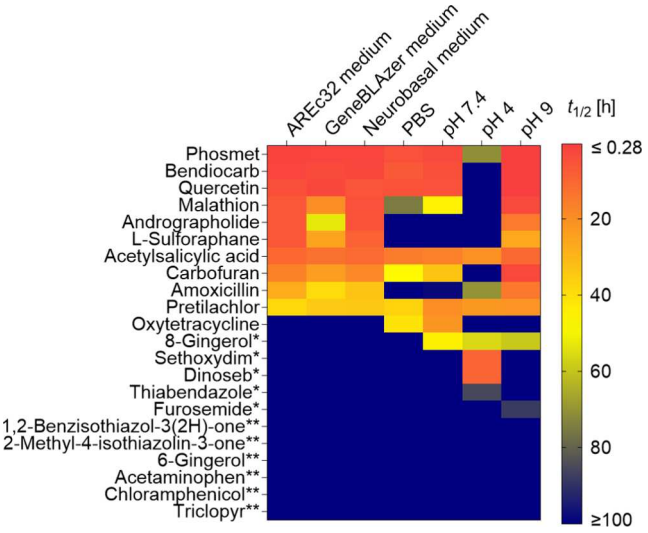

Figure 2. Stability of the test chemicals in three bioassay media, PBS, and three pH buffers. The different colors indicate the degradation half-life ($t_{1/2}$) of the chemical in the respective medium or buffer. Chemicals that were stable in all media and PBS are marked with an asterisk, and chemicals that were stable in all media and buffer are marked with two asterisks.

under bioassay conditions over 48 h. The degradation rate constants derived from the decay curves (Figure S4) and thereof derived $t_{1/2}$ of all chemicals and media are listed in Table S7. While experiments ran over 48 h, the extrapolation of $t_{1/2}$ up to 100 h was possible and all chemicals with $t_{1/2} \geq 100$ h were considered stable in the respective medium or PBS.

Acetylsalicylic acid, pretilachlor, phosmet, bendiocarb, and quercetin had similar $t_{1/2}$ in all media as well as PBS, indicating that hydrolysis and possibly autoxidation in the case of quercetin (Table S8) were responsible for the degradation. Phosmet showed the fastest degradation with $t_{1/2}$ below 5 h in all media. Malathion, carbofuran, amoxicillin, andrographolide, and L-sulforaphane showed faster degradation in the assay media than in PBS. For these chemicals, the protein content of the medium appeared to affect the degradation rate. However, the rapid degradation of some of these chemicals in the neurobasal medium was unexpected (*e.g.*, $t_{1/2}$ malathion 4.37 h, $t_{1/2}$ andrographolide 5.01 h, and $t_{1/2}$ L-sulforaphane 8.73 h). The protein content of the neurobasal medium (2.58 mL/L) was slightly below that of the GeneBLAzer medium (4.84 mL/L), so the $t_{1/2}$ in GeneBLAzer and neurobasal medium were expected to be very similar. However, the $t_{1/2}$ in the neurobasal medium

Table 2. *In Silico* Prediction Models Used for the Prediction of Chemical Degradation

transformation process	provider	module	description
hydrolysis	EPA	HYDROWIN	aqueous hydrolysis rate constants for acid- and base-catalyzed hydrolysis and degradation half-lives for esters, carbamates, epoxides, halomethanes, and selected alkyl halides[22]
		Chemical Transformation Simulator (CTS)	environmental and biological transformation pathways and products by comparison of the test chemical with existing reaction libraries; the abiotic hydrolysis reaction library contains 25 reaction schemes; a rank is assigned to each of the reaction schemes at pH 5, 7, or 9 at 25 °C, with which an approximate degradation half-life can be determined[19]
autoxidation	OECD QSAR Toolbox	autoxidation simulator	simulates the abiotic oxidation pathways of chemicals under air or oxygen exposure at room temperature, atmospheric pressure, and pH 7−9; contains 325 structurally generalized molecular transformations, extracted from observed autoxidation pathways for 140 training set chemicals[69,70]
		autoxidation simulator (alkaline conditions)	simulates the abiotic oxidation pathways of chemicals under air or oxygen exposure at room temperature, atmospheric pressure, and pH 10.2; contains 308 structurally generalized molecular transformations, extracted from the observed autoxidation pathways of 139 training set chemicals[69,70]
reactivity toward proteins		protein binding OECD	102 reaction profiles and structural alerts for the capability of a directly acting electrophile to form covalent bonds with a protein[71]
		protein binding OASIS	OASIS TIMES model for skin sensitization; contains 112 structural alerts related to interactions with (skin) proteins[72]
		protein binding potency Lys	alerts for the capability of a chemical to react with lysine (Lys); the 77 structural alerts were developed based on data from the direct peptide reactivity assay (DPRA)[73−75]
		protein binding potency Cys	alerts for the capability of a chemical to react with cysteine (Cys); the 77 structural alerts were developed based on data from the direct peptide reactivity assay (DPRA)[73−75]
reactivity toward proteins	OECD QSAR Toolbox	protein binding potency GSH	potency of a chemical to react with proteins based on the capability to react with the thiol group of glutathione (GSH); the 137 protein binding alerts were developed based on experimental GSH RC50 values[76]
photodegradation	EPA	Chemical Transformation Simulator (CTS)	environmental and biological transformation pathways and products by comparison of the test chemical with existing reaction libraries; the direct photolysis reaction library contains 155 reaction schemes but is currently unranked, so no degradation half-life can be determined[20]

https://doi.org/10.1021/acs.chemrestox.2c00030
Chem. Res. Toxicol. 2022, 35, 867−879

were almost as high as those measured in the AREc32 medium, which had a much higher protein content (*e.g.*, L-sulforaphane: AREc32 medium = 6.27 h and neurobasal medium = 8.73 h). It may be that the different composition of the neurobasal medium influenced the degradation rate of the test chemicals since it is an FBS-free medium. The neurobasal medium contains two supplements of undefined components that might be responsible for the accelerated degradation of the chemicals.

Oxytetracycline was the only chemical that showed degradation only in PBS and not in the bioassay media. Reversible binding to proteins of the media may stabilize the structure of oxytetracycline and prevent a hydrolytic degradation.

Chemical Stability at Different pH Values. In addition to the stability of the chemicals in cell culture media and PBS as a physiological buffer, the chemical stability was investigated at three different pH values over a maximum duration of 48 h to determine whether degradation of chemicals is more likely to be acid-catalyzed or neutral hydrolysis or might be accelerated by hydroxide ions. Autoxidation can also be pH-dependent if the redox potential of the chemical is dependent on the protonation state.[27,78] Evaluation of the pH dependence of degradation is important because the pH value of the bioassay medium can change during the course of the bioassay. The degradation kinetics plots of all chemicals (Figure S5) were used to derive k and $t_{1/2}$ at different pH values (Table S7).

Six chemicals were found to be stable at all three pH values with $t_{1/2} \geq 100$ h, and furosemide and thiabendazole showed only very slow degradation at one pH value (Figure 2). Acetylsalicylic acid, pretilachlor, and 8-gingerol showed similar $t_{1/2}$ at all pH values (Figure 2); thus, the degradation was independent of the hydroxide or proton concentration. For these chemicals, the nucleophile is either water or the hydrolysis is an S_N1 reaction.

Most of the test chemicals (phosmet, bendiocarb, quercetin, malathion, carbofuran, andrographolide, and L-sulforaphane) showed fastest degradation at pH 9 and decreasing degradation rates at pH 7.4 and 4. The degradation of these chemicals is apparently accelerated by hydroxide ions since they were stable at low hydroxide concentrations (pH 4, $[OH^-] = 10^{-10}$ M) and degraded more rapidly with increasing hydroxide concentrations, pH 7.4 ($[OH^-] = 10^{-6.6}$ M) and pH 9 ($[OH^-] = 10^{-5}$ M). For andrographolide and quercetin, there was evidence of possible autoxidation.[69,70,79] For the other chemicals, it was probably a hydrolytic degradation. In this case, the overall reaction followed pseudo-first-order kinetics between the test chemicals and the hydroxide ions, despite the fact that the concentration of hydroxide ions at the highest pH values tested was not higher than the chemical concentration (*e.g.*, [carbofuran] = 2.26×10^{-5} M and $[OH^-]$ at pH 9 = 1×10^{-5} M). The reactions took place in a buffered system to maintain the pH, and thus the hydroxide ion concentration was probably kept constant throughout the duration of the test. The pH of the buffers was measured after 48 h incubation with the chemicals and showed no significant deviation from the initial pH values within 0.1 pH units.

Bendiocarb, phosmet, and quercetin showed the lowest $t_{1/2}$ at pH 9 with 0.28 h (bendiocarb), 0.26 h (phosmet), and <0.28 h (quercetin) (Table S7). The time required to perform the experiments was approx. 17 min (0.28 h). Therefore, for chemicals with very rapid degradation, which were already degraded without additional incubation, $t_{1/2} < 0.28$ h was reported.

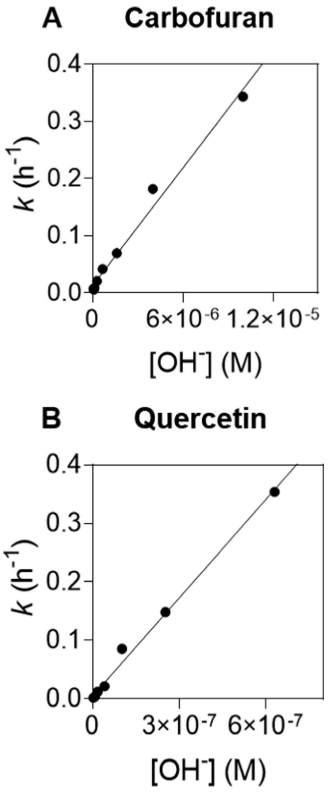

Figure 3. Experimental degradation constant (k) of (A) carbofuran and (B) quercetin plotted against the concentration of hydroxide ions [OH^-].

For two of the test chemicals (carbofuran and quercetin), the degradation was measured from pH 6.6 to 8.6 (carbofuran) or from pH 5.4 to 7.8 (quercetin) (Table S3). The k increased linearly with increasing [OH^-] for carbofuran (Figure 3A) and quercetin (Figure 3B). For carbofuran, the hydroxide ion acted as a nucleophile and the measured degradation constant k can be broken down into hydrolysis (k_{H_2O}) and reaction with OH^- (k_{OH^-}) (eq 5)

$$k = k_{H_2O} + k_{OH^-} \times [OH^-] \quad (5)$$

Thus, a linear regression of k plotted against [OH^-] has a slope of k_{OH^-} and an intercept of k_{H_2O}. Acid-catalyzed hydrolysis and reaction with water were negligible as the intercept of the linear regression of eq 5 in Figure 3 with a k_{H_2O} of 0.014 ± 0.006 h^{-1} demonstrated. The k_{OH^-} was $(3.42 \times 10^4) \pm (1.69 \times 10^3)$ M^{-1} h^{-1}.

For quercetin, which showed a structural alert for autoxidation, the reaction rate also increased linearly with increasing pH because the autoxidation is also pH-dependent.[27] Hydroxide ions can deprotonate the transition state of this reaction, which accelerates the reaction.[26,78] The intercept of Figure 3B was <0.01 h^{-1}, which means that protons do not play a role but k_{OH^-} was $(5.58 \times 10^5) \pm (1.87 \times 10^4)$ M^{-1} h^{-1} for the OH^--facilitated autoxidation (eq 7)

$$k = k_{OH^-} \times [OH^-] \quad (6)$$

Dinoseb and sethoxydim were rapidly degraded at pH 4 but had $t_{1/2} \geq 100$ h at pH 7.4 and 9. There is no evidence of hydrolysis of dinoseb in the literature, but the photocatalytic degradation was much faster at pH 4 than at higher pH values.[80] Dinoseb has an acidity constant (pK_a) of 4.62,[81] and the anion present at pH

https://doi.org/10.1021/acs.chemrestox.2c00030
Chem. Res. Toxicol. 2022, 35, 867−879

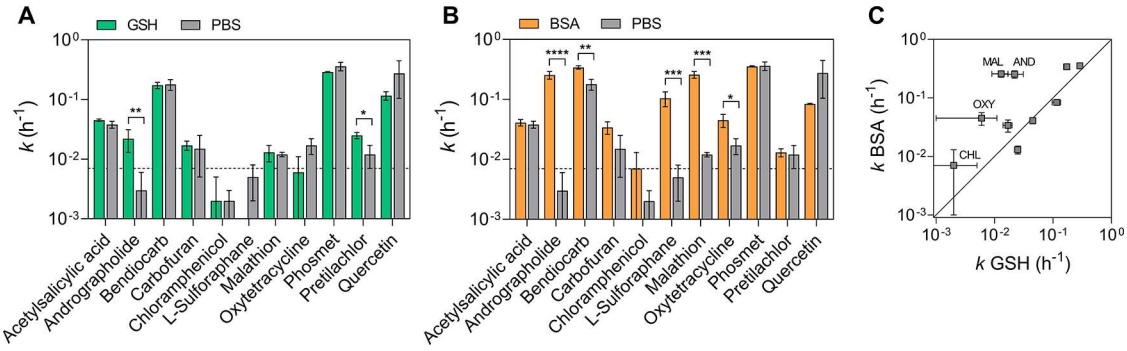

Figure 4. (A) Comparison of experimental degradation constants (k) of the test chemicals in glutathione (GSH) in phosphate-buffered saline (PBS) compared with k in PBS. (B) The k of the test chemicals in bovine serum albumin (BSA) in PBS compared with k in PBS. (C) The k in BSA in PBS compared with k in GSH in PBS. Only chemicals with $k > 0.007$ in at least one test solution are shown. For L-sulforaphane, no k could be measured in GSH because $t_{1/2}$ was ≤0.28 h. The difference between k measured in the GSH or BSA solution and in PBS was tested with an unpaired t-test (A, B). The asterisks above the columns indicate the level of significance. If no asterisks are shown, the difference was not significant. CHL, chloramphenicol; OXY, oxytetracycline; MAL, malathion; and AND, andrographolide (C).

7.4 and 9 is stabilized by the delocalization of the π-electrons over the benzene ring into the electron-withdrawing nitro-substituents. For sethoxydim, the observations are consistent with the literature since hydrolysis of the oxime group is catalyzed by protons.[82]

Oxytetracycline was the only test chemical that showed degradation only at pH 7.4. At lower or higher pH, $t_{1/2}$ was ≥100 h for that chemical. This observation is consistent with the literature where it has been demonstrated that oxytetracycline is hydrolyzed to apo-oxytetracycline.[54] Oxytetracycline has three acidic functions with pK_a values of 3.28, 6.68, and 12.52 and one basic amino group with a pK_a of 9.00.[83] At pH 7.4, the molecule is 84% anionic and 16% zwitterionic. Differences in speciation could influence the susceptibility to hydrolytic degradation.

Reactivity toward Proteins. The reactivity of the test chemicals toward proteins was tested with BSA and GSH as model nucleophiles. The pH of all solutions was adjusted to 7.4, and the nucleophile was always used in excess to ensure pseudo-first-order kinetics.

The reduced glutathione (GSH) was quantified with Ellman's assay.[66] The measured GSH concentration equaled the nominal concentration when measured immediately but deviated from the initial concentration by up to a factor of 10 after 48 h (Figure S6). Since this observation did not occur at all concentrations, it could be an artifact. Although GSH was used in 10-fold excess to the chemical concentration, GSH could have been partially depleted after 48 h, which could slow down the reaction. The plots of degradation kinetics of the test chemicals in a GSH or BSA solution in PBS (Figure S7) were used to derive k as fit parameter and $t_{1/2}$ (Table S7).

Eight chemicals showed degradation in the GSH solution with $t_{1/2} < 100$ h, *i.e.*, $k > 0.007$ h^{-1} (Figure 4A). For five of the chemicals (acetylsalicylic acid, andrographolide, carbofuran, malathion, and pretilachlor), k in the GSH solution was higher than k measured for the PBS control, but there was only a significant difference for andrographolide and pretilachlor (unpaired t-test). There was an immediate degradation of 1,2-benzisothiazol-3(2*H*)-one, 2-methyl-4-isothiazolinone, and L-sulforaphane, so that no k could be fitted and $t_{1/2}$ was ≤0.28 h for these chemicals. It is well known that isothiazolinone biocides like 1,2-benzisothiazol-3(2*H*)-one and 2-methyl-4-isothiazolinone can react with the cysteine residue of GSH.[84] However, there was no degradation of either chemical in BSA solution nor in the bioassay media up to 48 h of incubation. The size and three-dimensional structure of the BSA molecule may be a steric hindrance that prevents a reaction with the free cysteine, also explaining the stability of 1,2-benzisothiazol-3(2*H*)-one and 2-methyl-4-isothiazolinone in the bioassay medium (Figure 2 and Table S7). In this case, the stability test in GSH solutions did not reflect stability in the bioassay medium, so GSH should not generally be used as a sole surrogate for determining reactivity toward proteins in the assay medium.

Eleven chemicals had $k > 0.007$ h^{-1} in the BSA solution (Figure 4B). The k in the BSA solution was higher than k in PBS for nine of the chemicals, but the difference was significant only for andrographolide, bendiocarb, L-sulforaphane, malathion, and oxytetracycline (unpaired t-test; Figure 4B). L-Sulforaphane showed a very fast degradation in GSH and BSA solutions and was stable at pH 7.4 in PBS; thus, the reaction with proteins must be the main degradation pathway for this substance. This is consistent with the observation of Hanschen et al.[52] who demonstrated that L-sulforaphane can react with the thiol group of cysteine as well as with the amino group of, *e.g.*, lysine.

Bendiocarb, malathion, and oxytetracycline were all hydrolyzed at pH 7.4, which makes it difficult to say whether there is an additional reaction with proteins or whether the hydrolysis might be accelerated due to the presence of BSA. Only malathion showed faster degradation in the bioassay medium than in PBS, which also indicates a reactivity toward proteins for this chemical. Yamagishi et al.[85] recently showed that malathion can form various adducts with human serum albumin. For most chemicals, k measured in the presence of BSA or GSH did not differ greatly (Figure 4C). However, four of the test chemicals (chloramphenicol, oxytetracycline, andrographolide, malathion) showed faster degradation with BSA than with GSH. Chloramphenicol and oxytetracycline showed low k and high standard deviations with both nucleophiles, hampering the evaluation of this result. Malathion and andrographolide showed a significantly faster degradation in the presence of BSA compared to that of GSH (up to a factor of 19.9 difference). GSH has a freely accessible thiol group, but BSA contains other reactive amino acids (*e.g.*, lysines) that can play a role in reactivity. The results obtained with both nucleophiles are generally comparable for most of the chemicals but since some chemicals showed a significantly faster reaction with GSH than with BSA and vice versa, testing with both nucleophiles is advisable.

https://doi.org/10.1021/acs.chemrestox.2c00030
Chem. Res. Toxicol. 2022, 35, 867−879

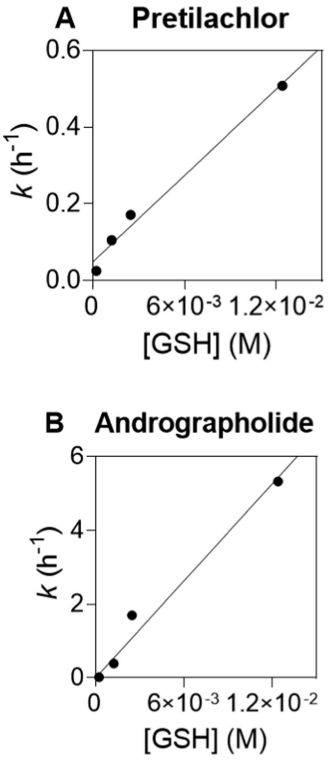

Figure 5. Experimental degradation constant (k) of (A) pretilachlor and (B) andrographolide plotted against the concentration of glutathione [GSH].

The degradation kinetics were measured for additional GSH concentrations for andrographolide and pretilachlor to determine the second-order rate constant with GSH k_{GSH} (eq 7).

$$k = k_{H_2O} + k_{GSH} \times [GSH] \quad (7)$$

Figure 5 shows k plotted against the GSH concentration for pretilachlor (A) and andrographolide (B). For pretilachlor, k_{GSH} determined from the fit was 37.55 M^{-1} h^{-1} and k_{H_2O} was 0.049 h^{-1}. This is slightly higher but in the same range as stability measured in PBS (0.022 ± 0.010 h^{-1}) because pretilachlor showed slow degradation at pH 7.4. Although pretilachlor reacted with GSH, it showed no reactivity to BSA (Figure 4B) because k in the BSA solution was higher than k_{H_2O}, but the difference was not significant (unpaired t-test).

Andrographolide had a k_{GSH} of 437.90 M^{-1} h^{-1} and was found to be stable at pH 7.4 with $k \leq 0.007$, so the intercept was set to 0. Michael addition is the mechanism of the second-order reaction of andrographolide with GHS.[41] Andrographolide showed an even faster reaction with BSA, which could be caused by other reactive amino acids in addition to cysteine.

Photodegradation. The susceptibility of the test substances to photodegradation was tested by incubation in a xenon test chamber. The chemicals were exposed to the radiation of the lamp for up to 7.5 h, which corresponds to a multiple of the light intensity to which chemicals are normally exposed under laboratory conditions. The degradation plots of all chemicals can be found in the Supporting Information (Figure S8). The sample temperature could not be monitored in the xenon chamber, and the samples were prone to evaporation after longer incubation. Therefore, there were volume variations in the samples from different time points. Since the volume of the desorption solution was constant, these variations should not have a large effect on the relative chemical concentration, but no kinetics for photodegradation were fitted since these would not be comparable with the kinetics of the other test systems.

An overview of the qualitative photodegradation results for the test chemicals can be found in the Supporting Information (Table S7). Eleven chemicals showed degradation within 7.5 h incubation in the xenon test chamber. Three of these chemicals (bendiocarb, phosmet, and quercetin) showed $t_{1/2}$ < 7.5 h in PBS in the dark, so the degradation of these chemicals might be caused by hydrolysis (or autoxidation) and not by photodegradation. 1,2-Benzisothiazol-3(2*H*)-one, chloramphenicol, and furosemide, which were all stable in PBS in the dark, and oxytetracycline showed the fastest degradation in the xenon test chamber, so these chemicals are very likely to be prone to photodegradation, which is also in line with the literature.[47,50,54,86] All chemicals that showed fast photodegradation were found to be stable in the bioassay medium. This observation proves that for a normal use of the chemicals in the *in vitro* bioassay, photodegradation does not play a significant role, as the chemicals are not exposed to high light intensities over a longer period of time. For other *in vitro* systems such as algal toxicity, where incubation in light is necessary, these processes could play a more important role.[87]

Oxidation. Although autoxidation in the bioassay medium is possible for some chemicals, this reaction cannot be separated from the other processes and is therefore difficult to detect. Potentially comparing stability in the presence and absence of antioxidants could shed more light on autoxidation. The general susceptibility for oxidation was checked by incubation of the test chemicals with the mild oxidant *N*-bromosuccinimide (NBS). NBS was used in excess to ensure a complete reaction of the chemicals. The reaction was very fast, and the half-lives were lower than the process time of the experiment. The degradation plots of all chemicals can be found in the Supporting Information (Figure S9), and an overview over the results can be found in Table S7. Fifteen of the 22 test chemicals were degraded by NBS within 2 h incubation (Figure S9 and Table S7). 2-Methyl-4-isothiazolinone, acetylsalicylic acid, bendiocarb, chloramphenicol, pretilachlor, thiabendazole, and triclopyr were not oxidized within the total incubation time of 48 h. The observed degradation of acetylsalicylic acid, bendiocarb, and pretilachlor after 48 h was caused by hydrolysis since the chemical concentration in the NBS solution did not differ from the concentration in the PBS controls (Figure S9). Most of the other test chemicals were degraded rapidly (<10 min) by NBS. The test with NBS showed that most of the test substances were principally oxidizable but oxidation does not appear to be relevant under bioassay conditions because many chemicals that were degraded by NBS were stable in the bioassay medium (1,2-benzisothiazol-3(2*H*)-one, 6-gingerol, 8-gingerol, acetaminophen, dinoseb, furosemide, sethoxydim). Thus, NBS is not a good substitute to detect oxidation under bioassay conditions (autoxidation); however, the reaction with NBS may indicate that these chemicals can also be oxidized within cells by metabolizing enzymes (cytochrome P450 enzymes).[88]

***In Silico* Prediction of Chemical Stability.** Three different *in silico* models were used to determine the susceptibility of the test chemicals to hydrolysis at different pH values, photodegradation, and their reaction potential toward proteins. All models were designed for the prediction of environmental degradation processes or structural alerts for chemical reactivity. We wanted to evaluate if these models could be used to identify unstable chemicals in *in vitro* bioassays as well. The *in silico*

https://doi.org/10.1021/acs.chemrestox.2c00030
Chem. Res. Toxicol. 2022, 35, 867−879

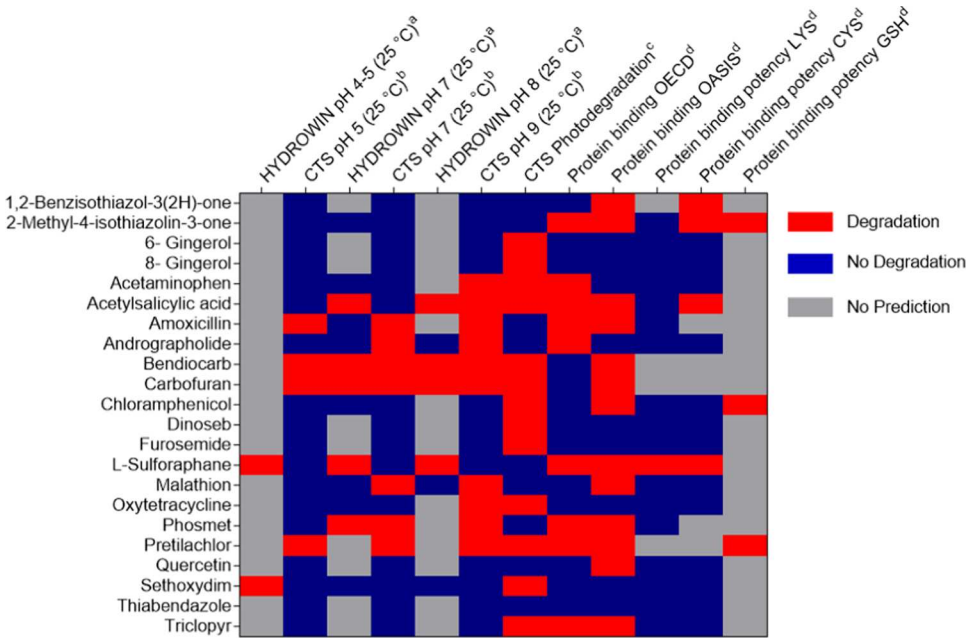

Figure 6. Overview of the *in silico* stability predictions for all test chemicals. Underlying data are given in Table S9. The *in silico* prediction models used for hydrolysis prediction also predict degradation half-lives ($t_{1/2}$). All chemicals with predicted $t_{1/2} \leq 60$ days were classified as degradable (red) and those with $t_{1/2} > 60$ days were classified as not degradable (blue). The gray boxes indicate chemicals and conditions where no prediction was possible. Only qualitative predictions were made for photodegradation and reactivity toward proteins using the QSAR Toolbox. [a]HYDROWIN was accessed *via* EPI-Suite version 4.1.[22] [b]Chemical transformation simulator version 1.1 (CTS) was accessed *via* the Internet (https://qed.epa.gov/cts/, 20 April 2021).[19] [c]Chemical transformation simulator version 1.1 (CTS) was accessed *via* the Internet (https://qed.epa.gov/cts/, 20 April 2021).[20] [d]Accessed *via* QSAR Toolbox version 4.4.1.[71−76]

models predicted degradation for all chemicals except thiabendazole for at least one test condition (Figure 6). More detailed information can be found in the Supporting Information (Table S9).

Two models (HYDROWIN and CTS) were used to predict hydrolysis of the test chemicals at three pH values. The models often provided different predictions of chemical stability, and HYDROWIN often lacked data for predicting stability at higher and lower pH values. The predicted $t_{1/2}$ (Table S9) were often very high (days to years), compared to the normal duration of an *in vitro* bioassay (24−48 h), which was also performed at higher temperature.

As a conservative approximation, all chemicals with predicted $t_{1/2} \leq 60$ days were considered degradable according to the persistence criterion of the European chemical regulation REACH.[89] For 10 of the chemicals, both models predicted no degradation at all pH values. At pH 4 or 5, HYDROWIN predicted degradation for two chemicals (L-sulforaphane, sethoxydim) and CTS for four chemicals (amoxicillin, bendiocarb, carbofuran, pretilachlor). At pH 7, HYDROWIN predicted the degradation of 5 and CTS of 7 chemicals, and at pH 9, degradation was predicted for 4 chemicals by HYDROWIN and 10 chemicals by CTS.

CTS was also used to predict photodegradation, and 13 of the test chemicals were predicted to be prone to photodegradation. There were no $t_{1/2}$ predicted for photodegradation, so all chemicals with predicted photodegradation were considered unstable.

Five models from the QSAR Toolbox were used for the prediction of reactivity toward proteins. The protein binding OECD model classified nine chemicals as reactive, and the protein binding OASIS model classified 13 chemicals as reactive. The protein binding potency LYS model predicted degradation only for L-sulforaphane, and the protein binding potency CYS model predicted degradation for 1,2-benzisothiazol-3(2*H*)-one, 2-methyl-4-isothiazolinone, acetylsalicylic acid, and L-sulforaphane. 2-Methyl-4-isothiazolinone, chloramphenicol, and pretilachlor were predicted to be unstable by the protein binding potency GSH model.

Comparison of Experimentally Determined Stability with *In Silico* Predictions. The models used for the prediction of hydrolysis or photodegradation were developed to predict these processes in the environment. The protein reactivity models are based on structural alerts and do not give any indication of reaction rates or conditions.

Since the pH of the bioassay medium is 7.4, hydrolysis at neutral pH should be a major degradation process in the bioassay medium. The HYDROWIN model was able to give a prediction for 13 of the test chemicals at pH 7. Acetylsalicylic acid, bendiocarb, carbofuran, L-sulforaphane, and phosmet were predicted to be degradable. All of these chemicals, except L-sulforaphane, also showed degradation in the experiment. However, two chemicals (malathion and oxytetracycline) that showed degradation at pH 7.4 in the experiment were predicted to be stable by the model. According to CTS, amoxicillin, andrographolide, bendiocarb, carbofuran, malathion, phosmet, and pretilachlor were prone to degradation at pH 7. Amoxicillin and andrographolide were found to be stable in the experiment, but 8-gingerol, acetylsalicylic acid, and oxytetracycline showed degradation, which was not predicted by CTS. Quercetin, which also showed degradation at pH 7.4 in the experiment, was probably not degraded hydrolytically but oxidized, which is why it was classified as stable by CTS. Table S10 compares model predictions with experimental results. For HYDROWIN, the agreement was 77% and for CTS, it was 76%.

https://doi.org/10.1021/acs.chemrestox.2c00030
Chem. Res. Toxicol. 2022, 35, 867−879

Reactivity toward proteins is a major potential degradation route for chemicals in bioassays, along with hydrolysis, since most media contain high levels of FBS or protein-rich supplements. In the experiments, six chemicals (1,2-benzisothiazol-3(2*H*)-one, 2-methyl-4-isothiazolinone, andrographolide, L-sulforaphane, malathion, and pretilachlor) reacted with GSH and/or BSA.

The models used to predict reactivity toward proteins are normally used to get early warnings about a possible skin sensitization potential of chemicals.[73−75] Therefore, they only give structural warnings indicating potentially reactive groups of the test chemical but do not give any indication of conditions and rate of a possible reaction. None of the models were able to identify all chemicals that showed reactivity toward proteins in the experiment. The protein binding OECD and the protein binding OASIS models gave alerts for approx. half of the chemicals. Still, both models could not identify all chemicals that showed reactivity toward proteins in the experiment. The protein binding OECD model classified 1,2-benzisothiazol-3(2*H*)-one and malathion as nonreactive, and the protein binding OASIS model gave no alert for andrographolide. The agreement of both models with the experimental findings was 59%. 1,2-Benzisothiazol-3(2*H*)-one, 2-methyl-4-isothiazolinone, acetylsalicylic acid, and L-sulforaphane were predicted to be reactive by the protein binding potency CYS model, but it did not give a warning for andrographolide and malathion and could not make a prediction for pretilachlor. The agreement with the experimental results was 76% for the protein binding potency CYS model, which was the best agreement of all models predicting reactivity toward proteins. The protein binding potency GSH model had an agreement of 67% with the experimental results and predicted reactivity for 2-methyl-4-isothiazolinone, chloramphenicol, and pretilachlor, and no prediction was possible for the other chemicals. L-Sulforaphane was the only chemical classified as reactive by the protein binding LYS model. L-Sulforaphane showed degradation in the presence of BSA, but from these results, it is not possible to conclude which amino acids were involved in the reaction.

CONCLUSIONS

The proposed HT workflow for the determination of the abiotic stability and characterization of degradation processes of chemicals in *in vitro* bioassays was used to evaluate the stability of 22 environmentally unstable test chemicals under bioassay conditions. Hydrolysis at pH 7.4, autoxidation (specifically for quercetin), and reactivity toward proteins were identified as the main responsible processes for the degradation of chemicals in the bioassay medium. All chemicals that showed degradation in assay media were either degraded in PBS alone or showed reactivity toward proteins. The experiments showed that the abiotic stability of chemicals played a relevant role even in the relatively short time frame of *in vitro* bioassays and that stability tests are necessary to obtain reliable bioassay results.

The depicted workflow (Figure 1) suggests that first, the concentration of the test chemicals in the respective bioassay medium should be measured and compared with the initial concentration. If no reduction of the initial concentration can be detected in this test, the chemicals can be considered abiotically stable and no further tests are necessary. However, if a reduction in the chemical concentration of >20% compared to the initial concentration is observed, the $t_{1/2}$ should be determined in the respective medium. If chemicals are not stable, the concentrations should be quantified in the bioassay and measured effect concentrations should be reported.

To identify the responsible degradation processes, the $t_{1/2}$ at pH 7.4 should be determined first, and if they are found to be higher than the corresponding $t_{1/2}$ in the medium, the reactivity toward proteins should be tested with BSA or GSH. In this case, the BioSPME 96-Pin device can be used for a HT measurement of the relative concentration, but also other extraction techniques can be used for more hydrophilic (*e.g.*, protein precipitation) or hydrophobic (*e.g.*, liquid−liquid extraction) chemicals.

According to the results of the present study, tests for photodegradation are not necessary if the bioassays are performed under laboratory conditions and incubated in the dark. Tests with NBS could not mimic oxidation under bioassay conditions in the present study but might be used to give an indication of metabolic degradability.

In silico models for the prediction of hydrolysis and reactivity toward proteins can be used in support of experimental tests to screen test chemicals for possible degradation or reactivity prior to bioassay. The models generally showed good agreement with the experimental data, but no model could predict all chemicals that showed degradation in the experiment. The models were not designed for the specific conditions in the bioassay and are therefore not sufficient on their own to evaluate the stability of chemicals in this context. Having a larger set of experimental stability data under bioassay conditions, it may be possible to develop a model capable of reliably predicting stability in the bioassay in the future, but until this is achieved, experimental stability measurements are indispensable for a reliable evaluation of the abiotic stability of chemicals and should be routinely integrated in future *in vitro* bioassay workflows.

Abiotic degradation processes that reduce the stability of the test chemical in the bioassay medium may lead to misinterpretation of the bioassay results. For example, if less active transformation products are formed, the chemical will be classified as inactive in the corresponding assay. Further research is needed to determine whether comparable degradation processes can also occur in humans. If nominal effect concentrations of unstable chemicals in *in vitro* assays are used as input parameters for QIVIVE models, the effect *in vivo* may be underestimated. QIVIVE models are usually based on the nominal concentration, which does not take into account either partitioning processes (*e.g.*, binding to proteins or plate material) or loss processes (abiotic degradation, metabolism, volatilization) of the test chemicals during the assay.[18,90,91] Differences in the stability of the test chemicals between the *in vitro* bioassays and *in vivo* in humans may be a major impediment for using bioassay data for human health risk assessment.

ASSOCIATED CONTENT

Supporting Information

The Supporting Information is available free of charge at https://pubs.acs.org/doi/10.1021/acs.chemrestox.2c00030.

Additional information about the test chemicals, the plate layout of the stability tests, instrumental analysis, uptake kinetics and reproducibility of the SPME pin device, compositions of additional pH buffers, and GSH stability and degradation plots of all chemicals in all test systems (PDF)

Detailed results from *in silico* stability prediction models and experimental stability tests (XLSX)

https://doi.org/10.1021/acs.chemrestox.2c00030
Chem. Res. Toxicol. 2022, 35, 867−879

AUTHOR INFORMATION

Corresponding Author

Beate I. Escher − *Department of Cell Toxicology, Helmholtz Centre for Environmental Research—UFZ, DE-04318 Leipzig, Germany; Environmental Toxicology, Center for Applied Geoscience, Eberhard Karls University Tübingen, DE-72076 Tübingen, Germany;* orcid.org/0000-0002-5304-706X; Email: beate.escher@ufz.de

Authors

Julia Huchthausen − *Department of Cell Toxicology, Helmholtz Centre for Environmental Research—UFZ, DE-04318 Leipzig, Germany;* orcid.org/0000-0003-4916-1174

Luise Henneberger − *Department of Cell Toxicology, Helmholtz Centre for Environmental Research—UFZ, DE-04318 Leipzig, Germany;* orcid.org/0000-0002-3181-0044

Sophia Mälzer − *Department of Cell Toxicology, Helmholtz Centre for Environmental Research—UFZ, DE-04318 Leipzig, Germany*

Beate Nicol − *Safety and Environmental Assurance Centre, Unilever, Bedford MK44 1LQ, U.K.*

Chris Sparham − *Safety and Environmental Assurance Centre, Unilever, Bedford MK44 1LQ, U.K.*

Complete contact information is available at: https://pubs.acs.org/10.1021/acs.chemrestox.2c00030

Funding

This work was funded by Unilever.

Notes

The authors declare no competing financial interest.

ACKNOWLEDGMENTS

The authors thank Jenny John for supporting the experiments and Daniel Kolb from the Department of Analytical Chemistry of UFZ for providing the xenon test chamber for the photodegradation experiments. The authors also thank Stefan Stolte and the team from SEAC (Unilever) for reviewing the manuscript.

REFERENCES

(1) Desprez, B.; Dent, M.; Keller, D.; Klaric, M.; Ouédraogo, G.; Cubberley, R.; Duplan, H.; Eilstein, J.; Ellison, C.; Grégoire, S.; Hewitt, N. J.; Jacques-Jamin, C.; Lange, D.; Roe, A.; Rothe, H.; Blaauboer, B. J.; Schepky, A.; Mahony, C. A strategy for systemic toxicity assessment based on non-animal approaches: The Cosmetics Europe Long Range Science Strategy programme. *Toxicol. In Vitro* **2018**, *50*, 137−146.

(2) Vinken, M.; Kramer, N.; Allen, T. E. H.; Hoffmans, Y.; Thatcher, N.; Levorato, S.; Traussnig, H.; Schulte, S.; Boobis, A.; Thiel, A.; Rietjens, I. M. C. M. The use of adverse outcome pathways in the safety evaluation of food additives. *Arch. Toxicol.* **2020**, *94*, 959−966.

(3) Westmoreland, C.; Carmichael, P.; Dent, M.; Fentem, J.; MacKay, C.; Maxwell, G.; Pease, C.; Reynolds, F. Assuring safety without animal testing: Unilever's ongoing research programme to deliver novel ways to assure consumer safety. *Altex* **2010**, *27*, 207−2011.

(4) Collins, F. S.; Gray, G. M.; Bucher, J. R. Toxicology - Transforming environmental health protection. *Science* **2008**, *319*, 906−907.

(5) Escher, B.; Neale, P.; Leusch, F. *Bioanalytical Tools in Water Quality Assessment*; IWA Publishing, 2021.

(6) Attene-Ramos, M. S.; Miller, N.; Huang, R.; Michael, S.; Itkin, M.; Kavlock, R. J.; Austin, C. P.; Shinn, P.; Simeonov, A.; Tice, R. R.; Xia, M. The Tox21 robotic platform for the assessment of environmental chemicals − from vision to reality. *Drug Discovery Today* **2013**, *18*, 716−723.

(7) Burden, N.; Chapman, K.; Sewell, F.; Robinson, V. Pioneering better science through the 3Rs: an introduction to the national centre for the replacement, refinement, and reduction of animals in research (NC3Rs). *J. Am. Assoc. Lab. Anim. Sci.* **2015**, *54*, 198−208.

(8) Wetmore, B. A. Quantitative in vitro-to-in vivo extrapolation in a high-throughput environment. *Toxicology* **2015**, *332*, 94−101.

(9) Wambaugh, J. F.; Hughes, M. F.; Ring, C. L.; MacMillan, D. K.; Ford, J.; Fennell, T. R.; Black, S. R.; Snyder, R. W.; Sipes, N. S.; Wetmore, B. A.; Westerhout, J.; Setzer, R. W.; Pearce, R. G.; Simmons, J. E.; Thomas, R. S. Evaluating in vitro-in vivo extrapolation of toxicokinetics. *Toxicol. Sci.* **2018**, *163*, 152−169.

(10) Groothuis, F. A.; Heringa, M. B.; Nicol, B.; Hermens, J. L. M.; Blaauboer, B. J.; Kramer, N. I. Dose metric considerations in in vitro assays to improve quantitative in vitro−in vivo dose extrapolations. *Toxicology* **2015**, *332*, 30−40.

(11) Fischer, F. C.; Henneberger, L.; König, M.; Bittermann, K.; Linden, L.; Goss, K. U.; Escher, B. I. Modeling exposure in the Tox21 in vitro bioassays. *Chem. Res. Toxicol.* **2017**, *30*, 1197−1208.

(12) Henneberger, L.; Mühlenbrink, M.; Fischer, F. C.; Escher, B. I. C18-coated solid-phase microextraction fibers for the quantification of partitioning of organic acids to proteins, lipids, and cells. *Chem. Res. Toxicol.* **2019**, *32*, 168−178.

(13) Kramer, N. I.; Krismartina, M.; Rico-Rico, A.; Blaauboer, B. J.; Hermens, J. L. Quantifying processes determining the free concentration of phenanthrene in basal cytotoxicity assays. *Chem. Res. Toxicol.* **2012**, *25*, 436−445.

(14) Kisitu, J.; Hollert, H.; Fisher, C.; Leist, M. Chemical Concentrations in Cell Culture Compartments (C5) - Free Concentrations. *Altex* **2020**, *37*, 693−708.

(15) Hung, S.; Mohan, A.; Reckhow, D. A.; Godri Pollitt, K. J. Assessment of the in vitro toxicity of the disinfection byproduct 2,6-dichloro-1,4-benzoquinone and its transformed derivatives. *Chemosphere* **2019**, *234*, 902−908.

(16) Tentscher, P. R.; Escher, B. I.; Schlichting, R.; König, M.; Bramaz, N.; Schirmer, K.; von Gunten, U. Toxic effects of substituted p-benzoquinones and hydroquinones in in vitro bioassays are altered by reactions with the cell assay medium. *Water Res.* **2021**, *202*, No. 117415.

(17) Shen, L.; Ji, H. F. The pharmacology of curcumin: is it the degradation products? *Trends Mol. Med.* **2012**, *18*, 138−144.

(18) Henneberger, L.; Huchthausen, J.; Wojtysiak, N.; Escher, B. I. Quantitative In Vitro-to-In Vivo Extrapolation: Nominal versus Freely Dissolved Concentration. *Chem. Res. Toxicol.* **2021**, *34*, 1175−1182.

(19) Tebes-Stevens, C.; Patel, J. M.; Jones, W. J.; Weber, E. J. Prediction of hydrolysis products of organic chemicals under environmental pH conditions. *Environ. Sci. Technol.* **2017**, *51*, 5008−5016.

(20) Yuan, C.; Tebes-Stevens, C.; Weber, E. J. Reaction library to predict direct photochemical transformation products of environmental organic contaminants in sunlit aquatic systems. *Environ. Sci. Technol.* **2020**, *54*, 7271−7279.

(21) Dimitrov, S. D.; Diderich, R.; Sobanski, T.; Pavlov, T. S.; Chankov, G. V.; Chapkanov, A. S.; Karakolev, Y. H.; Temelkov, S. G.; Vasilev, R. A.; Gerova, K. D.; Kuseva, C. D.; Todorova, N. D.; Mehmed, A. M.; Rasenberg, M.; Mekenyan, O. G. QSAR Toolbox − workflow and major functionalities. *SAR QSAR Environ. Res.* **2016**, *27*, 203−219.

(22) Howard, P. H.; Meylan, W. M. *Hydrolysis Rate Program*; Taylor & Francis, 1992.

(23) Villeneuve, D. L.; Coady, K.; Escher, B. I.; Mihaich, E.; Murphy, C. A.; Schlekat, T.; Garcia-Reyero, N. High-throughput screening and environmental risk assessment: State of the science and emerging applications. *Environ. Toxicol. Chem.* **2019**, *38*, 12−26.

(24) Judson, R.; Houck, K.; Martin, M.; Knudsen, T.; Thomas, R. S.; Sipes, N.; Shah, I.; Wambaugh, J.; Crofton, K. In Vitro and Modelling Approaches to Risk Assessment from the US Environmental Protection Agency ToxCast Programme. *Basic Clin. Pharmacol. Toxicol.* **2014**, *115*, 69−76.

(25) Crounse, J. D.; Nielsen, L. B.; Jørgensen, S.; Kjaergaard, H. G.; Wennberg, P. O. Autoxidation of Organic Compounds in the Atmosphere. *J. Phys. Chem. Lett.* **2013**, *4*, 3513−3520.
(26) Jiang, C.; Garg, S.; Waite, T. D. Hydroquinone-Mediated Redox Cycling of Iron and Concomitant Oxidation of Hydroquinone in Oxic Waters under Acidic Conditions: Comparison with Iron−Natural Organic Matter Interactions. *Environ. Sci. Technol.* **2015**, *49*, 14076−14084.
(27) Dangles, O.; Fargeix, G.; Dufour, C. One-electron oxidation of quercetin and quercetin derivatives in protic and non protic media. *J. Chem. Soc., Perkin Trans.* **1999**, *2*, 1387−1396.
(28) EPA. *Fate, Transport and Transformation Test Guidelines: OPPTS 835.2120 Hydrolysis*; EPA, 2008.
(29) Schwarzenbach, R. P.; Gschwend, P. M.; Imboden, D. M. *Environmental Organic Chemistry*; Wiley, 2016.
(30) Zepp, R. G.; Cline, D. M. Rates of direct photolysis in aquatic environment. *Environ. Sci. Technol.* **1977**, *11*, 359−366.
(31) OECD. *Test No. 316: Phototransformation of Chemicals in Water—Direct Photolysis*; OECD, 2008.
(32) Adimurthy, S.; Patoliya, P. N-Bromosuccinimide: A facile reagent for the oxidation of benzylic alcohols to aldehydes. *Synth. Commun.* **2007**, *37*, 1571−1577.
(33) Roy, K. S.; Nazdrajić, E.; Shimelis, O. I.; Ross, M. J.; Chen, Y.; Cramer, H.; Pawliszyn, J. Optimizing a High-Throughput Solid-Phase Microextraction System to Determine the Plasma Protein Binding of Drugs in Human Plasma. *Anal. Chem.* **2021**, *93*, 11061−11065.
(34) Mutschler, J.; Gimenez-Arnau, E.; Foertsch, L.; Gerberick, G. F.; Lepoittevin, J. P. Mechanistic assessment of peptide reactivity assay to predict skin allergens with Kathon (R) CG isothiazolinones. *Toxicol. In Vitro* **2009**, *23*, 439−446.
(35) Bhattarai, S.; Tran, V. H.; Duke, C. C. The stability of gingerol and shogaol in aqueous solutions. *J. Pharm. Sci.* **2001**, *90*, 1658−1664.
(36) Zhou, C.; Zhou, Q.; Zhang, X. Transformation of acetaminophen in natural surface water and the change of aquatic microbes. *Water Res.* **2019**, *148*, 133−141.
(37) Bakar, S. K.; Niazi, S. Stability of aspirin in different media. *J. Pharm. Sci.* **1983**, *72*, 1024−1026.
(38) Andreozzi, R.; Caprio, V.; Ciniglia, C.; de Champdoré, M.; Lo Giudice, R.; Marotta, R.; Zuccato, E. Antibiotics in the environment: Occurrence in Italian STPs, fate, and preliminary assessment on algal toxicity of amoxicillin. *Environ. Sci. Technol.* **2004**, *38*, 6832−6838.
(39) Xu, H.; Cooper, W. J.; Jung, J.; Song, W. Photosensitized degradation of amoxicillin in natural organic matter isolate solutions. *Water Res.* **2011**, *45*, 632−638.
(40) Phattanawasin, P.; Sotanaphun, U.; Burana-Osot, J.; Piyapolrungroj, N. Isolation and characterization of the acid and base degradation products of andrographolide. *Pharmazie* **2018**, *73*, 559−562.
(41) Zhang, Z. Q.; Chan, G. K. L.; Li, J. L.; Fong, W. F.; Cheung, H. Y. Molecular interaction between andrographolide and glutathione follows second order kinetics. *Chem. Pharm. Bull.* **2008**, *56*, 1229−1233.
(42) Kumar, K. S.; Suvardhan, K.; Rekha, D.; Kiran, K.; Jayaraj, B.; Janardhanam, K.; Chiranjeevi, P. Development of simple and sensitive spectrophotometric method for the determination of bendiocarb in its formulations and environmental samples. *Environ. Monit. Assess.* **2007**, *127*, 67−72.
(43) Climent, M. J.; Miranda, M. A. Gas chromatographic-mass spectrometric study of photodegradation of carbamate pesticides. *J. Chromatogr. A* **1996**, *738*, 225−231.
(44) Seiber, J. N.; Catahan, M. P.; Barril, C. R. Loss of carbofuran from rice paddy water: Chemical and physical factors. *J. Environ. Sci. Health, Part B* **1978**, *13*, 131−148.
(45) Campbell, S.; David, M. D.; Woodward, L. A.; Li, Q. X. Persistence of carbofuran in marine sand and water. *Chemosphere* **2004**, *54*, 1155−1161.
(46) Mitchell, S. M.; Ullman, J. L.; Teel, A. L.; Watts, R. J. Hydrolysis of amphenicol and macrolide antibiotics: Chloramphenicol, florfenicol, spiramycin, and tylosin. *Chemosphere* **2015**, *134*, 504−511.
(47) Marson, E. O.; Paniagua, C. E. S.; Costa-Serge, N. M.; Sousa, R. M. F.; Silva, G. D.; Becker, R. W.; Sirtori, C.; Starling, M.; Carvalho, S. R.; Trovó, A. G. Chemical and toxicological evaluation along with unprecedented transformation products during photolysis and heterogeneous photocatalysis of chloramphenicol in different aqueous matrices. *Environ. Sci. Pollut. Res. Int.* **2021**, *28*, 23582−23594.
(48) Matsuo, H.; Casida, J. E. Photodegradation of two dinitrophenolic pesticide chemicals, dinobuton and dinoseb, applied to bean leaves. *Bull. Environ. Contam. Toxicol.* **1970**, *5*, 72−78.
(49) Cruz, J. E.; Maness, D. D.; Yakatan, G. J. Kinetics and mechanism of hydrolysis of furosemide. *Int. J. Pharm.* **1979**, *2*, 275−281.
(50) Bundgaard, H.; Nørgaard, T.; Nielsen, N. M. Photodegradation and hydrolysis of furosemide and furosemide esters in aqueous solutions. *Int. J. Pharm.* **1988**, *42*, 217−224.
(51) Franklin, S. J.; Dickinson, S. E.; Karlage, K. L.; Bowden, G. T.; Myrdal, P. B. Stability of sulforaphane for topical formulation. *Drug Dev. Ind. Pharm.* **2014**, *40*, 494−502.
(52) Hanschen, F. S.; Brüggemann, N.; Brodehl, A.; Mewis, I.; Schreiner, M.; Rohn, S.; Kroh, L. W. Characterization of products from the reaction of glucosinolate-derived isothiocyanates with cysteine and lysine derivatives formed in either model systems or broccoli sprouts. *J. Agric. Food Chem.* **2012**, *60*, 7735−7745.
(53) Wolfe, N. L.; Zepp, R. G.; Gordon, J. A.; Baughman, G. L.; Cline, D. M. Kinetics of chemical degradation of malathion in water. *Environ. Sci. Technol.* **1977**, *11*, 88−93.
(54) Xuan, R.; Arisi, L.; Wang, Q.; Yates, S. R.; Biswas, K. C. Hydrolysis and photolysis of oxytetracycline in aqueous solution. *J. Environ. Sci. Health, Part B* **2009**, *45*, 73−81.
(55) Sinderhauf, K.; Schwack, W. Photolysis experiments on phosmet, an organophosphorus insecticide. *J. Agric. Food Chem.* **2003**, *51*, 5990−5995.
(56) Choudhury, P. P.; Barman, K. K.; Varshney, J. G. Photolysis of pretilachlor on soil surface. *Indian J. Weed Sci.* **2009**, *41*, 87−89.
(57) Clarke, E. D.; Greenhow, D. T.; Adams, D. Metabolism-related assays and their application to agrochemical research: Reactivity of pesticides with glutathione and glutathione transferases. *Pestic. Sci.* **1998**, *54*, 385−393.
(58) Zenkevich, I. G.; Eshchenko, A. Y.; Makarova, S. V.; Vitenberg, A. G.; Dobryakov, Y. G.; Utsal, V. A. Identification of the products of oxidation of quercetin by air oxygenat ambient temperature. *Molecules* **2007**, *12*, 654−672.
(59) Dall'Acqua, S.; Miolo, G.; Innocenti, G.; Caffieri, S. The photodegradation of quercetin: Relation to oxidation. *Molecules* **2012**, *17*, 8898−8907.
(60) Sevilla-Morán, B.; López-Goti, C.; Alonso-Prados, J. L.; Sandín-España, P. Aqueous photodegradation of sethoxydim herbicide: Qtof elucidation of its by-products, mechanism and degradation pathway. *Sci. Total Environ.* **2014**, *472*, 842−850.
(61) Smitka, J.; Lemos, A.; Porel, M.; Jockusch, S.; Belderrain, T. R.; Tesařová, E.; Da Silva, J. P. Phototransformation of benzimidazole and thiabendazole inside cucurbit[8]uril. *Photochem. Photobiol. Sci.* **2014**, *13*, 310−315.
(62) Mccall, P. J.; Gavit, P. D. Aqueous photolysis of triclopyr and its butoxyethyl ester and calculated environmental photodecomposition rates. *Environ. Toxicol. Chem.* **1986**, *5*, 879−885.
(63) Henneberger, L.; Mühlenbrink, M.; König, M.; Schlichting, R.; Fischer, F. C.; Escher, B. I. Quantification of freely dissolved effect concentrations in in vitro cell-based bioassays. *Arch. Toxicol.* **2019**, *93*, 2295−2305.
(64) Lee, J.; Braun, G.; Henneberger, L.; König, M.; Schlichting, R.; Scholz, S.; Escher, B. I. Critical membrane concentration and mass-balance model to identify baseline cytotoxicity of hydrophobic and ionizable organic chemicals in mammalian cell lines. *Chem. Res. Toxicol.* **2021**, *34*, 2100−2109.
(65) Stevens, R.; Stevens, L.; Price, N. C. The stabilities of various thiol compounds used in protein purifications. *Biochem. Educ.* **1983**, *11*, 70.
(66) Ellman, G. L. Tissue sulfhydryl groups. *Arch. Biochem. Biophys.* **1959**, *82*, 70−77.

https://doi.org/10.1021/acs.chemrestox.2c00030
Chem. Res. Toxicol. 2022, 35, 867−879

(67) Frost, A. A.; Pearson, R. G. *Kinetics and Mechanism*, 2nd ed.; Wiley: New York, 1953.
(68) Laidler, K. J. *Chemical Kinetics*, 3rd ed.; Harper & Row: New York, 1987.
(69) Dimitrov, S.; Dimitrova, G.; Pavlov, T.; Dimitrova, N.; Patlewicz, G.; Niemela, J.; Mekenyan, O. A Stepwise Approach for Defining the Applicability Domain of SAR and QSAR Models. *J. Chem. Inf. Model.* **2005**, *45*, 839−849.
(70) Hagvall, L.; Bäcktorp, C.; Norrby, P.-O.; Karlberg, A.-T.; Börje, A. Experimental and Theoretical Investigations of the Autoxidation of Geranial: A Dioxolane Hydroperoxide Identified as a Skin Sensitizer. *Chem. Res. Toxicol.* **2011**, *24*, 1507−1515.
(71) Enoch, S. J.; Ellison, C. M.; Schultz, T. W.; Cronin, M. T. A review of the electrophilic reaction chemistry involved in covalent protein binding relevant to toxicity. *Crit. Rev. Toxicol.* **2011**, *41*, 783−802.
(72) OECD. OECD QSAR Toolbox v.4.1 Example for predicting Skin Sensitization of mixture. *The OECD QSAR Toolbox for Grouping of Chemicals into Categories*; OECD, 2017.
(73) Natsch, A.; Gfeller, H. LC-MS−based characterization of the peptide reactivity of chemicals to improve the in vitro prediction of the skin sensitization potential. *Toxicol. Sci.* **2008**, *106*, 464−478.
(74) Jaworska, J. S.; Natsch, A.; Ryan, C.; Strickland, J.; Ashikaga, T.; Miyazawa, M. Bayesian integrated testing strategy (ITS) for skin sensitization potency assessment: a decision support system for quantitative weight of evidence and adaptive testing strategy. *Arch. Toxicol.* **2015**, *89*, 2355−2383.
(75) Urbisch, D.; Mehling, A.; Guth, K.; Ramirez, T.; Honarvar, N.; Kolle, S.; Landsiedel, R.; Jaworska, J.; Kern, P. S.; Gerberick, F.; Natsch, A.; Emter, R.; Ashikaga, T.; Miyazawa, M.; Sakaguchi, H. Assessing skin sensitization hazard in mice and men using non-animal test methods. *Regul. Toxicol. Pharmacol.* **2015**, *71*, 337−351.
(76) Schwöbel, J. A. H.; Koleva, Y. K.; Enoch, S. J.; Bajot, F.; Hewitt, M.; Madden, J. C.; Roberts, D. W.; Schultz, T. W.; Cronin, M. T. D. Measurement and estimation of electrophilic reactivity for predictive toxicology. *Chem. Rev.* **2011**, *111*, 2562−2596.
(77) EPA. *CTS: Chemical Transformation Simulator*, 2019. From https://qed.epa.gov/cts/gentrans/ (Feb 01, 2021).
(78) Canada, A. T.; Giannella, E.; Nguyen, T. D.; Mason, R. P. The production of reactive oxygen species by dietary flavonols. *Free Radical Biol. Med.* **1990**, *9*, 441−449.
(79) Dangles, O.; Fargeix, G.; Dufour, C. One-electron oxidation of quercetin and quercetin derivatives in protic and non protic media. *J. Chem. Soc., Perkin Trans. 2* **1999**, *2*, 1387−1395.
(80) Mir, N. A.; Haque, M. M.; Khan, A.; Muneer, M.; Boxall, C. Photoassisted Degradation of a Herbicide Derivative, Dinoseb, in Aqueous Suspension of Titania. *Sci. World J.* **2012**, *2012*, No. 251527.
(81) Worthing, C.; Walker, S. *The Pesticide Manual—A World Compendium*, 7th ed.; Lavenham Press Limited: Lavenham, Suffolk, U.K., 1983.
(82) Kalia, J.; Raines, R. T. Hydrolytic stability of hydrazones and oximes. *Angew. Chem., Int. Ed.* **2008**, *47*, 7523−7526.
(83) ACD/Percepta. *Build 2726*; Advanced Chemistry Development, Inc.: Toronto, ON, Canada, 2015. http://www.acdlabs.com.
(84) Cóllier, P. J.; Ramsey, A.; Waigh, R. D.; Douglas, K. T.; Austin, P.; Gilbert, P. Chemical reactivity of some isothiazolone biocides. *J. Appl. Bacteriol.* **1990**, *69*, 578−584.
(85) Yamagishi, Y.; Iwase, H.; Ogra, Y. Effects of human serum albumin on post-mortem changes of malathion. *Sci. Rep.* **2021**, *11*, No. 11573.
(86) Varga, Z.; Nicol, E.; Bouchonnet, S. Photodegradation of benzisothiazolinone: Identification and biological activity of degradation products. *Chemosphere* **2020**, *240*, No. 124862.
(87) Glauch, L.; Escher, B. I. The combined algae test for the evaluation of mixture toxicity in environmental samples. *Environ. Toxicol. Chem.* **2020**, *39*, 2496−2508.
(88) Omiecinski, C. J.; Vanden Heuvel, J. P.; Perdew, G. H.; Peters, J. M. Xenobiotic metabolism, disposition, and regulation by receptors: from biochemical phenomenon to predictors of major toxicities. *Toxicol. Sci.* **2011**, *120*, S49−S75.
(89) European Chemicals Agency. *Guidance on Information Requirements and Chemical Safety Assessment Chapter R.11: PBT/vPvB assessment*; European Chemicals Agency, 2017.
(90) Mielke, H.; Di Consiglio, E.; Kreutz, R.; Partosch, F.; Testai, E.; Gundert-Remy, U. The importance of protein binding for the in vitro−in vivo extrapolation (IVIVE)—example of ibuprofen, a highly protein-bound substance. *Arch. Toxicol.* **2017**, *91*, 1663−1670.
(91) Algharably, E. A. H.; Kreutz, R.; Gundert-Remy, U. Importance of in vitro conditions for modeling the in vivo dose in humans by in vitro−in vivo extrapolation (IVIVE). *Arch. Toxicol.* **2019**, *93*, 615−621.

https://doi.org/10.1021/acs.chemrestox.2c00030
Chem. Res. Toxicol. 2022, 35, 867−879

Publication II

Reactivity of Acrylamides Causes Cytotoxicity and Activates Oxidative Stress Response

Julia Huchthausen[†], Beate I. Escher[†, §, *], Nico Grasse[¶], Maria König[†], Stephan Beil[‡], Luise Henneberger[†]

[†] Helmholtz Centre for Environmental Research – UFZ, Department of Cell Toxicology, Permoserstr. 15, 04318 Leipzig, Germany

[§] Eberhard Karls University Tübingen, Environmental Toxicology, Department of Geosciences, Scharrenbergstr. 94-96, 72076 Tübingen, Germany

[¶] Helmholtz Centre for Environmental Research – UFZ, Department of Analytical Chemistry, Permoserstr. 15, 04318 Leipzig, Germany

[‡] Technische Universität Dresden, Institute of Water Chemistry, 01069 Dresden, Germany

Corresponding author: beate.escher@ufz.de

Published in Chemical Research in Toxicology, 10.1021/acs.chemrestox.3c00115.

Chemical Research in Toxicology

pubs.acs.org/crt

Article

Reactivity of Acrylamides Causes Cytotoxicity and Activates Oxidative Stress Response

Julia Huchthausen, Beate I. Escher,* Nico Grasse, Maria König, Stephan Beil, and Luise Henneberger

Cite This: *Chem. Res. Toxicol.* 2023, 36, 1374−1385

Read Online

ABSTRACT: Acrylamides are widely used industrial chemicals that cause adverse effects in humans or animals, such as carcinogenicity or neurotoxicity. The excess toxicity of these reactive electrophilic chemicals is especially interesting, as it is mostly triggered by covalent reactions with biological nucleophiles, such as DNA bases, proteins, or peptides. The cytotoxicity and activation of oxidative stress response of 10 (meth)acrylamides measured in three reporter gene cell lines occurred at similar concentrations. Most acrylamides exhibited high excess toxicity, while methacrylamides acted as baseline toxicants. The (meth)-acrylamides showed no reactivity toward the hard biological nucleophile 2-deoxyguanosine (2DG) within 24 h, and only acrylamides reacted with the soft nucleophile glutathione (GSH). Second-order degradation rate constants (k_{GSH}) were measured for all acrylamides with *N,N′*-methylenebis(acrylamide) (NMBA) showing the highest k_{GSH} (134.800 M^{-1} h^{-1}) and *N,N*-diethylacrylamide (NDA) the lowest k_{GSH} (2.574 M^{-1} h^{-1}). Liquid chromatography coupled to high-resolution mass spectrometry was used to confirm the GSH conjugates of the acrylamides with a double conjugate formed for NMBA. The differences in reactivity between acrylamides and methacrylamides could be explained by the charge density of the carbon atoms because the electron-donating inductive effect of the methyl group of the methacrylamides lowered their electrophilicity and thus their reactivity. The differences in reactivity within the group of acrylamides could be explained by the energy of the lowest unoccupied molecular orbital and steric hindrance. Cytotoxicity and activation of oxidative stress response were linearly correlated with the second-order reaction rate constants of the acrylamides with GSH. The reaction of the acrylamides with GSH is hence not only a detoxification mechanism but also leads to disturbances of the redox balance, making the cells more vulnerable to reactive oxygen species. The reactivity of acrylamides explained the oxidative stress response and cytotoxicity in the cells, and the lack of reactivity of the methacrylamides led to baseline toxicity.

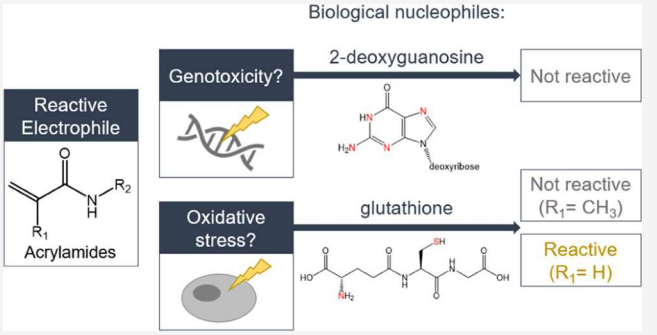

INTRODUCTION

Monomeric acrylamide (prop-2-enamide) is used in the chemical industry for the production of adhesives, sealants, coating products, and inks. Acrylamide is the building block of polyacrylamide, which is widely used in research, water treatment, and papermaking.[1,2] Acrylamide can also be formed during food processing at high temperatures.[3] It has been identified as a rodent carcinogen and probable human carcinogen[4,5] and is known to cause neurotoxicity in humans.[6,7] This is why, the European Union established a benchmark level for acrylamide in food in 2017.[8] The toxicity of acrylamide is well studied, and risks are known for this chemical, but the chemical group of acrylamides includes a large number of chemicals with different physicochemical properties and few data are available concerning the toxicity of differently *N*-substituted acrylamides (CH_2=CHC(O)NR_2) and methacrylamides (CH_2=C(CH_3)C(O)NR_2) even though some of these chemicals are produced in large quantities and also find application in industry and research.[9,10]

Acrylamides belong to the group of electrophilic reactive chemicals. The toxicity of reactive chemicals exceeds baseline toxicity (narcosis),[11] which is the lowest toxicity a chemical can have and is caused by the incorporation of the chemicals into the cell membrane.[12] Reactive chemicals are of special concern since they usually have 10 to 10,000 times higher toxicity than baseline toxic chemicals,[11] and their toxicity can have different modes of action (MOA),[13] but is mostly triggered by irreversible reactions with thiol, amino, or hydroxyl groups of biological nucleophiles such as proteins, peptides, and DNA.[14−16] The reaction of acrylamides with nucleophiles is a Michael addition where the α,β-unsaturated

Received: April 21, 2023
Published: August 2, 2023

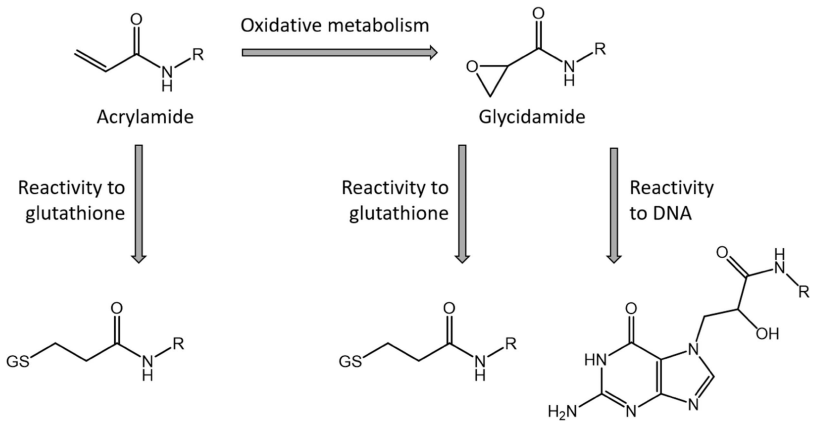

Figure 1. Potential reaction pathways of acrylamide chemicals in in vitro bioassays. Adapted from Katen et al.[28]

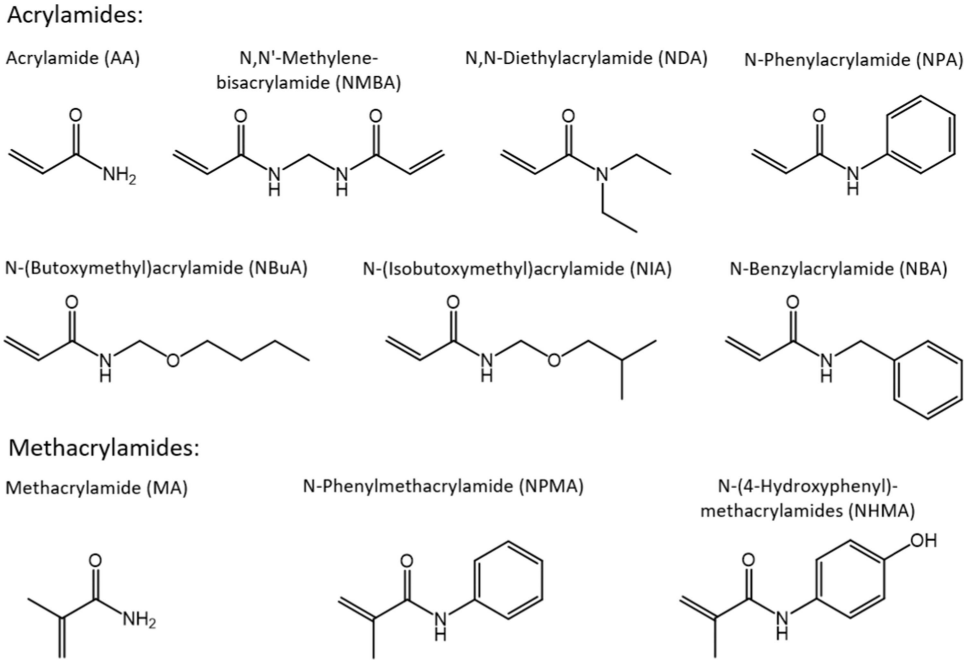

Figure 2. Structures of the test chemicals.

carbonyl moiety of the acrylamide acts as the Michael acceptor and the biological nucleophile acts as the Michael donor.[17,18] Especially the tripeptide glutathione (γ-L-glutamyl-L-cysteinyl-glycin, GSH) is a target of reactive chemicals since it has a free thiol group and is present in large amounts in the cell (Figure 1).[19] Acrylamide can also be metabolized by cytochrome P450 2E1 to its metabolite glycidamide, which reacts with DNA bases and causes genotoxicity (Figure 1).[20,21] All of these processes play a role in the toxicity of reactive chemicals and may lead to a variety of adverse effects of these chemicals.

Even though acrylamides are reactive chemicals and their reactivity is unspecific, they do not react equally well with all biological nucleophiles. For example, acrylamide reacts very rapidly with the thiol GSH but requires metabolic activation to react with DNA.[22,23] The selectivity in the reaction between electrophilic and nucleophilic chemicals can be explained by Pearson's theory of hard and soft acids and bases (HSAB).[24] According to this concept, reactive molecules are classified based on their respective polarizabilities as either soft (polarizable) or hard (nonpolarizable) electrophiles or nucleophiles. Furthermore, chemicals with the same softness or hardness react preferentially with each other.[25,26] The polarizability of a molecule depends on its electron distribution. The conjugated α,β-unsaturated carbonyl structure of acrylamides is a soft electrophile because of the delocalized pi-electron system. Therefore, they react preferentially with soft nucleophiles, such as thiols, which are easily polarized due to the large atomic radius of sulfur. The nitrogen and oxygen nucleophiles in DNA or RNA have smaller atomic radii and thus represent harder nucleophiles, which react preferentially with hard electrophiles, such as epoxides or organochlorides.[25,27] Quantum chemical calculations can be used to rationalize the chemical reactivity. The lowest unoccupied molecular orbital (LUMO) of the electrophile and the highest occupied molecular orbital (HOMO) of the nucleophile determine the reaction rate. The selectivity of the reaction can be modeled by the energies of these orbitals. Hard electrophiles usually have a relatively high energy (ε) of the LUMO (ε_{LUMO}) and soft electrophiles have rather low or negative ε_{LUMO}. However, other molecular structures can also play a role in reactivity if they sterically hinder the reaction.[26,27]

https://doi.org/10.1021/acs.chemrestox.3c00115
Chem. Res. Toxicol. 2023, 36, 1374−1385

The determination of the molecular target of reactive chemicals is important for the assessment of their toxicity and for the identification of possible adverse outcomes in humans.[16,29] Therefore, various studies have focused on the relationship between the reactivity of chemicals and toxicity in different species, such as bacteria, ciliophoran, algae, and fish.[30−34]

The aim of this study was to investigate whether the *in vitro* toxicity of different substituted (meth)acrylamides depends on their reactivity toward biological nucleophiles and whether this reactivity can be explained by their chemical structure. There are major knowledge gaps regarding the toxicity of substituted (meth)acrylamides, but these chemicals are used in large quantities in industry and may pose a potential hazard to humans and the environment. For this study, we selected (meth)acrylamides with different physicochemical properties that are produced in large quantities to investigate a possible influence of the substituent on reactivity and toxicity. The final test set of chemicals consisted of one bipolarized compound, two primary amines, six secondary amines, and one tertiary amine with seven chemicals being acrylamides and three being methacrylamides (Figure 2). The hydrophobicity of the test chemicals ranged over 2 orders of magnitude (Table S1). The cytotoxicity of the test chemicals was measured in three reporter gene cell lines (GR-*bla*, ARE-*bla*, and AREc32). GR-*bla* is based on a HEK293T cell line, ARE-*bla* is based on a HepG2 cell line, and AREc32 is based on an MCF7 cell line.

Previous work has demonstrated that GR-*bla* has no cytochrome P450 activity, while ARE-*bla* has a higher basal CYP1 level and CYP1 is inducible by chemical exposure in AREc32.[35] Three cell lines with different metabolic capacities were chosen to relate possible differences in cytotoxicity to differences in metabolic activity since it has been shown that metabolic activation of acrylamide to the reactive glycidamide is necessary for the reaction with DNA.[36]

ARE-*bla* and AREc32 also carry a reporter gene for the antioxidant response element, allowing measurement of the oxidative stress response via the Nuclear Factor Erythroid 2-related Factor 2/Kelch-like ECH-associated protein 1 (Nrf-2/Keap-1) pathway. This metabolic pathway is mostly activated by the generation of reactive oxygen species (ROS) in the exposed cells, but for some reactive chemicals, the oxidative stress response can also be triggered by direct binding of the chemicals to Keap-1.[37,38] The end point can also be an indirect measure of the reaction of the test chemicals with GSH, which maintains the redox status of the cells. GSH also functions as a detoxification molecule, as a deficiency of GSH leads to reduced protection against ROS, which can ultimately lead to cell death.[39] Since acrylamides, as soft electrophiles, react preferentially with soft nucleophiles such as GSH or cysteine residues in cellular proteins, two assays were selected that reflect this MOA. Direct reactions with DNA were not expected[40] and hence no assay for genotoxicity was selected. GR-*bla* carries a reporter gene for glucocorticoid receptor, which is not of interest for reactive chemicals[41] and only the cytotoxicity was quantified for this cell line.

Reactivity toward the hard nucleophile 2-deoxyguanosine (2DG) was investigated to confirm our hypothesis that reaction with DNA is not the molecular initiating event. Degradation rates and half-lives of the test chemicals toward the soft biological nucleophile GSH were measured and compared to the toxicity and activation of the Nrf-2/Keap-1 pathway and used to derive information on the MOA of the test chemicals. The reactivity of acrylamides with GSH has been previously described,[36,42] but we expanded systematically to acrylamides and methacrylamides with substitute groups to investigate how the substitution affects the toxicity and reactivity of the chemicals. In addition, we used nontarget screening to identify the GSH conjugates of acrylamides and quantum chemical calculations to explain the reactivity of the chemicals to GSH.

MATERIALS AND METHODS

Chemicals. The chemicals acrylamide (79-06-1, AA), *N*,*N*′-methylenebis(acrylamide) (110-26-9, NMBA), *N*-(butoxymethyl)-acrylamide (1852-16-0, NBuA), *N*-(isobutoxymethyl)acrylamide (16669-59-3, NIA), *N*,*N*-diethylacrylamide (2675-94-7, NDA), methacrylamide (79-39-0, MA), *N*-benzylacrylamide (13304-62-6, NBA), *N*-phenylmethacrylamide (1611-83-2, NPMA), *N*-phenyl-acrylamide (2210-24-4, NPA), and *N*-(4-hydroxyphenyl)-methacrylamide (19243-95-9, NHMA) were used in this study. Chemical structures are shown in Figure 2, and more information about the test chemicals can be found in the Supporting Information (Table S1).

Materials. All components of the bioassay media and GeneBLAzer ARE-*bla* and GeneBLAzer GR-UAS-*bla* cells were purchased from Thermo Fisher Scientific. AREc32 cells[43] were obtained from Cancer Research UK. 2′-Deoxyguanosine monohydrate (Cayman Chemical; Cay9002864-5; 312693-72-4) and reduced glutathione (Sigma-Aldrich; G4251-5G; 70-18-8) had a purity of ≥98%. All solvents used were of LC-MS grade and had a purity of ≥99%. Acetonitrile and 2-propanol were purchased from Honeywell or Chemsolute. Methanol was purchased from Honeywell, and formic acid was purchased from Serva. Water was obtained from a Milli-Q water purification system from Merck. Supel BioSPME 96-Pin Devices (Sigma-Aldrich; 59683-U) coated with C18-particles embedded in polyacrylonitrile (PAN) were used. The coating length was 2.1 mm, and the average coating thickness was 12.5 μm, resulting in an approximate coating volume of 80 nL.[44,45] Polystyrene 384-well plates (Product Nos. 3765 and 356663) from Corning were used for the *in vitro* bioassays, and the reactivity tests were performed in glass-coated deep-well plates (Product No. 60180P336) from Thermo Fisher Scientific which were sealed with sealing film from Brand (Product No. 701367).

***In Vitro* Bioassay.** ARE-*bla* bioassay medium (90% DMEM with GlutaMAX phenol red-free, 10% dialyzed fetal bovine serum (FBS), 0.1 mM nonessential amino acids, 25 mM HEPES, 100 U/mL penicillin-streptomycin), GR-*bla* bioassay medium (98% Opti-MEM, 2% charcoal-stripped FBS, 100 U/mL penicillin-streptomycin), and AREc32 bioassay medium (90% DMEM with GlutaMAX, 10% FBS, 100 U/mL penicillin-streptomycin) were used. A detailed description of the bioassay procedure can be found in the literature.[46−48]

Briefly, 30 μL of cell suspension in assay medium was dispensed into each well of a poly-D-lysine treated black 384-well plate with clear bottom (Product No. 356663, ARE-*bla* and GR-*bla*) or a white 384-well plate with clear bottom (Product No. 3765, AREc32) using a MultiFlo Dispenser (Biotek, Vermont, USA). The final cell numbers were 4100 cells/well (ARE-*bla*), 6000 cells/well (GR-*bla*) and 2650 cells/well (AREc32). The plates were incubated at 37 °C and 5% CO_2 for 24 h, and the confluency of the cells was measured with an IncuCyte S3 Live-Cell Analysis System (Essen BioScience, Sartorius) before and 24 h after chemical dosing. Chemical dilutions in the respective bioassay media were prepared by dissolving the pure chemical directly in the medium (AA, NMBA, NBuA, NIA, NDA, MA) or by using stock solutions in methanol (NBA, NPMA, NPA, NHMA). The final methanol content in the well was kept below 1%. All chemicals were tested in all assays in three independent replicates in 11-step serial dilutions. Dosing plates containing the chemicals in serial dilution were prepared using a Hamilton Microlab Star robotic system (Hamilton, Bonaduz, Switzerland). The diluted chemicals were dosed in duplicates by transferring two times 10 μL from the dosing plates to the cell plate. The cell plates were incubated at 37 °C

https://doi.org/10.1021/acs.chemrestox.3c00115
Chem. Res. Toxicol. 2023, 36, 1374−1385

and 5% CO_2 for 24 h. The cytotoxicity was evaluated by comparing the relative confluency of the cells before and after dosing. The activation of the reporter genes was quantified as described in the literature.[46−48]

Solid-Phase Microextraction. A previously published high-throughput (HT) solid-phase microextraction (SPME) method[45] was used to extract the chemicals from the medium samples and reaction solutions. The method was automated using a Hamilton Microlab Star robotic system (Hamilton, Bonaduz, Switzerland) equipped with a CO-RE grip and iSWAP and two BioShake 3000-T elm (QInstruments, Jena, Germany) and the corresponding software Hamilton Run Control and Hamilton Method Editor (version 4.5.0.7977). More information about the experimental parameters and a depiction of the robot deck layout can be found in the Supporting Information (Table S2 and Figure S1). The pin device was positioned in an empty deep-well reservoir equipped with a customized metal frame in the Hamilton robot. The remaining labware was also positioned as described in Figure S1. The pin device was conditioned in isopropanol for 20 min, in Milli-Q water for 10 s, and then transported to the deep-well plate containing the sample solutions. The chemicals were extracted at 1000 rpm and 37 °C for 15 min, then the pin device was transferred to the desorption plate containing the respective desorption solutions (Table S1) and was desorbed at 1000 rpm and room temperature for 15 min. No wash was performed between the extraction and desorption. Finally, the pin device was transported back to its starting position. All desorption plates were sealed and stored at 4 °C until concentration measurement.

Stability in Assay Medium. The freely dissolved concentration (C_{free}) of the test chemicals was measured in ARE-*bla* bioassay medium, GR-*bla* bioassay medium, and AREc32 bioassay medium. Chemical stock solutions of the test chemicals were spiked into aliquots of the media at a final concentration of 5.0×10^{-4} M (AA, NMBA, and MA) or 3.0×10^{-4} M (NBuA, NIA, NDA, NBA, NPMA, NPA, NHMA). 600 μL of each reaction solution were transferred in duplicate into two glass-coated 96-deep-well plates. One of the plates was directly extracted using SPME. The other plate was incubated at 37 °C for 24 h before extraction.

Reactivity Testing. To determine the reactivity of the test chemicals, reduced glutathione (GSH) and 2′-deoxyguanosine (2DG) were dissolved in phosphate-buffered saline (PBS, 137 mM NaCl, 12 mM phosphate) at different concentrations, and the pH was adjusted to 7.4. The test chemicals were added to aliquots of the GSH or 2DG solutions, leading to the same final concentrations as described above for the medium samples. The concentration of GSH was the same, 2 times, 5 times, 10 times, 50 times, or 100 times higher than the chemical concentration. The concentration of 2DG was the same, two times, five times, 10 times, 20 times, or 30 times higher than the chemical concentration. 600 μL of each reaction solution were transferred in duplicate into seven glass-coated 96-deep-well plates. One of the plates was directly extracted using SPME. The other plates were incubated at 37 °C for 30 min and 1, 2, 4, 6, or 24 h before extraction. The experiments were performed three times for all chemicals and solutions if the chemicals were degraded in the first test.

Instrumental Analysis. The chemical concentration in the desorption solvent was measured using a liquid chromatography instrument (LC, Agilent 1260 Infinity II) coupled to a triple quadrupole mass spectrometer (MS, Agilent 6420 Triple Quad). A LunaOmega 1.6 μm, Polar C18, 100 Å, LC column (50 × 2.1 mm) was used for AA, NMBA, NBuA, NIA, NDA, and MA. A Kinetex 1.7 μm, C18, 100 Å, LC column (50 × 2.1 mm) was used for NBA, NPMA, NPA, and NHMA. All LC and MS parameters can be found in the Supporting Information (Table S3). Standard solutions in the respective desorption solvents (1−5000 ng/L) and acetonitrile blanks were measured together with the samples.

One replicate of the desorption solvents after SPME of the chemicals incubated with GSH (ratio GSH/acrylamide = 5:1 and 100:1) for 1, 4, and 24 h was transferred to HPLC vials with inserts and analyzed by ultraperformance liquid chromatography time-of-flight mass spectrometry (UPLC-TOF-MS) using a AQUITY UPLC I-Class system (Waters) equipped with a HSS T3 column (100 mm × 2.1 mm, 1.7 μm) coupled to a XEVO XS Q-TOF-MS (Waters) to identify conjugates of the reaction of the acrylamides with GSH. The samples were injected without further dilution and solvent blanks, control samples without the test chemical, as well as control samples without GSH were measured in parallel. A detailed description of the analytical method and the instrumental parameters can be found in the literature.[49] GSH adducts were detected by a screening approach using MarkerLynx (Waters, version 4.1). UPLC-MS data were evaluated in a retention time window of 1 to 10 min and a mass range of m/z 50−1200. The maximum deviation in retention time for peak picking was 0.1 min, and the maximum deviation in the exact mass was 0.01 Da. Peaks that were present only in the samples containing acrylamide and GSH and not in the solvent blanks and control samples of acrylamides without GSH were selected as candidate conjugates. Chemical formulas were generated using a mass tolerance of 5 ppm and elemental composition of C (0−100), H (0−100), N (0−20), O (0−20), S (0−20), and Na (0−2). Additionally, fragment ions were considered for the structure elucidation.

Data Evaluation. An automatic KNIME (version 4.6.1) workflow and GraphPad Prism (version 9.0.2) were used for the evaluation of the bioassay data. The measured cytotoxicity and effects were plotted against the chemical concentration in the linear range of the concentration−response curve and the inhibitory effect concentrations were derived from the slope of the regression.[50]

The IC_{10} for cytotoxicity is the concentration at which a reduction in cell viability of 10% is achieved and was calculated with eq 1.

$$IC_{10} = \frac{10\%}{\text{slope}} \tag{1}$$

For the evaluation of the activation of the oxidative stress response, the induction ratio (IR) was calculated and the $EC_{IR1.5}$ (eq 2) was derived from the slope of the concentration−response curve.[48]

$$EC_{IR1.5} = \frac{0.5}{\text{slope}} \tag{2}$$

The reference substances used were dexamethasone for GR-*bla* and *tert*-butylhydroquinone (tBHQ) for AREc32 and ARE-*bla*.

The $IC_{10,baseline}$ was calculated with the baseline quantitative structure−activity relationship (QSAR) from Lee et al. (2021),[51] where $K_{lip/w}$ stands for the liposome-water partition constant, a measure of hydrophobicity and affinity to biological membranes. $K_{lip/w}$ of all test chemicals were predicted using a linear solvation energy relationship (LSER) model (Table S1).[52]

$$\log[1/IC_{10,baseline}(\text{M})] = 1.23 + 4.97 \times (1 - e^{-0.236 \times \log K_{lip/w}(\text{pH7.4})}) \tag{3}$$

To compare the measured cytotoxicity IC_{10} with the baseline toxicity $IC_{10,baseline}$, the toxic ratio (TR) was calculated with eq 4.

$$\text{toxic ratio (TR)} = \frac{IC_{10,baseline}}{IC_{10,experimental}} \tag{4}$$

The specificity ratio (SR) was used to elucidate how much the reporter gene induction differs from cytotoxicity ($SR_{cytotoxicity}$, eq 5) or baseline toxicity ($SR_{baseline}$, eq 6).[53]

$$SR_{cytotoxicity} = \frac{IC_{10,experimental}}{EC_{IR1.5}} \tag{5}$$

$$SR_{baseline} = \frac{IC_{10,baseline}}{EC_{IR1.5}} \tag{6}$$

The freely dissolved concentrations of the chemicals in the bioassay medium (C_{free}) were calculated with eq 7 as a measure of the exposure concentration.[54] The total amount of chemicals in the medium (n_{total}) was calculated from the nominal concentration (C_{nom}) added to the medium. The pin-water distribution ratios ($D_{pin/w}$) were calculated

https://doi.org/10.1021/acs.chemrestox.3c00115
Chem. Res. Toxicol. 2023, 36, 1374−1385

Table 1. IC_{10} and $EC_{IR1.5}$ Values for All Chemicals and Assays[a]

	ARE-*bla*				AREc32				GR-*bla*	
chemical	IC_{10} [M]	CV [%]	$EC_{IR1.5}$ (M)	CV [%]	IC_{10} (M)	CV [%]	$EC_{IR1.5}$ (M)	CV [%]	IC_{10} (M)	CV [%]
AA	1.01×10^{-3}	26.1	4.34×10^{-4}	7.2	4.29×10^{-4}	7.0	3.10×10^{-4}	5.9	8.05×10^{-4}	4.9
NMBA	1.13×10^{-4}	16.2	1.54×10^{-5}	7.0	4.25×10^{-5}	11.3	1.16×10^{-5}	4.6	8.29×10^{-5}	7.2
NBuA	5.28×10^{-4}	10.0	4.96×10^{-5}	7.6	1.52×10^{-4}	7.7	5.43×10^{-5}	4.8	3.90×10^{-4}	5.3
NIA	8.74×10^{-4}	8.8	6.76×10^{-5}	7.5	2.74×10^{-4}	6.0	8.62×10^{-5}	5.9	5.34×10^{-4}	8.2
NDA	8.06×10^{-3}	8.5	6.08×10^{-4}	6.1	5.73×10^{-3}	6.1	6.89×10^{-4}	3.0	3.10×10^{-3}	5.3
MA	2.23×10^{-2}	14.9	4.28×10^{-3}	3.9	1.59×10^{-2}	13.4	2.53×10^{-3}	4.6	7.56×10^{-3}	6.4
NBA	2.96×10^{-3}	6.7	2.92×10^{-4}	8.3	2.33×10^{-3}	17.2	2.61×10^{-4}	2.3	1.44×10^{-3}	12.1
NPMA	6.20×10^{-3}	22.1	3.27×10^{-3}	10.3	2.66×10^{-3}	12.6	1.33×10^{-3}	7.5	1.42×10^{-3}	9.0
NPA	7.58×10^{-4}	6.8	4.01×10^{-5}	7.5	2.12×10^{-4}	9.2	6.00×10^{-5}	4.3	4.35×10^{-4}	9.9
NHMA	5.41×10^{-2}	34.7	7.55×10^{-3}	6.6	1.19×10^{-2}	21.2	3.88×10^{-3}	6.0	1.30×10^{-3}	6.7
tBHQ	$>1.73 \times 10^{-5}$		2.93×10^{-6}	3.4	$>1.73 \times 10^{-5}$		2.91×10^{-6}	2.0	not tested	

[a]Chemical structures are shown in Figure 2. CV represents the coefficient of variation based on three independent replicates.

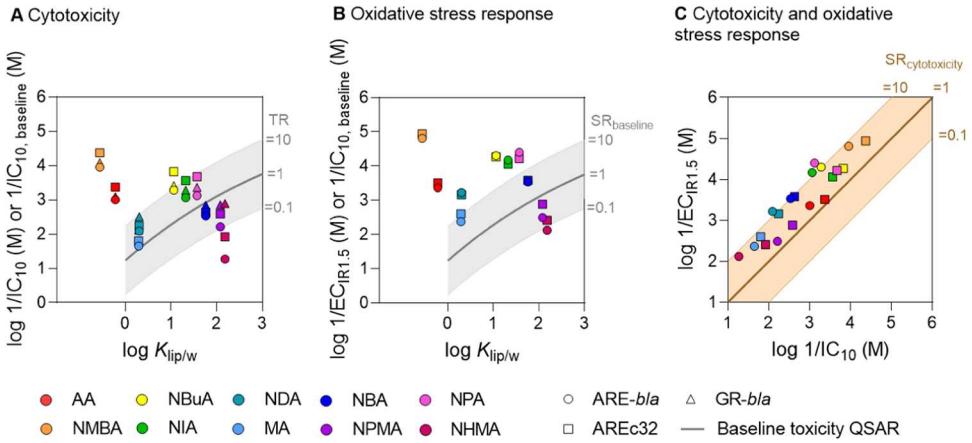

Figure 3. Visualization of toxic ratios (TR) and specificity ratios (SR) of the test chemicals. The thick gray lines in (A) and (B) represent the predicted baseline IC_{10} (eq 4) as a function of the logarithmic liposome-water partition constant $\log K_{lip/w}$ for chemicals with $K_{lip/w} \geq 0$.[51] (A) Cytotoxicity ($\log 1/IC_{10}$) plotted against $\log K_{lip/w}$. Gray areas show TR values between 0.1 and 10. (B) Activation of the oxidative stress response ($\log 1/EC_{IR1.5}$) plotted against $\log K_{lip/w}$. Gray areas show $SR_{baseline}$ values between 0.1 and 10. (C) Activation of the oxidative stress response ($\log 1/EC_{IR1.5}$) plotted against cytotoxicity ($\log 1/IC_{10}$). The thick brown line indicates an $SR_{cytotoxicity}$ of 1, and the brown area shows $SR_{cytotoxicity}$ values between 0.1 and 10. The different symbols indicate three different assays.

from samples in phosphate-buffered saline (PBS) (see the Supporting Information Text S1 for more information). Chemical concentrations in the pin coating (C_{pin}) were calculated from the measured concentrations in the desorption solution after SPME and the volume of the pin coating (V_{pin}) was approximately 80 nL.

$$C_{free} = \frac{n_{total}}{D_{pin/w} \times \left(\frac{n_{total}}{C_{pin}} \times V_{pin}\right)} \quad (7)$$

To determine the first-order degradation rate constant (k) and the degradation half-life ($t_{1/2}$) of the chemicals, the natural logarithm (ln) of the chemical concentration in the desorption solvent after SPME (C_{des}) was plotted against the incubation time (t). From the linear regression of this plot, k could be derived (eq 8).

$$\ln(C_{des})_t = -k \times t \quad (8)$$

The degradation half-life ($t_{1/2}$) was calculated from k using eq 9.

$$t_{1/2} = \frac{\ln(2)}{k} \quad (9)$$

The second-order rate constant from the reaction of acrylamides with GSH (k_{GSH}) was determined by linear regression of k plotted against the concentration of GSH (eq 10), where k_{GSH} is the slope of the regression and the intercept is k_{H_2O}, the reaction rate constant of the reaction with water.

$$k = k_{GSH} \times [GSH] + k_{H_2O} \quad (10)$$

Quantum Chemical Calculations. Charge densities of selected atoms ($q(C_\alpha)$, $q(C_\beta)$, and $q(C_1)$) and the energy of the lowest unoccupied orbital (ε_{LUMO}) were calculated for all test chemicals. 3D structure files of acrylamides were generated using Avogadro software, version 1.2.0,[55] and initially geometry-optimized via steepest descent algorithm in the UFF force field.[56] The resulting Cartesian coordinates were used as input for a detailed MP2 calculation (second-order Møller–Plesset perturbation theory) with the def2-TZVP basis set. The calculations were run with ORCA software, version 5.0.3.[57−59] Subsequently, the same software was applied to convert the obtained files to the molden file format. Orbitals of the final structures were visualized via IboView software, version 20211019-RevA.[60]

RESULTS AND DISCUSSION

Cytotoxicity. The measured cytotoxicity IC_{10} values (Table 1) were derived from the concentration–response curves shown in the Supporting Information (Figures S2–S4). NMBA was the most cytotoxic chemical, with the lowest IC_{10} values in all assays. The comparison of the IC_{10} values from ARE-*bla* and GR-*bla* with those from AREc32 showed that the measured cytotoxicity of the chemicals in the assays differed by less than 1 order of magnitude (Figure S5). The similar toxicity

https://doi.org/10.1021/acs.chemrestox.3c00115
Chem. Res. Toxicol. 2023, 36, 1374−1385

of the chemicals in cell lines of different origins suggests that differences in the metabolic activity of the cells do not affect the toxicity of the chemicals.

Activation of Oxidative Stress Response. Oxidative stress response was activated by all chemicals in the ARE-*bla* and the AREc32 assay (Table 1 and Figures S2 and S4), which is in line with previous studies which identified acrylamide as an activator of oxidative stress response *in vitro*[61,62] and *in vivo*.[63] NMBA showed the strongest effect in both assays.

The comparison of the measured $EC_{IR1.5}$ values in ARE-*bla* and AREc32 also showed almost perfect agreement. This suggests that the activation of ARE of the chemicals is independent of cell type and origin, so metabolic activation is not necessary to trigger the effect and the MOA is the same in different cell types.

Specificity Analysis. In Figure 3, the cytotoxicity log $1/IC_{10}$ (Figure 3A) and the activation of the oxidative stress response log $1/EC_{IR1.5}$ (Figure 3B) are plotted against the hydrophobicity ($K_{lip/w}$) of the test chemical. There was no apparent relationship between log $K_{lip/w}$ and cytotoxicity or activation of the oxidative stress response. Additionally, the baseline toxicity QSAR[51] was plotted as a function of the $K_{lip/w}$ to visualize the toxic ratios (TR) and specificity ratios ($SR_{baseline}$) of the chemicals, showing the comparison of the measured effects, namely, IC_{10} and $EC_{IR1.5}$, with the predicted $IC_{10,baseline}$. Baseline toxicity is the lowest toxicity a substance can have and is triggered by the incorporation of the chemical into the cell membrane.[11,12] The baseline toxicity QSAR is not defined at log $K_{lip/w}$ below 0, because no experimental data were recorded. In addition, very hydrophilic chemicals do not tend to be incorporated into the cell membrane and, thus, are unlikely to act through this mode of action. Unsubstituted acrylamide, like all small and polar molecules, does not accumulate in the cell membrane but rapidly permeates it.[64] Therefore, it cannot reach the critical membrane concentrations required to trigger baseline toxicity but must cause its toxicity through another mechanism. As hydrophobicity is affected by substitution, methacrylamides and acrylamides with long side chains have a higher log $K_{lip/w}$ and thus a greater tendency to integrate into the cell membrane.

Two of the chemicals (AA and NMBA) were too hydrophilic for a TR to be calculated. However, both showed high cytotoxicity in all assays (AA: log $1/IC_{10}$ up to 3.37, and NMBA: log $1/IC_{10}$ up to 4.37). Chemicals with TR > 10 were classified as reactive or specifically acting.[11,65] Four of the chemicals with log $K_{lip/w}$ > 0 (NBuA, NIA, NDA, and NPA) showed TR between 1 and 10 in all assays, which is why they can be classified as reactive toxicants.[11,17] However, TR were not orders of magnitude higher than baseline toxicity but close to the threshold. MA, NBA, NPMA, and NHMA showed TR around 1 and were classified as baseline toxicants.[11,17]

The $SR_{baseline}$ for most of the chemicals was higher than 10 indicating a specific mode of action. Only NPMA and NHMA had an $SR_{baseline}$ around 1, and activation of oxidative stress response can be considered as a result of the cytotoxicity burst phenomenon.[53,66] Figure 3C shows log $1/EC_{IR1.5}$ plotted against log $1/IC_{10}$ for the ARE-*bla* and AREc32 assay. This comparison displays the $SR_{cytotoxicity}$, which was between 1 and 10 for most chemicals. The activation of the oxidative stress response and cytotoxicity appear to be linked and do not occur independently of each other in both cell lines.

Solid-Phase Microextraction. The time until 95% equilibrium was reached ($t_{95\%}$), recovery, and logarithmic pin-water distribution ratios (log $D_{pin/w}$) were quantified for all test chemicals (Figure S6 and Table S4). The $t_{95\%}$ was below 15 min for all test chemicals and, for most, below 5 min. The recovery was between 86% (NDA) and 118% (NPA). Log $D_{pin/w}$ at equilibrium was between 0.61 (MA) and 1.48 (NPA), with $D_{pin/w}$ increasing with the hydrophobicity of the test chemicals.

Stability in Assay Medium. The freely dissolved concentration (C_{free}) of the test chemicals in GR-*bla*, ARE-*bla*, and AREc32 assay medium was determined without incubation and after 24 h of incubation at 37 °C (Figure 4).

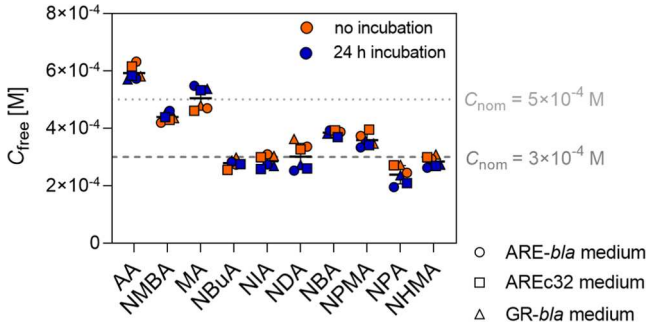

Figure 4. Freely dissolved concentration (C_{free}) of the test chemicals in three bioassay media without incubation (orange) or after 24 h of incubation (blue). Different symbols represent different media. AA, NMBA, and MA were dosed at a nominal concentration (C_{nom}) of 5×10^{-4} M (gray dotted line), and the other test chemicals were dosed at C_{nom} of 3×10^{-4} M (dark gray dashed line).

The C_{free} values of all chemicals were very close (up to a factor of 1.5) to the nominal concentration (C_{nom}). There was no difference between the C_{free} values of the chemicals in the three bioassay media. This is in line with previous results of the measured C_{free} of hydrophilic chemicals in *in vitro* bioassays, which showed no or very weak partitioning to proteins in the medium and are therefore almost completely freely dissolved.[54]

For most of the chemicals, there was no difference between C_{free} without incubation and C_{free} after 24 h, so most chemicals seem to be stable in the bioassay media over 24 h. Only for NDA there was a decrease of C_{free} within 24 h of 25%, in the GR-*bla* and ARE-*bla* media and 20% in the AREc32 medium. For NPA, there was a decrease of C_{free} of 20% in the ARE-*bla* and 23% in the AREc32 medium. This loss could be caused by covalent reactions of the chemicals with components of the medium since the chemicals showed no degradation over 24 h in aqueous buffer (PBS, pH 7.4) (Figures S7−S10). However, the observed loss of <30% may also be due to experimental variations or measurement uncertainties. This means that the test chemicals do not react or only react slowly with the components of the medium and the concentration is stable for the duration of the bioassay. The proteins in the medium are mostly from fetal bovine serum (FBS), and the results are consistent with previously reported slow reaction of acrylamides and albumin.[42]

Chemical Reactivity. The test chemicals showed no degradation with 2DG with $t_{1/2}$ close to or higher than 50 h (Figures S7 and S8). This value was defined as a threshold, as it is approximately twice the longest incubation time (24 h). To determine more reliable $t_{1/2}$ for the reaction with 2DG, longer incubation times would be necessary, but these would not be biologically relevant, since reactive chemicals are rapidly degraded in the body.[40,67] These results are consistent with the

https://doi.org/10.1021/acs.chemrestox.3c00115
Chem. Res. Toxicol. 2023, 36, 1374−1385

literature as acrylamides show no or only very low reactivity with hard nucleophiles such as DNA bases.[14,22] Only metabolic activation to more reactive glycidamide enables a reaction with DNA and therefore also causes the mutagenicity of acrylamides.[20,21,68]

Eight chemicals showed $t_{1/2}$ below 50 h with the biological nucleophile glutathione (GSH) (Figures S9 and S10), and reactions were much faster than with 2DG. The associated degradation rate constants (k) are shown in Table S5. Figure 5A shows the degradation half-lives ($t_{1/2}$) of the chemicals

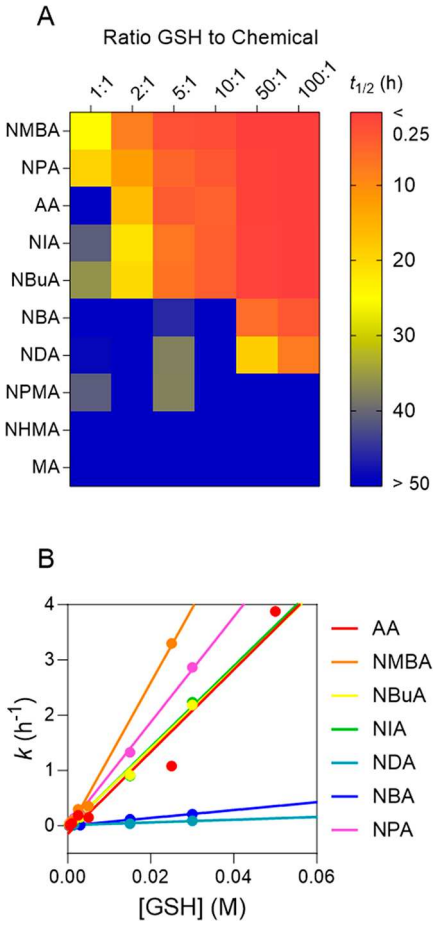

Figure 5. Degradation kinetics of the test chemicals with glutathione (GSH). (A) Degradation half-lives ($t_{1/2}$) of the test chemicals with different concentrations of GSH. (B) Linear regression of pseudo-first-order degradation rate constants (k) plotted against the concentration of GSH.

incubated with different concentrations of GSH. The concentration of the test chemical was kept constant so that only the ratio of nucleophile to chemical was changed. The lowest ratio of nucleophile to chemical was 1:1, and the highest was 100:1. MA and NHMA were not reactive and showed $t_{1/2}$ above 50 h for all GSH concentrations, and NPMA showed $t_{1/2}$ of 41.0 h (GSH/NPMA = 1:1) and 37.4 h (GSH/NPMA = 5:1), but $t_{1/2}$ above 50 h for the other GSH ratios. For the other seven chemicals, $t_{1/2}$ decreased with increasing concentration of GSH. NMBA showed the overall lowest $t_{1/2}$ and NDA the highest $t_{1/2}$ (Table S5). At the highest concentration of GSH, the reaction of NMBA was faster than the sample preparation time (15 min) so that $t_{1/2}$ could not be determined (Table S5). The measured pseudo-first-order degradation rate constants (k) were plotted against the concentration of GSH for all chemicals that showed degradation (Figure 5B). Linear regression was used to derive the second-order degradation rate constants (k_{GSH}) of the chemicals from the slope of this plot (eq 9).

The intercept of the fit gave the reaction constant of the reaction with water (k_{H_2O}). For all chemicals, the intercept was close to 0 (Table S5), so the reaction with water is negligible for all chemicals. This is consistent with the observation that none of the substances showed degradation in PBS (Figures S7−S10). NMBA showed the highest k_{GSH} (Table S5, 134.800 M^{-1} h^{-1}) and NDA the lowest (Table S5, 2.574 M^{-1} h^{-1}). As NBMA has two reactive groups, it had a k_{GSH} approximately twice as high as AA, NBuA, and NIA because, unlike the other test substances, it can react with two GSH molecules. NPMA, NHMA, and MA showed no degradation with GSH and no k_{GSH} values could be determined.

It is known that acrylamides react with GSH via a Michael addition.[17,18,69] The resulting Michael adducts were identified as common metabolites of acrylamides, making the reaction with GSH an important detoxification process of acrylamides *in vivo*.[70,71] Mass spectrometry was used to identify the transformation products of the reaction with GSH. As expected, Michael conjugation products with GSH were found for eight test chemicals. Chemical structures and MS/MS spectra of the conjugation products are shown in Figure S11. No conjugation products were found for MA and NHMA. Since NBMA has two reactive groups, only the conjugation product with two GSH molecules was found, and the conjugation product with one GSH molecule could not be detected for this chemical. The relative amount of GSH-conjugate was measured for two GSH/acrylamide ratios (5:1 and 100:1) and three time points (1, 4, and 24 h). Figure S12 shows that at a ratio GSH/acrylamide of 5:1, the relative amount of GSH-conjugate increased over time for GSH conjugates of AA, NMBA, NBuA, NIA, NDA, NBA, and NPA. At a GSH/acrylamide ratio of 100:1, relative amounts of GSH-conjugate were already high at the shortest incubation time and showed higher variation. For AA, NMBA, NBuA, NIA, and NPA, the relative amount of GSH-conjugate decreased slightly over time. The high excess of GSH accelerates the conjugation reaction, resulting in high relative amounts of GSH-conjugate in the 100:1 samples. The GSH conjugates appear to be further degraded over time, which is why their relative amount decreases, but the resulting transformation products could not be identified. GSH conjugates of NPMA could only be found at a GSH/acrylamide ratio of 100:1.

To rationalize the GSH reactivity of the chemicals, quantum chemical calculations were performed and the charge densities of selected atoms ($q(C_\alpha)$, $q(C_\beta)$, and $q(C_1)$) and the energy of the lowest unoccupied orbitals (ε_{LUMO}) were calculated (Table S6, Figure S13). The methacrylamides (MA, NPMA, and NHMA), which showed no reactivity with GSH in the experiment, had calculated q for C_α, which were significantly less negative than those for the acrylamides (factor 4). So, the electron-donating effect of the methyl group causes the reduced reactivity of these chemicals.[72,73] For the differently substituted acrylamides, ε_{LUMO} and the q of the atoms C_α, C_β, and C_1 showed no difference (Table S6). Nevertheless, NDA and NBA had much lower k_{GSH} values than the other acrylamides (factors 35 and 10, respectively). In the case of NDA, the formation of the intermediate state of the reaction

https://doi.org/10.1021/acs.chemrestox.3c00115
Chem. Res. Toxicol. 2023, 36, 1374−1385

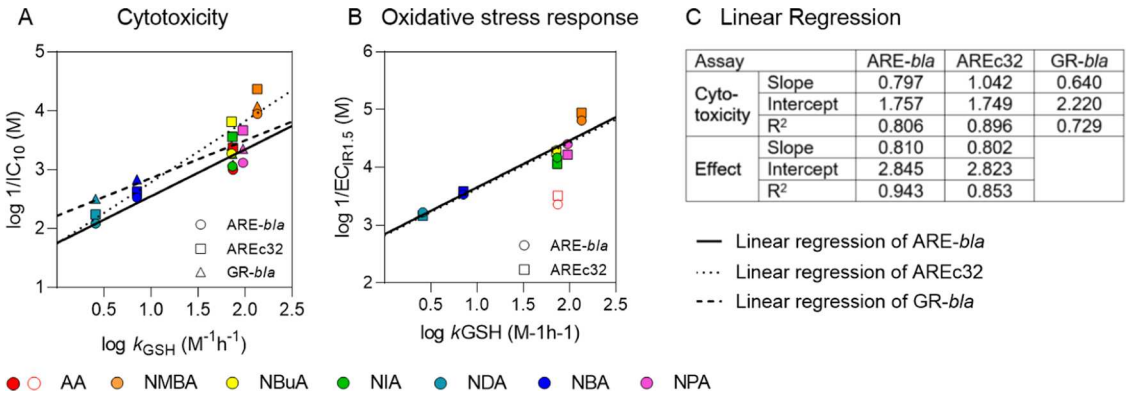

Assay		ARE-*bla*	AREc32	GR-*bla*
Cyto-toxicity	Slope	0.797	1.042	0.640
	Intercept	1.757	1.749	2.220
	R^2	0.806	0.896	0.729
Effect	Slope	0.810	0.802	
	Intercept	2.845	2.823	
	R^2	0.943	0.853	

Figure 6. Linear regression of cytotoxicity (log $1/IC_{10}$) (A) and activation of the oxidative stress response ($EC_{IR1.5}$) (B) plotted against reactivity with GSH (k_{GSH}). (C) Regression parameters of linear regression. AA was excluded from the fit of the oxidative stress response. No k_{GSH} could be quantified for MA, NPMA, and NHMA.

with GSH is sterically hindered by the two ethyl groups on the nitrogen, which leads to a deceleration of the reaction rate.[74] The low reactivity of NBA was surprising at first glance since its structure and the results of the quantum chemical calculations (Table S6) are very similar to those of the highly reactive NPA. These observations could be explained by looking at the depiction of the LUMO (Figure S13). While for NPA the orbitals of the phenyl ring and the α,β-unsaturated carbonyl group are clearly separated from each other, for NBA the orbitals of the phenyl ring merge with those of C_α and C_β lowering the electrophilicity, which explains the low reactivity.

Comparison of Toxicity and Reactivity. All methacrylamides and NDA and NBA showed the lowest effects and acted as baseline toxicants in all assays (Table 1 and Figure 3). These chemicals also showed no reactivity (methacrylamides) or low reactivity to GSH (NDA and NBA, Table S5). For the acrylamides, the measured effect concentrations for cytotoxicity (log $1/IC_{10}$) and the activation of the oxidative stress response (log $1/EC_{IR1.5}$) increased log-linearly with an increase in log k_{GSH} (Figure 6). Methacrylamides are not included, as they did not show reactivity toward GSH.

The log-linear relationship of the cytotoxicity (Figure 6A) or oxidative stress response (Figure 6B) and the reactivity toward GSH was shown by linear regression (Figure 6C). AA was excluded from the fit of the oxidative stress response since it showed lower effects than predicted by the fit (Figure 6B). The reason for the deviation of AA from the fit is unclear, but degradation in the medium or loss due to volatilization over the time of the assay can be excluded (Figure 4). Thus, cellular processes such as metabolism must be responsible for the low effects. However, these processes must occur to the same extent in both cell lines since no difference in the effect concentrations was observed for the different assays. Further tests on acrylamide metabolism are necessary to explain this observation. Even though a test set of 7 chemicals (cytotoxicity) or 6 chemicals (oxidative stress response) is rather small for the establishment of a QSAR, the R^2 of the linear regression were between 0.792 and 0.943 for the three cell lines (Figure 6C). While the fits for the activation of the oxidative stress response were almost identical in both cell lines, the fits for cytotoxicity differed slightly for the three cell lines tested, which can be explained by the generally higher variability of the cytotoxicity measurement. We therefore conclude that the predominant MOA of the test substances is the formation of ROS, which leads to an activation of the oxidative stress response. In addition, a decrease in the intracellular GSH level by direct reaction of GSH with the test substances disrupts the intracellular redox homeostasis and thus the protection against ROS. In this study, no intracellular GSH or ROS levels were measured; therefore, a confirmation of the proposed MOA in the tested cells is not possible. However, both *in vitro* and *in vivo* studies have shown that exposure to acrylamides leads to an increase in intracellular ROS levels and a decrease in GSH levels.[75−77] For other reactive chemicals, another possible mechanism of activation of the Nrf-2/Keap-1 pathway has been described. For example, Dinkova-Kostova et al.[78] and Suzuki et al.[37] have shown that some electrophilic chemicals react directly with cysteine residues of Kelch-like ECH-associated protein 1 (Keap-1), an important protein of the oxidative stress signal chain and thus trigger the activation of the oxidative stress response.[79] In this case, the reactivity of the chemicals with GSH can serve as a measure of the reactivity with cysteine-rich proteins in the cell.[80] However, this mechanism has not been verified for acrylamide or related chemicals.[81,82]

CONCLUSIONS

In this study, we investigated the cytotoxicity and activation of oxidative stress response via the Nrf-2/Keap-1 pathway of seven acrylamides and three methacrylamides and compared both *in vitro* effects with the reactivity toward the biological nucleophile GSH. The identification of the molecular initiating event is important for the interpretation of *in vitro* results of reactive chemicals with respect to possible adverse effects in humans. DNA damage and reactivity toward proteins or peptides are important MOAs of reactive chemicals. The softness or hardness of the electrophile determines the preferred reaction partner and thus the toxic effect.[24] DNA damage is caused mainly by the reaction of hard electrophiles such as epoxides or organochlorides with DNA bases, whereas soft electrophiles such as the acrylamides tested in this study preferentially react with soft nucleophiles such as cysteine residues of cellular proteins or peptides.[25] Reaction of the test chemicals with the hard nucleophile 2DG was much slower than the incubation time of a cell-based *in vitro* bioassay (24 h). Therefore, a direct genotoxic effect of the test chemicals through the formation of DNA adducts could be excluded. Nevertheless, acrylamide shows carcinogenic effects *in vivo*, because it can be metabolized to the hard nucleophile glycidamide, which shows reactivity toward DNA.[22,40] For a

https://doi.org/10.1021/acs.chemrestox.3c00115
Chem. Res. Toxicol. 2023, 36, 1374−1385

complete evaluation of the carcinogenicity of the test chemicals, further genotoxicity tests, such as the micronucleus test or a reporter gene assay for the induction of the tumor suppression factor p53 after metabolic activation, would be required to assess the mutagenic potential of possible metabolites. In addition, external metabolization using, for example, S9 or microsomes would be necessary, as the reporter gene cell lines used show only low cytochrome P450 activity.[35,83]

For the acrylamides tested in this study, the activation of the oxidative stress response via the Nrf-2/Keap-1 pathway was probably triggered by the intracellular formation of ROS as well as a disturbance of the redox balance by the reduction of the intracellular GSH level.[77] This adverse outcome pathway (AOP)[84] has already been shown for different adverse effects, such as hepatotoxicity[85] and neurotoxicity[76] of acrylamides. However, for some chemicals, the oxidative stress response can also be triggered by direct binding of the test chemicals to Keap-1, which has been identified as a molecular initiating event for skin sensitization,[79] but direct reactions with Keap-1 and acrylamides have not yet been demonstrated.[81] The results of this study can be used to deduce the probable behavior of the chemicals in humans and their potential effects on human health. The relationship between reactivity and toxicity of electrophiles has been extensively studied in the past and a number of QSAR models are available for predicting toxicity in different *in vitro* systems.[31,86,87] Comparable QSARs have also been developed to predict the toxicity of acrylates in *in vitro* cell lines.[88] We have found a linear relationship between the reactivity of the chemicals toward GSH and the activation of oxidative stress response *in vitro* (Figure 6). This result can be used to predict *in vitro* effects for other test chemicals, although a larger and more diverse set of test chemicals would be needed for reliable quantitative prediction and an elucidation of the MOA of the test chemicals. Nevertheless, the measurement of k_{GSH}, which can be done in HT format, together with quantum chemical calculations of the chemical reactivity allows a suitable estimation of the bioassay results and simplifies their interpretation.

■ ASSOCIATED CONTENT

Supporting Information

The Supporting Information is available free of charge at https://pubs.acs.org/doi/10.1021/acs.chemrestox.3c00115.

> Test chemicals, layout of the robot, analytical methods, concentration−response curves, uptake kinetics, pin-water distribution ratios, degradation kinetics, degradation rate constants, structures and MS/MS spectra of transformation products, quantum chemical calculations, and lowest unoccupied molecular orbitals (PDF)

■ AUTHOR INFORMATION

Corresponding Author

Beate I. Escher − *Department of Cell Toxicology, Helmholtz Centre for Environmental Research − UFZ, 04318 Leipzig, Germany; Department of Geosciences, Eberhard Karls University Tübingen, Environmental Toxicology, 72076 Tübingen, Germany;* orcid.org/0000-0002-5304-706X; Email: beate.escher@ufz.de

Authors

Julia Huchthausen − *Department of Cell Toxicology, Helmholtz Centre for Environmental Research − UFZ, 04318 Leipzig, Germany;* orcid.org/0000-0003-4916-1174

Nico Grasse − *Department of Analytical Chemistry, Helmholtz Centre for Environmental Research − UFZ, 04318 Leipzig, Germany*

Maria König − *Department of Cell Toxicology, Helmholtz Centre for Environmental Research − UFZ, 04318 Leipzig, Germany*

Stephan Beil − *Institute of Water Chemistry, Technische Universität Dresden, 01069 Dresden, Germany*

Luise Henneberger − *Department of Cell Toxicology, Helmholtz Centre for Environmental Research − UFZ, 04318 Leipzig, Germany;* orcid.org/0000-0002-3181-0044

Complete contact information is available at: https://pubs.acs.org/10.1021/acs.chemrestox.3c00115

Funding

This project has received funding from the European Union's Horizon 2020 research and innovation program under Grant Agreement No. 965406. The work presented in this publication was performed as part of the ASPIS cluster. The results and conclusions reflect only the authors' view and the European Commission cannot be held responsible for any use that may be made of the information contained therein.

Notes

The authors declare no competing financial interest.

■ ACKNOWLEDGMENTS

The authors thank Jenny Braasch and Christin Kühnert for supporting the experiments and establishment of the robot method, as well as Bettina Seiwert for conducting the UPLC-TOF-MS measurement and Stefan Stolte and Stefan Scholz for reviewing the manuscript.

■ REFERENCES

(1) Doble, M.; Kumar, A. Degradation of Polymers. In *Biotreatment of Industrial Effluents*; Doble, M.; Kumar, A., Eds.; Butterworth-Heinemann: Burlington, 2005; Chapter 9, pp 101−110.

(2) Taeymans, D.; Wood, J.; Ashby, P.; Blank, I.; Studer, A.; Stadler, R. H.; Gondé, P.; Van Eijck, P.; Lalljie, S.; Lingnert, H.; Lindblom, M.; Matissek, R.; Müller, D.; Tallmadge, D.; O'Brien, J.; Thompson, S.; Silvani, D.; Whitmore, T. A review of acrylamide: an industry perspective on research, analysis, formation, and control. *Crit. Rev. Food Sci. Nutr.* **2004**, *44*, 323−347.

(3) Stadler, R. H.; Blank, I.; Varga, N.; Robert, F.; Hau, J.; Guy, P. A.; Robert, M. C.; Riediker, S. Acrylamide from Maillard reaction products. *Nature* **2002**, *419*, 449−450.

(4) Bull, R. J.; Robinson, M.; Laurie, R. D.; Stoner, G. D.; Greisiger, E.; Meier, J. R.; Stober, J. Carcinogenic effects of acrylamide in Sencar and A/J mice. *Cancer Res.* **1984**, *44*, 107−111.

(5) International Agency for Research on Cancer (IARC). (1994) Monographs on the evaluation of carcinogenic risks to humans: Some industrial chemicals. Vol. *60*, Geneva, Switzerland. https://publications.iarc.fr/Book-And-Report-Series/Iarc-Monographs-On-The-Identification-Of-Carcinogenic-Hazards-To-Humans/Some-Industrial-Chemicals-1994.

(6) Zhao, M.; Lewis Wang, F. S.; Hu, X.; Chen, F.; Chan, H. M. Acrylamide-induced neurotoxicity in primary astrocytes and microglia: Roles of the Nrf2-ARE and NF-κB pathways. *Food Chem. Toxicol.* **2017**, *106*, 25−35.

(7) LoPachin, R. M.; Gavin, T. Toxic neuropathies: Mechanistic insights based on a chemical perspective. *Neurosci. Lett.* **2015**, *596*, 78−83.
(8) Commission Regulation (EU) 2017/2158 of 20 November 2017 *establishing mitigation measures and benchmark levels for the reduction of the presence of acrylamide in food.*, Official Journal of the European Union L *304*, 24−44.
(9) European Chemicals Agency (18/04/2023). "Methacrylamide." Methacrylamide." Retrieved 19/04/2023, from https://echa.europa.eu/de/substance-information/-/substanceinfo/100.001.094.
(10) European Chemicals Agency (06/05/2023). "N,N'-Methylenediacrylamide." Retrieved 19/04/2023, from https://echa.europa.eu/de/substance-information/-/substanceinfo/100.003.411.
(11) Verhaar, H. J. M.; van Leeuwen, C. J.; Hermens, J. L. M. Classifying environmental pollutants. *Chemosphere* **1992**, *25*, 471−491.
(12) Wezel, A. P. v.; Opperhuizen, A. Narcosis due to environmental pollutants in aquatic organisms: residue-based toxicity, mechanisms, and membrane burdens. *Crit. Rev. Toxicol.* **1995**, *25*, 255−279.
(13) Freidig, A. P.; Verhaar, H. J. M.; Hermens, J. L. M. Comparing the Potency of Chemicals with Multiple Modes of Action in Aquatic Toxicology: Acute Toxicity Due to Narcosis versus Reactive Toxicity of Acrylic Compounds. *Environ. Sci. Technol.* **1999**, *33*, 3038−3043.
(14) Harder, A.; Escher, B. I.; Landini, P.; Tobler, N. B.; Schwarzenbach, R. P. Evaluation of bioanalytical assays for toxicity assessment and mode of toxic action classification of reactive chemicals. *Environ. Sci. Technol.* **2003**, *37*, 4962−4970.
(15) Richter, M.; Escher, B. I. Mixture toxicity of reactive chemicals by using two bacterial growth assays as indicators of protein and DNA damage. *Environ. Sci. Technol.* **2005**, *39*, 8753−8761.
(16) Schultz, T. W.; Carlson, R. E.; Cronin, M. T. D.; Hermens, J. L. M.; Johnson, R.; O'Brien, P. J.; Roberts, D. W.; Siraki, A.; Wallace, K. B.; Veith, G. D. A conceptual framework for predicting the toxicity of reactive chemicals: modeling soft electrophilicity. *SAR QSAR Environ. Res.* **2006**, *17*, 413−428.
(17) Hermens, J. L. M. Electrophiles and Acute Toxicity to Fish. *Environ. Health Perspect.* **1990**, *87*, 219−225.
(18) Ramirez-Montes, S.; Zarate-Hernandez, L. A.; Rodriguez, J. A.; Santos, E. M.; Cruz-Borbolla, J. A DFT Study of the Reaction of Acrylamide with L-Cysteine and L-Glutathione. *Molecules* **2022**, *27*, 8220.
(19) Ketterer, B. The role of nonenzymatic reactions of glutathione in xenobiotic metabolism. *Drug Metab. Rev.* **1982**, *13*, 161−187.
(20) Sumner, S. C. J.; Fennell, T. R.; Moore, T. A.; Chanas, B.; Gonzalez, F.; Ghanayem, B. I. Role of Cytochrome P450 2E1 in the Metabolism of Acrylamide and Acrylonitrile in Mice. *Chem. Res. Toxicol.* **1999**, *12*, 1110−1116.
(21) Wang, R. S.; McDaniel, L. P.; Manjanatha, M. G.; Shelton, S. D.; Doerge, D. R.; Mei, N. Mutagenicity of acrylamide and glycidamide in the testes of big blue mice. *Toxicol. Sci.* **2010**, *117*, 72−80.
(22) van Welie, R. T. H.; van Dijck, R. G. J. M.; Vermeulen, N. P. E.; van Sittert, N. J. Mercapturic Acids, Protein Adducts, and DNA Adducts as Biomarkers of Electrophilic Chemicals. *Crit. Rev. Toxicol.* **1992**, *22*, 271−306.
(23) Segerbäck, D.; Calleman, C. J.; Schroeder, J. L.; Costa, L. G.; Faustman, E. M. Formation of N-7-(2-carbamoyl-2-hydroxyethyl)-guanine in DNA of the mouse and the rat following intraperitoneal administration of [14C]acrylamide. *Carcinogenesis* **1995**, *16*, 1161−1165.
(24) Pearson, R. G. Hard and soft acids and bases—the evolution of a chemical concept. *Coord. Chem. Rev.* **1990**, *100*, 403−425.
(25) Lopachin, R. M.; Gavin, T.; Decaprio, A.; Barber, D. S. Application of the Hard and Soft, Acids and Bases (HSAB) theory to toxicant−target interactions. *Chem. Res. Toxicol.* **2012**, *25*, 239−251.
(26) LoPachin, R. M.; Geohagen, B. C.; Nordstroem, L. U. Mechanisms of soft and hard electrophile toxicities. *Toxicology* **2019**, *418*, 62−69.
(27) Melnikov, F.; Geohagen, B. C.; Gavin, T.; LoPachin, R. M.; Anastas, P. T.; Coish, P.; Herr, D. W. Application of the hard and soft, acids and bases (HSAB) theory as a method to predict cumulative neurotoxicity. *Neurotoxicology* **2020**, *79*, 95−103.
(28) Katen, A. L.; Roman, S. D. The genetic consequences of paternal acrylamide exposure and potential for amelioration. *Mutat. Res., Fundam. Mol. Mech. Mutagen.* **2015**, *777*, 91−100.
(29) Schwöbel, J. A. H.; Koleva, Y. K.; Enoch, S. J.; Bajot, F.; Hewitt, M.; Madden, J. C.; Roberts, D. W.; Schultz, T. W.; Cronin, M. T. Measurement and estimation of electrophilic reactivity for predictive toxicology. *Chem. Rev.* **2011**, *111*, 2562−2596.
(30) Blaschke, U.; Eismann, K.; Böhme, A.; Paschke, A.; Schüürmann, G. Structural alerts for the excess toxicity of acrylates, methacrylates, and propiolates derived from their short-term and long-term bacterial toxicity. *Chem. Res. Toxicol.* **2012**, *25*, 170−180.
(31) Harder, A.; Escher, B. I.; Schwarzenbach, R. P. Applicability and limitation of QSARs for the toxicity of electrophilic chemicals. *Environ. Sci. Technol.* **2003**, *37*, 4955−4961.
(32) Böhme, A.; Thaens, D.; Paschke, A.; Schüürmann, G. Kinetic Glutathione Chemoassay To Quantify Thiol Reactivity of Organic Electrophiles—Application to α,β-Unsaturated Ketones, Acrylates, and Propiolates. *Chem. Res. Toxicol.* **2009**, *22*, 742−750.
(33) Niederer, C.; Behra, R.; Harder, A.; Schwarzenbach, R. P.; Escher, B. I. Mechanistic approaches for evaluating the toxicity of reactive organochlorines and epoxides in green algae. *Environ. Toxicol. Chem.* **2004**, *23*, 697−704.
(34) Freidig, A. P.; Hermens, J. L. M. Narcosis and chemical reactivity QSARs for acute fish toxicity. *Quant. Struct.-Act. Relat.* **2000**, *19*, 547−553.
(35) Fischer, F. C.; Abele, C.; Henneberger, L.; Kluver, N.; Konig, M.; Muhlenbrink, M.; Schlichting, R.; Escher, B. I. Cellular Metabolism in High-Throughput In Vitro Reporter Gene Assays and Implications for the Quantitative In Vitro-In Vivo Extrapolation. *Chem. Res. Toxicol.* **2020**, *33*, 1770−1779.
(36) Watzek, N.; Scherbl, D.; Schug, M.; Hengstler, J. G.; Baum, M.; Habermeyer, M.; Richling, E.; Eisenbrand, G. Toxicokinetics of acrylamide in primary rat hepatocytes: coupling to glutathione is faster than conversion to glycidamide. *Arch. Toxicol.* **2013**, *87*, 1545−1556.
(37) Suzuki, T.; Yamamoto, M. Stress-sensing mechanisms and the physiological roles of the Keap1-Nrf2 system during cellular stress. *J. Biol. Chem.* **2017**, *292*, 16817−16824.
(38) Suzuki, T.; Muramatsu, A.; Saito, R.; Iso, T.; Shibata, T.; Kuwata, K.; Kawaguchi, S. I.; Iwawaki, T.; Adachi, S.; Suda, H.; Morita, M.; Uchida, K.; Baird, L.; Yamamoto, M. Molecular Mechanism of Cellular Oxidative Stress Sensing by Keap1. *Cell Rep.* **2019**, *28*, 746−758.
(39) Tang, J. Y. M.; Glenn, E.; Thoen, H.; Escher, B. I. In vitro bioassay for reactive toxicity towards proteins implemented for water quality monitoring. *J. Environ. Monit.* **2012**, *14*, 1073−1081.
(40) Besaratinia, A.; Pfeifer, G. P. DNA adduction and mutagenic properties of acrylamide. *Mutat. Res., Genet. Toxicol. Environ. Mutagen.* **2005**, *580*, 31−40.
(41) Ramamoorthy, S.; Cidlowski, J. A. Corticosteroids: Mechanisms of Action in Health and Disease. *Rheum. Dis. Clin. North Am.* **2016**, *42*, 15−31.
(42) Tong, G. C.; Cornwell, W. K.; Means, G. E. Reactions of acrylamide with glutathione and serum albumin. *Toxicol. Lett.* **2004**, *147*, 127−131.
(43) Wang, X. J.; Hayes, J. D.; Wolf, C. R. Generation of a stable antioxidant response element-driven reporter gene cell line and its use to show redox-dependent activation of Nrf2 by cancer chemotherapeutic agents. *Cancer Res.* **2006**, *66*, 10983−10994.
(44) Roy, K. S.; Nazdrajić, E.; Shimelis, O. I.; Ross, M. J.; Chen, Y.; Cramer, H.; Pawliszyn, J. Optimizing a High-Throughput Solid-Phase Microextraction System to Determine the Plasma Protein Binding of Drugs in Human Plasma. *Anal. Chem.* **2021**, *93*, 11061−11065.
(45) Huchthausen, J.; Henneberger, L.; Mälzer, S.; Nicol, B.; Sparham, C.; Escher, B. I. High-Throughput Assessment of the

Abiotic Stability of Test Chemicals in In Vitro Bioassays. *Chem. Res. Toxicol.* **2022**, *35*, 867−879.
(46) König, M.; Escher, B. I.; Neale, P. A.; Krauss, M.; Hilscherova, K.; Novak, J.; Teodorovic, I.; Schulze, T.; Seidensticker, S.; Hashmi, M. A. K.; Ahlheim, J.; Brack, W. Impact of untreated wastewater on a major European river evaluated with a combination of in vitro bioassays and chemical analysis. *Environ. Pollut.* **2017**, *220*, 1220−1230.
(47) Neale, P. A.; Altenburger, R.; Ait-Aissa, S.; Brion, F.; Busch, W.; de Aragao Umbuzeiro, G.; Denison, M. S.; Du Pasquier, D.; Hilscherova, K.; Hollert, H.; Morales, D. A.; Novak, J.; Schlichting, R.; Seiler, T. B.; Serra, H.; Shao, Y.; Tindall, A. J.; Tollefsen, K. E.; Williams, T. D.; Escher, B. I. Development of a bioanalytical test battery for water quality monitoring: Fingerprinting identified micropollutants and their contribution to effects in surface water. *Water Res.* **2017**, *123*, 734−750.
(48) Escher, B. I.; Dutt, M.; Maylin, E.; Tang, J. Y. M.; Toze, S.; Wolf, C. R.; Lang, M. Water quality assessment using the AREc32 reporter gene assay indicative of the oxidative stress response pathway. *J. Environ. Monit.* **2012**, *14*, 2877−2885.
(49) Seiwert, B.; Nihemaiti, M.; Troussier, M.; Weyrauch, S.; Reemtsma, T. Abiotic oxidative transformation of 6-PPD and 6-PPD quinone from tires and occurrence of their products in snow from urban roads and in municipal wastewater. *Water Res.* **2022**, *212*, 118122.
(50) Escher, B. I.; Neale, P. A.; Villeneuve, D. L. The advantages of linear concentration-response curves for in vitro bioassays with environmental samples. *Environ. Toxicol. Chem.* **2018**, *37*, 2273−2280.
(51) Lee, J.; Braun, G.; Henneberger, L.; König, M.; Schlichting, R.; Scholz, S.; Escher, B. I. Critical Membrane Concentration and Mass-Balance Model to Identify Baseline Cytotoxicity of Hydrophobic and Ionizable Organic Chemicals in Mammalian Cell Lines. *Chem. Res. Toxicol.* **2021**, *34*, 2100−2109.
(52) Ulrich, N.; Endo, S.; Brown, T. N.; Watanabe, N.; Bronner, G.; Abraham, M. H.; Goss, K.-U. (2017) UFZ-LSER database v 3.2.1 [Internet], Helmholtz Centre for Environmental Research-UFZ, Leipzig, Germany. http://www.ufz.de/lserd.
(53) Escher, B. I.; Henneberger, L.; König, M.; Schlichting, R.; Fischer, F. C. Cytotoxicity Burst? Differentiating Specific from Nonspecific Effects in Tox21 in Vitro Reporter Gene Assays. *Environ. Health Perspect.* **2020**, *128*, 077007.
(54) Henneberger, L.; Mühlenbrink, M.; König, M.; Schlichting, R.; Fischer, F. C.; Escher, B. I. Quantification of freely dissolved effect concentrations in in vitro cell-based bioassays. *Arch. Toxicol.* **2019**, *93*, 2295−2305.
(55) Hanwell, M. D.; Curtis, D. E.; Lonie, D. C.; Vandermeersch, T.; Zurek, E.; Hutchison, G. R. Avogadro: an advanced semantic chemical editor, visualization, and analysis platform. *J. Cheminf.* **2012**, *4*, No. 17.
(56) Rappe, A. K.; Casewit, C. J.; Colwell, K. S.; Goddard, W. A.; Skiff, W. M. Uff, a Full Periodic-Table Force-Field for Molecular Mechanics and Molecular-Dynamics Simulations. *J. Am. Chem. Soc.* **1992**, *114*, 10024−10035.
(57) Neese, F. The ORCA program system. *Wires Comput. Mol. Sci.* **2012**, *2*, 73−78.
(58) Neese, F. Software update: the ORCA program system, version 4.0. *Wires Comput. Mol. Sci.* **2018**, *8*, No. e1327.
(59) Neese, F.; Wennmohs, F.; Becker, U.; Riplinger, C. The ORCA quantum chemistry program package. *J. Chem. Phys.* **2020**, *152*, 224108.
(60) Knizia, G.; Klein, J. E. M. N. Electron Flow in Reaction Mechanisms-Revealed from First Principles. *Angew. Chem., Int. Ed.* **2015**, *54*, 5518−5522.
(61) Prasad, S. N.; Muralidhara. Evidence of acrylamide induced oxidative stress and neurotoxicity in Drosophila melanogaster - its amelioration with spice active enrichment: relevance to neuropathy. *Neurotoxicology* **2012**, *33*, 1254−1264.
(62) Hong, Y.; Nan, B.; Wu, X.; Yan, H.; Yuan, Y. Allicin alleviates acrylamide-induced oxidative stress in BRL-3A cells. *Life Sci.* **2019**, *231*, 116550.
(63) Firouzabadi, A. M.; Imani, M.; Zakizadeh, F.; Ghaderi, N.; Zare, F.; Yadegari, M.; Pourentezari, M.; Fesahat, F. Evaluating effect of acrylamide and ascorbic acid on oxidative stress and apoptosis in ovarian tissue of wistar rat. *Toxicol. Rep.* **2022**, *9*, 1580−1585.
(64) Schabacker, J.; Schwend, T.; Wink, M. Reduction of Acrylamide Uptake by Dietary Proteins in a Caco-2 Gut Model. *J. Agric. Food Chem.* **2004**, *52*, 4021−4025.
(65) Maeder, V.; Escher, B. I.; Scheringer, M.; Hungerbühler, K. Toxic Ratio as an Indicator of the Intrinsic Toxicity in the Assessment of Persistent, Bioaccumulative, and Toxic Chemicals. *Environ. Sci. Technol.* **2004**, *38*, 3659−3666.
(66) Fay, K. A.; Villeneuve, D. L.; Swintek, J.; Edwards, S. W.; Nelms, M. D.; Blackwell, B. R.; Ankley, G. T. Differentiating Pathway-Specific From Nonspecific Effects in High-Throughput Toxicity Data: A Foundation for Prioritizing Adverse Outcome Pathway Development. *Toxicol. Sci.* **2018**, *163*, 500−515.
(67) Solomon, J. J.; Fedyk, J.; Mukai, F.; Segal, A. Direct alkylation of 2′-deoxynucleosides and DNA following in vitro reaction with acrylamide. *Cancer Res.* **1985**, *45*, 3465−3470.
(68) Hölzl-Armstrong, L.; Kucab, J. E.; Moody, S.; Zwart, E. P.; Loutkotová, L.; Duffy, V.; Luijten, M.; Gamboa da Costa, G.; Stratton, M. R.; Phillips, D. H.; Arlt, V. M. Mutagenicity of acrylamide and glycidamide in human TP53 knock-in (Hupki) mouse embryo fibroblasts. *Arch. Toxicol.* **2020**, *94*, 4173−4196.
(69) Nair, D. P.; Podgórski, M.; Chatani, S.; Gong, T.; Xi, W.; Fenoli, C. R.; Bowman, C. N. The Thiol-Michael Addition Click Reaction: A Powerful and Widely Used Tool in Materials Chemistry. *Chem. Mater.* **2014**, *26*, 724−744.
(70) Luo, Y. S.; Long, T. Y.; Chiang, S. Y.; Wu, K. Y. Characterization of primary glutathione conjugates with acrylamide and glycidamide: Toxicokinetic studies in Sprague Dawley rats treated with acrylamide. *Chem. Biol. Interact.* **2021**, *350*, 109701.
(71) Sumner, S. C. J.; MacNeela, J. P.; Fennell, T. R. Characterization and quantitation of urinary metabolites of [1,2,3−13C]-acrylamide in rats and mice using carbon-13 nuclear magnetic resonance spectroscopy. *Chem. Res. Toxicol.* **1992**, *5*, 81−89.
(72) Freidig, A. P.; Verhaar, H. J. M.; Hermens, J. L. M. Quantitative structure-property relationships for the chemical reactivity of acrylates and methacrylates. *Environ. Toxicol. Chem.* **1999**, *18*, 1133−1139.
(73) McCarthy, T. J.; Hayes, E. P.; Schwartz, C. S.; Witz, G. The reactivity of selected acrylate esters toward glutathione and deoxyribonucleosides in vitro: structure-activity relationships. *Fundam. Appl. Toxicol.* **1994**, *22*, 543−548.
(74) Bent, G.-A.; Maragh, P.; Dasgupta, T.; Fairman, R. A.; Grierson, L. Kinetic and density functional theory (DFT) studies of in vitro reactions of acrylamide with the thiols: captopril, l-cysteine, and glutathione. *Toxicol. Res.* **2015**, *4*, 121−131.
(75) Zhao, M.; Wang, P.; Zhu, Y.; Liu, X.; Hu, X.; Chen, F. The chemoprotection of a blueberry anthocyanin extract against the acrylamide-induced oxidative stress in mitochondria: unequivocal evidence in mice liver. *Food Funct.* **2015**, *6*, 3006−3012.
(76) Zhao, M.; Deng, L.; Lu, X.; Fan, L.; Zhu, Y.; Zhao, L. The involvement of oxidative stress, neuronal lesions, neurotransmission impairment, and neuroinflammation in acrylamide-induced neurotoxicity in C57/BL6 mice. *Environ. Sci. Pollut. Res.* **2022**, *29*, 41151−41167.
(77) Zhao, M.; Zhang, B.; Deng, L. The Mechanism of Acrylamide-Induced Neurotoxicity: Current Status and Future Perspectives. *Front. Nutr.* **2022**, *9*, No. 488.
(78) Dinkova-Kostova, A. T.; Holtzclaw, W. D.; Cole, R. N.; Itoh, K.; Wakabayashi, N.; Katoh, Y.; Yamamoto, M.; Talalay, P. Direct evidence that sulfhydryl groups of Keap1 are the sensors regulating induction of phase 2 enzymes that protect against carcinogens and oxidants. *Proc. Natl. Acad. Sci. U.S.A.* **2002**, *99*, 11908−11913.
(79) Natsch, A.; Emter, R. Skin sensitizers induce antioxidant response element dependent genes: application to the in vitro testing

https://doi.org/10.1021/acs.chemrestox.3c00115
Chem. Res. Toxicol. 2023, 36, 1374−1385

of the sensitization potential of chemicals. *Toxicol. Sci.* **2008**, *102*, 110−119.
(80) Ebbrell, D. J.; Madden, J. C.; Cronin, M. T.; Schultz, T. W.; Enoch, S. J. Development of a Fragment-Based in Silico Profiler for Michael Addition Thiol Reactivity. *Chem. Res. Toxicol.* **2016**, *29*, 1073−1081.
(81) Zhang, L.; Gavin, T.; Barber, D. S.; LoPachin, R. M. Role of the Nrf2-ARE pathway in acrylamide neurotoxicity. *Toxicol. Lett.* **2011**, *205*, 1−7.
(82) Barber, D. S.; Stevens, S.; LoPachin, R. M. Proteomic analysis of rat striatal synaptosomes during acrylamide intoxication at a low dose rate. *Toxicol. Sci.* **2007**, *100*, 156−167.
(83) Qu, W.; Crizer, D. M.; DeVito, M. J.; Waidyanatha, S.; Xia, M.; Houck, K.; Ferguson, S. S. Exploration of xenobiotic metabolism within cell lines used for Tox21 chemical screening. *Toxicol. In Vitro* **2021**, *73*, 105109.
(84) Ankley, G. T.; Bennett, R. S.; Erickson, R. J.; Hoff, D. J.; Hornung, M. W.; Johnson, R. D.; Mount, D. R.; Nichols, J. W.; Russom, C. L.; Schmieder, P. K.; Serrrano, J. A.; Tietge, J. E.; Villeneuve, D. L. Adverse outcome pathways: a conceptual framework to support ecotoxicology research and risk assessment. *Environ. Toxicol. Chem.* **2010**, *29*, 730−741.
(85) Banc, R.; Popa, D.-S.; Cozma-Petruţ, A.; Filip, L.; Kiss, B.; Fărcaş, A.; Nagy, A.; Miere, D.; Loghin, F. Protective Effects of Wine Polyphenols on Oxidative Stress and Hepatotoxicity Induced by Acrylamide in Rats. *Antioxidants* **2022**, *11*, 1347.
(86) Schultz, T. W.; Yarbrough, J. W.; Koss, S. K. Identification of reactive toxicants: structure-activity relationships for amides. *Cell Biol. Toxicol.* **2006**, *22*, 339−349.
(87) Schultz, T. W.; Aptula, A. O. Kinetic-Based Reactivity for Michael Acceptors: Structural Activity Relationships and Its Relationship to Excess Acute Fish Toxicity. *Bull. Environ. Contam. Toxicol.* **2016**, *97*, 752−756.
(88) Chan, K.; O'Brien, P. J. Structure-activity relationships for hepatocyte toxicity and electrophilic reactivity of alpha,beta-unsaturated esters, acrylates and methacrylates. *J. Appl. Toxicol.* **2008**, *28*, 1004−1015.

https://doi.org/10.1021/acs.chemrestox.3c00115
Chem. Res. Toxicol. 2023, 36, 1374−1385

Publication III

Effects of Chemicals in Reporter Gene Bioassays with Different Metabolic Activity Compared to Baseline Toxicity

Julia Huchthausen[†], Jenny Braasch[†], Beate I. Escher[†,§], Maria König[†], Luise Henneberger[†,*]

[†] Helmholtz Centre for Environmental Research – UFZ, Department of Cell Toxicology, Permoserstr. 15, 04318 Leipzig, Germany

[§] Eberhard Karls University Tübingen, Environmental Toxicology, Department of Geosciences, Scharrenbergstr. 94-96, 72076 Tübingen, Germany

Corresponding author: luise.henneberger@ufz.de

Published in Chemical Research in Toxicology, DOI: 10.1021/acs.chemrestox.4c00017.

Chemical Research in Toxicology

pubs.acs.org/crt

Article

Effects of Chemicals in Reporter Gene Bioassays with Different Metabolic Activities Compared to Baseline Toxicity

Published as part of Chemical Research in Toxicology virtual special issue "Women in Toxicology".

Julia Huchthausen, Jenny Braasch, Beate I. Escher, Maria König, and Luise Henneberger*

Cite This: https://doi.org/10.1021/acs.chemrestox.4c00017

Read Online

ACCESS | Metrics & More | Article Recommendations | Supporting Information

ABSTRACT: High-throughput cell-based bioassays are used for chemical screening and risk assessment. Chemical transformation processes caused by abiotic degradation or metabolization can reduce the chemical concentration or, in some cases, lead to the formation of more toxic transformation products. Unaccounted loss processes may falsify the bioassay results. Capturing the formation and effects of transformation products is important for relating the *in vitro* effects to *in vivo*. Reporter gene cell lines are believed to have low metabolic activity, but inducibility of cytochrome P450 (CYP) enzymes has been reported. Baseline toxicity is the minimal toxicity a chemical can have and is caused by the incorporation of the chemical into cell membranes. In the present study, we improved an existing baseline toxicity model based on a newly defined critical membrane burden derived from freely dissolved effect concentrations, which are directly related to the membrane concentration. Experimental effect concentrations of 94 chemicals in three bioassays (AREc32, ARE-*bla* and GR-*bla*) were compared with baseline toxicity by calculating the toxic ratio (TR). CYP activities of all cell lines were determined by using fluorescence-based assays. Only ARE-*bla* showed a low basal CYP activity and inducibility and AREc32 showed a low inducibility. Overall cytotoxicity was similar in all three assays despite the different metabolic activities indicating that chemical metabolism is not relevant for the cytotoxicity of the tested chemicals in these assays. Up to 28 chemicals showed specific cytotoxicity with TR > 10 in the bioassays, but baseline toxicity could explain the effects of the majority of the remaining chemicals. Seven chemicals showed TR < 0.1 indicating inaccurate physicochemical properties or experimental artifacts like chemical precipitation, volatilization, degradation, or other loss processes during the *in vitro* bioassay. The new baseline model can be used not only to identify specific cytotoxicity mechanisms but also to identify potential problems in the experimental performance or evaluation of the bioassay and thus improve the quality of the bioassay data.

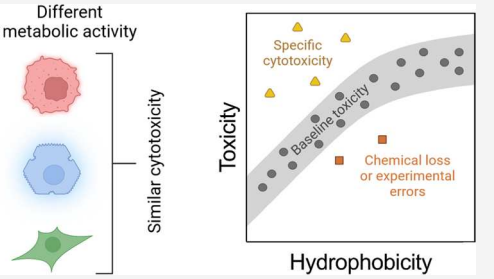

INTRODUCTION

Risk assessment of chemicals using high-throughput tests is becoming more and more important since the number of chemicals is increasing year by year. The conventional approach of using animal studies to assess the risk of chemicals to humans has been used for many years. However, a comprehensive risk assessment of chemicals using animal-based studies is not feasible, as animal testing for the risk assessment of single chemicals is extremely costly and can take several years to complete.[1]

Therefore, there has been a recent shift in the focus of risk assessment to so-called "New Approach Methodologies" (NAMs) which include a wide range of experimental approaches such as *in vitro* bioassays and omics methods, as well as *in silico* approaches such as quantitative structure−activity relationships (QSARs), and machine learning approaches. While these methods are not new, a combination of *in silico*, *in chemico* and *in vitro* approaches can provide information to assess the risks of even data-poor chemicals and reduce or eliminate the use of animals.[2−4] The PrecisionTox initiative started in February 2021 and was funded by the European Commission as part of the Horizon 2020 program for the development of NAMs for testing the safety of chemicals. The goal of PrecisionTox is to understand the systemic toxicity of chemicals by applying evolutionary principles to compare toxicological responses in different species. The concept of "toxicity by descent" suggests that the mechanisms of chemical toxicity may be similar in distantly related species due to a shared biology. PrecisionTox uses five model species (*Drosophila melanogaster*, *Caenorhabditis elegans*, *Daphnia magna*, and embryos of *Xenopus laevis* and *Danio rerio*) as well as human cell lines for high-throughput testing. The project integrates phenotype, metabolome, and transcriptome analysis to identify toxicity pathways.[5] The present study investigated the *in vitro* effects of 94 chemicals

Received: January 12, 2024
Revised: April 5, 2024
Accepted: April 9, 2024

with diverse physicochemical properties selected within the PrecisonTox project for analysis in three different *in vitro* cell-based bioassays.

A major impediment for the use of *in vitro* bioassays for risk assessment is the lack of exposure assessment of the chemicals. The prerequisite to generate reliable *in vitro* data is a stable chemical concentration over the course of the assay. Chemicals are subject to a variety of loss processes during the assay, which have been discussed in numerous publications. Binding to medium components,[6] binding to the plate material,[7] volatilization,[8] and abiotic[9] and biotic[10] degradation processes can only be reliably excluded for the large spectrum of chemicals by measuring the chemical concentration. Although methods exist for the experimental measurement of chemical concentration in 96- and 384-well plates,[11,12] these methods are very time-consuming and labor-intensive and therefore are not compatible with high-throughput screening of hundreds of chemicals. Mass-balance models can confidently predict loss processes due to partitioning/binding to plates, medium, and loss to air.[13,14]

An indirect way to estimate if there might be problems associated with loss of chemicals is to compare the measured *in vitro* cytotoxicity data with predicted baseline toxicity,[8] *i.e.*, the minimum toxicity of every chemical.[15] Baseline toxicity is caused by the incorporation of the chemical into the cell membrane and its resulting destabilization. It occurs at critical membrane burdens (CMBs) that are constant and independent of the chemical properties. Linear low concentration−response curves have been established for cell-based reporter gene bioassays to avoid artifacts caused by the so-called cytotoxicity burst.[16] Furthermore, problems with solubility can be avoided by focusing on the low concentration range. Therefore, CMBs for reporter gene cell lines are determined at the 10% inhibitory concentration of cell viability (IC_{10}). Escher et al.[8] estimated a CMB ($IC_{10,membrane}$) of 69 mmol/L_{lip} for cell-based bioassays, which appeared to be not only independent of the chemicals but also of the cell types.

Lee et al.[17] developed an empirical QSAR model for the prediction of baseline toxicity in reporter gene cell lines, which only requires the liposome−water distribution ratio ($D_{lip/w}$) of the chemical as an input parameter. The toxic ratio (TR) can be calculated to compare the measured toxicity with baseline toxicity. If chemicals show higher toxicity than baseline toxicity (TR > 10), this is indicating a specific cytotoxicity mechanism.[18] If chemicals show lower toxicity than baseline toxicity (TR < 0.1), this may be an artifact caused by a loss of the chemical in the course of the bioassay. However, the existing empirical QSAR model is limited to chemicals with log $D_{lip/w}$ > 0 and has not been validated for the prediction of the toxicity of anions.[17] Recently, Qin et al. developed a baseline toxicity QSAR for neutral and anionic per- and polyfluorinated substances (PFAS) based on the same critical membrane concentration.[19]

The $IC_{10,membrane}$ of 69 mmol/L_{lip} used in these mass-balance models was derived from nominal effect concentrations ($IC_{10,nom}$). An improved estimation of $IC_{10,membrane}$ is possible using measured freely dissolved effect concentrations ($IC_{10,free}$), as these account for distribution processes of the chemicals between water and medium components. $IC_{10,membrane}$ can be directly derived from $IC_{10,free}$ using the $D_{lip/w}$ values of the test chemicals.

$$IC_{10,membrane} = IC_{10,free} \times D_{lip/w} \quad (1)$$

$IC_{10,free}$ equals $IC_{10,nom}$ for hydrophilic chemicals that do not show significant binding to medium components.[11] This premise allows for the improvement of baseline toxicity predictions by redefining $IC_{10,membrane}$ based on $IC_{10,free}$ of hydrophilic chemicals. In the present study, a subset of nonvolatile, hydrophilic chemicals with measured $D_{lip/w}$ and without specific effects was selected and their cytotoxicity was measured in the AREc32, ARE-*bla*, and GR-*bla* assay to develop this refined baseline toxicity model. Additionally, ionizable chemicals with measured $IC_{10,free}$ values were included to generate a QSAR model that is also applicable to anionic chemicals.

Reporter gene cells are often derived from cancer cell lines and assumed to have very limited metabolic activity.[20−23] However, it has been shown that the formation of cytochrome P450 (CYP) enzymes can be induced by xenobiotic chemicals.[10,24,25] Metabolization can lead to the loss of the parent chemical. For example, the metabolic transformation of benzo[*a*]pyrene led to a decrease in cellular concentration over time as shown by Fischer et al.[10,26] meaning that cellular metabolism may lead to false effect concentrations. However, the formation of reactive metabolites with a higher toxicity is also possible. The comparison of effect data from cell lines with different metabolic activity can therefore provide an indication of the relevance of metabolization of the test chemicals in *in vitro* bioassays.

In this study, three representative reporter gene cell lines were selected based on three frequently used cell lines with different origins. AREc32 is based on the MCF-7 breast cancer cell line, ARE-*bla* is based on a HepG2 liver cell line and GR-*bla* is based on a HEK293T embryonic kidney cell line. Over half of the bioassays of the Tox21 test battery[27] are based on HEK293T (42%) and HepG2 (14%) cells.[10] Two of the cell lines (AREc32 and ARE-*bla*) carry a reporter gene for the activation of the oxidative stress response[28,29] and one cell line (GR-*bla*) carries a reporter gene for the glucocorticoid receptor,[30] representing two important toxicological end points. The three selected cell lines showed different activity and inducibility of CYP1 in a previous study.[10]

Cellular CYP activities without and with chemical induction were investigated with fluorescence-based assays. 7-Ethoxyresorufin-*O*-deethylase (EROD) assay was used to measure CYP1A1/2 activity,[31] 7-ethoxy-4-trifluoromethylcoumarin-*O*-deethylase (EFCOD) assay was used to measure CYP2B6 activity,[32] and 7-benzyloxy-4-trifluoromethylcoumarin-*O*-debenzyloxylase (BFCOD) assay was used to measure CYP3A4/5 activity.[33]

The objectives of this study were: (1) to develop a novel baseline toxicity model for *in vitro* bioassays that is applicable to hydrophilic and charged chemicals; (2) to determine the metabolic activity of three reporter gene cell lines with different cellular origins; (3) to measure the effects of 94 chemicals with diverse physicochemical properties in high-throughput screening in the three cell lines; and (4) to compare the cytotoxicity measured in the three cell lines with each other and with baseline toxicity predictions. Thus, it may be possible to correlate the *in vitro* effects with the metabolic activity of the cell lines if the resulting metabolites lead to higher or lower effects. This combined approach can increase confidence in *in vitro* data, as valuable information on chemical exposure can be obtained by careful analysis of in *vitro* effect concentrations. Possible loss processes that would otherwise have remained unobserved can be uncovered, thus, preventing misinterpretation of *in vitro* data.

https://doi.org/10.1021/acs.chemrestox.4c00017
Chem. Res. Toxicol. XXXX, XXX, XXX−XXX

Table 1. Chemicals of This Study

chemical	ID	chemical	ID
1,2-dimethyl-1*H*-imidazole	12DMIZ	genistein	GEN
1-ethyl-1*H*-imidazole	1E1HIZ	haloperidol	HPD
1*H*-imidazole-1-propanamine	1HIZ1P	HC yellow 13	HCY
1-methylimidazole	1MIZ	hexachlorophene	HCP
1-vinylimidazole	1VIZ	hydroxyurea	HU
2-ethyl-4-methyl-1*H*-imidazole	2E4MIZ	imazalil	IMZ
2-ethylimidazole	2EIZ	imidacloprid	IMI
2-methylimidazole	2MIZ	imidazole	IZ
4-methylimidazole	4MIZ	lidocaine	LIDO
5,5-diphenylhydantoin	55DH	mebendazole	MBZ
5-fluorouracil	5FU	methacrylamide	MAA
acetaminophen	APAP	methimazole	MMI
acrylamide	AA	methotrexate	MTX
all-trans retinoic acid	ATRA	*N*-(butoxymethyl)acrylamide	NBuAA
arsenic(III) oxide	As_2O_3	*N*-(isobutoxymethyl)acrylamide	NIAA
aspartame	ASP	*N*,*N*′-bis(2-hydroxyethyl)-2-nitro-p-phenylenediamine	NBNP
atorvastatin	ATO	*N*,*N*-diethylacrylamide	NDAA
atrazine	ATZ	*N*,*N*-dimethylacetamide	DMA
azacytidine	AZA	*N*,*N*-dimethylformamide	DMF
azoxystrobin	AZ	*N*,*N*′-methylenebisacrylamide	NMBAA
bisphenol A	BPA	nicotine	NIC
bromodeoxyuridine	BDU	niflumic acid	NIFA
butoxyethanol	BE	*N*-methylaniline	NMA
cadmium chloride	$CdCl_2$	*N*-methylolacrylamide	NMAA
caffeine	CAF	*o*-aminophenol	oAP
camptothecin	CPT	PCB28	PCB28
carbamazepine	CBZ	perfluorooctanoic acid	PFOA
carbendazim	CBD	picoxystrobin	PXS
chlorpromazine	CPZ	pirinixic acid	WY-14643
chlorpyrifos	CP	pregnenolone	PREG
chlorpyrifos-oxon	CPO	propofol	PPF
citalopram	CT	propylthiouracil	PTU
clofibric acid	CFA	rotenone	RTN
colchicine	CC	sodium arsenite	$NaAsO_2$
cyclophosphamide	CPA	tamoxifen	TAM
cyclosporin A	CSA	tebuconazole	TCZ
cyproconazole	CPCZ	tetracycline	TET
cytosinearabinoside	CARA	tetraethylthiuram disulfide	TETD
dexamethasone	DEXA	thiamethoxam	TMX
diclofenac	DCL	tigecycline	TG
dimethyl sulfoxide	DMSO	toluene-2,5-diamine	T25D
diphenylamine	DPA	triadimenol	TDM
ethoprophos	EPP	tributyltin	TBT
ethylenethiourea	ETU	trichlorfon	TCF
fingolimod	FGM	triethyl-tin bromide	TEtT
fipronil	FIP	valproic acid	VPA
fluoxetine	FLX	verapamil	VRP

MATERIAL AND METHODS

Chemicals. A total of 94 chemicals (Table 1) were tested in three bioassays. Volatile or very hydrophobic chemicals were not included. More information on the test chemicals can be found in the Supporting Information in Table S1. The method for pK_a measurement is described in the literature[12,34] and the method for $\log K_{ow}$ measurement can be found in the Supporting Information (Text S1). Chemicals were either dosed as stock solutions in dimethyl sulfoxide (DMSO), methanol, or water or directly dissolved in bioassay medium depending on the dosing concentration and chemical solubility. Information on the additional hydrophilic chemicals ($\log K_{lip/w}$ between −1.04 and 0.81) for the development of a baseline QSAR model can be found in Table S2. Chemicals for CYP activity assays were purchased from Sigma-Aldrich (omeprazole, benzo[*a*]pyrene, resorufin, 7-ethoxyresorufin, 7-hydroxy-4-trifluoromethylcoumarin) with a purity ≥95% and from Chemodex (7-ethoxy-4-trifluoromethylcoumarin, 7-benzyloxy-4-trifluoromethyl-coumarin) with a purity ≥98%. Rat liver S9 was purchased from Molecular Toxicology and nicotinamide adenine dinucleotide phosphate tetrasodium salt (NADPH, purity ≥95%) was obtained from Roth.

Materials. All components of the bioassay media as well as CellSensor ARE-*bla* and GeneBLAzer GR-UAS-*bla* cells were purchased from Thermo Fisher Scientific. AREc32 cells were purchased from Cancer Research UK. Poly-D-lysine-treated black 384-well plates with a clear bottom (Product No. 356663) for ARE-*bla* and GR-*bla* assay and white 384-well plates with a clear bottom (Product No. 3765)

https://doi.org/10.1021/acs.chemrestox.4c00017
Chem. Res. Toxicol. XXXX, XXX, XXX−XXX

for AREc32 were purchased from Corning. Water was obtained from a Milli-Q water purification system from Merck.

***In Vitro* Bioassays.** All chemicals were tested in the ARE-*bla* and AREc32 assay for the detection of the oxidative stress response activation *via* the Nuclear Factor Erythroid 2 related Factor 2/Kelch-like ECH-associated protein 1 (Nrf-2/Keap-1) pathway. GR-*bla* cells carry a reporter gene for the glucocorticoid receptor (GR). The procedure of the *in vitro* bioassays has been described in detail in the literature.[35−37] ARE-*bla* bioassay medium (90% DMEM phenol red-free, 10% dialyzed fetal bovine serum (d-FBS), 0.1 mM nonessential amino acids, 25 mM HEPES, 1 mM sodium pyruvate, 4.97 mM GlutaMAX, 100 U/mL penicillin-streptomycin), GR-*bla* bioassay medium (98% Opti-MEM, 2% charcoal-stripped FBS (cs-FBS), 100 U/mL penicillin-streptomycin), and AREc32 bioassay medium (90% DMEM with GlutaMAX, 10% FBS, 100 U/mL penicillin-streptomycin) were prepared. A MultiFlo dispenser (Biotek, Vermont) was used to dispense 30 μL of a cell suspension per well. Final cell counts were 4100 cells/well (ARE-*bla*), 6000 cells/well (GR-*bla*), and 2650 cells/well (AREc32). Plates were incubated for 24 h at 37 °C and 5% CO_2, and cell confluency was measured before and 24 h after chemical dosing using an IncuCyte S3 Live-Cell Analysis System (Essen BioScience, Sartorius) in HD phase contrast mode with 10× magnification at room temperature. Cell confluency was determined from customized confluency masks created with the basic analyzer software (Incucyte 2023A). The chemicals were either directly dissolved in bioassay medium or dosed as DMSO, methanol or water stock solutions. The final DMSO content in the wells was kept below 0.5%, the methanol content was kept below 1%. For acids and bases which are charged at pH 7.4, an equimolar aliquot of sodium hydroxide or hydrochloric acid was added to the dosing vials. Dosing plates containing the chemicals in serial dilution were prepared using a Hamilton Microlab Star robotic system (Hamilton, Bonaduz, Switzerland). *tert*-Butylhydroquinone (final concentration in cell plate 1.73×10^{-5} M − 1.35×10^{-8} M) was used as positive control for ARE-*bla* and AREc32 and dexamethasone (final concentration in cell plate 5.05×10^{-8} M − 1.53×10^{-12} M) was used as positive control for GR-*bla*. The diluted chemicals were dispensed in duplicate by transferring 10 μL from the dosing plates to the cell plate twice. Chemicals with high air−water partitioning constants (K_{aw}) (NMA, NIC, IMZ and PCB28) were tested on a separate plate, which was sealed with a gas-permeable plate cover (Product No. 4ti-0516/384, Azenta Life Sciences), with one row of bioassay medium between the rows containing the chemicals. The cell plates were incubated at 37 °C and 5% CO_2 for 24 h after dosing. Cytotoxicity was determined by comparing the confluency of the dosed wells with control wells without chemical addition. Reporter gene activation was quantified as described in the literature.[35−37] Briefly, for AREc32 the medium was removed, and the cells were washed 3 times with phosphate-buffered saline (PBS, 137 mM NaCl, 2.7 mM KCl, 8.1 mM disodium phosphate dihydrate, 1.8 mM potassium dihydrogen phosphate). 10 μL of lysis buffer (50 mM Tris, 2% Triton-X 100, 4 mM ethylenediaminetetraacetic acid (EDTA), 4 mM DL-dithiothreitol (DTT), 20% glycerol) were added to each well and incubated at room temperature and 1500 rpm (BioShake iQ, QInstruments) for 20 min. 40 μL of D-luciferin buffer (pH 7.7−7.8, 20 mM tricine, 2.67 mM magnesium sulfate pentahydrate, 33.3 mM DTT, 0.1 mM EDTA, 0.261 mM coenzyme A, 0.53 mM adenosine 5′-triphosphate, 0.235 mM D-luciferin added immediately before use) were added to all wells. The plates were shaken for 30 s and 1000 rpm (BioShake iQ, QInstruments), and luminescence was detected with a multimode plate reader (Tecan Reader Infinite 1000 Pro). For ARE-*bla* and GR-*bla*, ToxBLAzer working solution (Product No. K1138, Thermo Fischer) was prepared according to the manufacturer's protocol. 8 μL of working solution were added per well and fluorescence was measured (Ex/Em: 409/460; 409/530 and 590/665 nm). Plates were incubated for 2 h at room temperature in the dark, and fluorescence was measured again. ToxBLAzer reagent contains also a cytotoxicity indicator that detects cell membrane integrity and esterase activity as a measure of cytotoxicity next to reporter gene activation. All chemicals were tested in all assays in three independent replicates.

Baseline Toxicity. The target site of baseline toxicants is the membrane; therefore, baseline toxicity can be predicted if the CMB is known. Since baseline toxicity is unspecific, the CMB should be similar for all chemicals and cell lines.[8,38] Partitioning processes of the chemicals to proteins or lipids of the bioassay medium can reduce the freely dissolved effect concentration for cytotoxicity ($IC_{10,free}$) of the chemicals and must be considered for the determination of the CMB. Ideally, measured $IC_{10,free}$ values should be used to calculate the CMB, as these represent the actual available concentration that can partition into the cell membrane. The CMB can also be determined from neutral, hydrophilic chemicals, as these do not bind to medium components or only to a negligible extent, and therefore the nominal effect concentration $IC_{10,nom}$ equals $IC_{10,free}$ and internal and external freely dissolved concentrations can be assumed to be equal.

Fourteen chemicals with measured log $K_{lip/w}$ values between −1.04 and 0.81 were selected to calculate the $IC_{10,membrane}$ (Table S2). All chemicals were tested once in serial and twice in linear dilution in the AREc32, ARE-*bla* and GR-*bla* assay. The assays were performed as described above, but only cytotoxicity was measured *via* confluency measurement, not reporter gene activation or ToxBLAzer cytotoxicity. Additionally, 15 chemicals with experimental log $D_{lip/w}$ (0.08−4.73), previously measured $IC_{10,free}$ and without known specific cytotoxicity were included for the calculation of $IC_{10,membrane}$.[39]

For more hydrophobic chemicals, the nominal concentration of the test chemicals causing baseline toxicity ($IC_{10,nom,baseline}$) can be calculated from the $IC_{10,membrane}$ using a mass-balance model to estimate chemical partitioning to medium components.[13] Partitioning to cells is negligible in protein-rich bioassay media as they only constitute a very small percentage of the total protein and lipid volume of the bioassay.[19]

$$IC_{10,nom,baseline} = \frac{IC_{10,membrane}}{D_{lip/w}} \times (1 + D_{BSA/w} \times VF_{protein,medium} + D_{lip/w} \times VF_{lipid,medium}) \quad (2)$$

As there is a linear relationship between the distribution ratios of the test chemicals to bovine serum albumin ($D_{BSA/w}$) and the distribution ratios to liposomes ($D_{lip/w}$), the only input parameters for the mass-balance model are the volume fractions (VF) of protein and lipid of the media used which were obtained from the literature[19] (Table S3) and the $D_{lip/w}$ of the test chemicals. Experimental $D_{lip/w}$ were obtained from the literature or predicted using Linear Solvation Energy Relationship (LSER) or QSAR models and are summarized in Table S1.[40,41]

A linear QSAR for the calculation of log $D_{BSA/w}$ from log $D_{lip/w}$ has been developed for neutral chemicals (eq 3).[42]

$$\log D_{BSA/w}\ (\text{neutral}) = 0.70 \times \log D_{lip/w} + 0.34 \quad (3)$$

Recently, a similar QSAR has been developed for anionic perfluoroalkyl and polyfluoroalkyl substances (PFAS). However, it will be evaluated if this QSAR is also applicable to other organic anions tested in the present study (eq 4).[19]

$$\log D_{BSA/w}\ (\text{anionic}) = 0.75 \times \log D_{lip/w} + 1.01 \quad (4)$$

By insertion of eqs 3 or 4 in eq 2, a nominal baseline toxicity QSAR can be derived for neutral chemicals (eq 5) and anionic chemicals (eq 6) which requires only $D_{lip/w}$ as input parameter.

$$IC_{10,nom,baseline}\ (\text{neutral}) = \frac{IC_{10,membrane}}{D_{lip/w}} \times (1 + 10^{0.70 \times \log D_{lip/w} + 0.34} \times VF_{protein,medium} + D_{lip/w} \times VF_{lipid,medium}) \quad (5)$$

https://doi.org/10.1021/acs.chemrestox.4c00017
Chem. Res. Toxicol. XXXX, XXX, XXX−XXX

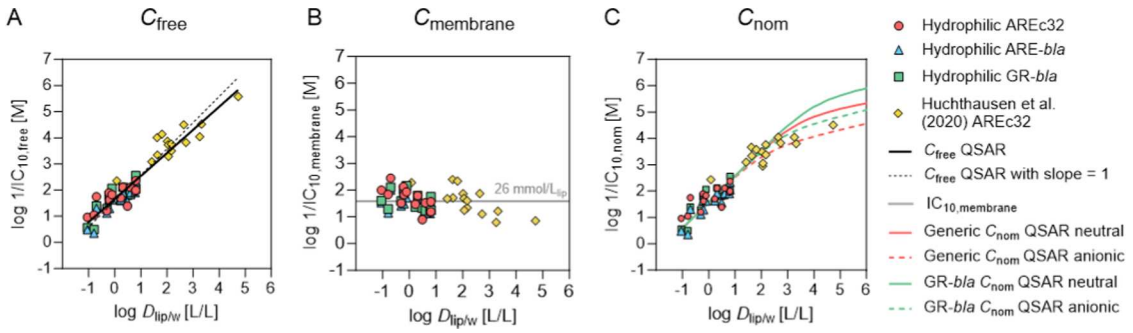

Figure 1. Experimental derivation of nominal baseline toxicity QSARs for neutral and anionic chemicals for AREc32, ARE-*bla*, and GR-*bla* cell lines. (A) Logarithmic reciprocal $IC_{10,free}$ (log $1/IC_{10,free}$) of test chemicals were plotted against logarithmic liposome−water distribution ratios (log $D_{lip/w}$). The black solid line is the linear regression of the data points, and the dotted black line is the linear regression with a slope fixed to 1, which was used to derive the critical membrane concentration for baseline toxicity ($IC_{10,membrane}$). (B) Logarithmic reciprocal $IC_{10,membrane}$ (log $1/IC_{10,membrane}$) of test chemicals were plotted against log $D_{lip/w}$. The solid gray line indicates the constant CMB of 26 mmol/L_{lip} derived from the linear regression from A. (C) Logarithmic reciprocal $IC_{10,nom}$ (log $1/IC_{10}$) of test chemicals plotted against log $D_{lip/w}$ derived with the mass-balance models for neutral and anionic chemicals. The red solid line indicates the generic QSAR for AREc32 and ARE-bla for neutral chemicals, and the red dotted line indicates the generic anionic QSAR. The green solid line indicates the QSAR for GR-*bla* for neutral chemicals, and the green dotted line indicates the anionic QSAR for GR-*bla*.

$$IC_{10,nom,baseline}\ (anionic) = \frac{IC_{10,membrane}}{D_{lip/w}} \times (1 + 10^{0.75\times \log D_{lip/w}+1.01} \times VF_{protein,medium} + D_{lip/w} \times VF_{lipid,medium}) \quad (6)$$

The toxic ratio (TR) was calculated to compare the measured cytotoxicity (IC_{10}) with the baseline toxicity ($IC_{10,baseline}$). A TR between 0.1 and 10 means that the chemical is a baseline toxicant, and a TR higher than 10 indicates a specific mode of action.

$$TR = \frac{IC_{10,baseline}}{IC_{10,experimental}} \quad (7)$$

Metabolic Characterization. To determine cytochrome P450 (CYP) enzyme activity and inducibility of CYP activity, the fluorescence-based EROD, EFCOD and BFCOD assays were used. The substrates are metabolized by different CYP enzymes (CYP1A1/2, CYP2B6 and CYP3A4/5) and form fluorescent metabolites. The fluorescence of the respective metabolites can be detected, and thus the CYP activity can be quantified.

For all three assays, 90 μL of cell suspension were dispensed in black 96-well plates (Corning, AREc32 Product No. 3603, ARE-*bla* and GR-*bla* Product No. 354640) with 11000 cells/well (AREc32 and ARE-*bla*) or 20000 cells/per well (GR-*bla*). The plates were incubated at 37 °C and 5% CO_2. After 24 h, 30 μL of a dilution of the CYP inducers omeprazole or benzo[*a*]pyrene in bioassay medium was dosed to the cells. The concentration in the plate was below cytotoxicity (IC_{10}) for all three cell lines (Text S2 and Figures S1−S3). The final chemical concentrations can be found in Table S4. Wells with only the medium were included to determine basal CYP activity. After chemical dosing, the plates were incubated at 37 °C and 5% CO_2 for 24 h. The confluency of the cells was measured before and after incubation using an IncuCyte S3 Live-Cell Analysis System (Essen BioScience, Sartorius) to monitor the cell viability and calculate the cell growth. For the detection of CYP activity, the medium was removed from all wells and the cells were washed with 120 μL of PBS twice. 7-Ethoxyresorufin (ETX), 7-ethoxy-4-trifluoromethylcoumarin (EFC) and 7-benzyloxy-4-trifluoromethylcoumarin (BFC) working solutions in PBS were prepared. The concentrations of ETX, EFC and BFC were optimized (Text S2 and Figure S4) and were 2 μM (ETX) and 5 μM (EFC and BFC). Calibration standards of resorufin and 7-hydroxy-4-trifluoromethylcoumarin (HFC) were prepared by serial dilution in PBS. The concentration range of the calibration standards was 3.13×10^{-7} M − 2.45×10^{-10} M (resorufin) and 1.00×10^{-6} M − 7.81×10^{-11} M (HFC). 120 μL of either EROD, EFCOD and BFCOD working solution were added to all wells containing cells and to all control wells without cells. 120 μL of each calibration standard were added to empty wells. The fluorescence intensity of resorufin (Ex/Em: 560:584 nm) or HFC (Ex/Em: 405:520 nm) was measured in a preheated microplate reader (plate reader Infinite M1000 PRO, Tecan) at 37 °C for 10 min with measurement intervals of 30 s. The formed resorufin or HFC amount ($n_{resorufin}$ or n_{HFC}) was calculated after background subtraction from the control wells without cells with the respective calibration curve. From the slope (k) of a linear regression of $n_{resorufin}$ or n_{HFC} against time (t) with an intercept of $n_{resorufin}$ or n_{HFC} at the beginning of measurement ($n_{resorufin}$ or $n_{HFC})_{t0}$ (eq 8), the CYP activity was determined as the amount of resorufin or HFC formed per minute ($n_{resorufin}$ or n_{HFC} mol $min^{-1})_t$.

$$(n_{resorufin\ or\ HFC})_t\ [mol] = k \times t + (n_{resorufin\ or\ HFC})_{t0} \quad (8)$$

This was normalized to the mass of protein in the wells ($mg_{protein}$) which was calculated from the cell number after 48 h and the protein content of the cells which were 0.70 $mg_{protein}$ per 10^6 cells for AREc32,[6] 0.21 $mg_{protein}$ per 10^6 cells for ARE-*bla*, and 0.45 $mg_{protein}$ per 10^6 cells for GR-*bla*.[10]

As positive control, EROD, EFCOD and BFCOD assay were performed with rat liver S9 (Moltox, protein content 39.3 mg/mL). Rat liver S9 was diluted with PBS to a final protein concentration of 0.1 mg/mL. NADPH was added at a final concentration of 80 μM. 60 μL of the mix was added to the wells of a black 96-well plate (Corning, Product No. 3603). EROD, EFCOD and BFCOD working solutions and resorufin and HFC calibration standards were prepared as described above. 60 μL of either EROD, EFCOD and BFCOD working solution was added to all wells containing S9 and to all control wells, and 120 μL of the respective calibration standards was added to empty wells. CYP activity was measured as described above.

Data Evaluation. Bioassay raw data was processed using an automatic KNIME (version 4.6.1) workflow, and GraphPad Prism (version 10.1.0) was used for data visualization. Cytotoxicity and reporter gene activation were plotted against the chemical concentration to derive concentration−response curves for all chemicals.

The concentration at which cell viability was reduced by 10% (IC_{10}) was calculated from the slope of the regression of the linear range of the concentration−response curves using eq 9.[43]

$$IC_{10} = \frac{10\%}{slope} \quad (9)$$

The induction ratio (IR) was calculated for the evaluation of the activation of the oxidative stress response, and the $EC_{IR1.5}$ (eq 10) was derived from the slope of the linear part of concentration−response

https://doi.org/10.1021/acs.chemrestox.4c00017
Chem. Res. Toxicol. XXXX, XXX, XXX−XXX

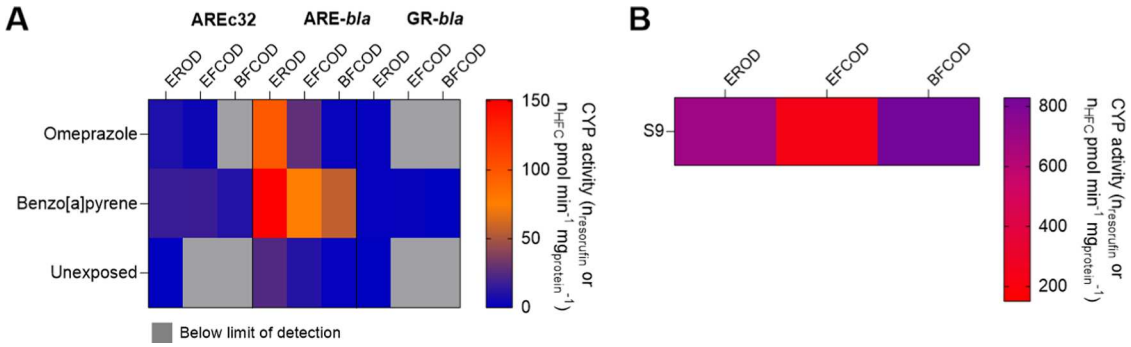

Figure 2. Results of EROD, EFCOD and BFCOD assay for AREc32, ARE-*bla*, and GR-*bla* cells without chemical exposure and after exposure to omeprazole or benzo[*a*]pyrene (A) and for rat liver S9 as a positive control (B). CYP activity was measured as the amount of resorufin ($n_{resorufin}$, EROD) or the amount of 7-hydroxy-4-trifluoromethylcoumarin (n_{HFC}, EFCOD and BFCOD) formed per minute and per $mg_{protein}$.

curve. Only concentrations below 10% cytotoxicity were used for the calculation.[37]

$$EC_{IR1.5} = \frac{0.5}{slope} \quad (10)$$

For activation of GR, the concentration at which 10% of the maximum effect was reached (EC_{10}) was calculated from the slope of the linear part of the concentration−response curve. Only concentrations below 10% of cytotoxicity were used for the calculation. The maximum effect was calculated from the concentration−response curve of the reference chemical dexamethasone.

$$EC_{10} = \frac{10\%}{slope} \quad (11)$$

The specificity ratio (SR) was used to compare the reporter gene activation with cytotoxicity ($SR_{cytotoxicity}$) or baseline toxicity ($SR_{baseline}$).[16] An SR > 10 means that the reporter gene activation is specific and not linked to cytotoxicity.

$$\text{specificity ratio } (SR_{cytotoxicity} \text{ or } SR_{baseline}) = \frac{IC_{10,experimental} \text{ or } IC_{10,baseline}}{EC_{IR1.5} \text{ or } EC_{10}} \quad (12)$$

RESULTS AND DISCUSSION

Baseline Toxicity. Concentration−response curves (CRCs) of 14 hydrophilic chemicals in all three assays are shown in Figures S5 and S7, and IC_{10} values are listed in Table S5. Measured $IC_{10,free}$ of 15 additional chemicals from Huchthausen et al.[39] are shown in Table S6.

Logarithmic reciprocal $IC_{10,free}$ of all chemicals were plotted against logarithmic $D_{lip/w}$ and linear regression of all data points had a slope of 0.8837 ± 0.0403 and an intercept of 1.658 ± 0.0550 (Figure 1A). As the CMB is independent of hydrophobicity, the ideal slope of the regression is 1. The measured slope is close to the ideal slope, and the deviation is probably caused by variation of the cytotoxicity or concentration measurements. However, it was in line with QSARS for other species,[44,45] so the slope of the regression was set to 1 resulting in an intercept of 1.585 ± 0.0519 which converts to a constant $IC_{10,membrane}$ of 26 ± 3.3 mmol/L_{lip} (Figure 1B). This CMB is 2.6 times lower than the previously reported CMB of 69 mmol/L_{lip}. The earlier $IC_{10,membrane}$ was only modeled from $IC_{10,nom}$ of a set of chemicals with a limited hydrophobicity range. Therefore, the new $IC_{10,membrane}$ of 26 mmol/L_{lip} can be considered more reliable and robust, but should be validated with measured C_{free} for more hydrophobic chemicals in future studies.

The newly derived $IC_{10,membrane}$ as well as the respective protein and lipid contents of the media (Table S3) were inserted in eqs 5 and 6 resulting in the new nominal baseline QSAR equations for neutral (eqs 13 and 15) and anionic chemicals (eqs 14 and 16).

$$IC_{10,nom,baseline}\ (\text{neutral; 10\% FBS}) = \frac{0.026\ \text{mol/L}_{lip}}{D_{lip/w}} \times (1 + 10^{0.70 \times \log D_{lip/w} + 0.34} \times 3.00 \times 10^{-3}\text{L/L} + D_{lip/w} \times 7.00 \times 10^{-5}\text{L/}L) \quad (13)$$

$$IC_{10,nom,baseline}\ (\text{anionic; 10\% FBS}) = \frac{0.026\ \text{mol/L}_{lip}}{D_{lip/w}} \times (1 + 10^{0.75 \times \log D_{lip/w} + 1.01} \times 3.00 \times 10^{-3}\text{L/L} + D_{lip/w} \times 7.00 \times 10^{-5}\text{L/L}) \quad (14)$$

$$IC_{10,nom,baseline}\ (\text{neutral; 2\% cs} - \text{FBS}) = \frac{0.026\ \text{mol/L}_{lip}}{D_{lip/w}} \times (1 + 10^{0.70 \times \log D_{lip/w} + 0.34} \times 9.40 \times 10^{-4}\text{L/L} + D_{lip/w} \times 1.47 \times 10^{-5}\text{L/L}) \quad (15)$$

$$IC_{10,nom,baseline}\ (\text{anionic; 2\% cs} - \text{FBS}) = \frac{0.026\ \text{mol/L}_{lip}}{D_{lip/w}} \times (1 + 10^{0.75 \times \log D_{lip/w} + 1.01} \times 9.40 \times 10^{-4}\text{L/L} + D_{lip/w} \times 1.47 \times 10^{-5}\text{L/L}) \quad (16)$$

Logarithmic reciprocal nominal IC_{10} values of the test chemicals were plotted against $D_{lip/w}$ (Figure 1C). AREc32 and ARE-*bla* assay media had a similar protein and lipid content as both were supplemented with 10% FBS or d-FBS (Table S3), so a generic QSAR was developed for both assays for neutral (eq 13) and anionic (eq 14) chemicals (Figure 1C, red lines). GR-*bla* medium had a lower protein and lipid content as it was supplemented with 2% cs-FBS (Table S3), so a separate GR-*bla* QSAR was developed for neutral (eq 15) and anionic (eq 16) chemicals (Figure 1C, green lines).

Metabolic Characterization. Reporter gene cell lines are often cited to have a lack of metabolic capacity.[20,22,23] However, it has also been reported that the activity of CYP enzymes in cell lines can be activated by chemicals.[10,24,25] Different metabolic

https://doi.org/10.1021/acs.chemrestox.4c00017
Chem. Res. Toxicol. XXXX, XXX, XXX−XXX

activity makes it difficult to compare *in vitro* data from different cell lines because metabolization of the test chemicals affects *in vitro* effect data. Fischer et al. have shown that the medium and cellular concentration of benzo[*a*]pyrene decreased and the concentration of formed metabolites increased significantly in the course of an *in vitro* bioassay with AREc32 and ARE-*bla* cells.[10] Therefore, in this study, CYP enzyme activity of all three cell lines was measured using three different assays (EROD, EFCOD, and BFCOD assays). Basal CYP activities were low for all cell lines and were below the detection limit for EFCOD and BFCOD assay in case of AREc32 and GR-*bla*. ARE-*bla* had the highest basal EROD activity with 24.36 pmol resorufin formed per minute per $mg_{protein}$ (Figure 2A). CYP activities were also measured after incubation with the CYP inducers benzo[*a*]-pyrene (B[*a*]P)[10] and omeprazole.[24] B[*a*]P induces CYP1 gene expression *via* binding to the aryl hydrocarbon receptor (AhR)[25,46] while omeprazole does not bind directly to the AhR but induces CYP1 gene expression *via* modulation of a protein tyrosine kinase-mediated pathway.[47] GR-*bla* showed no increased CYP activity after incubation with omeprazole and only a minor increase after incubation with B[*a*]P (Figure 2A). CYP activities were slightly increased in AREc32 by both inducers, with the highest CYP activity being 16.59 pmol of resorufin formed per minute per $mg_{protein}$ in the EROD assay after incubation with B[*a*]P. ARE-*bla* showed a stronger induction of the CYP activity by both inducers. The highest CYP activity was measured in the EROD assay after incubation with B[*a*]P with 151.00 pmol of resorufin formed per minute per $mg_{protein}$.

As a comparison with a commonly used metabolization system with increased CYP activity, EROD, EFCOD, and BFCOD assays were also performed with rat liver S9 (Figure 2B). EFCOD activity was lowest (230.56 pmol HFC min^{-1} $mg_{protein}{}^{-1}$) and BFCOD activity was highest (827.29 pmol HFC min^{-1} $mg_{protein}{}^{-1}$) for rat liver S9 (0.1 mg/mL). EROD activity was 695.17 pmol of resorufin min^{-1} $mg_{protein}{}^{-1}$ which is 4.6 times higher than the highest EROD activity of the cell lines. However, it should be noted that S9 from chemically induced rats has a higher metabolic activity than liver fractions from humans and therefore does not simulate the metabolism in humans.[48]

***In Vitro* Effect Concentrations.** All *in vitro* effect concentrations can be found in the Supporting Information (Table S7). Corresponding concentration response curves are shown in Table S8. For five chemicals (ATZ, PCB28, 55DH, IMI, ASP) no cytotoxicity could be determined *via* confluency measurement in all three assays. Nine additional chemicals (CPO, PREG, DEXA, PXS, TAM, HPD, TMX, AZ and 5FU) did not show any cytotoxicity in the AREc32 assay up to the highest tested concentrations, which are also listed in Table S7. No cytotoxicity could be measured *via* confluency for 11 additional chemicals (DMSO, $NaAsO_2$, CPO, PREG, DEXA, ETU, CBD, NBNP, TG, TMX, and TETD) in the ARE-*bla* assay and for two additional chemicals (TG and TETD) in the GR-*bla* assay. The chemical with the highest cytotoxicity in all three assays was colchicine (IC_{10} = 3.76 × 10^{-9} M in AREc32, 1.81 × 10^{-8} M in ARE-*bla*, and 2.48 × 10^{-9} M in GR-*bla*). The high toxicity of colchicine can be explained by its antimitotic properties caused by tubulin binding.[49]

For the ARE-*bla* and GR-*bla* assay, cytotoxicity was also measured with the ToxBLAzer reagent (Table S7). Linear fitting of the concentration−response curves was not possible for some chemicals for the ToxBLAzer responses (IZ, 4MIZ, 1MIZ, 1HIZ1P, PPF, 2EIZ, 1E1HIZ, 1VIZ, CARA, HU, and MTX in ARE-*bla* and IZ, 4MIZ, 2MIZ, 1MIZ, 1HIZ1P, 1E1HIZ, 1VIZ, and CARA in GR-*bla*). For these chemicals, cell viability did not decrease with increasing chemical concentration, but appeared to increase. However, the phenomenon only occurred for certain classes of chemicals (*e.g.*, imidazoles). A comparison of $IC_{10,ToxBLAzer}$ and $IC_{10,confluency}$ is shown in Figure S8. For some chemicals, cytotoxicity could only be detected with one of the methods (DMSO, $NaAsO_2$, CPO, NBNP, TG, 55DH, TETD, and ASP in ARE-*bla* and DEXA, 55DH, HU, and ASP in GR-*bla*). For chemicals for which IC_{10} could be measured with both detection methods, IC_{10} agreed well (Figure S8). $IC_{10,ToxBLAzer}$ values were lower than $IC_{10,confluency}$ values for some chemicals. In the GR-*bla* assay only trichlorfon had a significantly lower $IC_{10,ToxBLAzer}$ (factor of 716). In ARE-*bla* seven chemicals showed differences between both IC_{10} that were higher than a factor of 10. The highest difference was also observed for trichlorfon (factor of 170). Cytotoxicity assays using fluorescent dyes to detect a decrease in metabolic activity are widely used, but have been shown to be prone to artifacts in other studies.[16,50] However, these methods can be used to detect cell death involving cell swelling (necrosis),[51] which cannot be detected by confluency-based methods.

Comparison of Oxidative Stress Response Measured in Two Different Cell Lines. AREc32 and ARE-*bla* carry a reporter gene for the oxidative stress response. In AREc32, 31 chemicals activated the oxidative stress response at concentrations below IC_{10}. In ARE-*bla*, 17 chemicals activated oxidative stress response. Thirteen chemicals activated oxidative stress response in both assays. Figure 3 shows a comparison of the specificity ratios ($SR_{cytotoxicity}$ or $SR_{baseline}$) of oxidative stress response activation in both assays. The specificity ratio compares the oxidative stress response activation with cytotoxicity or baseline toxicity. $SR_{baseline}$ is shown only if no cytotoxicity could be measured. Five chemicals had specific effects ($SR_{cytotoxicity}$ > 10) in the AREc32 assay ($CdCl_2$, 1HIZ1P, GEN, HCY, and oAP) and seven chemicals in the ARE-*bla* assay (NMBAA, NBuAA, NIAA, NDAA, 1HIZ1P, T25D, and oAP). The chemicals with the highest $SR_{cytotoxicity}$ were oAP in AREc32 ($SR_{cytotoxicity}$ = 53.66) and 1HIZ1P in the ARE-*bla* assay ($SR_{cytotoxicity}$ = 83.51) which were also the only chemicals with $SR_{cytotoxicity}$ > 10 in both assays. TMX had $SR_{baseline}$ > 10 in both assays. The inorganic $CdCl_2$ activated the reporter gene in

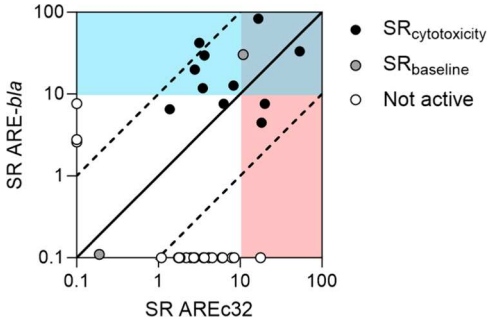

Figure 3. Specificity ratios (SR) of oxidative stress response activation in ARE-*bla* plotted against SR in AREc32. $SR_{cytotoxicity}$ is shown when the cytotoxicity could be determined in both assays (black circles). For chemicals without measured cytotoxicity in at least one assay, $SR_{baseline}$ was used (gray circles). Chemicals which showed oxidative stress response activation only in one assay are indicated with white circles. The solid black line indicates a perfect agreement of SR from both cell lines, and the dashed black lines indicate a deviation by a factor of 10.

https://doi.org/10.1021/acs.chemrestox.4c00017
Chem. Res. Toxicol. XXXX, XXX, XXX−XXX

AREc32 but was not active at concentrations below cytotoxicity in ARE-*bla*. However, baseline toxicity analysis was not possible for inorganic chemicals, and metabolism also cannot play a role for $CdCl_2$.

Seventeen chemicals that showed moderately specific effects ($1 < SR < 10$) in AREc32 did not activate oxidative stress response below cytotoxicity in ARE-*bla*. The high number of moderately specific chemicals in AREc32 compared with ARE-*bla* is surprising. While 41% of the chemicals that activated oxidative stress response in ARE-*bla* had SR > 10, it was only 16% in AREc32.

The limit of detection (LOD) and limit of quantification (LOQ) were calculated for both assays using eqs 17 and 18 where μ is the average IR and σ is the standard deviation of the unexposed cells.

$$LOD = \mu_n + 3 \times \sigma_n \quad (17)$$

$$LOQ = \mu_n + 10 \times \sigma_n \quad (18)$$

The LODs were 0.28 ± 0.08 and 0.24 ± 0.13 for AREc32 and ARE-*bla*, respectively, and LOQs were 0.93 ± 0.28 (AREc32) and 0.79 ± 0.42 (ARE-*bla*), respectively. Even though the LOD and LOQ of the two assays were very similar and the LOQ for ARE-*bla* was slightly lower than that of AREc32, ARE-*bla* showed a higher standard deviation. Figure S9 shows the $EC_{IR1.5}$ values of the reference substance *tert*-butylhydroquinone (tBHQ) for both assays. The average $EC_{IR1.5}$ was 2.33×10^{-6} M for AREc32 and a factor of 1.75 higher for ARE-*bla* (4.08×10^{-6} M). There was greater variation in the values of the individual plates for ARE-*bla*. It appears that ARE-*bla* has a sensitivity lower than that of AREc32 and therefore cannot detect chemicals that activate the oxidative stress response with only moderate specificity.

GR-*bla* detects glucocorticoid receptor (GR) activation. Only dexamethasone, which is also the reference chemical for the assay, activated GR with an EC_{10} of 3.58×10^{-10} M and an $SR_{cytotoxicity}$ of 10.21.

Comparison of Cytotoxicity Measured in Three Different Cell Lines. If the metabolic activity of the cell lines has an influence on the bioassay results, then differences in cytotoxicity between the cell lines should be apparent. It can be assumed that the highest toxicity is present in GR-*bla*, as there is no metabolic degradation of the test substances and therefore no detoxification. However, for some chemicals, there may also be bioactivation of the test substances, meaning a transformation into reactive metabolites with higher toxicity. As mentioned above, most chemicals without measured IC_{10} were present in ARE-*bla* (16 chemicals) and least chemicals without measured IC_{10} were present in GR-*bla* (7 chemicals) (Table S7).

Dexamethasone showed high cytotoxicity in GR-*bla*, but no cytotoxicity in AREc32 and ARE-*bla*, although the highest tested concentrations were 136,220 (AREc32) or 173,694 (ARE-*bla*) times higher than the IC_{10} values of dexamethasone in GR-*bla*. Dexamethasone is the reference chemical for the GR-*bla* assay and a known GR agonist.[52] This means that dexamethasone has a specific toxicity mechanism in GR-*bla* that is not present in the other two cell lines. Even if binding to the GR does not lead directly to cell death, a high dose of the receptor agonist restricts the normal function of the reporter gene cell, which ultimately leads to cell death.

Chlorpyrifos-oxon was not cytotoxic in AREc32 and ARE-*bla* and picoxystrobin was not cytotoxic in AREc32. There was a ratio of 140 between AREc32 (highest tested concentration) and GR-*bla* (IC_{10}) and a ratio of 279 for ARE-*bla* for chlorpyrifos-oxon. Similarly, the ratio AREc32 (highest tested concentration)/GR-*bla* (IC_{10}) was 131 for picoxystrobin. It should be noted that AREc32 and ARE-*bla* both use an assay medium with 10% fetal bovine serum (FBS) and GR-*bla* a medium with only 2% cs-FBS. Particularly in the case of hydrophobic chemicals or protein-reactive chemicals, this can lead to lower bioavailability of the test chemical due to reversible binding to medium proteins or covalent reaction with these proteins.[6,9] Chlorpyrifos-oxon showed no cytotoxicity in AREc32 and ARE-*bla* although the highest tested concentration was at least 86 times higher than the baseline toxicity. Reactivity toward the proteins of the bioassay medium could explain this observation as protein reactivity of chlorpyrifos-oxon was reported in the literature.[53]

Figure 4A shows that the toxicity of most of the chemicals was slightly lower in ARE-*bla* compared to that of the other two cell lines. An analysis of variance (ANOVA) was performed using Prism 10.1.0. to investigate the significance of the deviation of the log $1/IC_{10}$ values of the three assays. The log $1/IC_{10}$ values were normally distributed for all assays as shown in Figure S10. The one-way ANOVA showed no significant difference between the means of the three data sets with a *P*-value of 0.3647.

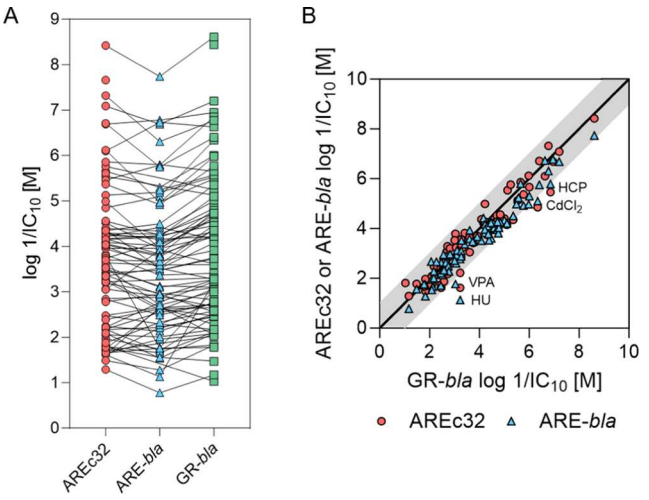

Figure 4. Comparison of cytotoxicity (log $1/IC_{10}$) of all cell lines. (A) All measured log $1/IC_{10}$ values from all assays.. (B) Log $1/IC_{10}$ measured in AREc32 or ARE-*bla* plotted against $1/IC_{10}$ measured in GR-*bla*. Red circles indicate results for AREc32, blue triangles indicate results for ARE-*bla*, and green squares indicate results for GR-*bla*. The black line in (B) indicates a perfect agreement of the results of the cell lines. The gray area indicates a deviation of a factor of 10. HCP = hexachlorophene, $CdCl_2$ = cadmium chloride, VPA = valproic acid, HU = hydroxyurea.

Figure 4B shows a comparison of the cytotoxicity measured in GR-*bla* that showed no metabolic activity in the EROD, EFCOD and BFCOD assays with the cytotoxicity measured in AREc32 and ARE-*bla*. For the majority of the tested chemicals, IC_{10} from AREc32 and ARE-*bla* agreed within a factor of 10 with the IC_{10} from GR-*bla*. However, the IC_{10} values of hydroxyurea, cadmium chloride and hexachlorophene (AREc32 and ARE-*bla*) and valproic acid (ARE-*bla*) showed more than 10 times deviation from the IC_{10} values of GR-*bla*.

Apparently the higher basal CYP activity of ARE-*bla* compared to GR-*bla* does not influence the cytotoxicity of most chemicals measured in this study, and the chemicals tested

https://doi.org/10.1021/acs.chemrestox.4c00017
Chem. Res. Toxicol. XXXX, XXX, XXX−XXX

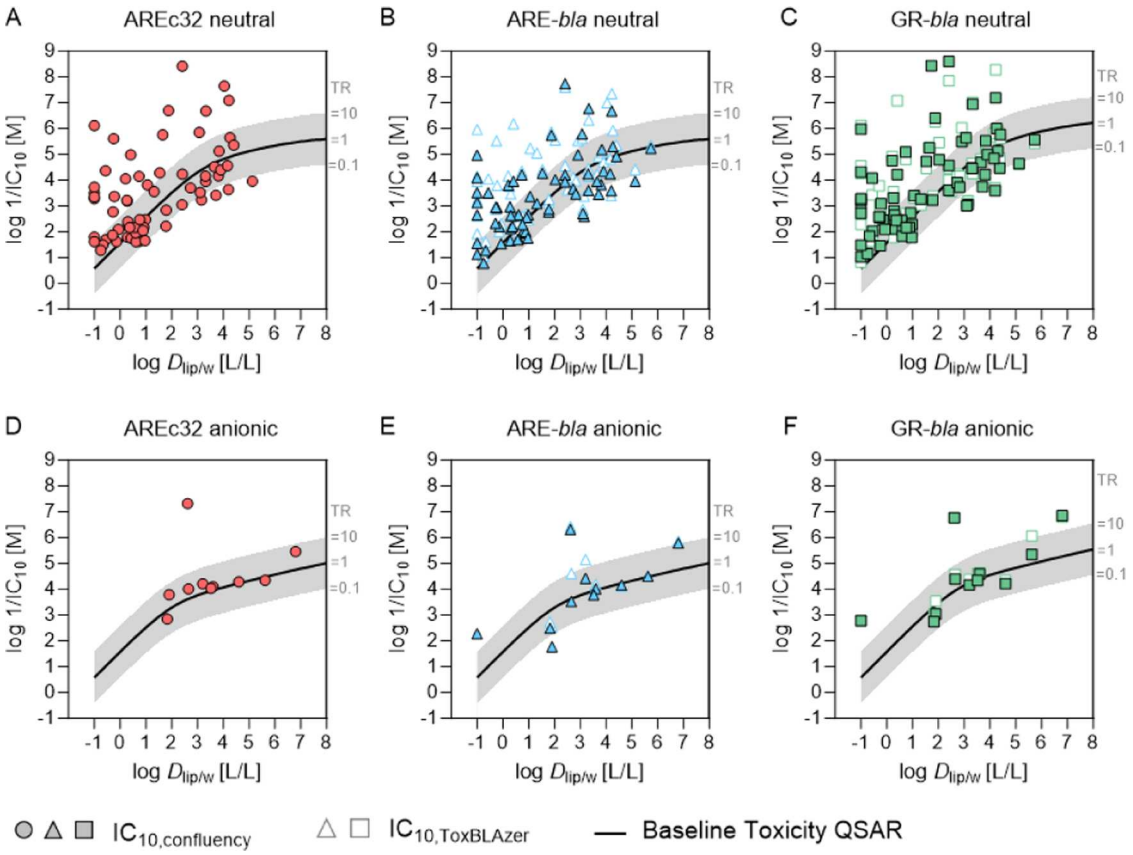

Figure 5. Cytotoxicity of test chemicals compared to baseline toxicity. Logarithmic reciprocal $IC_{10,confluency}$ and logarithmic reciprocal $IC_{10,ToxBLAzer}$ were plotted against the logarithmic liposome−water distribution ratios (log $D_{lip/w}$) of the test chemicals. The black line indicates $IC_{10,baseline}$, and the gray area indicates a toxic ratio (TR) between 0.1 and 10. (A, D) Data from AREc32 assay for neutral (A) and anionic chemicals (D). (B, E) Data from ARE-*bla* assay for neutral (B) and anionic chemicals (E). (C, F) Data from GR-*bla* assay for neutral (C) and anionic chemicals (F).

do not increase CYP activity. Although the IC_{10} values of most chemicals were higher in ARE-*bla* than in the other two cell lines (Figure 4A), the difference was less than a factor of 10 for most chemicals and larger deviations for few chemicals were not only detected for ARE-*bla* but also for AREc32. AREc32 showed a slight inducibility of metabolic activity, but it was significantly lower than the metabolic activity of ARE-*bla*. Chemicals with largest deviations between GR-*bla* and ARE-*bla* and AREc32 (hydroxyurea, cadmium chloride, and hexachlorophene) are not known to be highly metabolized *in vivo*. None of the chemicals showed a higher toxicity in ARE-*bla* or AREc32 compared to GR-*bla* which speaks against metabolic activation of the chemicals.

Comparison of Cytotoxicity Measured in Three Different Cell Lines with Baseline Toxicity. Even if there were no clear differences in cytotoxicity between the different cell lines, individual chemicals can be affected by cellular metabolism. To identify these chemicals, the measured cytotoxicity can be compared with the predicted minimum toxicity (baseline toxicity). If the measured toxicity is lower than the baseline toxicity (TR < 0.1), this may indicate a loss of the chemical. However, this approach only identifies loss of baseline toxicants. Experimental artifacts or loss of specifically acting chemicals with TR > 10 cannot be identified with this approach, as they might just have a reduced TR or be wrongly classified as baseline toxicants.

The measured cytotoxicity of the chemicals was compared with baseline toxicity using the newly defined baseline IC_{10} based on a critical membrane concentration of 26 mmol/L_{lip} for neutral and anionic chemicals and for the media with either 10% FBS or 2% cs-FBS. Figure 5 shows the logarithmic reciprocal IC_{10} values of all chemicals plotted against log $D_{lip/w}$. Four chemicals ($CdCl_2$, As_2O_3, $NaAsO_2$, and TEtT) were metals or inorganic chemical without measured $D_{lip/w}$, so no $IC_{10,baseline}$ could be predicted.

From the remaining 90 chemicals, 27 showed specific toxicity in AREc32 (26 neutral and one anionic chemical, Figure 5A,5D), and 22 showed specific toxicity in ARE-*bla* (19 neutral and three anionic chemicals, Figure 5B,5E) when using $IC_{10,confluency}$ and 32 chemicals (29 neutral and three anionic chemicals, Figure 5B,5E) when using $IC_{10,ToxBLAzer}$. In GR-*bla*, 28 chemicals showed specific toxicity (25 neutral and three anionic chemicals, Figure 5C,5F) when using $IC_{10,confluency}$ and 27 chemicals (23 neutral and four anionic chemicals, Figure 5C,F) when using $IC_{10,ToxBLAzer}$. The chemical with the highest TR in all assays was azacytidine, a cytostatic drug used in cancer therapy. Azacytidine exerts toxic effects by intercalating into DNA and inhibition of DNA methyltransferases which ultimately leads to chromosomal instability and cell death.[54] The majority of the chemicals were baseline toxicants, and the new baseline toxicity QSAR could predict baseline toxicity for both neutral chemicals and anionic chemicals.

For five chemicals (AREc32 and GR-*bla*) or six chemicals (ARE-*bla*), calculated TR values were below 0.1. Valproic acid (VPA) was the only anionic chemical with a TR < 0.1, but only in ARE-*bla*. VPA is an anticonvulsant drug which is rapidly

https://doi.org/10.1021/acs.chemrestox.4c00017
Chem. Res. Toxicol. XXXX, XXX, XXX−XXX

metabolized in the liver,[55] so possibly metabolic degradation could be responsible for the low TR in ARE-*bla* which is also confirmed by the comparison with GR-*bla* (Figure 4) which showed a significantly lower IC_{10} for VPA.

For other chemicals with TR < 0.1, low TRs were observed in all assays suggesting that cellular metabolism was not involved. It is more likely to be an artifact as baseline toxicity is the minimal toxicity a chemical can have. TR below 0.1 can be caused by experimental errors, *e.g.*, precipitation of the chemical or by wrong physicochemical properties as input parameters for the baseline toxicity QSAR. $D_{lip/w}$ of all chemicals with TR < 0.1 were predicted with LSER or QSAR models, so inaccurate $D_{lip/w}$ could be responsible for this artifact. Also, chemical loss processes like volatilization or degradation can lead to TR < 0.1. Chemicals with TR < 0.1 in at least one assay were EPP, NMA, TDM, CP, DPA, VPA, and CBZ.

There are no indications of possible abiotic instability in the literature for most of the chemicals. Only ethoprophos (EPP) and chlorpyrifos (CP) could possibly be hydrolyzed in the course of bioassay like it has been observed for other organophosphates.[9,56] *N*-Methylaniline (NMA) and CP have predicted water−air partitioning constants of 3.62×10^{-4} and 1.19×10^{-4}, so volatilization could be responsible for the low TR of these two chemicals, especially in bioassay medium with a low FBS content. In order to clarify the cause of the low TR for these chemicals, the concentration in the bioassay should be determined experimentally, and possible metabolites should be identified.

CONCLUSIONS

The revised baseline toxicity QSAR is a clear improvement over previous models as it extends the QSAR to more hydrophilic chemicals than previously published studies,[8,17] down to a log $D_{lip/w}$ of −1, and includes specifically anionic chemicals. In protein-rich medium, two different QSAR lines apply for neutral and anionic chemicals due to the stronger binding of anions to proteins. The model for neutral chemicals (eqs 13 and 15) is also applicable to cations and zwitterions, provided the log $D_{lip/w}$ accounts for speciation.[17] The revised baseline toxicity QSAR is shifted 0.42 log units higher (lower $IC_{10,baseline}$) than the previously used QSAR (Figure S11), which means that some chemicals that were previously classified as moderately specific will now still be classified as baseline toxicants.

The improved baseline toxicity QSAR can be used to distinguish between baseline toxicants and specifically acting chemicals. In the present study, the chemicals with the most specific cytotoxicity (highest TR) were azacytidine and colchicine in all assays. Although there were seven chemicals with TR < 0.1, they amounted to less than 10% of the tested chemicals. The reason for this artifact could not fully be explained, but it is likely that experimental artifacts or incorrectly predicted physicochemical properties are a major cause of the inaccurate prediction of baseline toxicity. TR < 0.1 can also be an indication of chemical loss processes, but only for baseline toxicants and cannot differentiate between loss of specifically acting chemicals and reduction of their effect. For this reason, experimental measurement of the freely dissolved or total concentration in the bioassay should be performed to ensure stable chemical exposure during the bioassay.

This study has shown that a number of points (Figure 6) need to be considered before and after the high-throughput screening of single chemicals in order to obtain reliable results. A careful consideration of the physicochemical properties of the

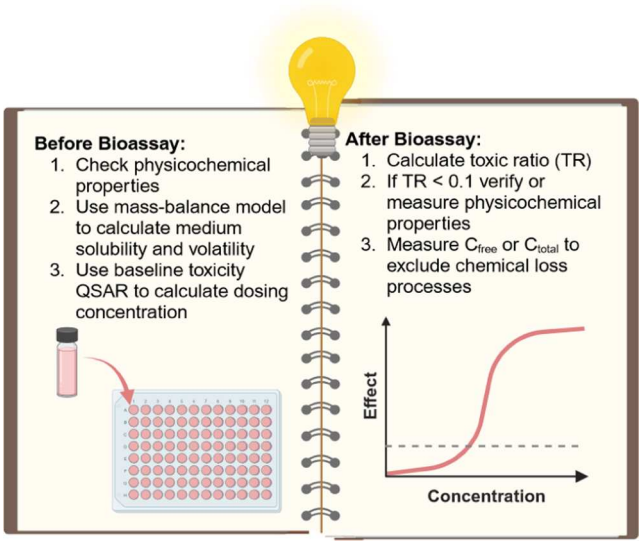

Figure 6. Testing strategies for single chemical screening in high-throughput *in vitro* bioassays.

chemicals can exclude chemical precipitation or volatilization during the assay. Mass-balance models can be used to calculate solubility in bioassay medium and medium-air partitioning constants to identify possibly volatile chemicals.[8,57] Experimental $D_{lip/w}$ of the chemical will give a better prediction of baseline toxicity, because predicted values are often subject to uncertainty, especially if they are based on predicted K_{ow} or if speciation is incorrectly measured or predicted. A dosing concentration of 3 times the calculated baseline toxicity is recommended if this is below medium solubility. After the experiment, TR can be calculated to identify chemicals with specific modes of action, but also to identify chemicals with experimental issues such as precipitation, volatilization, or degradation. Effect concentrations of problematic chemicals should be reevaluated, and loss processes should be experimentally excluded if these data are to be used for chemical risk assessment.

Another aim of this study was to evaluate the impact of the metabolic activity of reporter gene cell lines on *in vitro* results. The metabolic activity of the three reporter gene cell lines of this study was found to be low, as already described in the literature.[23] The highest activity was observed for the ARE-*bla* cell line, which is explained by its liver origin. For the 94 chemicals tested in this study, no clear difference in cytotoxicity in the three different cell lines could be identified, even though a higher metabolic activity of the HepG2-based ARE-*bla* cell line was measured. Although ARE-*bla* showed a slightly lower chemical susceptibility with slightly higher IC_{10} values for the majority of chemicals compared to the other two cell lines, this difference was found to be not significant. Nevertheless, ARE-*bla* showed a lower sensitivity for the activation of the oxidative stress response, as a much smaller number of chemicals showed activity in ARE-*bla* than in AREc32. The more sensitive AREc32 assay should preferably be used for a conservative risk assessment as chemicals with less specific effects can also be identified. Such chemicals may not pose a high risk as individual substances, but in mixtures with other chemicals with the same mode of action, they can contribute to mixture effects.[58]

Although strong CYP inducers, such as benzo[*a*]pyrene, were able to induce metabolic enzymes in ARE-*bla* and AREc32,

https://doi.org/10.1021/acs.chemrestox.4c00017
Chem. Res. Toxicol. XXXX, XXX, XXX−XXX

metabolism rates must be high enough to significantly reduce the internal chemical concentration and, thus, alter the measured toxicity. Since the cell lines showed a low basal CYP activity and even after chemical induction it was almost 5 times lower than the CYP activity of rat liver S9, metabolic activity of the three cell lines used is apparently not sufficient to influence the cytotoxicity of the chemicals of the present study or metabolites and parent chemicals have similar cytotoxicity. It has been shown that despite the different metabolic activity of the three cell lines, there is no systematic change in the measured *in vitro* effects. This result is positive, as it indicates a good comparability of the *in vitro* data from different cell lines. However, if metabolism in the *in vitro* system is desired to study the toxic effects of metabolites that might be formed *in vivo*, a separate metabolism system such as liver microsomes, S9 fractions or purified enzymes must be added to the chemicals either before or during the *in vitro* bioassay.[20]

■ ASSOCIATED CONTENT

Supporting Information

The Supporting Information is available free of charge at https://pubs.acs.org/doi/10.1021/acs.chemrestox.4c00017.

Chemicals for baseline toxicity QSAR development with effect concentrations and concentration response curves; details on CYP inducers and metabolic characterization; comparison of confluency measurement and ToxBLAzer measurement for cytotoxicity determination; oxidative stress response activation of reference compound tBHQ, normal distribution of cytotoxicity; and comparison of newly defined baseline toxicity QSAR with QSAR from the literature (PDF)

Test chemicals and effect concentrations and concentration response curves of all chemicals and assays (XLSX)

■ AUTHOR INFORMATION

Corresponding Author

Luise Henneberger − *Department of Cell Toxicology, Helmholtz Centre for Environmental Research − UFZ, 04318 Leipzig, Germany;* orcid.org/0000-0002-3181-0044; Email: luise.henneberger@ufz.de

Authors

Julia Huchthausen − *Department of Cell Toxicology, Helmholtz Centre for Environmental Research − UFZ, 04318 Leipzig, Germany;* orcid.org/0000-0003-4916-1174

Jenny Braasch − *Department of Cell Toxicology, Helmholtz Centre for Environmental Research − UFZ, 04318 Leipzig, Germany*

Beate I. Escher − *Department of Cell Toxicology, Helmholtz Centre for Environmental Research − UFZ, 04318 Leipzig, Germany; Environmental Toxicology, Department of Geosciences, Eberhard Karls University Tübingen, 72076 Tübingen, Germany;* orcid.org/0000-0002-5304-706X

Maria König − *Department of Cell Toxicology, Helmholtz Centre for Environmental Research − UFZ, 04318 Leipzig, Germany*

Complete contact information is available at: https://pubs.acs.org/10.1021/acs.chemrestox.4c00017

Author Contributions

CRediT: **Julia Huchthausen** data curation, investigation, visualization, writing-original draft; **Jenny Braasch** investigation, writing-review & editing; **Beate I. Escher** conceptualization, funding acquisition, project administration, supervision, writing-review & editing; **Maria König** investigation, writing-review & editing; **Luise Henneberger** data curation, formal analysis, supervision, writing-review & editing.

Funding

This project has received funding from the European Union's Horizon 2020 research and innovation program under Grant Agreement No 965406 (PrecisionTox). The work presented in this publication was performed as part of the ASPIS cluster. The results and conclusions reflect only the authors' view, and the European Commission cannot be held responsible for any use that may be made of the information contained therein.

Notes

The authors declare no competing financial interest.

■ ACKNOWLEDGMENTS

The authors thank Niklas Wojtysiak and Christin Kühnert for supporting the *in vitro* bioassay experiments, as well as Stefan Scholz for coordinating the PrecisionTox project at UFZ and reviewing the manuscript. The authors thank Rita Schlichting for providing the KNIME workflows for data evaluation. They also gratefully acknowledge funding of access to the platform CITEPro (Chemicals in the Terrestrial Environment Profiler) by the Helmholtz Association.

■ REFERENCES

(1) Van Norman, G. A. Limitations of Animal Studies for Predicting Toxicity in Clinical Trials: Is it Time to Rethink Our Current Approach? *JACC Basic Transl. Sci.* **2019**, *4* (7), 845−854.

(2) Isaacs, K. K.; Egeghy, P.; Dionisio, K. L.; Phillips, K. A.; Zidek, A.; Ring, C.; Sobus, J. R.; Ulrich, E. M.; Wetmore, B. A.; Williams, A. J.; Wambaugh, J. F. The chemical landscape of high-throughput new approach methodologies for exposure. *J. Exposure Sci. Environ. Epidemiol.* **2022**, *32* (6), 820−832.

(3) Schmeisser, S.; Miccoli, A.; von Bergen, M.; Berggren, E.; Braeuning, A.; Busch, W.; Desaintes, C.; Gourmelon, A.; Grafström, R.; Harrill, J.; Hartung, T.; Herzler, M.; Kass, G. E. N.; Kleinstreuer, N.; Leist, M.; Luijten, M.; Marx-Stoelting, P.; Poetz, O.; van Ravenzwaay, B.; Roggeband, R.; Rogiers, V.; Roth, A.; Sanders, P.; Thomas, R. S.; Marie Vinggaard, A.; Vinken, M.; van de Water, B.; Luch, A.; Tralau, T. New approach methodologies in human regulatory toxicology - Not if, but how and when! *Environ. Int.* **2023**, *178*, No. 108082.

(4) van der Zalm, A. J.; Barroso, J.; Browne, P.; Casey, W.; Gordon, J.; Henry, T. R.; Kleinstreuer, N. C.; Lowit, A. B.; Perron, M.; Clippinger, A. J. A framework for establishing scientific confidence in new approach methodologies. *Arch. Toxicol.* **2022**, *96* (11), 2865−2879.

(5) Freedman, J.; The PrecisionTox Consortium, Colbourne JK. The Precision Toxicology initiative. *Toxicol. Lett.* **2023**, *383*, 33−42.

(6) Henneberger, L.; Mühlenbrink, M.; Fischer, F. C.; Escher, B. I. C18-Coated Solid-Phase Microextraction Fibers for the Quantification of Partitioning of Organic Acids to Proteins, Lipids, and Cells. *Chem. Res. Toxicol.* **2019**, *32* (1), 168−178.

(7) Fischer, F. C.; Cirpka, O. A.; Goss, K. U.; Henneberger, L.; Escher, B. I. Application of Experimental Polystyrene Partition Constants and Diffusion Coefficients to Predict the Sorption of Neutral Organic Chemicals to Multiwell Plates in in Vivo and in Vitro Bioassays. *Environ. Sci. Technol.* **2018**, *52* (22), 13511−13522.

(8) Escher, B. I.; Glauch, L.; König, M.; Mayer, P.; Schlichting, R. Baseline Toxicity and Volatility Cutoff in Reporter Gene Assays Used for High-Throughput Screening. *Chem. Res. Toxicol.* **2019**, *32* (8), 1646−1655.

(9) Huchthausen, J.; Henneberger, L.; Mälzer, S.; Nicol, B.; Sparham, C.; Escher, B. I. High-Throughput Assessment of the Abiotic Stability of Test Chemicals in In Vitro Bioassays. *Chem. Res. Toxicol.* **2022**, *35* (5), 867−879.
(10) Fischer, F. C.; Abele, C.; Henneberger, L.; Klüver, N.; König, M.; Mühlenbrink, M.; Schlichting, R.; Escher, B. I. Cellular Metabolism in High-Throughput In Vitro Reporter Gene Assays and Implications for the Quantitative In Vitro-In Vivo Extrapolation. *Chem. Res. Toxicol.* **2020**, *33* (7), 1770−1779.
(11) Henneberger, L.; Mühlenbrink, M.; König, M.; Schlichting, R.; Fischer, F. C.; Escher, B. I. Quantification of freely dissolved effect concentrations in in vitro cell-based bioassays. *Arch. Toxicol.* **2019**, *93* (8), 2295−2305.
(12) Huchthausen, J.; König, M.; Escher, B. I.; Henneberger, L. Experimental exposure assessment for in vitro cell-based bioassays in 96- and 384-well plates. *Front. Toxicol.* **2023**, *5*, No. 1221625.
(13) Fischer, F. C.; Henneberger, L.; König, M.; Bittermann, K.; Linden, L.; Goss, K. U.; Escher, B. I. Modeling Exposure in the Tox21 in Vitro Bioassays. *Chem. Res. Toxicol.* **2017**, *30* (5), 1197−1208.
(14) Armitage, J. M.; Sangion, A.; Parmar, R.; Looky, A. B.; Arnot, J. A. Update and Evaluation of a High-Throughput In Vitro Mass Balance Distribution Model: IV-MBM EQP v2.0. *Toxics* **2021**, *9* (11), No. 31.
(15) Verhaar, H. J. M.; Ramos, E. U.; Hermens, J. L. M. Classifying environmental pollutants. 2. Separation of class 1 (baseline toxicity) and class 2 ('polar narcosis') type compounds based on chemical descriptors. *J. Chem.* **1996**, *10* (2), 149−162.
(16) Escher, B. I.; Henneberger, L.; König, M.; Schlichting, R.; Fischer, F. C. Cytotoxicity Burst? Differentiating Specific from Nonspecific Effects in Tox21 in Vitro Reporter Gene Assays. *Environ. Health Perspect.* **2020**, *128* (7), No. 77007.
(17) Lee, J.; Braun, G.; Henneberger, L.; König, M.; Schlichting, R.; Scholz, S.; Escher, B. I. Critical Membrane Concentration and Mass-Balance Model to Identify Baseline Cytotoxicity of Hydrophobic and Ionizable Organic Chemicals in Mammalian Cell Lines. *Chem. Res. Toxicol.* **2021**, *34* (9), 2100−2109.
(18) Maeder, V.; Escher, B. I.; Scheringer, M.; Hungerbühler, K. Toxic ratio as an indicator of the intrinsic toxicity in the assessment of persistent, bioaccumulative, and toxic chemicals. *Environ. Sci. Technol.* **2004**, *38* (13), 3659−3666.
(19) Qin, W.; Henneberger, L.; Glüge, J.; König, M.; Escher, B. I. Baseline toxicity model to identify the specific and non-specific effects of per- and polyfluoroalkyl substances in cell-based bioassays. *Environ. Sci. Technol.* **2024**, *58* (13), 5727−5738.
(20) Coecke, S.; Ahr, H.; Blaauboer, B. J.; Bremer, S.; Casati, S.; Castell, J.; Combes, R.; Corvi, R.; Crespi, C. L.; Cunningham, M. L.; Elaut, G.; Eletti, B.; Freidig, A.; Gennari, A.; Ghersi-Egea, J. F.; Guillouzo, A.; Hartung, T.; Hoet, P.; Ingelman-Sundberg, M.; Munn, S.; Janssens, W.; Ladstetter, B.; Leahy, D.; Long, A.; Meneguz, A.; Monshouwer, M.; Morath, S.; Nagelkerke, F.; Pelkonen, O.; Ponti, J.; Prieto, P.; Richert, L.; Sabbioni, E.; Schaack, B.; Steiling, W.; Testai, E.; Vericat, J. A.; Worth, A. Metabolism: a bottleneck in in vitro toxicological test development. The report and recommendations of ECVAM workshop 54. *Altern. Lab. Anim.* **2006**, *34* (1), 49−84.
(21) Ooka, M.; Lynch, C.; Xia, M. Application of In Vitro Metabolism Activation in High-Throughput Screening. *Int. J. Mol. Sci.* **2020**, *21* (21), No. 8182.
(22) Hopperstad, K.; Deisenroth, C. Development of a bioprinter-based method for incorporating metabolic competence into high-throughput in vitro assays. *Front. Toxicol.* **2023**, *5*, No. 1196245.
(23) Qu, W.; Crizer, D. M.; DeVito, M. J.; Waidyanatha, S.; Xia, M.; Houck, K.; Ferguson, S. S. Exploration of xenobiotic metabolism within cell lines used for Tox21 chemical screening. *Toxicol. In Vitro.* **2021**, *73*, No. 105109.
(24) Choi, J. M.; Oh, S. J.; Lee, S. Y.; Im, J. H.; Oh, J. M.; Ryu, C. S.; Kwak, H. C.; Lee, J. Y.; Kang, K. W.; Kim, S. K. HepG2 cells as an in vitro model for evaluation of cytochrome P450 induction by xenobiotics. *Arch. Pharm. Res.* **2015**, *38* (5), 691−704.
(25) Iwanari, M.; Nakajima, M.; Kizu, R.; Hayakawa, K.; Yokoi, T. Induction of CYP1A1, CYP1A2, and CYP1B1 mRNAs by nitro-polycyclic aromatic hydrocarbons in various human tissue-derived cells: chemical-, cytochrome P450 isoform-, and cell-specific differences. *Arch. Toxicol.* **2002**, *76* (5−6), 287−298.
(26) Fischer, F. C.; Abele, C.; Droge, S. T. J.; Henneberger, L.; König, M.; Schlichting, R.; Scholz, S.; Escher, B. I. Cellular Uptake Kinetics of Neutral and Charged Chemicals in in Vitro Assays Measured by Fluorescence Microscopy. *Chem. Res. Toxicol.* **2018**, *31* (8), 646−657.
(27) Attene-Ramos, M. S.; Miller, N.; Huang, R.; Michael, S.; Itkin, M.; Kavlock, R. J.; Austin, C. P.; Shinn, P.; Simeonov, A.; Tice, R. R.; Xia, M. The Tox21 robotic platform for the assessment of environmental chemicals-from vision to reality. *Drug Discovery Today* **2013**, *18* (15−16), 716−723.
(28) Wang, X. J.; Hayes, J. D.; Wolf, C. R. Generation of a stable antioxidant response element-driven reporter gene cell line and its use to show redox-dependent activation of nrf2 by cancer chemotherapeutic agents. *Cancer Res.* **2006**, *66* (22), 10983−10994.
(29) Shukla, S. J.; Huang, R.; Simmons, S. O.; Tice, R. R.; Witt, K. L.; Vanleer, D.; Ramabhadran, R.; Austin, C. P.; Xia, M. Profiling environmental chemicals for activity in the antioxidant response element signaling pathway using a high throughput screening approach. *Environ. Health Perspect.* **2012**, *120* (8), 1150−1156.
(30) Wilkinson, J. M.; Hayes, S.; Thompson, D.; Whitney, P.; Bi, K. Compound profiling using a panel of steroid hormone receptor cell-based assays. *J. Biomol. Screening* **2008**, *13* (8), 755−765.
(31) Kennedy, S. W.; Lorenzen, A.; James, C. A.; Collins, B. T. Ethoxyresorufin-O-deethylase and porphyrin analysis in chicken embryo hepatocyte cultures with a fluorescence multiwell plate reader. *Anal. Biochem.* **1993**, *211* (1), 102−112.
(32) DeLuca, J. G.; Dysart, G. R.; Rasnick, D.; Bradley, M. O. A direct, highly sensitive assay for cytochrome P-450 catalyzed O-deethylation using a novel coumarin analog. *Biochem. Pharmacol.* **1988**, *37* (9), 1731−1739.
(33) Renwick, A. B.; Surry, D.; Price, R. J.; Lake, B. G.; Evans, D. C. Metabolism of 7-benzyloxy-4-trifluoromethyl-coumarin by human hepatic cytochrome P450 isoforms. *Xenobiotica* **2000**, *30* (10), 955−969.
(34) Niu, L.; Henneberger, L.; Huchthausen, J.; Krauss, M.; Ogefere, A.; Escher, B. I. pH-Dependent Partitioning of Ionizable Organic Chemicals between the Silicone Polymer Polydimethylsiloxane (PDMS) and Water. *ACS Environ. Au* **2022**, *2* (3), 253−262.
(35) König, M.; Escher, B. I.; Neale, P. A.; Krauss, M.; Hilscherova, K.; Novak, J.; Teodorovic, I.; Schulze, T.; Seidensticker, S.; Hashmi, M. A. K.; Ahlheim, J.; Brack, W. Impact of untreated wastewater on a major European river evaluated with a combination of in vitro bioassays and chemical analysis. *Environ. Pollut.* **2017**, *220* (Pt B), 1220−1230.
(36) Neale, P. A.; Altenburger, R.; Ait-Aissa, S.; Brion, F.; Busch, W.; de Aragao Umbuzeiro, G.; Denison, M. S.; Du Pasquier, D.; Hilscherova, K.; Hollert, H.; Morales, D. A.; Novak, J.; Schlichting, R.; Seiler, T. B.; Serra, H.; Shao, Y.; Tindall, A. J.; Tollefsen, K. E.; Williams, T. D.; Escher, B. I. Development of a bioanalytical test battery for water quality monitoring: Fingerprinting identified micropollutants and their contribution to effects in surface water. *Water Res.* **2017**, *123*, 734−750.
(37) Escher, B. I.; Dutt, M.; Maylin, E.; Tang, J. Y.; Toze, S.; Wolf, C. R.; Lang, M. Water quality assessment using the AREc32 reporter gene assay indicative of the oxidative stress response pathway. *J. Environ. Monit.* **2012**, *14* (11), 2877−2885.
(38) Wezel, A. P. v.; Opperhuizen, A. Narcosis due to environmental pollutants in aquatic organisms: residue-based toxicity, mechanisms, and membrane burdens. *Crit. Rev. Toxicol.* **1995**, *25* (3), 255−279.
(39) Huchthausen, J.; Mühlenbrink, M.; König, M.; Escher, B. I.; Henneberger, L. Experimental Exposure Assessment of Ionizable Organic Chemicals in In Vitro Cell-Based Bioassays. *Chem. Res. Toxicol.* **2020**, *33* (7), 1845−1854.
(40) Ulrich, N.; Endo, S.; Brown, T. N.; Watanabe, N.; Bronner, G.; Abraham, M. H.; Goss, K.-U. UFZ-LSER database v 3.2.1 [Internet], 2017. http://www.ufz.de/lserd.

https://doi.org/10.1021/acs.chemrestox.4c00017
Chem. Res. Toxicol. XXXX, XXX, XXX−XXX

(41) Endo, S.; Escher, B. I.; Goss, K.-U. Capacities of Membrane Lipids to Accumulate Neutral Organic Chemicals. *Environ. Sci. Technol.* **2011**, *45* (14), 5912−5921.
(42) Endo, S.; Goss, K. U. Serum albumin binding of structurally diverse neutral organic compounds: data and models. *Chem. Res. Toxicol.* **2011**, *24* (12), 2293−2301.
(43) Escher, B. I.; Neale, P. A.; Villeneuve, D. L. The advantages of linear concentration-response curves for in vitro bioassays with environmental samples. *Environ. Toxicol. Chem.* **2018**, *37* (9), 2273−2280.
(44) Escher, B. I.; Schwarzenbach, R. P. Mechanistic studies on baseline toxicity and uncoupling of organic compounds as a basis for modeling effective membrane concentrations in aquatic organisms. *Aquat. Sci.* **2002**, *64* (1), 20−35.
(45) Escher, B. I.; Baumer, A.; Bittermann, K.; Henneberger, L.; König, M.; Kühnert, C.; Klüver, N. General baseline toxicity QSAR for nonpolar, polar and ionisable chemicals and their mixtures in the bioluminescence inhibition assay with Aliivibrio fischeri. *Environ. Sci.: Processes Impacts* **2017**, *19* (3), 414−428.
(46) Shah, U. K.; Seager, A. L.; Fowler, P.; Doak, S. H.; Johnson, G. E.; Scott, S. J.; Scott, A. D.; Jenkins, G. J. A comparison of the genotoxicity of benzo[a]pyrene in four cell lines with differing metabolic capacity. *Mutat. Res., Genet. Toxicol. Environ. Mutagen.* **2016**, *808*, 8−19.
(47) Kikuchi, H.; Hossain, A. Signal transduction-mediated CYP1A1 induction by omeprazole in human HepG2 cells. *Exp. Toxicol. Pathol.* **1999**, *51* (4), 342−346.
(48) Cox, J. A.; Fellows, M. D.; Hashizume, T.; White, P. A. The utility of metabolic activation mixtures containing human hepatic post-mitochondrial supernatant (S9) for in vitro genetic toxicity assessment. *Mutagenesis* **2016**, *31* (2), 117−130.
(49) Sackett, D. L.; Varma, J. K. Molecular mechanism of colchicine action: induced local unfolding of beta-tubulin. *Biochemistry* **1993**, *32* (49), 13560−13565.
(50) Hsieh, J. H.; Huang, R.; Lin, J. A.; Sedykh, A.; Zhao, J.; Tice, R. R.; Paules, R. S.; Xia, M.; Auerbach, S. S. Real-time cell toxicity profiling of Tox21 10K compounds reveals cytotoxicity dependent toxicity pathway linkage. *PLoS One* **2017**, *12* (5), No. e0177902.
(51) Martin, S. J.; Henry, C. M. Distinguishing between apoptosis, necrosis, necroptosis and other cell death modalities. *Methods* **2013**, *61* (2), 87−89.
(52) Li, H.; Qian, W.; Weng, X.; Wu, Z.; Li, H.; Zhuang, Q.; Feng, B.; Bian, Y. Glucocorticoid receptor and sequential P53 activation by dexamethasone mediates apoptosis and cell cycle arrest of osteoblastic MC3T3-E1 cells. *PLoS One* **2012**, *7* (6), No. e37030.
(53) Schopfer, L. M.; Lockridge, O. Mass Spectrometry Identifies Isopeptide Cross-Links Promoted by Diethylphosphorylated Lysine in Proteins Treated with Chlorpyrifos Oxon. *Chem. Res. Toxicol.* **2019**, *32* (4), 762−772.
(54) Raj, K.; Mufti, G. J. Azacytidine (Vidaza(R)) in the treatment of myelodysplastic syndromes. *Ther. Clin. Risk Manage.* **2006**, *2* (4), 377−388.
(55) Ghodke-Puranik, Y.; Thorn, C. F.; Lamba, J. K.; Leeder, J. S.; Song, W.; Birnbaum, A. K.; Altman, R. B.; Klein, T. E. Valproic acid pathway: pharmacokinetics and pharmacodynamics. *Pharmacogenet. Genomics* **2013**, *23* (4), 236−241.
(56) Silva, V. B.; Orth, E. S. Structure-Reactivity Insights on the Alkaline Hydrolysis of Organophosphates: Non-Leaving and Leaving Group Effects in a Bilinear Brønsted-Like Relationship. *ChemPhysChem* **2023**, *24* (6), No. e202200612.
(57) Fischer, F. C.; Henneberger, L.; Schlichting, R.; Escher, B. I. How To Improve the Dosing of Chemicals in High-Throughput in Vitro Mammalian Cell Assays. *Chem. Res. Toxicol.* **2019**, *32* (8), 1462−1468.
(58) Escher, B.; Braun, G.; Zarfl, C. Exploring the Concepts of Concentration Addition and Independent Action Using a Linear Low-Effect Mixture Model. *Environ. Toxicol. Chem.* **2020**, *39* (12), 2552−2559.

https://doi.org/10.1021/acs.chemrestox.4c00017
Chem. Res. Toxicol. XXXX, XXX, XXX−XXX